BEHAVIOUR OF UNSTIFFENED FLUSH END PLATE BEAM-TO-COLUMN CONNECTIONS IN STRUCTURAL STEELWORK

Zhi Min Wang

A thesis submitted in partial fulfilment
of the requirements of the
University of Abertay Dundee
for the degree of Doctor of Philosophy

January 1996

I certify that this thesis is the true and accurate version of the thesis approved by the examiners.

Signed .. [redacted] ..... Date 29/2/96

Director of Studies

Acknowledgements

The author would like to express his sincere gratitude to his supervisors Dr. B. Bose (Director of Studies) and Prof. S. Sarkar and his project advisor-Mr A. S. Malik, Senior Engineer, The Steel Construction Institute, for their guidance, encouragement and assistance throughout the course of this investigation. Without their support, it would have been impossible to accomplish the task successfully and in time.

The author would also like to acknowledge the University of Abertay Dundee for providing financial support for the project.

Further he wishes to extend his thanks to all the technical staff of the School of Construction and Environment, and in particular Messrs Galloway, Thomson, Smart and Webster, for their much valued help and co-operation. Thanks are also due to Mr. S. Gardener and other staff of the Computer Centre of the University for their assistance on computing.

Behaviour of unstiffened flush end plate beam-to-column connections in structural steelwork

Zhi Min Wang, B. Eng.

ABSTRACT

End plate connections are extensively used as moment resistant connections between members in steel frame. Surveys of the English and Scottish Steelwork Industry clearly indicate that the flush end plate connection is the most popular type of beam-to-column connection in steel-framed structures. The popularity of this connection can be attributed to the simplicity of the connection detail and economy associated with their fabrication and erection. Flush end plate connection is less rigid and has a lower moment capacity than that of an extended end plate connection. If a rigid joint is aimed extended end plate connection should be used, whereas if a semi-rigid joint is needed flush end plate can be employed.

The main objectives of this project were to carry out in-depth investigation of the behaviour of this type of connection by applying finite element technique and experimental means.

A three dimensional finite element prediction model of the unstiffened flush end plate beam-to-column connection was developed. Six full scale tests were conducted and the results were analysed. Comparison between analytical and experimental results was made. The analytical investigation into the contribution of the various connection components toward the moment rotation characteristics was carried out. The investigation of bolt force and prying force were also carried out. Comparison between analytical, experimental results and the results obtained by applying the design rules of Eurocode 3 was made.

By comparing the experimental results with the analytical results using finite element method, it was found that the finite element method was quite capable of

tackling the complex problem of flush end plate connections. Finite element computer models can be used to simulate structural behaviour of the connections, which can be useful to the design of the connections. By comparing the results of the tests, finite element analyses and the design rules of Eurocode 3, it was found that the Annex J of Eurocode 3 significantly underestimated the moment resistance capacity of many joints and appear to predict the failure type incorrectly. Recommendations on future work on column web buckling, the effect of bolt heads and nuts, the sectional fillets and the effect of welding are also made which should be carried out before a comprehensive design procedure could be developed.

List of Tables

List of Figures

Notations

A	area of cross-section
A_s	tensile stress area of a bolt
A_{vc}	shear area of the column
b_{eff}	effective width of an equivalent T-stub
$B_{t,Rd}$	design tension resistance of a bolt-plate assembly
D	depth of the beam
d	diameter of a bolt
d_c	clear depth of the column web
$[D]$	elasticity matrix
E	Young's modulus of elasticity
e	distance between the bolt and the edge of T-stub
F	force
$F_{c,fb,Rd}$	design resistance of the beam flange and web in compression
$F_{c,wc,Rd}$	design resistance of the column web in compression
$F_{t,Rd}$	design tension resistance of an equivalent T-stub flange
f_{ub}	ultimate tensile strength of the bolts
f_y	yield strength
G	rigidity (shear) modulus of elasticity
h_b	depth of the beam
h_r	distance between bolt row r and the centre of compression
h, n_1	depth of the column section
I	second moment of the area
I_b	second moment of the beam cross-section
$[J]$	Jacobian matrix
k	stiffness of joint element
$k_{eff,r}$	effective stiffness coefficient for bolt row r taking into account the stiffness coefficients k_i for the basic components
k_{eq}	equivalent stiffness coefficient
k_i	stiffness coefficient representing component i
k_{ir}	stiffness coefficient representing component i relative to bolt row r
$[k^e]$	stiffness matrix of element e in global coordinate system
L	length of a beam
l	length of one-dimensional element
L_b	length of a beam
L_b	elongation length of the bolt
l_{eff}	effective length of an equivalent T-stub
l_{ij} , m_{ij} , n_{ij}	direction cosines of a bar element with nodes i and j

M	moment
m	clear distance between the bolt and the web of T-stub
$M_{c,Rd}$	design moment resistance of the beam cross section
$M_{j,Rd}$	moment resistance of the connection
N_i	interpolation function associated with the *i*th nodal degree of freedom
$[N]$	matrix of shape (nodal interpolation) functions
n	e_{min}, but $\leq$ 1.25m
P	distributed load
$\vec{p}_b^{(e)}$ ($\vec{P}_b^{(e)}$)	load vector due to body forces of element e in local (global) coordinate system
$\vec{\tilde{P}}_c$	vector of concentrated loads
$\vec{p}_i^{(e)}$ ($\vec{P}_i^{(e)}$)	load vector due to initial strains of element e in local (global) coordinate system
$\vec{p}_s^{(e)}$ ($\vec{P}_s^{(e)}$)	load vector due to surface forces of element e in local (global) coordinate system
$\vec{q}^{(e)}$ ($\vec{Q}^{(e)}$)	vector of nodal displacement of element e in local (global) coordinate system
$\vec{R}$	external force vector
r, *s*, *t*	natural coordinates of a hexahedron element
S	coefficient in elastic-plastic constitutive relationship
S_j	rotation stiffness
$S_{j,ini}$	initial rotational stiffness
S_s , b_1	length of stiff bearing
T	beam flange thickness
t	thickness of plate
t_w	weld size
$V_{wp,Rd}$	design shear resistance of a column web panel
Z	lever arm
β	transformation parameter
$\vec{\varepsilon}$	strain vector
$\vec{\varepsilon}_0$	initial strain vector
γ_d	displacement norm used for convergence
γ_{M0}	safety factor
γ_w	work norm used for convergence
γ_ψ	residual norm used for convergence

γ_{ψ_1}	root mean square of residuals convergence criterion
γ_{ψ_2}	maximum absolute residual convergence criterion
$[\lambda]$	coordinate transformation matrix
μ	stiffness ratio
μ, ν, ω	components of displacement parallel to x, y, z axes
ν	Poisson's ratio
ρ	reduction factor
$\overline{\sigma}$	generalised stress
σ_i	principal component of stress
σ_y	yield stress in simple tension
σ'_y	rate of change of σ_y with respect to plastic strain
σ'_{ij}	deviatoric component of stress
ϕ	rotation
ϕ_b	contribution of the bolt to the connection rotation
ϕ_{cd}	rotation capacity
ϕ_{cf}	contribution of the column flange to the connection rotation
ϕ_{ep}	contribution of the end plate to the connection rotation
$\overrightarrow{\Phi}$	surface force vector
$\overrightarrow{\phi}$	body force vector
$\bar{\psi}$	residual force vector
det[ ]	determinant of enclosed matrix

Contents

CHAPTER 1

INTRODUCTION

1.1 GENERAL INTRODUCTION

The flush end plate connection is the most popular type[1],[2] of beam-to-column connection in steel-framed structures. A typical flush end plate connection consists of a rectangular steel plate welded to the end of a beam, which in turn is connected to the flange of a column by one or two pairs of high-strength steel bolts positioned near the beam tension flange and a pair of bolts placed adjacent to the beam compression flange, as shown in Figure 1.1. A typical extended end plate connection consists of an end plate, which is longer than the depth of the beam, with one pair of high-strength steel bolts positioned on either side of the beam tension flange and one pair of bolts placed adjacent to the beam compression flange, as shown in Figure 1.2.

Although bolted connections have been used for shear joints for a long time, the extension of their use as moment resisting connections is a recent trend in steel construction. In a report on end plate connections published in 1962 Disque[3] described the advantages and disadvantages of the end plate connections from practical and fabrication points of view. Some of the advantages over other bolted connections that he listed are:

(a) saving in material weight and fabrication cost;

(b) reduced number of detail pieces to handle;

(c) no difficulty in correcting for overrun or underrun in beam depth;

(d) workmanship is simpler when all drilling is confined to plates which are then welded to beams.

Both flush and extended end plate connections are widely used as moment resisting joints in steel frame construction. Flush end plate connection is less rigid

and has a lower moment capacity than that of an extended end plate and is frequently used in order to achieve semi-rigid connections. Column stiffeners are generally provided at the level of beam flanges; however this involves costly fabrication and may interfere with the connection of cross beams to the web of the column. It may, therefore, be preferable to use a heavier column section in order to avoid stiffeners.

The flush end plate connection represents an extremely complex and highly indeterminate problem with a large number of parameters affecting its structural behaviour. Included among them are the depth of the beam, end plate thickness, type, size and pitch of bolts, and column flange/web thicknesses. The interactive forces between the end plate and column flange can also influence the characteristics of the connection.

In flush end plate connections the beam end moment is transferred through the end plate to the column flange via the bolts. This results in tension force acting on the column flange at bolt location in the tension region and compression force acting over some bearing zone in the compression region. The interaction at the interface of end plate and column flange is a complex problem which can be exacerbated by bolt tightening. The prying forces had been frequently disregarded even though they can have significant influence and in many cases they can lead to joint strength being controlled by premature bolt failure.

Although ideally all the components of the connection should fail simultaneously for maximum efficiency, this cannot be regarded as a good design practice. Bolts and welds behave in a brittle manner and their failure in a connection would cause a sudden loss of strength. If a thick end plate is used, there is negligible bending deformation of the end plate and failure of bolts or welds might occur, provided the column is strong enough to resist the external moment. It is therefore necessary to establish a right balance between the performance of the individual components in order to attain the desired stiffness and strength. Semi-rigid design is

allowed in BS5950[4], which recommends that semi-rigid connections shall be designed as idealised pinned joints and allowance of 10% of free moment shall be made for the end restraint moment. This design method is neither efficient nor economical and is not widely used. Another design approach is based on the yield line method where various yield line configurations are assumed in order to consider the plastic behaviour of the various components forming the connection. This approach tends to oversimplify the behaviour of the connection. It is acknowledged that prying forces exist, but no attempt is made to evaluate these forces. It is suggested that an increase of up to 33% in the tension bolt forces will be adequate to compensate for the prying action. This method results in conservative formulae for the design of end plate, column flange and bolts. The recently published draft Annex J of Eurocode 3[5] is based on the 'yield line' method. A comparative study of the provisions in Eurocode 3 and the results of tests carried out at the University of Abertay Dundee[6],[7] indicated significant anomalies. An appraisal of the design rules in Eurocode 3 for bolted end plate joints are carried out in chapter 8.

It is common knowledge that the 'yield line' method can only predict the ultimate strength of the connection but failed to provide any information regarding the actual deformation occurring in the connection at service loads. The method can not predict the relationship between bending moment and rotation. A satisfactory approach to comprehensive analysis and design of a connection must include the prediction of its performance at both service and ultimate loads.

The availability of high speed computers and powerful finite element software provide an ideal tool to carry out an in-depth study of the connection behaviour. In order to overcome the shortcomings of other methods the author chose finite element method for an in-depth study of the behaviour of flush end plate connections.

For any beam-to-column connection the rotational stiffness of the joint is of utmost importance. This is defined by the relationship between the moment, M,

transmitted by the connection and the angular rotation, ϕ, of the connection. The joint rotation, ϕ, is given by the change in angle between the longitudinal axes of the connecting members at their point of intersection. Figure 1.3 illustrates the M-ϕ relationship for a few popular types of connection: web cleats, flush end plates and extended end plates. An ideal pinned connection rotates without transmitting any moment, whereas an ideal rigid connection transmits moment without any rotation as represented by the x and y axes respectively. From Figure 1.3 it is clear that the rotational stiffness offered by various practical connections differ greatly. However, they exhibit some common characteristics which can be summarised as follows:

1. The M-ϕ curves are non-linear from the very start and continue to be non-linear over their whole loading range.
2. 'Flexible' connections like web cleats possess a degree of rotational stiffness and transmit some amount of moment, whereas 'rigid' connections like extended end plates exhibit some flexibility and give rise to appreciable joint rotations. Thus in reality all bolted beam-to-column connections are semi-rigid.

The three significant characteristics of a connection are:

- Moment resistance;
- Rotational stiffness;
- Rotation capacity.

Eurocode 3 defines of the above three connection characteristics as shown in Figure 1.4. In the figure $M_{j,Rd}$, $S_{j,ini}$ and ϕ_{cd} represent the moment resistance, rotational stiffness and rotation capacity respectively of the connection.

Eurocode 3 classifies connections as nominally pinned, semi-rigid and rigid on the basis of rotational stiffness of the connection. The connection is classified as nominally pinned, partial strength or full strength depending on the moment resistance of the connection. The suitability of a connection for use in plastically designed continuous/semi-continuous structures depends on the rotation capacity of the connection. The connection design of Eurocode 3, which is based on 'yield line'

method, will in future replace all the national codes in Europe, including the British Standard BS5950, currently in use in the UK.

At the ultimate limit state failure of the connection can be due to any of the following:

- Column web panel in shear;
- Column web in compression;
- Beam flange and web in compression;
- Column flange in bending;
- Column web in tension;
- End plate in bending;
- Beam web in tension;
- Bolts in tension;
- Bolts in shear;
- Bolts in bearing;

The finite element method was successfully applied at the University of Abertay Dundee by a research student for his work on 'extended endplate' connections[8]. The LUSAS[9] finite element package, acquired by the University, is a highly sophisticated and powerful program which can be used for an in-depth investigation into the behaviour of flush end plate connections. Other widely used finite element packages available in the market are ABAQUS and ANSYS.

1.2 SURVEY OF THE STRUCTURAL STEELWORK INDUSTRY

An important element in cost reduction in today's construction industry is the more economic use of manpower by applying computerised automatic and semi-automatic procedures. This pre-supposes a measure of standardization not currently present in the British constructional steelwork industry. The introduction of standardization not only reduces the numerous parameters involved in any connection design but also allows the designers to choose between a range of connections, once the beam and column section have been decided. This method provides a more efficient and

economical design than the present methods where all connections are designed individually. Standardization can only be achieved if adequate knowledge of connection responses is available. It is, therefore, essential to carry out a detailed study to understand the moment-rotation characteristics of different types of connection.

Traditional steel frames design method is based on the concept of 'rigid' or 'pinned' connections and ignores the end restraint provided by many practical connections. The consideration of this end restraint will provide efficiency in design and a saving of up to 15%[10]. The saving is the result of more realistic design without alteration to the existing design procedure; hence fabrication and erection costs remain unchanged. However, the recent increase in labour cost has overwhelmed the saving which can be made in material. It is, therefore, essential that the connection details be rationalised and the design procedure be standardized. Standardization can reduce manpower by increasing the productivity, which is achieved by means of repetition or computerised automatic and semi-automatic procedures. The overall cost of construction can be reduced by the combination of the reduction in material and manpower cost. The Australian Steel Industry, with only a single large fabricator, has achieved a measure of standardization of connections and has adopted a 20 mm diameter bolt (commercial grade) as standard. The diversity of fabricators and designers in Britain complicates the issue and contributes to the large number of connection types, bolts, weld sizes, plate thicknesses, etc. It will need considerable effort and a lot of convincing before standard connections will be adopted in the U.K.

1.2.1 A Survey of the English Structural Steelwork Industry

A survey of the English Structural Steelwork Industry[11],[12] was carried out by Hatfield Polytechnic to review current practices and the validity of existing design methods in England. Two part questionnaires were sent to steelwork fabricators and consulting engineers. The first part was about industrial practice in the use of

various beam-to-column connection types, use of stiffeners, bolt types and sizes, preloading of bolts. It was also seeking the frequency of universal beam and column usage, weld sizes and plate thicknesses. Other questions were concerned with design practice and connection performance. The second part of the questionnaire was intended to obtain industry's response to certain proposals for standardization of end plate types of beam-to-column connections.

A collection of ten popular connections from pinned to rigid, as identified in the BCSA 'Manual on Connections' [13], was sent to industry (Figure 1.5). According to their stiffness these connections were classified into three groups namely, flexible, semi-rigid and rigid. The survey indicated that connection types 1, 6, 7 and 10 were being used frequently by 48%, 83%, 31% and 71% of the fabricators respectively, as shown in Figure 1.6. The popularity of the connection type 10 is due to its extensive use in portal frame construction. End plate connection 6, 7 and 10 can be prefabricated in shop which allows a higher standard of quality control. The replies clearly indicate the connection types for which standardization of detail is a worthwhile task. Conversely the connections with the need for on site welding were the most unpopular, with less than 10% of respondent claiming a frequent use. This highlights the preference of steel industry for in shop opposed to on site welding.

As to bolts, similar convergence occurs. The one overwhelmingly preferred is M20 grade 8.8 despite the popularity of M16 and M24 grade 8.8 bolts (Figures 1.7-1.10). The use of H.S.F.G bolts is quite low, except where there is a possibility of nut working loose with dynamic loading or rigidity is critical or slip is an important factor. This is due to the need for on site supervision and access for pretensioning which lead to higher labour cost. This has contributed to general limitation in the use of preloaded bolts. Another pattern of practice shows that the grade 4.6 bolts are mostly used in flexible connections with grade 8.8 being used in semi-rigid and rigid connections where bolt tension is a more important factor than

shear. A comparative study of grade 8.8 and H.S.F.G[14] bolts has shown that grade 8.8 bolts are not significantly weaker in tension than H.S.F.G. bolts provided that grade 10 nuts are used to avoid premature stripping of the thread in the nuts. However, the discussion on that paper indicated that such mixing of grades is not practical and controllable on site. Therefore grade 8.8 bolts can be replaced by general grade H.S.F.G. bolts, which have larger head and nut (equivalent to grade 10 nut) and used without preload to prevent stripping and provide economy.

A wide range of universal sections are still being used; however the trend is for shallower beam and column sections to be used. Grade 43 steel (Euro standard S275) is almost universally in use. 69% of universal beams used are between the range 203x133 UB and 475x191 UB and 81% of column sections used are between 152x152 UC and 305x305 UC. Although heavier column and beam sections have been considered more economical than introducing stiffeners, there was little support from the replies for the suggestion. This indicates a lack of understanding of the behaviour of the unstiffened column web/flange. When stiffeners are introduced, tension/compression stiffeners are popular and are limited to flush, extended end plate and fully rigid connections. Table 1.1 summarises the results of the survey.

The thickness of end plate seems to be related to moment-rotation capacity requirements of the connection and therefore, not specifically predictable, but there is a relationship between the thickness of the end plate and the size of the weld as expressed by the rule of thumb formula:

$$t_w = 2\sqrt{t_p}$$

where t_w is the weld size and t_p is the thickness of end plate.

Standardization of bolts can be divided into two groups, with M16 and M20 bolts for beams in one group while M20 and M24 bolts for beams in other group, with a variation in bolt pitch and horizontal spacing. Connection standardization is unlikely to result in saving in the amount of steel used, but even if there is a slight

increase this would be more than compensated for by saving in labour cost. Additional results collected by the Hatfield Survey are summarised in Tables 1.2-1.6.

1.2.2 A Survey of the Scottish Structural Steelwork Industry

A similar survey of Structural Steelwork Industry in Scotland was carried out by the then Dundee Institute of Technology in 1993. Similar questionnaires and the same collection of ten popular connections (Figure 1.5) were sent to industry.

The survey suggests that the most frequently used beam-to-column connection is the flush end plate (connection type 6); 91% of the replies claimed to use this connection "frequently". The summary of the usage of the connection types is shown in Table 1.7.

Column stiffeners are generally limited to connection types 6, 7, 8, 9 and 10. Tension/compression stiffeners are "frequently" used; diagonal stiffeners, column web reinforcing plates and flange backing plates are not "frequently" used (Table 1.8).

The results of the survey of bolt types is shown in Table 1.9. The survey has shown that the most frequently used bolt is the grade 8.8; over 60% claim usage on all the connection types. Only one or two replies claimed to use H.S.F.G. on connection type 7 and 10. The general range of bolt diameters used is 16 to 24 mm (Table 1.10) with bolts outside this range being used exceptionally. Over 50% of the respondents stated that the bolt diameters were confined to the 16 to 24 mm range, and 36% claimed to use bolt diameters in the 20 to 24 mm range.

Over half of the respondents claimed to punch less than 10% of holes. The remainder were in the over 70%, with only one respondent claiming to punch 10% to 20%, and one claiming to 20% to 30%. The results are set out in Table 1.11. Over 50% of respondents claimed they did not preload bolts at all and 84% claimed preloading was less than 10% of all bolts. The results are shown in Table 1.12.

One of the possible results of standardization of connection is that under certain circumstances holes would be provided where bolts are not needed. In

answer to the question 'in the interests of economy and standardisation, would you accept holes without bolts?', 64% of respondents said 'no' and 36% said 'yes'. One of the problems that might occur with unused holes is the problem of corrosion.

73% of the respondents claimed to use the BCSA 'Manual on Connections', and 27% claimed not to use the Manual.

Table 1.13 shows the frequency of UB/UC usage. 63% of the UB's are in the range 203x133 to 457x191 and 83% of UC's are in the range of 152x152 to 305x305. Table 1.14 shows the results of survey of weld sizes and plate thicknesses for end plate connections.

Generally speaking, the industry seems willing and indeed eager to accept the standardization of connections as long as such standardization entailed no more expenditure of time or effort than the present methods. There were, however, two areas where reluctance was shown. First, replies indicated an unwillingness to make use of heavier columns instead of using horizontal stiffeners in the column flange, despite the saving in manpower. Second, the suggestion that fabricated end plates should be provided with more holes than needed for a specific connection was rejected on ground of susceptibility to corrosion and adverse public reaction.

It seems that in view of the results of the questionnaire a standardized design should be sought. While complete mass production of end plate is not popular and there is marked opposition to unfilled holes and punched holes, consideration should be given to the use of standard universal flats rolled to width at the mill for end plates.

1.3 OBJECTIVES OF THE PROJECT

The main objectives of the investigation are as follows:

(a) Develop an analytical prediction model of the unstiffened flush end plate beam-to-column connection using the finite element technique to ascertain its behaviour.

(b) Predict connection behaviour in both elastic and plastic ranges.

(c) Carry out an in-depth investigation of this type of connection at both service and ultimate loads.

(d) Conduct full scale tests and compare the test results with those obtained using the finite element analysis.

(e) Identify the contribution of individual components to the overall performance of the connection.

(f) Compare the results of finite element analysis and full scale tests with the design rules of Eurocode 3.

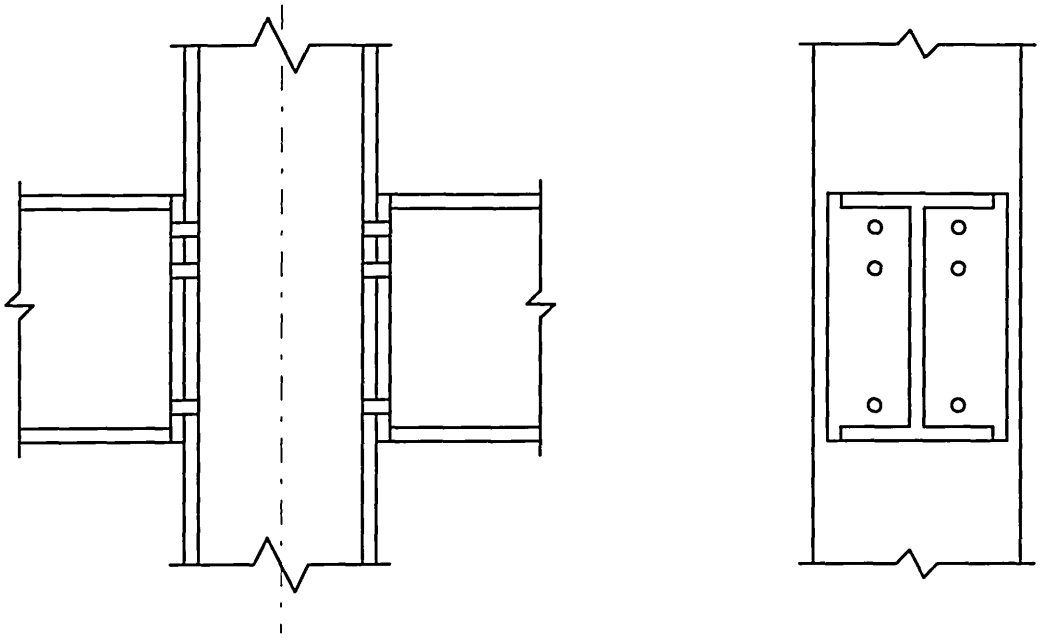

Fig.1.1 Flush end plate connection

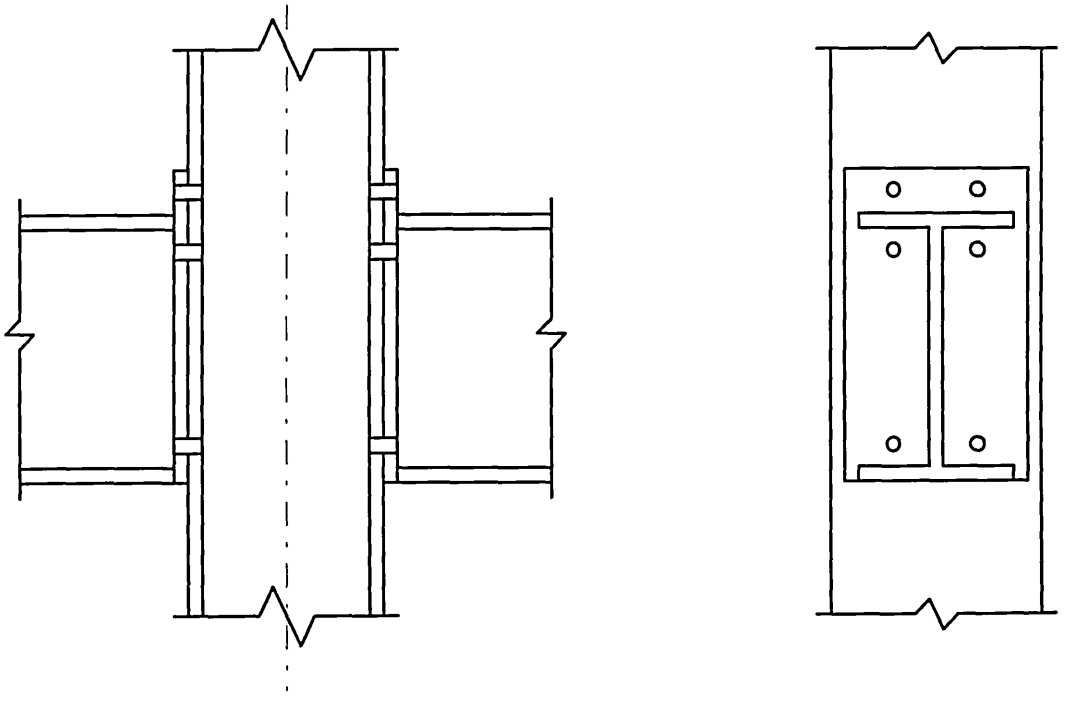

Fig.1.2 Extended end plate connection

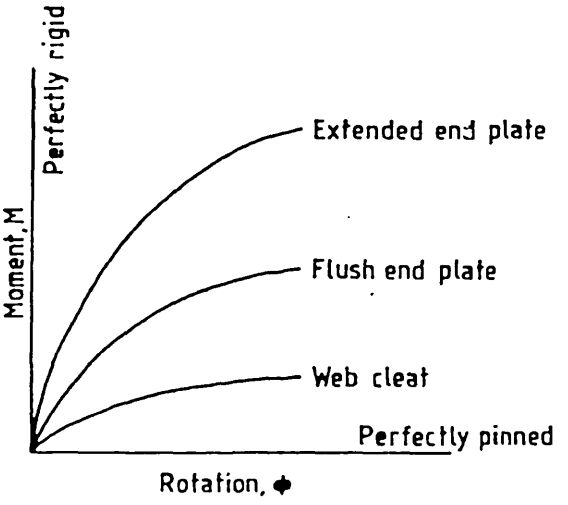

Fig.1.3 Moment-rotation (M-ϕ) relationships

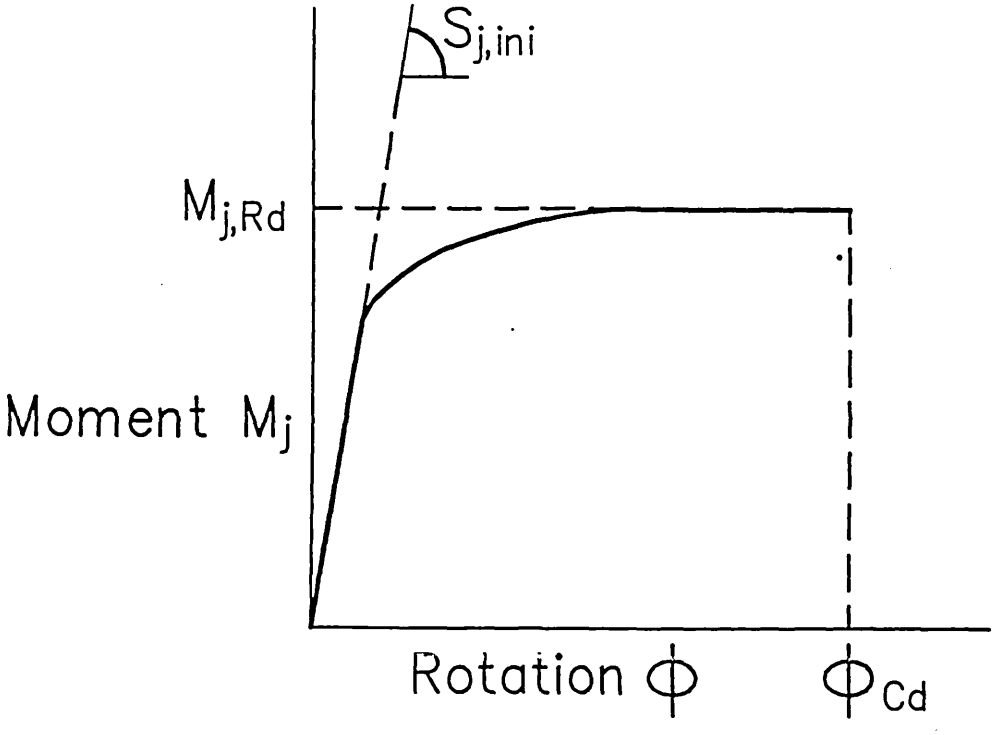

Fig.1.4 Moment-rotation (M-ϕ) characteristics of a connection

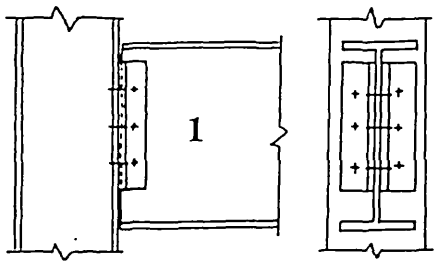

Web cleat

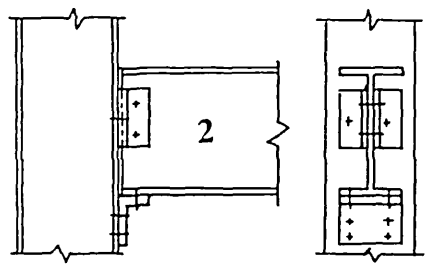

Bottom flange cleat with web cleat

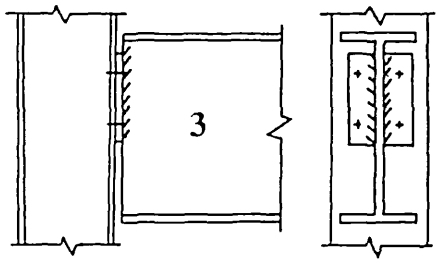

Flexible end plate

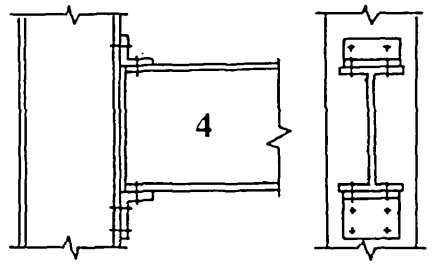

Flange cleat

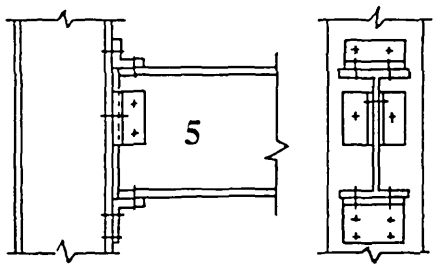

Web and flange cleat

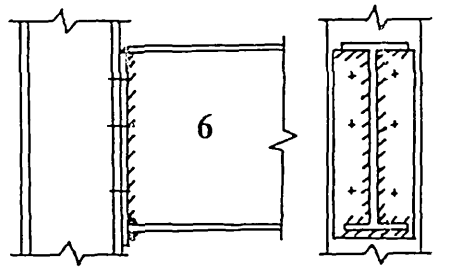

Flush end plate

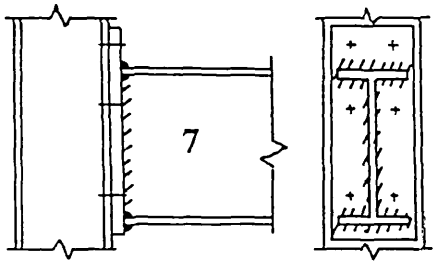

Extended end plate

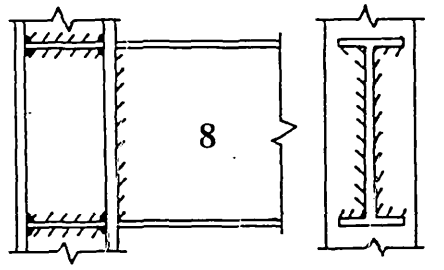

Directly welded with horizontal stiffeners

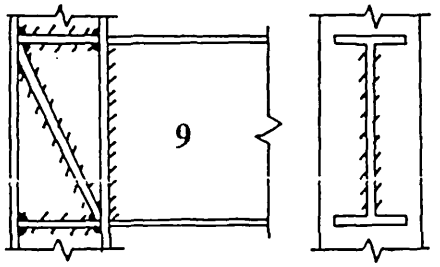

Directly welded with diagonal stiffeners

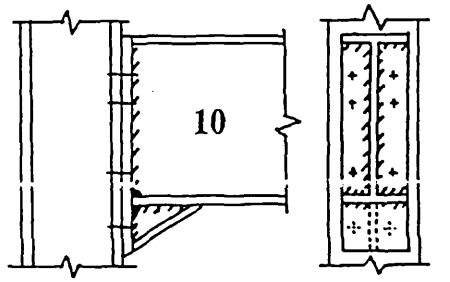

Extended end plate with haunch

Fig.1.5 Connection types

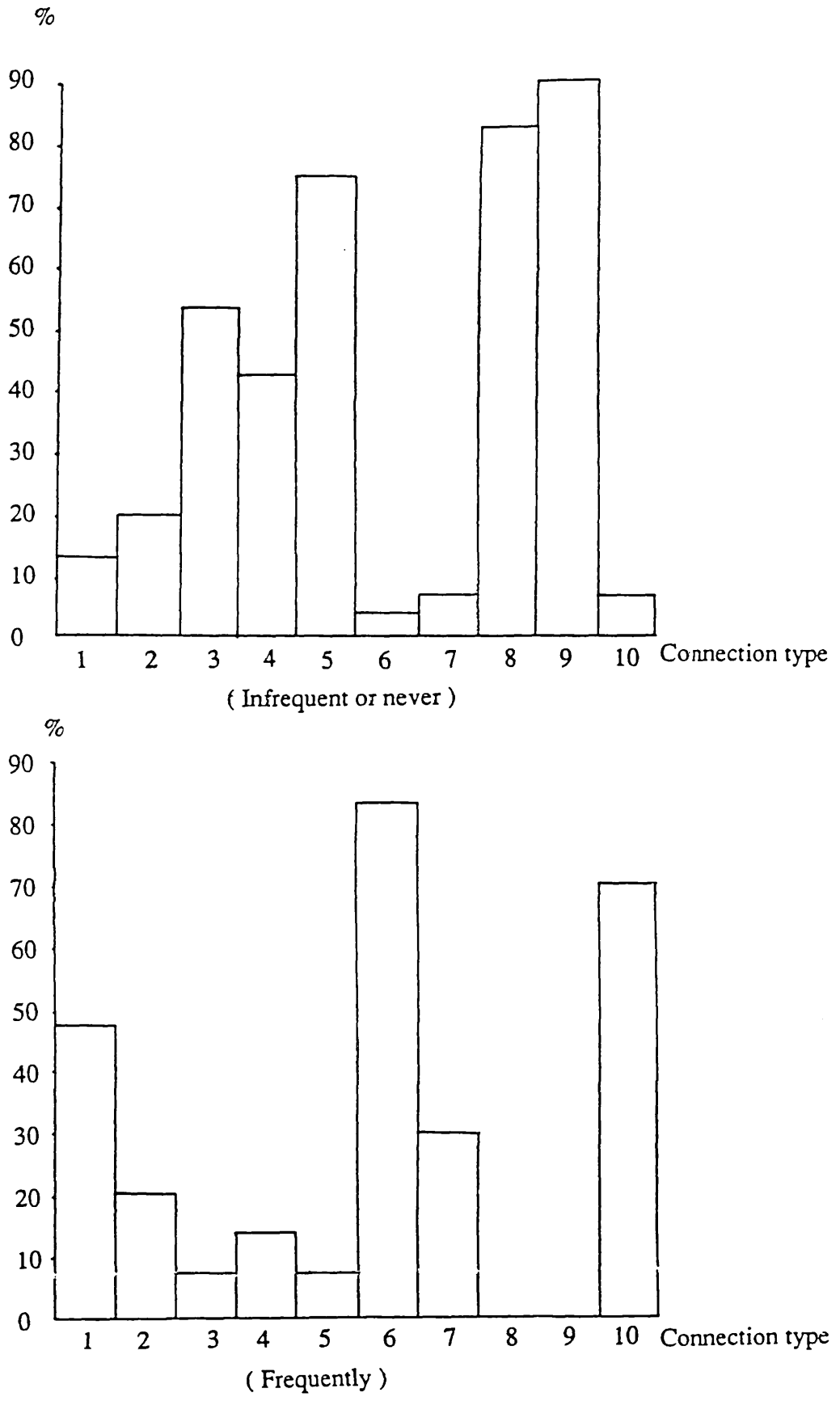

Fig.1.6 Usage of connection types

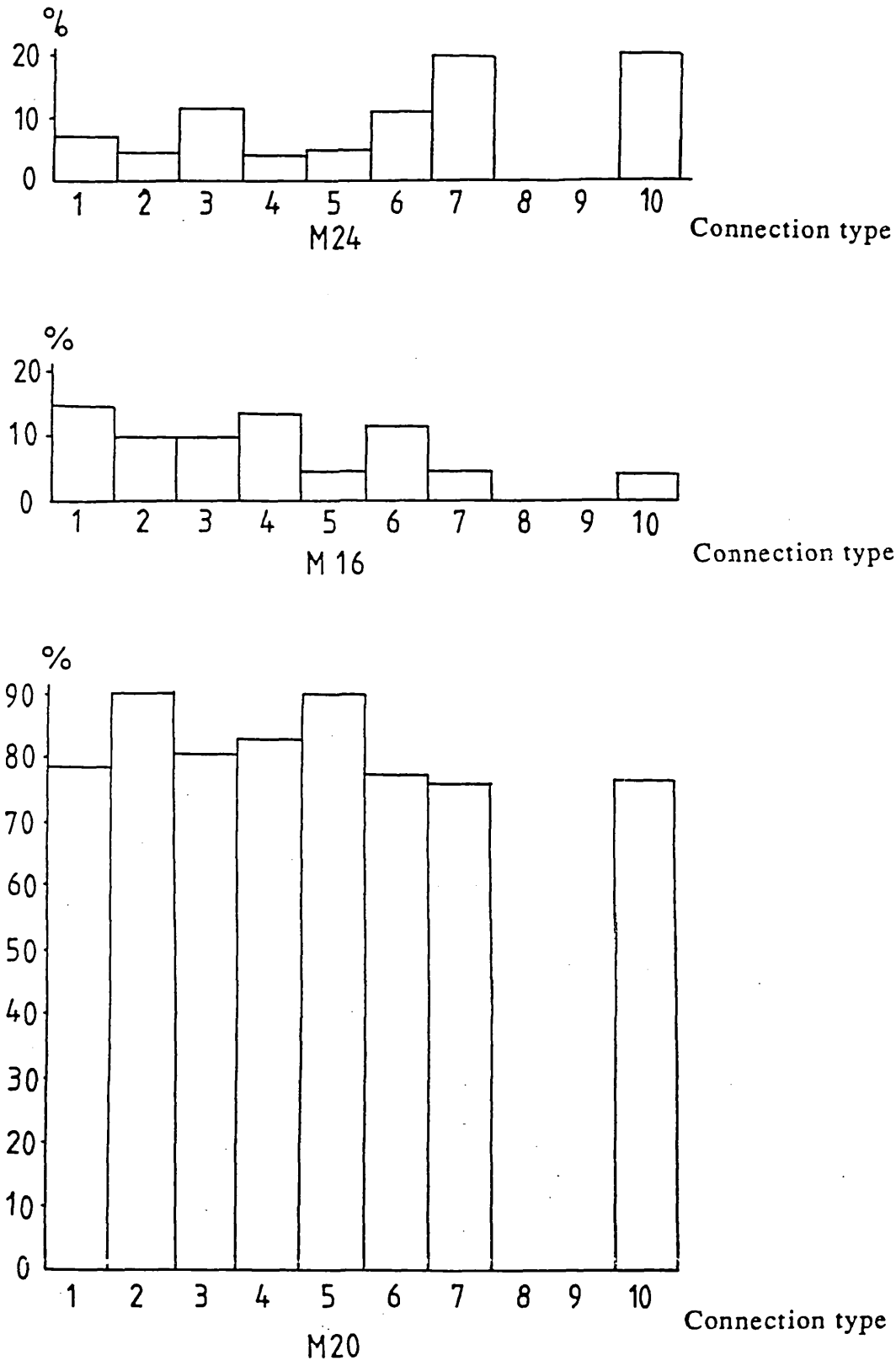

Fig.1.7 Most frequently used bolt diameter

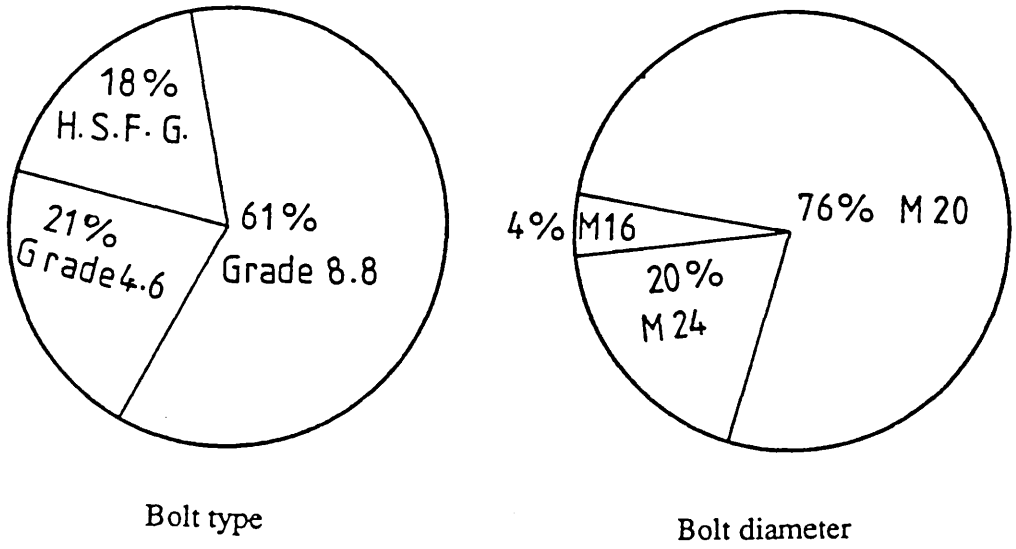

Fig.1.8 Frequently used bolt type and diameter for extended end plate connections

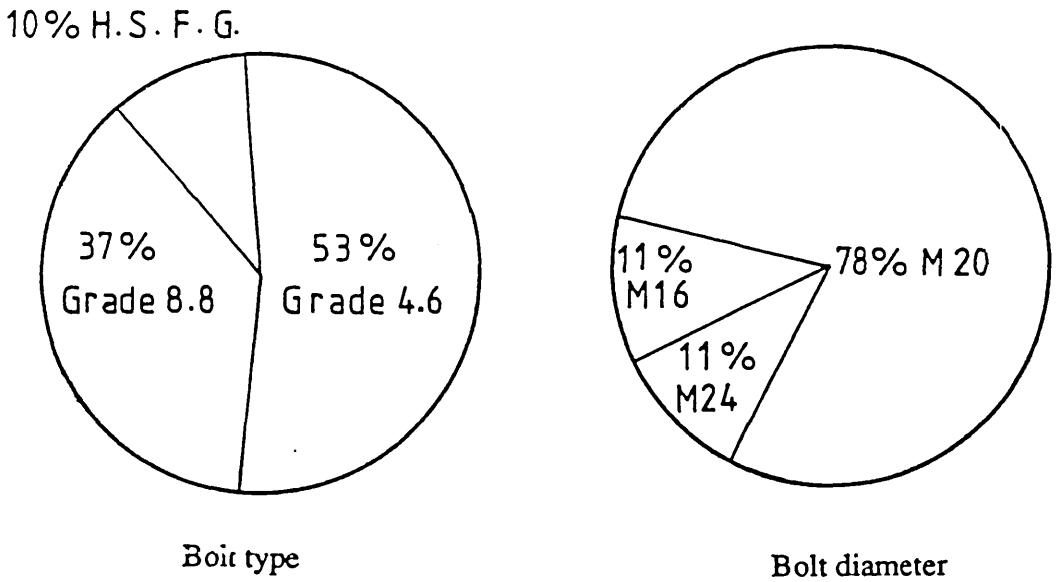

Fig.1.9 Frequently used bolt type and diameter for flush end plate connections

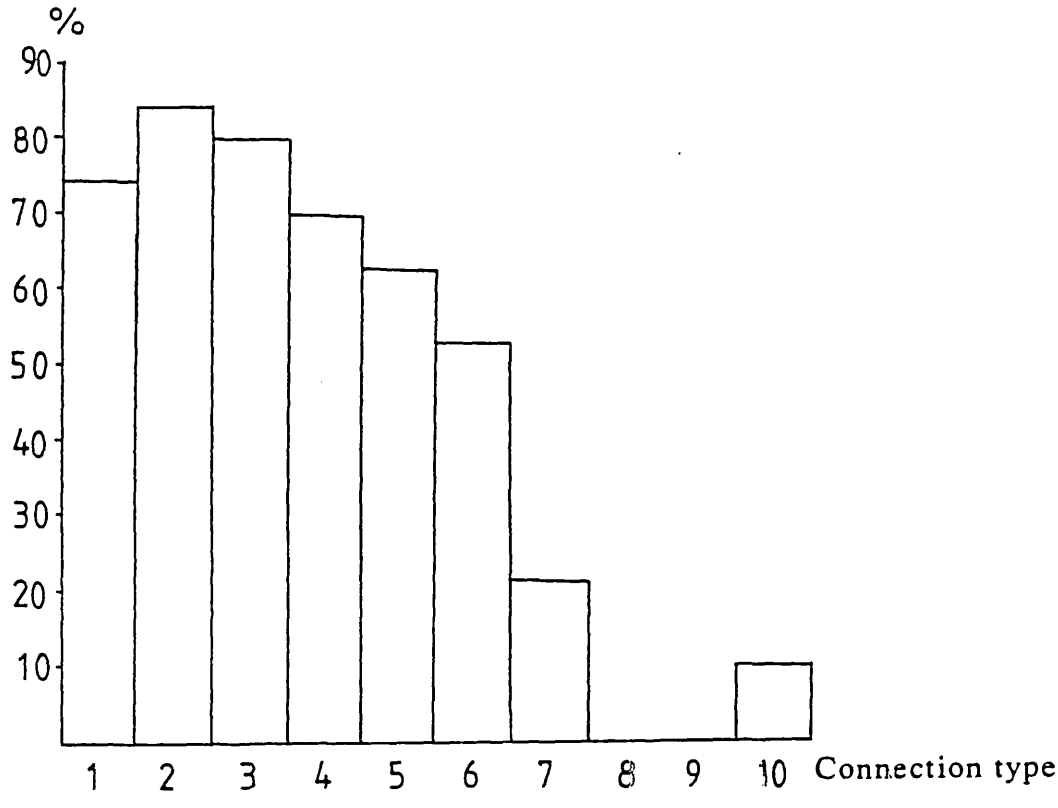

(Grade 4.6 bolt)

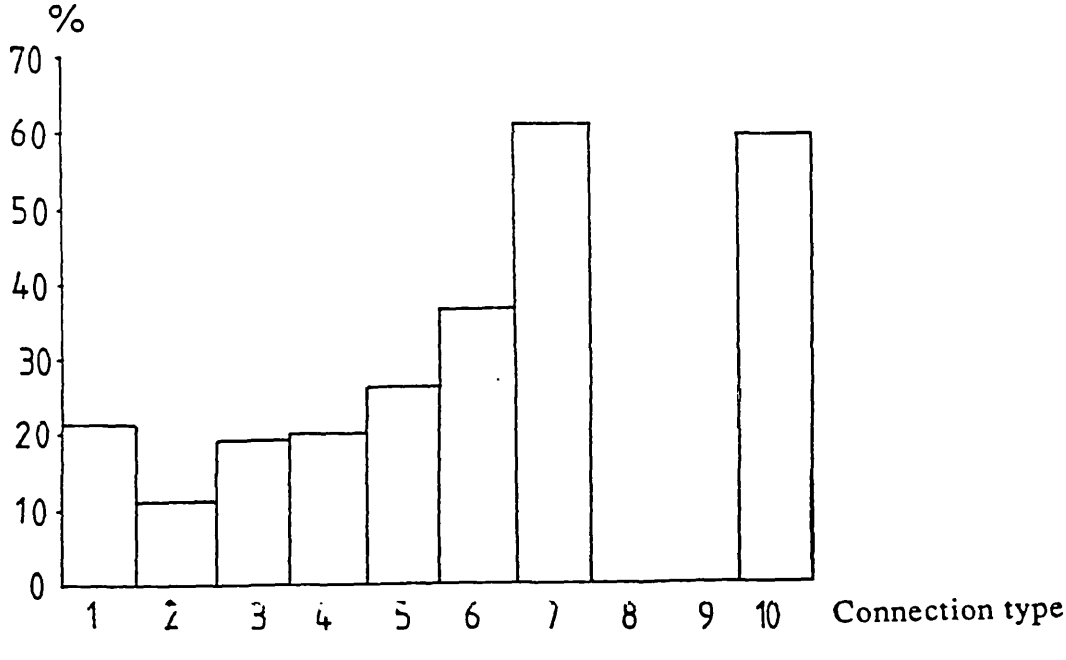

(Grade 8.8 bolt)

Fig.1.10 Most frequently used bolt in connections

	Connection type				
	6	7	8	9	10
Stiffeners in tension/ compression	31	54	40	23	66
Diagonal Stiffeners	3	6	6	10	10
Column web reinforcing plate	6	11	11	3	11
Flange backing plate	6	14	0	0	14

(Figures indicate % of respondents using stiffeners frequently)

Table 1.1 Use of column stiffeners

	% range of holes punched						
	0-10	10-20	20-30	30-40	40-50	50-60	60
(%) Respondents	48	8	19	8	7	7	3

Table 1.2 Use of punched holes

	% of bolt preloaded					Measuring method		
	0	4-5	6-10	11-15	>15	Torque Wrench	Part Turn	Load Indicating Washers
Respondents %	24	31	28	7	10	20	12	68

Table 1.3 Preloading of bolts

UB / UC	914X 419 to 762X267	686 X 254 to 533X 210	457X191 to 356X127	305X165 to 203X133	Total (UC)
356X406 to 356X368	5	7	3	4	19
305X 305 to 254X 254	4	11	20	8	43
203X203 to 152X152	0	4	13	21	38
Total (UB)	9	22	36	33	100

(Figures are percentages)

Table 1.4 Usage of UB and UC

t_p (mm) \ UB	914 X 419 to 762 X 267	686X 254 to 533X 210	457X191 to 357X127	305X165 to 203X133
40	59	47	37	37
40-30	68	74	52	52
30-20	79	85	76	70
20-10	70	95	100	95
<10	45	57	80	90

Table 1.5 Percentage of respondents using end plate

t_p (mm) \ UB	914X419 to 762X 267	686X 254 to 533X 210	457X191 to 357X127	305X165 to 203X133
40	12	12	10	10
40-30	10	10	10	8
30-20	8	10	8	8
20-10	8	8	6	6
<10	6	6	6	6

Table 1.6 Average weld size (mm) quoted by respondents

No.	Connection types	F (%)	S (%)	N (%)
1	Web cleats	25	67	8
2	Flange cleats	0	68	32
3	Web and flange cleats	0	51	49
4	Bottom flange cleat with web cleat	0	37	63
5	Flexible end plate	12	48	40
6	Flush end plate	91	9	0
7	Extended end plate	55	36	9
8	Directly welded with horizontal stiffeners	0	12	88
9	Directly welded with diagonal stiffeners	0	4	96
10	Extended end plate with haunch	67	33	0

F = "frequently"; S = "sometimes"; N = "infrequently or never".

Table 1.7 Usage of connection types (Scotland)

Column stiffener	Connection type				
	6	7	8	9	10
Stiffeners in tension/compression	63	71	21	21	92
Diagonal stiffeners	12	16	4	4	28
Column web reinforcing plate	9	21	4	4	25
Flange backing plate	12	21	0	0	25

Figures indicate % of respondents using stiffeners "frequently".

Table 1.8 Use of column stiffeners (Scotland)

Bolt types		Connection type							
		1	2	3	4	5	6	7	10
Most frequently used bolt (%)	4.6	34	37	37	20	16	13	9	0
	8.8	71	68	68	71	80	88	88	92
	H.S.F.G	0	0	0	0	0	0	9	13

Table 1.9 Use of bolt types (Scotland)

Bolt diameters		Connection type							
		1	2	3	4	5	6	7	10
Most frequently used bolt diameters (%)	M16	33	33	29	33	25	0	0	5
	M20	68	64	71	59	71	100	100	79
	M24	0	4	0	0	0	0	0	17

Table 1.10 Use of bolt diameters (Scotland)

	% range of holes punched							
	0-10	10-20	20-30	30-40	40-50	50-60	60-70	> 70
Respondents (%)	53	9	9	0	0	0	0	29

Table 1.11 Use of punched holes (Scotland)

	% of bolts preloaded				
	0	1-5	5-10	10-20	> 20
Respondents (%)	58	17	9	4	9

Table 1.12 Preloading of bolts (Scotland)

UB / UC	914 x 419 to 762 x 267	686 x 254 to 533 x 210	457 x 191 to 356 x 127	305 x 165 to 203 x 133	Total UC
356 x 406 to 356 x 368	4	5	4	4	17
305 x 305 to 254 x 254	6	4	23	13	46
203 x 203 to 152 x 152	6	12	13	6	37
Total UB	16	21	40	23	100

All figures in percentages.

Table 1.13 Usage of UB/UC (Scotland)

End plate thickness (mm) / UB	914 x 419 to 762 x 267		686 x 254 to 533 x 210		457 x 191 to 356 x 127		305 x 165 to 203 x 133	
	a	b	a	b	a	b	a	b
> 40	18	13	18	11	18	9	18	9
40 - 30	45	12	36	11	36	10	27	7
30 - 20	64	10	73	8	73	8	64	7
20 - 10	64	8	64	8	64	7	73	6
< 10	55	6	55	6	55	6	55	6

a = % respondents using end plate thickness quoted;
b = average weld size quoted by respondents (leg length mm).

Table 1.14 End plate thickness and weld size (Scotland)

CHAPTER 2

REVIEW OF PREVIOUS RESEARCH WORK

2.1 EXPERIMENTAL STUDY AND RESEARCH BASED ON YIELD LINE METHOD

Investigation into semi-rigid connections started at the beginning of this century. In 1917, Wilson and Moore[15] carried out an experimental investigation with the aim of determining the rigidity of riveted joints in steel structures and highlighted the significance of end restraint provided by semi-rigid connections. In the 1930's Batho[16], and Young[17] established the relationship between the moment transmitted and the relative change of angle between the beam and the column in an attempt to provide data for semi-rigid design of connections. Batho proposed a graphical method for predicting the end restraint provided by a connection for which experimentally derived moment-rotation relationship was known. Such proposals were based on extensive experimental programmes. During the 1940's Hetchman and Johnson[18] conducted a large experimental programme comprising 47 riveted tests. The result of all this work led to the prediction of 15%-20% economies in semi-rigid design compared with pinned connections.

During the first half of this century the only way to find out joint behaviour was by conducting large number of tests and this was mainly confined to riveted connections. With the marketing of high strength steel bolts, riveted connections are now seldom used in structural steelwork. Since the 1950's, an increased number of countries have become involved in research into the behaviour of connections. In the past M-ϕ relationships for certain types of connections were established by physical tests of actual connections. As tests are time consuming and expensive and as these can be prohibitive to cover all possible connection details, it is necessary to develop a theoretical approach for predicting the connection behaviour.

The 'prying force' concept which forms the basis for the present T-stub and end plate design formulae was originally suggested by Schutz[19] in 1959. When a tensile load was applied to a T-stub, prying forces developed due to flexure of the flange of the T-stub. His design rules for determining the flange thickness and bolt size were based on experimental data. Prying forces were assumed to act at the extreme edge of the flange of the T-stub.

In 1965, Douty and McGuire[20] refined Schuz's method and developed semi-empirical equations for the prediction of the prying force in terms of the dimensions of the T-stub. A limited test programme involving beam-to-column end plate connections was included in their study. They concluded that the prying force increased with increasing bolt stiffness and local compressive stiffness of the T-stub flange, and decreased with the increasing distance of bolt to flange edge. In 1974, similar work was done by Nair, Birkemore and Munse[21] on the behaviour of high strength bolts in T-stub connections in both the elastic and inelastic ranges. They developed an alternative formula to Douty and McGuire's which was simpler and which showed that prying action could significantly reduce the ultimate load and fatigue strength of the bolted connections.

More recently, Agerskov[22],[23] presented another version of the prying theory. Three force distribution patterns were considered for establishing the failure mechanism in the T-stub flange. The case of no separation at the bolts, and the case of complete separation (no prying) were considered in addition to the force pattern that assumed separation at the bolts and prying at the edge of the T-stub flange. A new prying force formula was proposed in T-stub and end plate connections.

Sherbourne[24], Zoetemeijer[25] and Packer and Morris[26] published work on column flange behaviour for end plate connections. Sherbourne investigated the characteristics of the end plate connections with particular reference to the detailing of the end plate and the column stiffening. He carried out a series of tests on beam-to-column end plate connections. In the tests, the emphasis was on determining the

overall behaviour of the connection, while no attempt was made to determine the forces in the bolts. His tests focused on the ability of columns, with or without stiffeners, to develop the full plastic moment of the connection component. It was concluded that a nominal amount of stiffening was required for columns with thin flanges.

Zoetemeijer's work was based on the ultimate load approach employing 'yield line' theory. The 'equivalent length' of yield line was expressed in terms of the geometrical and physical properties of the connected parts for the two possible yield line patterns. The pattern that gives the lowest moment capacity is the failure pattern. The T-stub analysis procedure was then extended to end plate connections. The design method was based on plastic behaviour of the T-stub flange and the bolts. Formulae were given to compute the design load of a connection based on two possible failure modes - bolt fracture and flange failure. The effect of prying force was not considered in the method. His formulae could not provide any information about deformation and stress distribution when the material was in the elastic and plastic ranges, because the method was strictly an ultimate load approach.

Packer and Morris also applied 'yield line' theory to predict the moment capacity of end plate connections, but their effort was focused on the failure of the column flange. They suggested that the bolt load should be increased by 33% to account for prying, but no method was developed to determine the prying forces. They studied the behaviour of column flange which were less stiff than the end plate. It was suggested that in such a situation the extended end plate can be modelled as a T-stub. This model assumes that double curvature had developed, with yield lines forming at the bolt lines and at the plate-flange junction.

In the tests on beam-to-column connections reported by Surtees and Mann[27] the end plate and column flange were of similar thickness and the behaviour of the extended end plate, rather than the T-stub model, was examined. In

developing the proposed formula for end plate thickness, these authors included the restraint offered to the end plate by the beam web, assuming that the pattern of yield lines extended down to approximately half the depth of the beam. Though their experimental results did not verify the assumed yield line pattern, the results nevertheless validated their estimation of the end plate thickness.

In 1981, an International Conference on "Joints in Structural Steelwork" was held at Teesside Polytechnic, Middlesborough[28]. In a paper presented at the Conference Maxwell et al[10] explained how the experimental data could be transferred into design charts, based on a method developed some 50 years ago by Professor Batho. Attention was mainly focused on angle cleat connections.

Zoetermeijer[29] used the same procedure as above to develop a design chart based on collapse mechanisms, which could be used to design a flush end plate connection with stiffened column flanges. Prying force was not included in the analysis but he predicted that the prying action would not be larger than 30% of the bolt force.

Phillips and Packer[30] conducted a series of tests to investigate the effect of plate thickness on flush end plate connections. The results indicated that flush end plate connections with two tension bolt rows were suitable for semi-rigid construction.

Aggarwal[31] conducted eight tests to investigate flexible beam-to-column end plate connections. These joints were tested under gradually increasing static loads with 16 mm, 20 mm and 24 mm diameter bolts and 12 mm and 16 mm thick end plates for a constant beam and column cross-sections. He concluded that the rotation of the connections resulted from yielding of the flexible end plate and deformation in the column flange around the bolt holes.

Bose[32],[33] carried out twelve full scale tests of standard ductile connections which were developed at the Steel Construction Institute. These tests were conducted with various beam depths and connection details. Moment-rotation

curves, moment and rotation capacities and failure modes of each of the connections tested were ascertained. It was concluded that the standard connections which were tested to failure exhibit adequate rotation capacities to ensure that they act as plastic hinges in plastically designed semi-continuous frames. The moment-rotation curves provided reliable means of computing the rotational stiffness of the connections.

Bose and Hughes[6] used the tests data mentioned above to verify the performance of standard ductile connections for semi-continuous steel frames. They concluded that the SCI's standard ductile connections exhibit well-balanced performance for beam depths up to 700 mm. Satisfactory ductility is achieved without undue sacrifice of strength or stiffness. Above 700 mm beam depth ductility deteriorates and the standard detail may require modification. They suggested that further work would be needed to confirm whether and how this should be done.

Bose, Youngson and Wang (the author)[7] have made an appraisal of the design rules in Eurocode 3 for bolted end plate joints by comparison with experimental results. They found that unstiffened bolted end plate joints fail very frequently due to column web buckling. Unfortunately, Annex J of Eurocode 3 considers only crushing resistance of column web for evaluating the moment resistance of joints. It was also observed that Annex J greatly underestimates the moment resistance of many joints and predicts the failure type incorrectly. Large discrepancies between test and Eurocode 3 predicted values of rotational stiffness were detected. Many joints which did not meet the requirements of Annex J for sufficient rotation capacity, achieved rotation which may be deemed as adequate for plastic design.

2.2 RESEARCH BASED ON FINITE ELEMENT METHOD

It is common knowledge that 'yield line' method can only predict the ultimate strength of the connection and can not provide any information regarding the deformation occurring in the connection when it is subjected to service loads. Also it can not predict the degree of stiffness provided by the connection. A satisfactory

method of the design and analysis of a connection must include the performance at both service and ultimate loads.

With the appearance of high speed computers and a number of sophisticated finite element software, it is possible to carry out a thorough investigation into the behaviour of beam-to-column end plate connections by the finite element technique.

The finite element method was first employed by Krishnamurthy[34],[35],[36],[37],[38] for the analysis of end plate connection. He carried out 2 and 3 dimensional elastic analyses of the end plate connections. An iterative procedure was adopted to determine the location of contact points between the end plate and the column flange support. However, neither did he propose a method for the calculation of prying forces nor did he acknowledge their effect on bolt forces.

Tarpy and Cardinal[39] carried out a study of the behaviour of unstiffened beam-to-column end plate connections. Equations were produced which predicted the behaviour of the connection by using linear finite element method. By introducing joint elements in the model the interaction between end plate and column flange was taken into account. The investigation was limited to elastic analysis and no attempt was made to extend it to the inelastic range. A design method was proposed on the basis of elastic finite element analysis and experimental verification. Connection performance at the plastic range and ultimate load were not included in the study. Furthermore, they did not suggest a method to determine bolt forces.

Maxwell, Jenkins, and Howlett[40] studied the behaviour of extended end plate and cleated connections using an elastic-plastic layered finite element model. Some limited experimental testing and theoretical studies on the end plate connection were reported. The importance of moment rotation characteristic of the connections was stressed. Previous work, using the finite element method, was based on the classic 'Kirchhoff thin plate' theory in which shear deformations were neglected. In most connections the relative dimensions of the joint components make

it a 'thick' plate problem. It was pointed out that the effect of shear deformation should be included in the investigation on end plate connections.

Patel and Chen[41],[42] adopted a simple equivalent bar system, when simulating the response of a fully bolted moment connection. Plane stress, isoparametric elements were used for modelling the beam, column and connection plates, while three bar elements were used to simulate the pretension and shear carrying behaviour of the bolts. A linear stress-strain relationship was assumed for the bars, whose parameters were derived from experimental results. The possibility of slip was not taken into account in the proposed system. This factor was suggested as the main reason for the discrepancies observed between the numerical results and test data in the inelastic range.

Jenkins, Tong and Prescott[43],[44] developed two-dimensional finite element model and suggested a design method for stiffened beam-to-column connections. Moment-rotation curves were obtained by combining the separate analysis of end plate and column flange. The first analysis was based on the assumption that the rotation is principally due to deformation of end plate with no contribution from the flange, and the second analysis considered the column flange only with no deformation in the end plate. The theoretical modelling of column flange was simplified considerably by using column flange stiffeners in the tension and compression region. In order to account for the contribution of bolt stretching to connection rotation, the actual force-extension relationship of the bolts was used. Interactive forces generated between the end plate and column flange, which plays an important role in the connection, were neglected in their model. Standard details for both flush and extended end plate connections were proposed for a limited range of UB sections and a sample of only two UC sections, but their attention was mainly concentrated on flush end plates with at least four tension bolts. Extended end plate connections were considered only in passing and information regarding their structural behaviour was not reported. Their design method was based on the finite

element model and standard details they proposed. The method has not found favour with the construction industry.

Gendron, Beaulieu and Dhatt[45] proposed a 2-dimensional finite element model which takes account of plasticity for predicting the behaviour of bolted connections. A method similar to the one used by Patel and Chen was used to simulate the bolt behaviour. A contact element was added to model the shear behaviour of the bolt and account for the existing gap between the shank of the bolt and the edge of the hole. Four of these bolts were placed in each beam flange at actual bolt locations. As the entire connection assembly was modelled in two dimensions, the shear plate bolted to the beam web was generally allowed to overlap in the same plane while having different elements and different nodes. Only at the bolt positions they had common nodes. A load-deflection curve and a series of stress distribution graphs were produced, which did not reflect accurately the behaviour of finite element model. This model does not consider the effect of prying on the bolt behaviour.

A three-dimensional finite element model of unstiffened extended end plate beam-to-column connections was developed by Bose, Sarkar and Bahrami[46],[47]. In addition to the solid and bar elements used to discretize the plates and bolts respectively, non-linear joint elements were employed to model the interactive forces induced between the end plate and column flange. The properties of the joint elements were chosen to ensure displacement compatibility at nodes where end plate and column flange were in contact but allowed separation at other nodes. A three dimensional elastic-plastic analysis of the connection was carried out with the aim of predicting the ultimate moment capacity and moment-rotational characteristics of the connection over the entire loading range until collapse occurred. Twelve full scale tests involving three column-beam sets, and four end plate thicknesses for each of the three column-beam sets, were conducted and the results were analysed. Comparison was made between the results obtained by the finite element analysis

and the experimental investigation. A parametric study was also carried out for the purpose of the separating the contribution of the end plate, column and bolt towards the stiffness of the connection. They made significant contribution in finite element modelling of the complex beam-to-column extended end plate connections. But their model did not include bolt holes which could influence the deformation of end plate and the rotational behaviour of the whole connection.

Sherbourne and Bahaari[48] simulated a three-dimensional model for stiffened extended end plate connection. They used plastic quadrilateral shell elements to model beam web/flange, end plate, column web/flange, and stiffeners. Such shell elements are generally suitable for modelling 'thin plate' problems. If a heavier column section is used to avoid stiffening or thick end plate is used, prediction of the connection behaviour will not be accurate at the ultimate load range.

Having completed the literature survey the author came to the conclusion that there remained a gap in the investigation into the behaviour of unstiffened flush end plate connections. In response to this finding the author has created a three dimensional finite element model for unstiffened flush end plate connection which has not been attempted so far. He has used isoparametric solid elements with 16 nodes for plates, which is able to tackle 'thick plate' problems. He has also used eight bar elements to represent a bolt which has been modelled to coincide with the corresponding nodes of plate element on the boundary of the bolt hole. These features are considered to be original innovations in the application of the finite element model.

CHAPTER 3

FINITE ELEMENT METHOD

3.1 INTRODUCTION

The finite element method is now widely recognised as the most powerful technique for solving a large variety of engineering problems. Applications range from the stress analysis of solids to the solution of acoustical, neutron physics and fluid dynamics problems. Indeed the finite element method is now firmly established as a general numerical method for the solution of partial differential equation systems, subject to known boundary and/or initial conditions.

For linear analysis, the technique is widely employed as a design tool. Similar acceptance for non-linear situation is dependent on two major factors. Firstly, in view of the increased numerical operations associated with non-linear problems, considerable computing power is required. Developments in the last decade or so have ensured that high-speed computers which meet this need are now available and present indications are that reductions in unit computing costs will continue. Secondly, before the finite element method can be used in design, the accuracy of any proposed solution technique must be proven. The development of improved element characteristics and more efficient non-linear solution algorithms and the experience gained in their application to engineering problems have ensured that non-linear finite element analyses can now be performed with confidence. Hence barriers to the common use of non-linear finite element techniques have been removed and the process is already economically acceptable for industrial applications.

There are many excellent texts on Finite Element Method and the theory described in this chapter are extracted from references 9, 49, 50, 51, 52 and 53.

Although a tetrahedron element, having four corner nodes with three degrees of freedom per node, is used as a basic element to solve three-dimensional problems, a hexahedron element having eight corner nodes with three degrees of freedom per node is widely used to model three-dimensional structural components. On the basis of shape function of a hexahedron element having eight corner nodes, shape function of a more accurate and efficient hexahedron element having sixteen or twenty nodes can be developed. The shape function of bar element and joint element can also be derived.

3.2 HEXAHEDRON ELEMENT

3.2.1 Natural Coordinate System

As shown in Figure 3.1(a), the natural coordinates are *r*, *s* and *t* with the origin of the system taken at the centroid of the element. It can be seen that each of the coordinate axes *r*, *s* and *t* is associated with a pair of opposite faces, which are given by the coordinate value ± 1. Thus in the local (natural) coordinates, the element is a cube as shown in Figure 3.1(b) although in the global cartesian coordinate system it may be an arbitrarily warped and distorted six-sided solid as shown in Figure 3.1(a). The relationship between the local and global coordinates can be expressed as

$$\begin{Bmatrix} x \\ y \\ z \end{Bmatrix} = [N] \begin{Bmatrix} x_1 \\ y_1 \\ z_1 \\ x_2 \\ \vdots \\ z_8 \end{Bmatrix} \qquad (3.1)$$

where

$$[N] = \begin{bmatrix} N_1 & 0 & 0 & N_2 & \cdots & 0 \\ 0 & N_1 & 0 & 0 & \cdots & 0 \\ 0 & 0 & N_1 & 0 & 0 & N_8 \end{bmatrix}$$

and

$$N_i\,(r,s,t) = \frac{1}{8}(1+rr_i)(1+ss_i)(1+tt_i)\;;\; i = 1\,,\,2\,,\,\ldots\,,\,8 \qquad (3.2)$$

or

$$\begin{Bmatrix} x \\ y \\ z \end{Bmatrix} = \begin{Bmatrix} \sum_{i=1}^{8} N_i x_i \\ \sum_{i=1}^{8} N_i y_i \\ \sum_{i=1}^{8} N_i z_i \end{Bmatrix} \qquad (3.3)$$

3.2.2 Displacement Model

By assuming the variations of the displacement between the nodes to be linear, the displacements can be expressed by the same interpolation functions used to describe the geometry as (analogous to Equation (3.1))

$$\begin{Bmatrix} \mu \\ \upsilon \\ \omega \end{Bmatrix} = [N] \begin{Bmatrix} \mu_1 \\ \upsilon_1 \\ \omega_1 \\ \mu_2 \\ \vdots \\ \omega_8 \end{Bmatrix} = [N]\, \vec{Q}^{(e)} \qquad (3.4)$$

where $\vec{Q}^{(e)}$ is the vector of nodal displacement degrees of freedom and (μ_i , υ_i , ω_i) denote the displacements of node i, i = 1 to 8.

3.2.3 Strain-Displacement Relations

Using Equation (3.4) the three-dimensional strain-displacement relations can be expressed as

$$\vec{\varepsilon} = \begin{Bmatrix} \varepsilon_{xx} \\ \varepsilon_{yy} \\ \varepsilon_{zz} \\ \varepsilon_{xy} \\ \varepsilon_{yz} \\ \varepsilon_{zx} \end{Bmatrix} = \begin{Bmatrix} \frac{\partial \mu}{\partial x} \\ \frac{\partial \upsilon}{\partial y} \\ \frac{\partial \omega}{\partial z} \\ \frac{\partial \mu}{\partial y} + \frac{\partial \upsilon}{\partial x} \\ \frac{\partial \upsilon}{\partial z} + \frac{\partial \omega}{\partial y} \\ \frac{\partial \omega}{\partial x} + \frac{\partial \mu}{\partial z} \end{Bmatrix} = \underset{6\times24}{[B]} \underset{24\times1}{\vec{Q}^{(e)}} \qquad (3.5)$$

where

$$\underset{6\times24}{[B]} = [[B_1] \quad [B_2] \quad \cdots \quad [B_8]] \qquad (3.6)$$

and

$$\underset{6\times3}{[B_i]} = \begin{bmatrix} \frac{\partial N_i}{\partial x} & 0 & 0 \\ 0 & \frac{\partial N_i}{\partial y} & 0 \\ 0 & 0 & \frac{\partial N_i}{\partial z} \\ \frac{\partial N_i}{\partial y} & \frac{\partial N_i}{\partial x} & 0 \\ 0 & \frac{\partial N_i}{\partial z} & \frac{\partial N_i}{\partial y} \\ \frac{\partial N_i}{\partial z} & 0 & \frac{\partial N_i}{\partial x} \end{bmatrix}, \quad i = 1 \text{ to } 8 \qquad (3.7)$$

The derivatives in the matrix $[B_i]$ may be evaluated by applying the chain rule of differentiation as follows :

$$\begin{Bmatrix} \frac{\partial N_i}{\partial r} \\ \frac{\partial N_i}{\partial s} \\ \frac{\partial N_i}{\partial t} \end{Bmatrix} = \begin{Bmatrix} \frac{\partial N_i}{\partial x}\cdot\frac{\partial x}{\partial r} + \frac{\partial N_i}{\partial y}\cdot\frac{\partial y}{\partial r} + \frac{\partial N_i}{\partial z}\cdot\frac{\partial z}{\partial r} \\ \frac{\partial N_i}{\partial x}\cdot\frac{\partial x}{\partial s} + \frac{\partial N_i}{\partial y}\cdot\frac{\partial y}{\partial s} + \frac{\partial N_i}{\partial z}\cdot\frac{\partial z}{\partial s} \\ \frac{\partial N_i}{\partial x}\cdot\frac{\partial x}{\partial t} + \frac{\partial N_i}{\partial y}\cdot\frac{\partial y}{\partial t} + \frac{\partial N_i}{\partial z}\cdot\frac{\partial z}{\partial t} \end{Bmatrix}$$

$$= \begin{bmatrix} \frac{\partial x}{\partial r} & \frac{\partial y}{\partial r} & \frac{\partial z}{\partial r} \\ \frac{\partial x}{\partial s} & \frac{\partial y}{\partial s} & \frac{\partial z}{\partial s} \\ \frac{\partial x}{\partial t} & \frac{\partial y}{\partial t} & \frac{\partial z}{\partial t} \end{bmatrix} \begin{Bmatrix} \frac{\partial N_i}{\partial x} \\ \frac{\partial N_i}{\partial y} \\ \frac{\partial N_i}{\partial z} \end{Bmatrix} = [J] \begin{Bmatrix} \frac{\partial N_i}{\partial x} \\ \frac{\partial N_i}{\partial y} \\ \frac{\partial N_i}{\partial z} \end{Bmatrix} \qquad (3.8)$$

Where $[J]$ is the Jacobian matrix which can be expressed, using Equation (3.3), as

$$\underset{3\times3}{[J]} = \begin{bmatrix} \frac{\partial x}{\partial r} & \frac{\partial y}{\partial r} & \frac{\partial z}{\partial r} \\ \frac{\partial x}{\partial s} & \frac{\partial y}{\partial s} & \frac{\partial z}{\partial s} \\ \frac{\partial x}{\partial t} & \frac{\partial y}{\partial t} & \frac{\partial z}{\partial t} \end{bmatrix}$$

$$= \begin{bmatrix} \sum_{i=1}^{8}(\frac{\partial N_i}{\partial r}x_i) & \sum_{i=1}^{8}(\frac{\partial N_i}{\partial r}y_i) & \sum_{i=1}^{8}(\frac{\partial N_i}{\partial r}z_i) \\ \sum_{i=1}^{8}(\frac{\partial N_i}{\partial s}x_i) & \sum_{i=1}^{8}(\frac{\partial N_i}{\partial s}y_i) & \sum_{i=1}^{8}(\frac{\partial N_i}{\partial s}z_i) \\ \sum_{i=1}^{8}(\frac{\partial N_i}{\partial t}x_i) & \sum_{i=1}^{8}(\frac{\partial N_i}{\partial t}y_i) & \sum_{i=1}^{8}(\frac{\partial N_i}{\partial t}z_i) \end{bmatrix} \qquad (3.9)$$

The derivatives of the interpolation functions can be obtained from Equation (3.2) as

$$\left.\begin{aligned} \frac{\partial N_i}{\partial r} &= \tfrac{1}{8}r_i(1+ss_i)(1+tt_i) \\ \frac{\partial N_i}{\partial s} &= \tfrac{1}{8}s_i(1+rr_i)(1+tt_i) \\ \frac{\partial N_i}{\partial t} &= \tfrac{1}{8}t_i(1+rr_i)(1+ss_i) \end{aligned}\right\} \quad , \; i = 1 \text{ to } 8 \qquad (3.10)$$

and the coordinates of the nodes in the local system (r_i, s_i, t_i) are given by

$$\begin{Bmatrix} r_1 \\ r_2 \\ r_3 \\ r_4 \\ r_5 \\ r_6 \\ r_7 \\ r_8 \end{Bmatrix} = \begin{Bmatrix} -1 \\ 1 \\ 1 \\ -1 \\ -1 \\ 1 \\ 1 \\ -1 \end{Bmatrix}, \quad \begin{Bmatrix} s_1 \\ s_2 \\ s_3 \\ s_4 \\ s_5 \\ s_6 \\ s_7 \\ s_8 \end{Bmatrix} = \begin{Bmatrix} -1 \\ -1 \\ 1 \\ 1 \\ -1 \\ -1 \\ 1 \\ 1 \end{Bmatrix}, \quad \begin{Bmatrix} t_1 \\ t_2 \\ t_3 \\ t_4 \\ t_5 \\ t_6 \\ t_7 \\ t_8 \end{Bmatrix} = \begin{Bmatrix} -1 \\ -1 \\ -1 \\ -1 \\ 1 \\ 1 \\ 1 \\ 1 \end{Bmatrix}$$

(3.11)

By inverting Equation (3.8), we obtain

$$\begin{Bmatrix} \frac{\partial N_i}{\partial x} \\ \frac{\partial N_i}{\partial y} \\ \frac{\partial N_i}{\partial z} \end{Bmatrix} = [J]^{-1} \begin{Bmatrix} \frac{\partial N_i}{\partial r} \\ \frac{\partial N_i}{\partial s} \\ \frac{\partial N_i}{\partial t} \end{Bmatrix} \qquad (3.12)$$

from which the matrix $[B_i]$ can be evaluated.

3.2.4 Stress-Strain Relation

The stress-strain relations, in the case of three-dimensional analysis, can be expressed as

$$\vec{\sigma} = [D]\,\vec{\varepsilon} \qquad (3.13)$$

where

$$\vec{\sigma}^{T} = \{\sigma_{xx} \quad \sigma_{yy} \quad \sigma_{zz} \quad \sigma_{xy} \quad \sigma_{yz} \quad \sigma_{zx}\}$$

and

$$[D] = \frac{E}{(1+\upsilon)(1-2\upsilon)} \times$$

$$\begin{bmatrix} (1-\upsilon) & \upsilon & \upsilon & 0 & 0 & 0 \\ \upsilon & (1-\upsilon) & \upsilon & 0 & 0 & 0 \\ \upsilon & \upsilon & (1-\upsilon) & 0 & 0 & 0 \\ 0 & 0 & 0 & (\frac{1-2\upsilon}{2}) & 0 & 0 \\ 0 & 0 & 0 & 0 & (\frac{1-2\upsilon}{2}) & 0 \\ 0 & 0 & 0 & 0 & 0 & (\frac{1-2\upsilon}{2}) \end{bmatrix}$$

(3.14)

3.2.5 Element Stiffness Matrix

The element stiffness matrix is given by

$$\left[K^{(e)}\right] = \iiint_{V^{(e)}} [B]^T [D][B] dV \qquad (3.15)$$

Since the matrix $[B]$ is expressed in natural coordinates (evident from Equations (3.6), (3.7) and (3.12)), it is necessary to carry out the integration in Equation (3.15) in natural coordinates too, using the relationship

$$dV = dx\, dy\, dz = \det[J] \cdot dr\, ds\, st \qquad (3.16)$$

Thus Equation (3.15) can be rewritten as

$$\left[k^{(e)}\right] = \int_{-1}^{1}\int_{-1}^{1}\int_{-1}^{1} [B]^T [D][B] \det [J]\, dr\, ds\, dt \qquad (3.17)$$

3.2.6 Element Load Matrices

Element load vector due to initial strains:

$$\vec{P}_i^{(e)} = \iiint_{V^{(e)}} [B]^T [D] \vec{\varepsilon}_0 \cdot dV \qquad (3.18)$$

Element load vector due to surface forces:

$$\vec{P}_s^{(e)} = \iint_{S_1^{(e)}} [N]^T \vec{\Phi} \cdot dS_1 \qquad (3.19)$$

Element load vector due to body forces:

$$\vec{P}_b^{(e)} = \iiint_{V^{(e)}} [N]^T \vec{\phi} \cdot dV \qquad (3.20)$$

where

$\vec{\varepsilon}_0$ ------ vector of initial strain

$\vec{\Phi}$ ------ vector of surface force

$\vec{\phi}$ ------ vector of prescribed body force

3.3 THREE DIMENSIONAL (3D) BAR ELEMENT

3.3.1 Element Stiffness Matrix

Consider the bar element shown in Figure 3.2 where the local x-axis is taken in the axial direction of the element with origin at corner (or local node) 1. If a linear displacement field is assumed, we can express the axial displacement, $u(x)$, as

$$u(x) = \alpha_1 + \alpha_2 x \qquad (3.21)$$

The two constants α_1 and α_2 can be expressed in terms of the nodal displacement degrees of freedom by using the conditions

$$\begin{aligned} u(x) &= q_1 \text{ at } x = 0 \\ u(x) &= q_2 \text{ at } x = l \end{aligned} \qquad (3.22)$$

where q_1 and q_2 represent the nodal degrees of freedom in the local coordinate system (unknowns) and l denotes the length of the element. With the help of Equations (3.22), Equation (3.21) can be expressed as

$$u(x) = q_1 + (q_2 - q_1)\frac{x}{l}$$

i.e.,

$$\underset{1\times 1}{\{u(x)\}} = \underset{1\times 2}{[N]}\ \underset{2\times 1}{\vec{q}^{(e)}} \qquad (3.23)$$

where

$$[N] = \left[\left(1-\frac{x}{l}\right)\ \frac{x}{l}\right],$$

$$\vec{q}^{(e)} = \begin{Bmatrix} q_1 \\ q_2 \end{Bmatrix},$$

and the superscript e denotes the element number. The axial strain can be expressed as

$$\varepsilon_{xx} = \frac{\partial u(x)}{\partial x} = \frac{q_2 - q_1}{l}$$

i.e.,
$$\underset{1\times 1}{\{\varepsilon_{xx}\}} = \underset{1\times 2}{[B]}\ \underset{2\times 1}{\vec{q}^{(e)}} \qquad (3.24)$$

where

$$[B] = \begin{bmatrix} -\frac{1}{l} & \frac{1}{l} \end{bmatrix}$$

The stress-strain relation is given by

$$\sigma_{xx} = E\,\varepsilon_{xx}$$

i.e.,
$$\underset{1\times 1}{\{\sigma_{xx}\}} = \underset{1\times 1}{[D]}\ \underset{1\times 1}{\{\varepsilon_{xx}\}} \qquad (3.25)$$

where

$$[D] = [E]$$

and E is the Young's modulus of the material. Now the stiffness matrix of the element (in the local coordinate system) can be obtained, from Equation (3.15), as

$$\underset{2\times 2}{\left[k^{(e)}\right]} = \iiint_{V^{(e)}} [B]^T [D][B]\,dV = A\int_{x=0}^{l} \begin{Bmatrix} -\frac{1}{l} \\ \frac{1}{l} \end{Bmatrix} E \begin{Bmatrix} -\frac{1}{l} & \frac{1}{l} \end{Bmatrix} dx$$

$$= \frac{AE}{l} \begin{bmatrix} 1 & -1 \\ -1 & 1 \end{bmatrix} \qquad (3.26)$$

where A is the area of cross section of the bar.

To find the stiffness matrix of the bar in the global coordinate system, we need to find the transformation matrix. In general, the element under consideration will be one of the elements of the whole structure. Let the (local) nodes 1 and 2 of the element correspond to nodes i and j respectively of the global system as shown in Figure 3.2. The local displacements q_1 and q_2 can be resolved into components Q_{3i-2} , Q_{3i-1} , Q_{3i} and Q_{3j-2} , Q_{3j-1} , Q_{3j} parallel to the global X , Y, Z axes respectively. Then the two sets of displacements are related as

$$q_1 = l_{ij}\, Q_{3i-2} + m_{ij}\, Q_{3i-1} + n_{ij}\, Q_{3i}$$
$$q_2 = l_{ij}\, Q_{3j-2} + m_{ij}\, Q_{3j-1} + n_{ij}\, Q_{3j}$$

i.e., $$\bar{q}^{(e)} = [\lambda]\, \bar{Q}^{(e)} \qquad (3.27)$$

where

$$[\lambda] = \begin{bmatrix} l_{ij} & m_{ij} & n_{ij} & 0 & 0 & 0 \\ 0 & 0 & 0 & l_{ij} & m_{ij} & n_{ij} \end{bmatrix}$$

= transformation matrix (3.28)

$$\bar{Q}^{(e)} = \begin{Bmatrix} Q_{3i-2} \\ Q_{3i-1} \\ Q_{3i} \\ Q_{3j-2} \\ Q_{3j-1} \\ Q_{3j} \end{Bmatrix}$$ = vector of nodal displacements of

elements e in the global coordinate system and l_{ij} , m_{ij} and n_{ij} denote the direction cosines of angles between the line i j and the directions OX , OY and OZ respectively. The direction cosines can be computed in terms of the global coordinates of nodes i and j as

$$l_{ij} = \frac{X_j - X_i}{l} \;,\; m_{ij} = \frac{Y_j - Y_i}{l} \;,\; n_{ij} = \frac{Z_j - Z_i}{l} \qquad (3.29)$$

where (X_i , Y_i , Z_i) and (X_j , Y_j , Z_j) are the global coordinates of nodes i and j respectively, and l is the length of the element i j given by

$$l = \left\{ (X_j - X_i)^2 + (Y_j - Y_i)^2 + (Z_j - Z_i)^2 \right\}^{1/2} \qquad (3.30)$$

Thus the stiffness matrix of the element in the global coordinate system can be obtained as

$$\underset{6\times6}{\left[K^{(e)}\right]} = \underset{6\times2}{\left[\lambda\right]^T} \underset{2\times2}{\left[k^{(e)}\right]} \underset{2\times6}{\left[\lambda\right]} = \frac{AE}{l} \underset{6\times6}{\left[L\right]} \qquad (3.31)$$

where

$$\underset{6\times6}{\left[L\right]} =$$

$$\begin{bmatrix} l_{ij}^2 & l_{ij}m_{ij} & l_{ij}n_{ij} & -l_{ij}^2 & -l_{ij}m_{ij} & -l_{ij}n_{ij} \\ l_{ij}m_{ij} & m_{ij}^2 & m_{ij}n_{ij} & -l_{ij}m_{ij} & -m_{ij}^2 & -m_{ij}n_{ij} \\ l_{ij}n_{ij} & m_{ij}n_{ij} & n_{ij}^2 & -l_{ij}n_{ij} & -m_{ij}n_{ij} & -n_{ij}^2 \\ -l_{ij}^2 & -l_{ij}m_{ij} & -l_{ij}n_{ij} & l_{ij}^2 & l_{ij}m_{ij} & l_{ij}n_{ij} \\ -l_{ij}m_{ij} & -m_{ij}^2 & -m_{ij}n_{ij} & l_{ij}m_{ij} & m_{ij}^2 & m_{ij}n_{ij} \\ -l_{ij}n_{ij} & -m_{ij}n_{ij} & -n_{ij}^2 & l_{ij}n_{ij} & m_{ij}n_{ij} & n_{ij}^2 \end{bmatrix} \qquad (3.32)$$

3.3.2 Consistent Load Vector

The consistent load vectors can be computed using Equations (3.18) to (3.20)

$$\vec{p}_i^{(e)} = \text{load vector due to initial strains } (\varepsilon_0) = \iiint_{V^{(e)}} [B]^T [D] \vec{\varepsilon}_0 \cdot dV$$

$$= AE\varepsilon_0 \begin{Bmatrix} -1/l \\ 1/l \end{Bmatrix} \int_0^l dx = AE\varepsilon_0 \begin{Bmatrix} -1 \\ 1 \end{Bmatrix} \qquad (3.33)$$

$$\vec{p}_b^{(e)} = \text{load vector due to constant body force } (\phi_0) = \iiint_{V^{(e)}} [N]^T \vec{\phi} \cdot dV$$

$$= A\phi_0 \int_0^l \begin{Bmatrix} \left(1 - \frac{x}{l}\right) \\ (x/l) \end{Bmatrix} dx = \frac{Al\phi_0}{2} \begin{Bmatrix} 1 \\ 1 \end{Bmatrix} \qquad (3.34)$$

The only surface stress that can exist is p_x and this must be applied at one of the nodal points. Assuming that p_x is applied at node 1, the load vector becomes

$$\vec{p}_{s^1}^{(e)} = \iint_{S_1^{(e)}} [N]^T \{p_x\}\, ds_1 = p_0 \begin{Bmatrix} 1 \\ 0 \end{Bmatrix} \iint_{S_1} ds_1 = p_0\, A_1 \begin{Bmatrix} 1 \\ 0 \end{Bmatrix} \qquad (3.35)$$

where $p_x = p_0$ is assumed to be a constant and the subscript 1 is used to denote the node. The matrix of shape functions $[N]$ reduces to $\begin{Bmatrix} 1 \\ 0 \end{Bmatrix}$ since the stress is located at node 1. Similarly, when $p_x = p_0$ is applied at node 2, the load vector becomes

$$\vec{p}_{s^2}^{(e)} = \iint_{S_2^{(e)}} [N]^T \{p_x\}\, ds_2 = p_0 \begin{Bmatrix} 0 \\ 1 \end{Bmatrix} \iint_{S_2} ds_2 = p_0\, A_2 \begin{Bmatrix} 0 \\ 1 \end{Bmatrix} \qquad (3.36)$$

The total consistent load vector in the local coordinate system is given by

$$\vec{p}^{(e)} = \vec{p}_i^{(e)} + \vec{p}_b^{(e)} + \vec{p}_{s^1}^{(e)} + \vec{p}_{s^2}^{(e)} \qquad (3.37)$$

This load vector, when referred to the global coordinate system, will be

$$\vec{P}^{(e)} = [\lambda]^T\, \vec{p}^{(e)} \qquad (3.38)$$

where $[\lambda]$ is given by Equation (3.28).

3.4 JOINT ELEMENT

3.4.1 Element Stiffness Matrix

Consider the joint element shown in Figure 3.3. We can derive the equation

$$\begin{Bmatrix} F_1 \\ F_2 \end{Bmatrix} = \begin{bmatrix} k & -k \\ -k & k \end{bmatrix} \begin{Bmatrix} u_1 \\ u_2 \end{Bmatrix} \qquad (3.39)$$

Stiffness matrix of the element (in the local coordinate system) can be obtained as

$$\underset{2\times 2}{\left[k^{(e)}\right]} = k \begin{bmatrix} 1 & -1 \\ -1 & 1 \end{bmatrix} \qquad (3.40)$$

If we use the same global coordinate system as shown in Figure 3.2, we can obtain the same transformation matrix $[\lambda]$ from the Equation (3.28). Thus the stiffness matrix of the element in global coordinate system can be obtained as

$$\underset{6\times6}{\left[K^{(e)}\right]} = \underset{6\times2}{[\lambda]^T}\underset{2\times2}{\left[k^{(e)}\right]}\underset{2\times6}{[\lambda]} = k\underset{6\times6}{[L]} \qquad (3.41)$$

3.4.2 Consistent Load Vector

$$\vec{p}_i^{(e)} = k\delta\begin{Bmatrix}-1\\1\end{Bmatrix} \qquad (3.42)$$

where δ is the initial displacement of joint.

$$\vec{p}_b^{(e)} = 0 \qquad (3.43)$$

$$\vec{p}_{s^1}^{(e)} = f_0\begin{Bmatrix}1\\0\end{Bmatrix} \qquad (3.44)$$

$$\vec{p}_{s^2}^{(e)} = f_0\begin{Bmatrix}0\\1\end{Bmatrix} \qquad (3.45)$$

where f_0 is assumed to be a constant. The total consistent load vector in the local coordinate system is given by

$$\vec{p}^{(e)} = \vec{p}_i^{(e)} + \vec{p}_{s^1}^{(e)} + \vec{p}_{s^2}^{(e)} \qquad (3.46)$$

This load vector, when referred to the global coordinate system takes the same form of Equation (3.38),

$$\vec{P}^{(e)} = [\lambda]^T\ \vec{p}^{(e)}$$

3.5 Equilibrium Equation

The desired equilibrium equations of the overall structure or body can now be expressed as

$$\left(\sum_{e=1}^{E}\left[K^{(e)}\right]\right)\vec{\tilde{Q}} = \vec{\tilde{P}}_c + \sum_{e=1}^{E}\left(\vec{P}_i^{(e)} + \vec{P}_s^{(e)} + \vec{P}_b^{(e)}\right) = \vec{\tilde{P}} \qquad (3.47)$$

or

$$\left[\tilde{K}\right]\vec{\tilde{Q}} = \vec{\tilde{P}} \qquad (3.48)$$

where

$\vec{\tilde{Q}}$ ------ global vector of nodal displacements

$\vec{\tilde{P}}_c$ ------ vector of concentrated loads

$\left[\tilde{K}\right] = \sum_{e=1}^{E}\left[K^{(e)}\right]$ ------ assembled (global) stiffness matrix (3.49)

$$\vec{\tilde{P}} = \vec{\tilde{P}}_c + \sum_{e=1}^{E}\vec{P}_i^{(e)} + \sum_{e=1}^{E}\vec{P}_s^{(e)} + \sum_{e=1}^{E}\vec{P}_b^{(e)}$$

------ assembled (global) nodal load vector (3.50)

In a linear problem, the $\left[D\right]$ matrix is considered constant in terms of linear elasticity. So Equation (3.48) can be solved directly. If the problem is non-linear, $\left[\tilde{K}\right]$ is a function of the unknown variable, displacement. The solution will not generally be satisfied unless non-linear computational technique is applied.

The steel deforms elastically at first with essentially constant values of Young's Modulus and Poisson's Ratio, but as soon as the stress reaches the yield value, plastic deformation occurs with a much lower effective modulus. The yield stress itself increases with strain due to work hardening, and stress is no longer proportional to strain, but is related to the strain increment.

It is essential to know how the material will react under a combination of stresses. For this purpose the well-known von Mises yield criterion is used. In terms of principal stresses, this criterion is usually written:

$$(\sigma_1 - \sigma_2)^2 + (\sigma_2 - \sigma_3)^2 + (\sigma_3 - \sigma_1)^2 = 2\sigma_y^2 \qquad (3.51)$$

The equation for an elastic-plastic finite element formation, a relationship between the incremental strain and the incremental stress in a plastically-deforming body can be expressed as :

$$d\vec{\sigma} = [D]_{ep}\, d\vec{\varepsilon} \qquad (3.52)$$

where

$$[D]_{ep} = [D] - [D]_p \qquad (3.53)$$

$[D]$ is the elastic stress/strain matrix; $[D]_p$ is the plastic stress/strain matrix and can be expressed as :

$$[D]_p = \frac{2G}{S} \times$$

$$\begin{bmatrix}
\sigma'_{11}\sigma'_{11} & \sigma'_{11}\sigma'_{22} & \sigma'_{11}\sigma'_{33} & \sigma'_{11}\sigma'_{12} & \sigma'_{11}\sigma'_{23} & \sigma'_{11}\sigma'_{13} \\
\sigma'_{22}\sigma'_{11} & \sigma'_{22}\sigma'_{22} & \sigma'_{22}\sigma'_{33} & \sigma'_{22}\sigma'_{12} & \sigma'_{22}\sigma'_{23} & \sigma'_{22}\sigma'_{13} \\
\sigma'_{33}\sigma'_{11} & \sigma'_{33}\sigma'_{22} & \sigma'_{33}\sigma'_{33} & \sigma'_{33}\sigma'_{12} & \sigma'_{33}\sigma'_{23} & \sigma'_{33}\sigma'_{13} \\
\sigma'_{12}\sigma'_{11} & \sigma'_{12}\sigma'_{22} & \sigma'_{12}\sigma'_{33} & \sigma'_{12}\sigma'_{12} & \sigma'_{12}\sigma'_{23} & \sigma'_{12}\sigma'_{13} \\
\sigma'_{23}\sigma'_{11} & \sigma'_{23}\sigma'_{22} & \sigma'_{23}\sigma'_{33} & \sigma'_{23}\sigma'_{12} & \sigma'_{23}\sigma'_{23} & \sigma'_{23}\sigma'_{13} \\
\sigma'_{13}\sigma'_{11} & \sigma'_{13}\sigma'_{22} & \sigma'_{13}\sigma'_{33} & \sigma'_{13}\sigma'_{12} & \sigma'_{13}\sigma'_{23} & \sigma'_{13}\sigma'_{13}
\end{bmatrix} \qquad (3.54)$$

where

$$G = \frac{E}{2(1+\upsilon)} \qquad (3.55)$$

and

$$S = \frac{3}{2}\bar{\sigma}^2\left(1+\frac{\sigma'_y}{3G}\right) \qquad (3.56)$$

where

$$\bar{\sigma} = \left(\frac{3}{2}\sigma'_{ij}\sigma'_{ij}\right)^{\frac{1}{2}} \qquad (3.57)$$

σ_y' is the rate of change of yield stress σ_y with respect to plastic strain $\bar{\varepsilon}^p$. σ_{ij}' is the deviatoric stress.

For small but finite increments of deformation, Equation (3.52) may be generalised as :

$$\Delta\vec{\sigma} = [D]_{ep}\,\Delta\vec{\varepsilon} \qquad (3.58)$$

It is assumed that the stiffness is constant over each small increment of deformation and a relationship between incremental displacement $\Delta\vec{\tilde{Q}}$ and incremental force $\Delta\vec{\tilde{P}}$ is obtained :

$$[\tilde{K}]\,\Delta\vec{\tilde{Q}} = \Delta\vec{\tilde{P}} \qquad (3.59)$$

The stiffness matrix takes the same form as the Equation (3.49), but the elastic-plastic constitutive matrix is used.

3.6 NONLINEAR ANALYSIS

Material nonlinear effects arise from a nonlinear constitutive model (that is, progressively disproportionate stresses and strains). Common example of nonlinear material behaviour is the plastic yielding of metals.

3.6.1 Nonlinear solution procedures

For nonlinear analysis, since it is no longer possible to directly obtain a stress distribution which equilibrates a given set of external loads, a solution procedure is usually adopted in which the total required load is applied in a number of increments. Within each increment a linear prediction of the nonlinear response is made, and subsequent iterative corrections are performed in order to restore equilibrium by the elimination of the residual or 'out of balance' forces. The iterative corrections are referred to some form of 'convergence' criteria which indicates to what extent an equilibrate state has been achieved. Such a solution procedure is therefore commonly referred to as an 'incremental-iterative' (or 'predictor-corrector')

method. There are two main forms of this method, both having their advantages and disadvantages. They are:

(a) The standard Newton Raphson method, and

(b) The modified Newton Raphson method.

3.6.2 The Standard Newton Raphson method

In the standard Newton Raphson method an initial guess at the displacements by using the linear stiffness equation is made, with the stiffness value being that for the previous load conditions. A value of strain is then calculated for this guess for which there is a specified stress value given by the computer model of the strain-stress curve, as contained in the input data. The stress level actually existing due to the applied loads is then compared with the stress from the curve, and any difference is called the residual force.

If this residual value is within strict limits of acceptance then the process is finished, and the strains that have been calculated are adopted as the true strains that the structure had been subjected to. If however, the residual value falls outside the limits, then it updates the stiffness of the structure and another guess is made about the displacement that occur, and the residual values again checked for the tolerance. The stiffness is updated for the calculation of each guess and is taken as tangent to the stress-strain curve at the point it previously considered.

In the standard Newton Raphson procedure each iterative calculation is always based upon the 'current tangent stiffness'. For finite element analysis, this involves the formation (and factorisation) of the tangent stiffness matrix at the start of each equilibrium iteration.

Although the standard Newton Raphson method generally converges rapidly (as shown in Figure 3.4), the continual manipulation of the stiffness matrix is often prohibitively expensive. The need for a robust yet inexpensive procedure leads to the development of the modified Newton Raphson method.

3.6.3 The modified Newton Raphson method

This method is almost exactly the same as the standard Newton Raphson method except that it uses the same stiffness value for all guesses. In this method the tangent stiffness matrix is formed less frequently, the iterative corrections being based on some previous stiffness evaluation (as shown in Figure 3.5).

3.6.4 Convergence

When using incremental/iterative solution algorithms, a measure of the convergence of the solution is required to define when equilibrium has been achieved. The selection of appropriate convergence criteria is of utmost importance. An excessively tight tolerance may result in unnecessary iterations and consequent waste of computer resources, whilst a slack tolerance may provide incorrect answers. Therefore an effective convergence criterion, used with a realistic tolerance, is a precondition for accurate and economic solutions.

Assigning tolerance values is very much a matter of experience. In general, sensitive geometrically nonlinear problems require a tight convergence criteria in order to maintain the solution on the correct equilibrium path, whereas a slack tolerance is usually more effective with predominantly materially nonlinear problems, where high local residuals may have to be tolerated. The method of monitoring convergence within LUSAS considers five criteria:

(1) EUCLIDIAN RESIDUAL NORM (rlnorm)

The Euclidian residual norm γ_ψ is defined as the norm of the residuals $\bar{\psi}$ as a percentage of the norm of the external forces $\bar{R}$ and is written as

$$\gamma_\psi = \frac{\|\bar{\psi}\|_2}{\|\bar{R}\|_2} \text{ x } 100 \qquad (3.60)$$

where $\bar{R}$ contains the external loads and reactions. Owing to the inconsistency of the units of displacement and rotation, only translational degrees of freedom are considered. For problems involving predominantly geometric nonlinearity, a

tolerance of $\gamma_\psi < 0.1$ is suggested. Where plasticity predominates, a more flexible tolerance of $1.0 < \gamma_\psi < 5.0$ is suggested.

(2) EUCLIDIAN DISPLACEMENT NORM (dlnorm)

The Euclidian displacement norm γ_d is defined as the norm of the iterative displacements $\delta\vec{\tilde{Q}}$ as a percentage of the norm of the total displacements $\vec{\tilde{Q}}$ and is written as

$$\gamma_d = \frac{\left\| \delta\vec{\tilde{Q}} \right\|_2}{\left\| \vec{\tilde{Q}} \right\|_2} \text{ x } 100 \qquad (3.61)$$

As in the residual norm only translation degrees of freedom are considered. The criterion is physical measure of how much the structure has moved during the current iteration. Typical values are: $0.1 < \gamma_d < 1.0$ (reasonable); $0.001 < \gamma_d < 0.1$ (tight).

(3) WORK NORM (wlnorm)

The work measure is defined as the work done by the residual forces on the current iteration as a percentage of the work done by the external forces on iteration zero i.e. for iteration *i*

$$\gamma_w = \frac{(\vec{\psi}^i)^T \delta\vec{\tilde{Q}}^i}{\vec{R}^T \delta\vec{\tilde{Q}}^1} \text{ x } 100 \qquad (3.62)$$

where $\vec{\psi}^i$ is the current residual force vector, $\vec{R}$ is the external force vector for the current increment, $\delta\vec{\tilde{Q}}^1$ is the iterative displacement for iteration 1, and $\delta\vec{\tilde{Q}}^i$ is the iterative displacement for the current increment. The following are typical values: $1.0E\text{-}3 < \gamma_w < 1.0E\text{-}1$ (slack); $1.0E\text{-}6 < \gamma_w < 1.0E\text{-}3$ (reasonable); $1.0E\text{-}9 < \gamma_w < 1.0E\text{-}6$ (tight).

(4) ROOT MEAN SQUARE OF RESIDUALS (rnoral)

This criterion evaluates the root mean square value of all the residuals in the problem i.e.

$$\gamma_{\psi_1} = \left\| \bar{\psi} \right\|_2 \qquad (3.63)$$

This criterion is dependent upon the units of the problem.

(5) MAXIMUM ABSOLUTE RESIDUAL (rmaxal)

This criterion limits the maximum absolute residual in a problem i.e.

$$\gamma_{\psi_2} = \max \left[\left| \bar{\psi} \right| \right] \qquad (3.64)$$

The criterion is dependent upon the units of the problem. It is an extremely stiff criterion, which may be useful near bifurcation points of sensitive geometrically nonlinear problems where large residuals may pollute the solution.

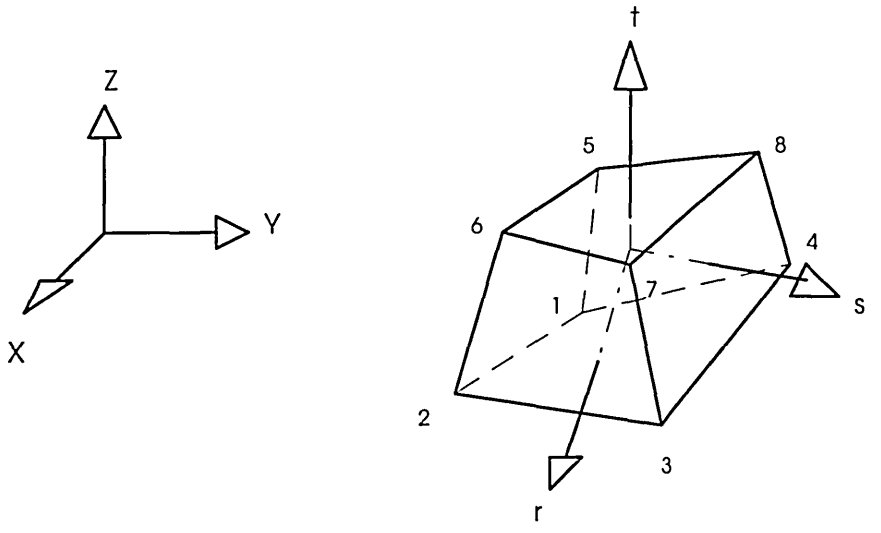

(a) in global xyz system

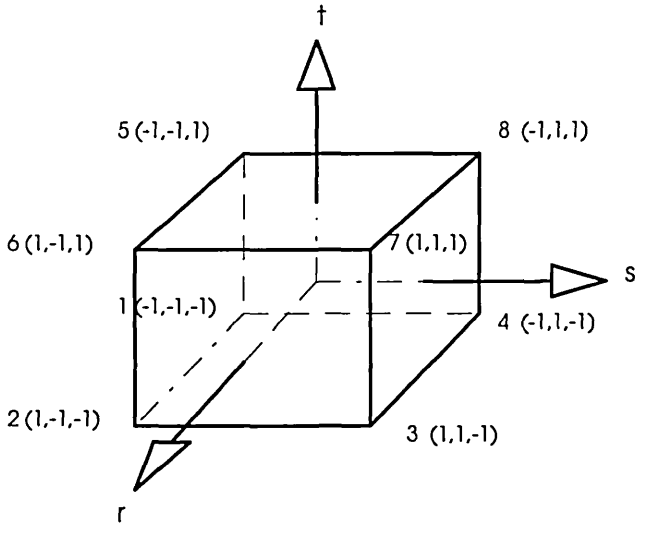

(b) in local rst system

Fig. 3.1 A hexahedron element with 8 nodes

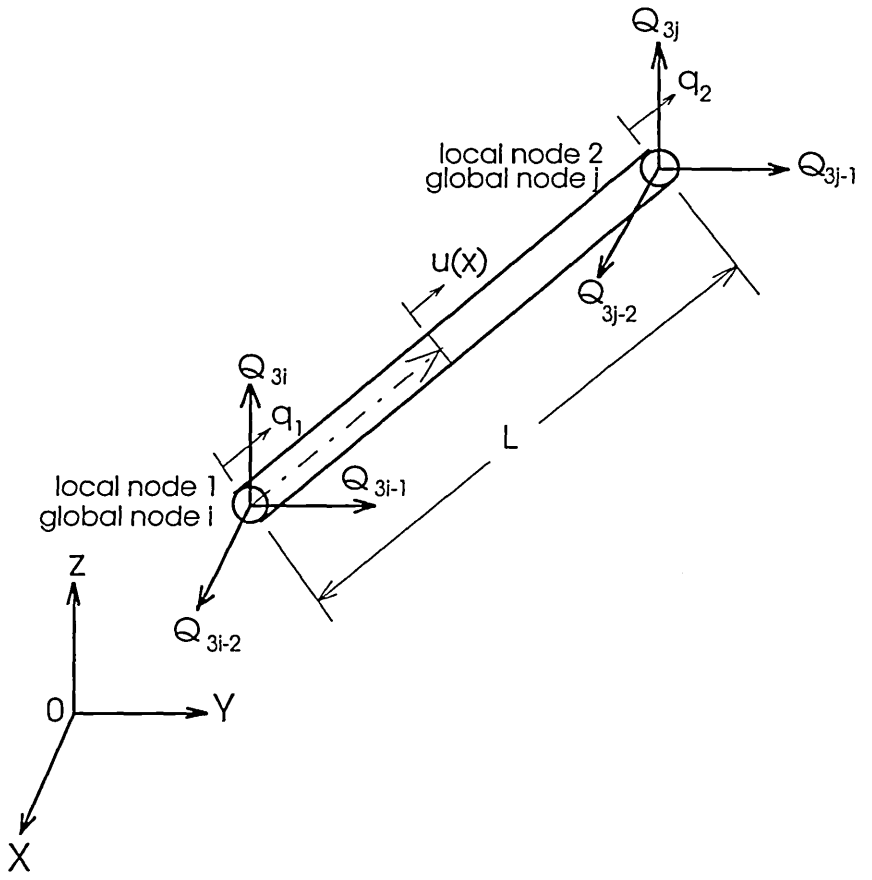

Fig. 3.2 3D bar element

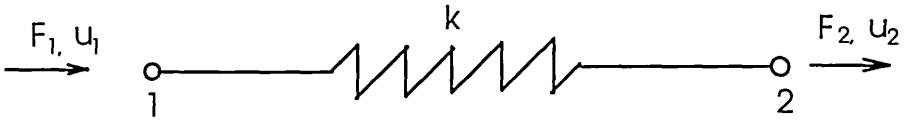

Fig. 3.3 Joint element

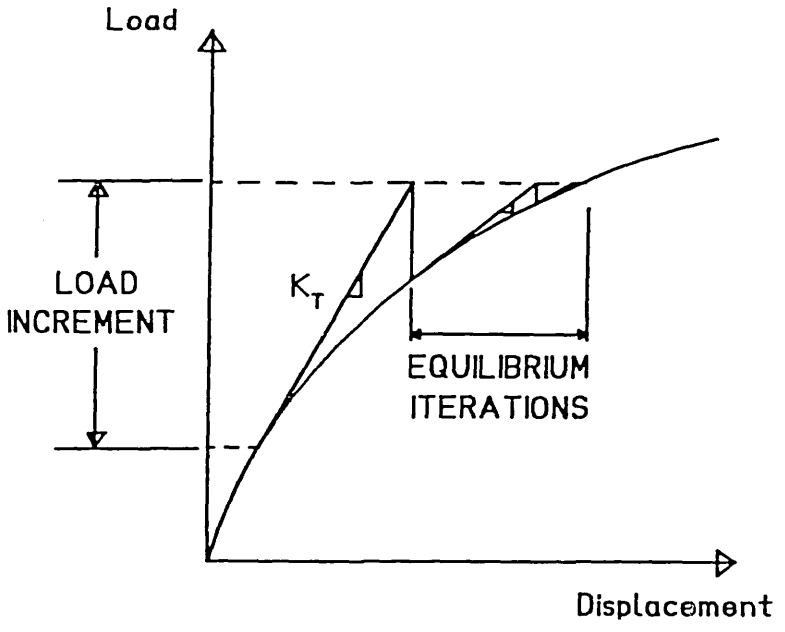

Fig. 3.4 The standard Newton Raphson method

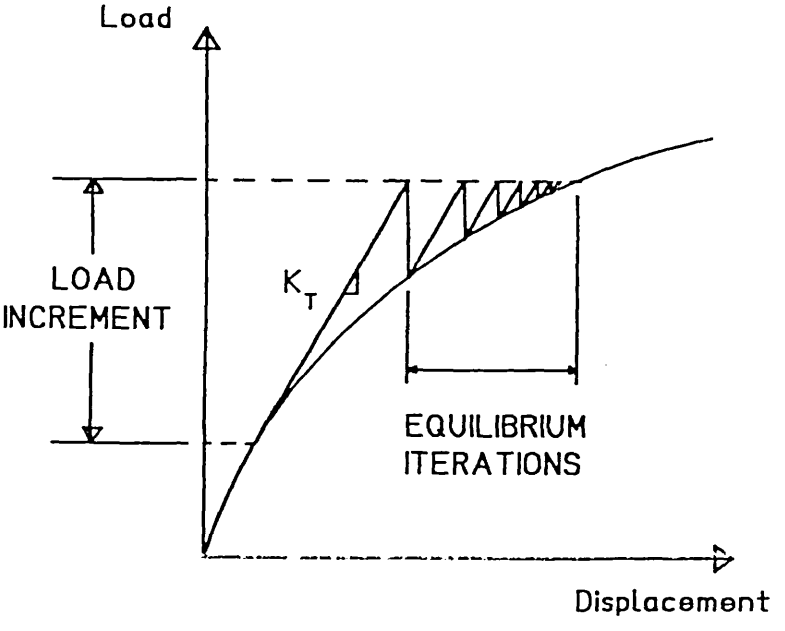

Fig. 3.5 The modified Newton Raphson method

CHAPTER 4

FINITE ELEMENT MODEL OF THE CONNECTION

4.1 INTRODUCTION

Flush end plate connection represents an extremely complex and highly indeterminate structural problem. A large number of parameters affect the behaviour of the connection, including end plate and column flange thickness, bolt size and grade, beam depth and connection details. The interaction between end plate and column flange, known as prying, further exacerbates the problem. Experimentally the moment-rotation characteristic of a connection can be ascertained. However, full scale tests are very expensive and time consuming. Also the number of variables are too many for a limited test programme to form the basis of any design method. It is, therefore, essential to develop an appropriate analytical method, which is capable of predicting accurately the structural properties of the connection and can lead to the formulation of design rules.

The finite element technique is ideally suited to handle such a complex problem. A number of powerful and efficient finite element softwares, namely LUSAS, ABAQUS and ANSYS, are now commercially available.

The LUSAS (London University Structural Analysis System) software was employed by the author for an in-depth study of the connection. LUSAS is a general purpose finite element software which incorporates a number of facilities including the following:

- Linear static analysis;
- Nonlinear static analysis;
- Linear material buckling analysis.

A range of linear and nonlinear constitutive models are available, covering most commonly used engineering materials. The constitutive models currently available include:

- Linear isotropic/orthotropic/anisotropic;
- Elasto-plastic isotropic/anisotropic with strain hardening and pressure dependence;
- Nonlinear concrete with strain softening.

The LUSAS element library contains over 100 element types, enabling a wide range of engineering applications to be efficiently modelled. The element types currently available include:

- Bars;
- Beams;
- 2-D continuum;
- 3-D continuum;
- Plates;
- Shells;
- Joints.

Nonlinear boundary condition joint models are also available for modelling smooth and frictional contact surfaces, using nonlinear joint models or slidelines. Boundary conditions may be applied to the finite element model as:

- Restrained/prescribed values;
- Springs;
- Slidelines.

In addition, a variety of loading conditions may be applied. The loading types currently available include:

- Prescribed displacements;
- Concentrated loads;
- Element loads;

- Distributed loads;
- Body force loads;
- Initial stresses and strains;
- Residual stresses.

LUSAS is a sophisticated finite element package but it is complex and a lot of hands on experience is needed before it can be applied to solve a complex structural engineering problem. The author spent a lot of time and effort in familiarising himself with the package and assessing its potentialities. Only then attention was focused on developing a finite element model of the connection.

Development of an accurate and economical model of the connection is a laborious and painstaking task. A comparative study of four finite element models of one flush end plate connection made of 254x254UC89 column, 406x178UB74 beams, 450x200x10 end plate and two rows of M20 grade 8.8 tension bolts was undertaken to consider the effect of the following variables on the performance of the model:

- Two types of three dimensional elements, HX8 and HX16
- Two column lengths, 2.5 times and 3 times the depth of beam (2.5D, 3D)
- Bolt holes ignored or incorporated in the model (NH, WH)

The four models had the following characteristics:

MODEL 1: element type HX16, no hole, column length 3D, number of elements 1203, number of nodes 6139;

MODEL 2: element type HX16, no hole, column length 2.5D, number of elements 1115, number of nodes 5403;

MODEL 3: element type HX8, no holes, column length 2.5D, number of elements 860, number of nodes 1534;

MODEL 4: element type HX16, with holes, column length 2.5D, number of elements 1117, number of nodes 5457.

The results of the comparative study is given in Table 4.1.

In previous research[8],[46],[47] it was assumed that the deformation of column flange in extended end plate connection permeated over a length equal to 3 times the depth of beam. After comparing the results of finite element analyses of MODEL1 and MODEL2, the author concluded that it was not necessary to consider a column length of '3D' for flush end plate connections, (the performance of these two models were identical). The conclusion was confirmed later, when elastic-plastic analysis was carried out. In order to achieve further economy, the author carried out a comparison between MODEL2 with sixteen noded HX16 solid elements and MODEL3 with eight noded HX8 solid elements. The results of MODEL2 and MODEL3 differed significantly with the maximum difference in displacement of 30%. The comparison of models with bolt holes and without bolt holes was also carried out. The maximum difference in displacement between the results of MODEL2 and MODEL4 was 6%. It should be emphasised that the above comparison is valid for linear analysis of the connection. On the basis of the above study the author tentatively adopted MODEL4 for further study of the connection. The author also developed one model for buckling analysis of the connection. Unfortunately, LUSAS can only perform linear material buckling analysis and is incapable of performing non-linear material buckling or collapse analysis. Hence an in-depth buckling analysis was not attempted.

The suitability of MODEL4 for elasto-plastic analysis was investigated next. The model finally chosen must be capable of predicting the performance of the connection over the entire loading history, covering both the elastic and the elasto-plastic range. Three connection models with column and beam sizes same as Test T1 and lengths of column equal to 2, 2.5 and 3 times the depth of beam were considered for the comparative study. Each model was made of HX16 solid elements and each included bolt holes. Load displacement characteristics of the three models, Model M1, Model M1a and Model M1b are recorded in Table 4.2. The

results confirm the earlier tentative finding that a column length equal to 2.5 times the depth of beam is adequate for the connection model.

The output from the LUSAS finite element analysis, covering the entire elasto-plastic range, consisted of the following:

- stresses and strains in the solid elements;
- forces and strains in the bar elements;
- forces and strains in the joint elements;
- displacements at nodes.

Finite element models of the six test specimens were developed and named M1 to M6. A few characteristics of these models are given in Table 4.3.

Finite element analysis of a complex structural engineering problem demands a lot of computing time. The computing time depends on the type of computer being used and the number of load increments being considered over the entire elasto-plastic range. Mainframe computer named ZIPPY (Alfa) was used which took 1 to 3 days to run the analysis. If the analyses of these models were run on a PC (486, DX 33MHZ), it would have taken 2 to 3 weeks for each model.

4.2 DESCRIPTION OF THE MODEL

An in-depth investigation of unstiffened flush end plate connection should examine the response of the connection over the entire elasto-plastic range, predict moment-rotation characteristic of the connection, ascertain magnitude and location of interacting forces at the interface of column flange and end plate, and compute the magnitude of bolt forces. In order to develop a suitable design method for the connection, it is also imperative to separate the contribution of different components of the connection.

A three-dimensional finite element model of the connection is shown in Figure 4.1, which incorporates the following LUSAS element types:

1. HX16 solid elements (Figure 4.2a) for the plates: this is a three-dimensional, isoparametric solid element capable of modelling curved boundary. This element comprises 16 nodes with three degrees of freedom u, v, w at each node.
2. BRS2 bar elements (Figure 4.2b) for the bolts: this is a straight isoparametric bar element in three dimensions which can accommodate varying cross-sectional area. It includes two nodes with three degrees of freedom u, v, w at each node. The axial force along the length is constant for this element.
3. JNT4 joint elements (Figure 4.2c) for the interactive forces generated at the interface of end plate and column flange: this is a three-dimensional joint element which connects two nodes by three springs in the local x, y, z directions. This element has four nodes with three degrees of freedom at each of the two active nodes while the third and fourth nodes are passive nodes used only to define the element's local x-axis and the xy-plane.

Symmetry of the connection configuration and load resisted by it about both the major and minor axes mean that only a quarter of the entire connection needs to be modelled for the analysis.

The HX16, solid elements are used to model column web/flanges, end plate and beam web/flanges. The column web and flange share common nodes (Figure 4.3a) at their junction. At the interface, the two coincident nodes of the column flange and end plate are connected (Figure 4.3b) to each other by non-linear joint elements, JNT4. Infinite (very large) stiffness in compression and zero stiffness in tension were assigned to these bi-linear joint elements. These ensure displacement compatibility at nodes where end plate and column flange are in contact but allows separation at all other nodes. Friction between column flange and end plate is not considered and the only degrees of freedom that are made compatible between the bodies are lateral displacements. HX16 elements with curved boundary (Figure 4.3c) are used to model bolt holes. The bolt is represented by eight bar elements (Figure 4.3c), BRS2, which connect appropriate nodes of the column flange and end plate at

hole position. The contribution of the beam towards the rotational stiffness of the connection is small and is not considered. However, its contribution towards the bending behaviour of the end plate is recognised and included in the model. A short length of the beam is incorporated in the model with fictitiously very high modulus of elasticity to ensure that the boundary of the end plate, where it is connected to the beam flanges and web, remains in a plane at all times during the loading cycle.

The connection model did not include the following:

- Welds;
- Column root fillets;
- Heat affected zones of end plate;
- Bolt heads and nuts.

As stated previously, a length of column equal to two and half times the depth of the beam was considered in the model.

The moment acting at the connection is decomposed into a pair equal and opposite distributed loads acting on the two flanges of the beam as shown in Figure 4.4. The total distributed load acting on each flange is given by

$$P = \frac{M}{D - T} \qquad (4.1)$$

in which

D is the depth of the beam;

T is the flange thickness.

4.3 BOUNDARY CONDITIONS

Since only a quarter of the whole connection is considered in the finite element model, appropriate boundary conditions are assigned. Only half of the actual thickness of the column web is included in the model. The section of web through the web centre line is subjected to in-plane action only and the nodes in the section are allowed vertical and horizontal in-plane displacements (y and z directions in

Figure 4.1). All the nodes in the column flange, end plate, beam flanges and web, which lie in the yz plane of symmetry through the column web centreline, have their horizontal displacement in the x direction restrained. Also at the column mid-depth all the nodes in xy plane of symmetry are restrained in z direction.

4.4 MATERIAL PROPERTIES

The reliable prediction of connection behaviour depends on a number of factors including a knowledge of the material properties. A series of tensile tests was carried out of grade 43 (S275) steel plates cut from test specimens and grade 8.8 steel bolts. In the elastic range, a modulus of elasticity of steel plate, E = 200 kN/mm^2, and a yield stress, σ_y = 300 N/mm^2, were used. For non-linear analysis, the stress-strain relationship for the elements of the column web/flange and end plate is decomposed into an equivalent trilinear stress-strain curve as shown in Figure 4.5a. The tangential stiffness after the yield point is defined as 0 at the yield plateau and 5% of the initial modulus of elasticity at hardening stage. The limit on the effective yield plateau is taken as 0.02. A modulus of elasticity of the bolt, E = 200 kN/mm^2, and a yield stress, σ_y = 600 N/mm^2, were used. The stress-strain relationship is taken as a bilinear curve as shown in Figure 4.5b, with post yield tangential stiffness defined as 10% of the initial modulus of elasticity. The test results are reported in Chapter 5.

The von Mises yield criterion, which is applicable to isotropic engineering material, is used to predict the onset of yielding. The behaviour upon further yielding is predicted by the flow rule and hardening law.

4.5 NONLINEAR ANALYSIS CONTROL

Incremental loading for non-linear problem in LUSAS can be specified in three ways:

- Manual incrementation;
- Automatic incrementation;
- Mixed manual and automatic incrementation.

Automatic load incrementation was used in the author's model. Automatic incrementation for non-linear problem is controlled via the INCREMENTATION section of the NONLINEAR CONTROL data chapter. In this case, only the initial LOAD CASE is specified and the incrementation is controlled by the INCREMENTATION and TERMINATION sections of the NONLINEAR CONTROL data chapter. When using automatic incrementation, the initial loading components specified in the LOAD CASE data chapter are multiplied by the current load factor. Two methods of automatic incrementation are available:

- Uniform incrementation;
- Variable incrementation.

Uniform incrementation was applied in author's model. That is, for each increment the starting load factor will be multiplied by the specified load components and added to the previous level. The incremental load factor was set at 1 in the model.

Two iterative procedures included in LUSAS were compared. It was found that although the modified Newton Raphson method took less time for each iteration, it needed lots of iterations for the analysis to meet the convergence criteria. The total running time of standard Newton Raphson method was less than that of modified Newton Raphson method. Therefore, standard Newton Raphson method was adopted for the investigation.

Two convergence criteria namely displacement norm (dlnorm) and the residual form norm (rlnorm), were specified. Both of them were set at 0.1 which represented the upper limit of the tight values.

Non-linear analysis may generate a vast amount of output. In addition to the normal nodal point and element output controls, the frequency of non-linear solution output may be restricted via the OUTPUT section in NONLINEAR CONTROL chapter. The following output controls are available:

- Iteration output frequency;
- Increment output frequency;
- Plot file output frequency.

The incremental interval for output of both analysis results and plotting data was set at 1, which meant that after each load incrementation output of both analysis results and plotting data occurred.

With automatic incrementation, the solution progresses one NONLINEAR CONTROL chapter at a time. The finish of each NONLINEAR CONTROL chapter is controlled by its TERMINATION data section. Termination may be specified in 3 ways:

- Limiting the maximum applied load factor;
- Limiting the maximum number of applied increments;
- Limiting the maximum value of named freedom.

The maximum number of applied increments in the model was used for TERMINATION data . They were varied depending on different initial load input and maximum load level obtained from test results (see Table 4.3).

4.6 MOMENT-ROTATION CHARACTERISTICS

Thus moment-rotation curve of a connection can be derived on the basis of data obtained from finite element analysis. The contribution of individual components to the rotational capacity of the connection can also be identified.

The deflection of the end plate at the beam tension flange is the transverse displacement, ab related to the undeformed beam as shown in Figure 4.6. This total deformation is the aggregate of the contributions of column, bolts and end plate. If the point of the rotation is assumed to be at the edge of the compression flange of the beam, the total rotation can be obtained by the following formula:

$$\phi = \frac{ab}{D - \frac{T}{2}} \qquad (4.2)$$

where:

D is the depth of the beam;

T is the thickness of the beam flange.

The contribution of the column flange, bolts and end plate can be determined as follows (Figure 4.7):

$$\phi_{cf} = \frac{a'c'}{D - \frac{T}{2}} \qquad (4.3)$$

$$\phi_{b} = \frac{c'd'}{D - \frac{T}{2}} \qquad (4.4)$$

$$\phi_{ep} = \frac{d'b'}{D - \frac{T}{2}} \qquad (4.5)$$

The total connection rotation is given by

$$\phi = \phi_{cf} + \phi_{b} + \phi_{ep} \qquad (4.6)$$

				MODEL1 HX16 NH 3D	MODEL2 HX16 NH 2.5D	MODEL3 HX8 NH 2.5D	MODEL4 HX16 WH 2.5D
LOAD(L)				53910	53910	53910	53910
PRYING FORCE (P)	NO. OF NODES IN TENSION REGION			13	13	7	12
	TOTAL NUMBER OF NODES			33	33	21	31
	MAGNITUDE IN TENSION REGION			15102.48	15102.48	11099	8548.66
P/L (%)				28	28	21	16
BOLT FORCE (B)	FIRST ROW			50700	50700	47330	46197
	SECOND ROW			28320	28320	27860	26535
	RATIO (%)			56	56	59	57
BOLT DISTANCE (see note)	FIRST ROW			348	348	348	348
	SECOND ROW			288	288	288	288
	RATIO (%)			83	83	83	83
DISPLA-CEMENT (z)	END PLATE	LEFT EDGE X=27.95	MAX	0.611	0.611	0.421	0.574
			MIN	-0.101	-0.101	-0.0856	-0.0998
		MIDDLE X=67.95	MAX	0.605	0.605	0.417	0.570
			MIN	-0.0869	-0.0869	-0.0730	-0.0861
		RIGHT EDGE X=127.95	MAX	0.600	0.600	0.413	0.565
			MIN	-0.0835	-0.0835	-0.0709	-0.0832
	COLUMN FLANGE	LEFT EDGE X=0.01	MAX	0.220	0.220	0.162	0.198
			MIN	-0.118	-0.118	-0.0978	-0.117
		MIDDLE X=67.95	MAX	0.151	0.151	0.120	0.153
			MIN	-0.0858	-0.0858	-0.0733	-0.0855
		RIGTH EDGE X=127.95	MAX	0.0438	0.0438	0.0419	0.0466
			MIN	-0.0699	-0.0698	-0.0637	-0.0699

Units: N mm.

Note: Distance of bolt row is measured from the bottom of the compression flange.

Table 4.1 Comparison of different model types

DISPLACEMENT (z) at node 7298 (mm)			
LOAD (kNm)	Model M1 (HX16 WH 2.5D)	Model M1a (HX16 WH 2D)	Model M1b (HX16 WH 3D)
0	0	0	0
18.3	0.169	0.169	0.169
36.6	0.337	0.338	0.337
54.9	0.531	0.531	0.531
73.2	0.809	0.812	0.809
91.5	1.355	1.357	1.355
109.8	2.313	2.317	2.313
128.1	3.703	3.709	3.703
146.4	5.391	5.397	5.392
164.7	7.549	7.558	7.549
183.0	10.286	10.297	10.288
201.3	13.313	13.331	13.314

Table 4.2 Load-displacement results of one node for three lengths of column

Model	Element number				Node number	Load increment	CPU (ZIPPY) (hour)	Elapsed time (hour)
	Solid	Bar	Joint	Total				
M1	856	16	657	1529	8317	11	4.5	39
M2	856	16	657	1529	8317	16	5.5	60
M3	970	16	683	1669	9125	9	5.5	30
M4	938	32	734	1704	9101	12	3.8	29
M5	1016	32	725	1773	9601	10	5.5	26
M6	1016	32	725	1773	9601	10	4.5	24

Note: Models M1 to M6 correspond to Test specimens T1 to T6 respectively.

Table 4.3 Model statistics

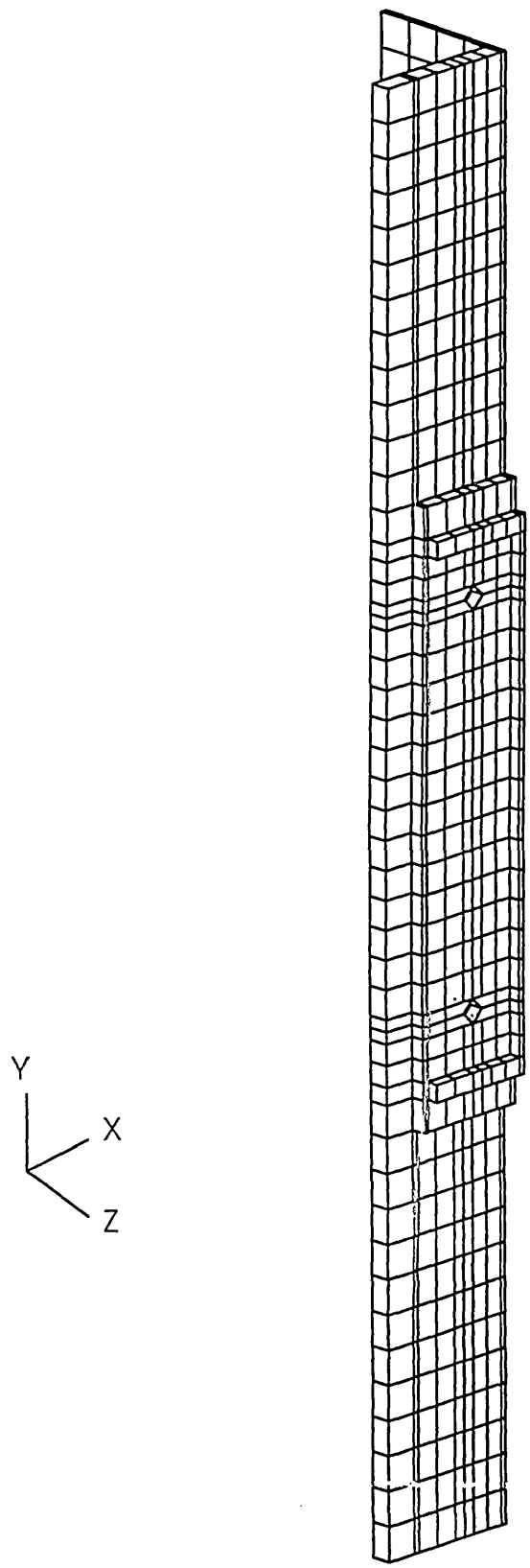

Fig. 4.1 Model of a quarter of the connection

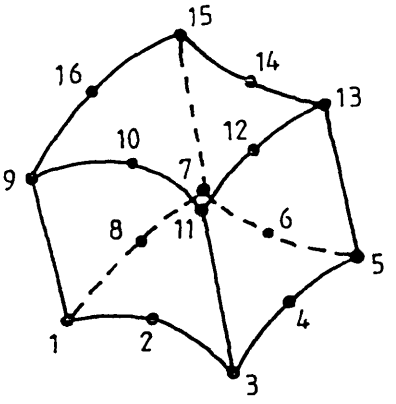

(a) HX16 for plates

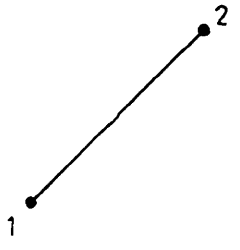

(b) BRS2 for grade 8.8 bolts

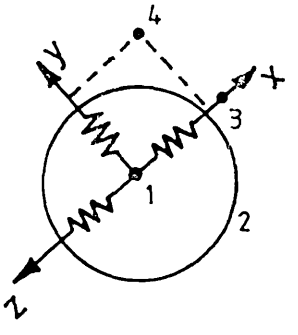

(c) JNT4 for interactive forces

Fig. 4.2 Finite elements used in the model

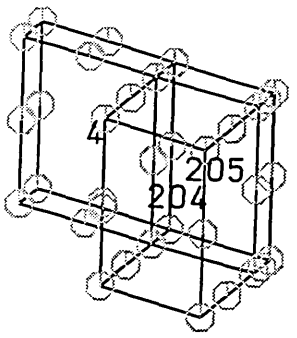

(a) Column web and flange

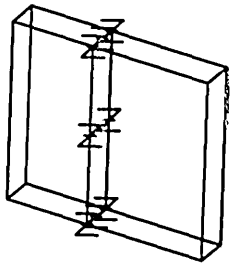

(b) Column flange and end plate

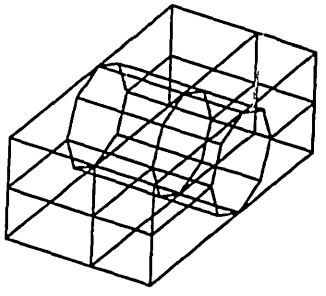

(c) Bolt hole and bolts

Fig. 4.3 Element relationships

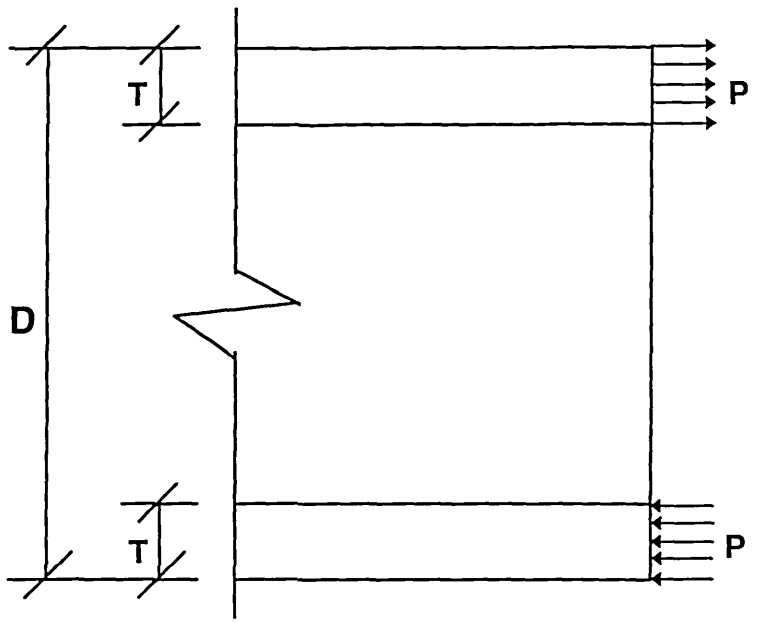

Fig. 4.4 Distributed load acting on beam flanges

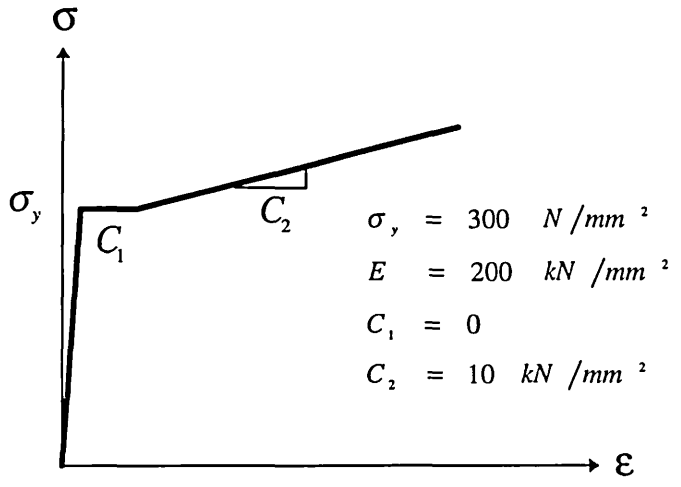

(a) Stress-strain curve for grade 43 (S275) plate

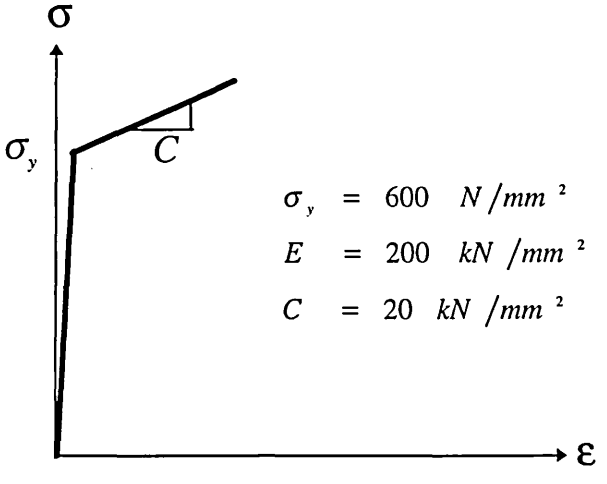

(b) Stress-strain curve for grade 8.8 bolt

Fig. 4.5 Stress-strain curves for nonlinear material model

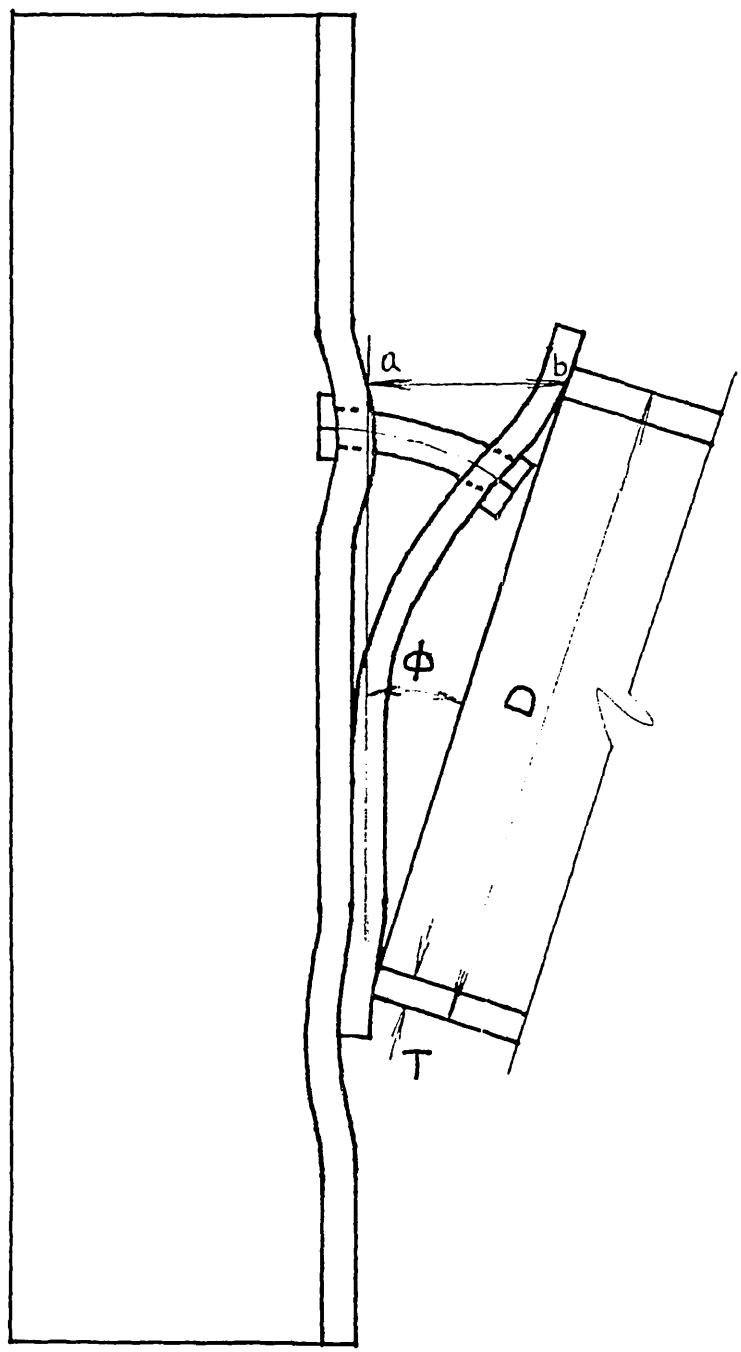

Fig. 4.6 Rotation of flush end plate connection

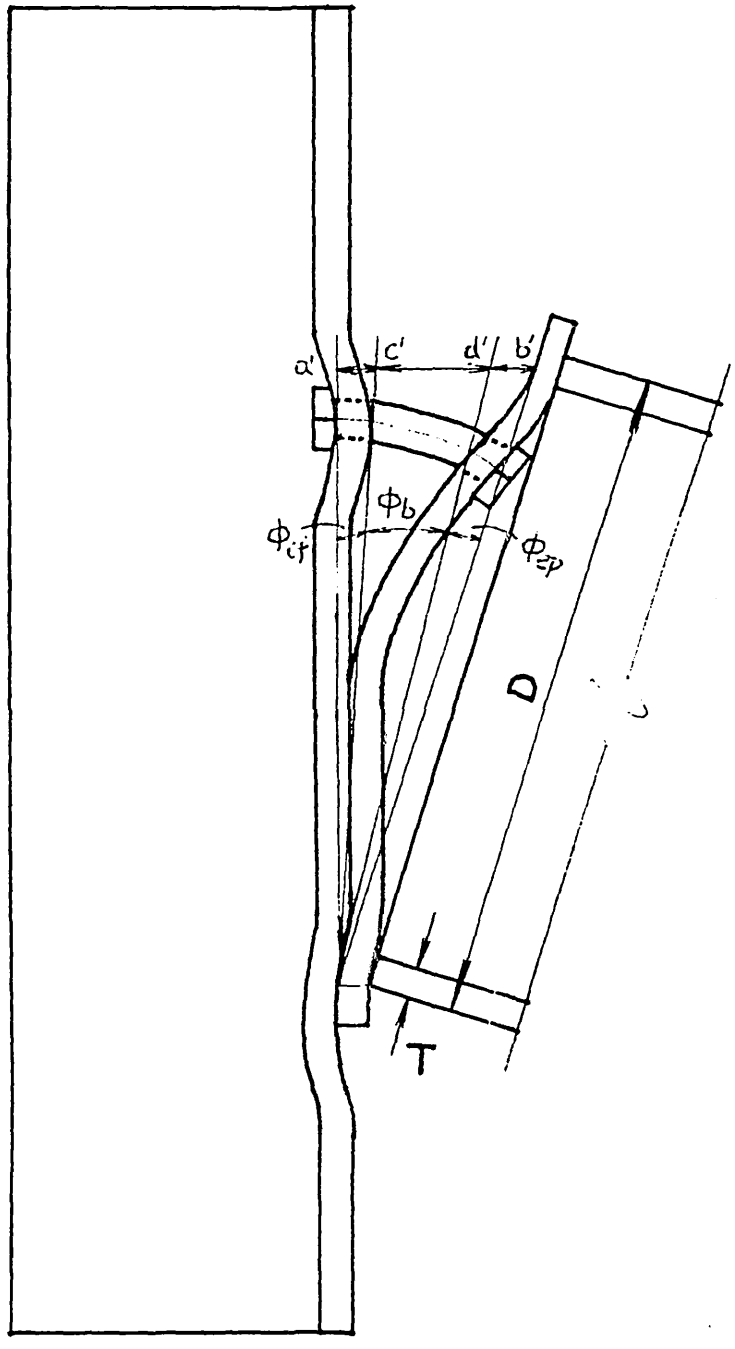

Fig. 4.7 Individual contributions of connection components

CHAPTER 5

EXPERIMENTAL INVESTIGATION

5.1 INTRODUCTION

In order to develop a practical design method for steel frames with unstiffened flush end plate connections, a knowledge of the moment capacity, rotational stiffness and rotation capacity of the connections over the entire elasto-plastic range is essential. The determination of such characteristics requires full understanding of the behaviour of each component of the connection as well as the way in which they interact. Although the finite element technique is an economical and efficient tool for conducting a comprehensive investigation into the overall behaviour of the connection and interaction between individual components, the accuracy and adequacy of the finite element model of the connection must be verified by comparison with full scale tests. If good agreement between the analytical model and experimental results is achieved, thorough investigation of connection performance can be undertaken through analytical models, something which is very difficult to achieve by experiments. An experimental study of the overall behaviour of the unstiffened flush end plate connections was, therefore, undertaken with the object of establishing the validity of the finite element model. All the tests were continued until failure occurred. The details of the comprehensive test programme are reported in this chapter.

5.2 TEST RIG

The tests were performed in the Heavy Structures Laboratory of the University of Abertay Dundee. The loading and instrumentation set up for the full-scale tests of flush end plate connections are shown in Figure 5.1. The Heavy Structures Laboratory is equipped with a 1000 kN capacity loading frame supported on strong floor. The load was applied by a 1000 kN capacity hydraulic jack and monitored by

a load cell of similar capacity. In the simple test set up the connections are subjected to combined moment and shear when loaded. As stated previously the effect of shear on connection rotation is small and can be ignored[8].

5.3 STANDARD DUCTILE CONNECTION

Connection standardisation has been identified as an important component in the campaign to deliver efficiency gains at all stages of the steelwork design and production process. The arguments are well rehearsed and widely accepted. They apply as much to moment connection as to any other.

The range of standard ductile connection details developed at the Steel Construction Institute was originally based around five bolt configurations, with either flush or extended end plate in two standard widths. Bolts are M24 or M20, 8.8. Figure 5.2 illustrates the range for M24 bolts; for M20 bolts the geometry is the same except that end plate thickness is one size down, e.g. 12 mm in place of 15 mm.

5.4 TEST PROGRAMME

A program of tests involving six standard flush end plate connections was planned which covered the following variables:

- two beam depths;
- two connection details;
- two column sizes;
- two bolt sizes (M20 and M24, 8.8).

Details of the test specimens are given in Figure 5.3 (a) and (b), Figure 5.4 and Table 5.1. Mackintosh Steel Structures, a local steel fabricator, was the supplier of the column stubs and beams with welded end plates. No attempt was made to control material or workmanship of the specimens, except punched (not drilled) holes were specified. In fact holes in end plates only could be punched; in column flange they had to be drilled. Weld contraction induced some convexity in the end plate, but it was minimised by good fabrication technique. It is unlikely that this

'initial imperfection' had much effect on the ultimate resistance of the connection, but it might have exerted some influence on the ductility and rotational stiffness. The test specimens were assembled in the Laboratory, using podger spanner to tighten the bolts.

5.5 INSTRUMENTATION AND MEASUREMENT

The most important characteristic of a semi-rigid connection is the relationship between the moment, M, transmitted by the connection and the rotation, ϕ, between the members connected at the connection. Joint rotation is defined as the change of angle between column and beam centre lines. Although the importance of correct measurement of these angular changes has been stressed by different researchers, there is still no standard method of measurement. During the past fifty years of research on semi-rigid connections various techniques have been devised to measure the moment-rotation characteristics. In the investigation carried out by the author, rotation was measured separately on each side of the column by two independent means, a pair of dial gauges and a pair of displacement transducers. A steel bar of square section was rigidly connected to the column web at position A and a steel angle section was attached to each of the beam webs at B, as shown in Figure 5.5. Point A was located in the column at the intersection of column and beam centre lines, whereas point B was positioned on the beam centre line very close to the welded end plate. Two dial gauges mounted on magnetic stands were set up on the beam attachment at 300 mm distance apart with their pointers resting on the column attachment. A pair of displacement transducers on magnetic stands were supported on a rigid steel frame with their pointers resting on the beam attachment at 300 mm distance apart. The steel frame was fixed to the laboratory floor at a short distance in front of the test specimen as shown in Figure 5.6 (a), (b), (c)[32]. Similar arrangements were made on either side of the column to measure the joint rotation. At any applied load the difference between the two dial gauge readings or two displacement transducer readings in mm divided by 300 mm represented the rotation

of the connection. The moment acting at the connection corresponding to an applied load is calculated by multiplying the support reaction (half of the applied load) by the distance between the roller support and the face of the column flange. The load cell and displacement transducers were connected to datalogger.

In order to determine the stress distribution, seven strain gauges were mounted on the specimens at locations shown in Figure 5.7. Two strain gauges were attached to the column web in line of the beam compression flange, one near the column flange and the other at the centre line of column web. These two strain gauges were meant to monitor the compression of the column web. Five strain gauges were located in the tension region of the connection along the bolt centre line, three on the column flange and two on the end plate. In the tests the bolt forces were computed by means of 3 strain gauges attached at 120 degree interval to the shank of the bolts between the threaded region and the head[11]. The strain gauges were mounted longitudinally in 1mm deep recesses milled in the bolt shank as shown in Figure 5.8. Only bolts in the tension region were strain gauged. The leads from the strain gauges passed through holes bored in the bolt head and were connected to a datalogger.

A sheet of carbon paper sandwiched between two sheets of cartridge paper was interposed between the end plate and column flange on each side. The purpose of the carbon paper was to map the contact area at the interface.

5.6 TEST PROCEDURE

As stated previously, each test specimen was lined up on the laboratory floor and assembled together by tightening the bolts with a podger spanner. It was then placed in the test frame and aligned accurately using a theodolite.

In order to measure the rotation of the connection, steel arms were connected to the column and beam webs and levelled using a precise engineering level. The dial gauges and displacement transducers were then mounted at the predetermined positions.

The load cell, the displacement transducers and strain gauges were connected to an RDP Translog 500 Data Logger which was calibrated before each test. Once the instrumentation was completed and checked, zero load readings were taken for all dial and strain gauges, the displacement transducers and load cell.

The load was applied at the top of the column stub through a hydraulic jack. Each specimen was loaded and unloaded once in the elastic range before being finally loaded to destruction. Load was applied gradually with constant increment in the elastic range. In the plastic region the load increment was gradually reduced. At every load increment the appropriate readings were taken and the axial load was kept constant during the measurement period. In the plastic region there was creep in the metal causing dial gauges to run and displacement transducers to move. Hence adequate time was allowed for dial gauge and displacement transducer movements to stop or become imperceptible. It was observed that there was a certain degree of slackness in the bolts after the initial loading and unloading. This was due to welding distortion of the end plate which prevented complete contact between the end plate and column flange.

Once the test was completed the instrumentation set up was removed and photographs were taken to record permanent deformation and failure mode of the specimens. The specimen was then dismembered and various components were carefully examined. Bolts and bolt holes were subjects of special examination after the test.

5.7 SUMMARY OF TEST RESULTS

In total six connections were tested under combined bending moment and shear force. In the tests bolts were hand tightened and when loaded the slip of the end plate caused the bolts to be in shear and bearing. It is however, reasonable to assume that in the tension region bolts were predominately subjected to tension due to moment. Furthermore, in small to medium span beams the two bolts in the compression region are adequate to resist the end shear from the beam. Therefore,

the bolts in the tension region may be assumed to transfer bending moment from the beam to the column flange and web through the end plates.

The factors which control the connection rotation are the end plate deformation, stretching of bolts and column flange and web deformation. In general if the end plate is relatively thin, the first sign of deformation is the separation of the end plate and column flange in the tension region. At subsequent loading, as the lack-of-fit is overcome, the end plate is forced into double curvature and separation between the end plate and column flange at the position of beam tension flange ensues. Also bolts in the tension region start to stretch. In this case the rotation is mainly due to the end plate bending. If, however, the end plate is thick enough to resist any significant deformation, connection rotation is attributed to column flange and web deformation and bolt extension. The column flange behaviour is like the plate fixed on one side when subjected to concentrated loads from the end plate through the connection bolts. In addition, the end plate serves to restrain the bending of the flange by providing a degree of fixity at the bolt location and other points of contact. This results in the column flange bending away from the column web. Column web is subjected to compression and tension. As a result of compression, column web may buckle.

The summary of test results is presented in Table 5.1. Connections T1, T2 and T3, each with one row of bolts in the tension region failed due to thread stripping. Buckling of column webs was observed in each of the connections T4, T5 and T6, with two rows of bolts. The combined moment-rotation curves for the six connections are presented in Figure 5.9.

Columns and beams sizes are identical in tests T1, T2 and T4, 254x254UC89 for columns and 457x191UB74 for beams. The differences between tests T1 and T2 lie in thickness of the end plates and the diameter of bolts. The only difference between tests T1 and T4 is the number of bolt rows, specimen of test T1 had a single row and test T4 had two rows of M20 bolts in each of the tension and

compression zones. Failure moments and rotations at failure differ considerably as shown in Figures 5.10 and 5.11 and Table 5.1.

In each of the tests T3, T5 and T6, the column size is 254x254UC73 and the beam size is 406x178UB60. Tests 3 and 5 differ in the number of bolt rows while test 5 and 6 differ in the thickness of end plate and bolt diameter. The failure moments and rotations at failure do not differ a great deal as shown in Figures 5.12 and 5.13 and Table 5.1.

5.8 MOMENT-ROTATION CURVES

The moment-rotation characteristic of a connection is expressed by a curve which plots the moment, M, transmitted by the connection against the rotation, ϕ, of the connection. For an ideally rigid joint the rotation is zero and the M-ϕ relationship is represented by the y axis of the graph. In the case of an ideally pinned connection the moment transmitted is zero and the relationship is expressed by the x axis. In practice connections which are termed as rigid exhibit some degree of rotation whereas connections which are classified as pinned offer appreciable moments of resistance. All practical joints differ from the ideal connections and can be termed as semi-rigid connections.

Moment-rotation curves are the product of a complex interaction between the connection components with significant contribution from a number of parameters. The components which contribute significantly to the connection rotation are as follows:

(a) end plate;

(b) column flange;

(c) bolts.

Each of these components has unique material properties and its contribution depends on its position within a connection. There are other components which also affect connection rotational behaviour, such as column web, beam flange and web,

welds and nuts. However, their effect on connection rotation is generally small and may be ignored.

The moment-rotation curves of all connections tested were found to be nonlinear through their entire loading history irrespective of their material and geometrical properties. Nonlinearity in the lower load range was caused by the lack-of-fit of the combination and imperfection of the connected parts; in the higher load range it was due to the elastic-plastic material properties. The end plate distortion caused by welding prevented a full contact between the end plate and column flange. Moreover, bolts were hand tightened. Consequently, each connection possessed a certain degree of in-built slackness which could cause slip, and relative local deformation between the end plate and column flange. These deformations were not recoverable completely. Before the connections were tested to failure they were subjected once to a loading and unloading cycle to eliminate, to a certain extent, any possible imperfection.

Throughout the experimental programme bolts were hand tightened with a podger spanner. From previous investigation[11] it is known that pretensioning has little influence on the moment-rotation characteristics of the connection at higher loading. The only difference in rotation between the hand-tightening and pretensioning arises from the absence of any contribution from the extension of the bolts in the preloaded connection. Once the pretensioning has been overcome the M-ϕ characteristics become identical. Therefore, a pretensioned joint shows a stiffer rotation response to the applied moment only in the low range. As far as moment resistance of a connection is concerned, there is clearly no advantage to be gained by pretensioning of bolts.

5.9 BOLT STRAINS

The end plate is connected to column flange via four or eight bolts. In four bolt configuration, two bolts are situated in a row in each of the tension region and compression regions. In the case of eight bolts, four are placed in two rows in the

tension region and the other four again in two rows in the compression region. This pattern of bolting is adopted with the knowledge that additional bolts will not add significantly to bending strength of the connection. The symmetry of connection configuration is preferred by steel industry and is suitable for wind moment connections.

Each bolt in the tension region had three strain gauges at 120 degree interval attached to the shank of the bolts between the threaded region and the head, as mentioned previously. The strains recorded in various tests are presented in chapter 6. The experimental results clearly demonstrated that the bolts were not subjected to pure tension and many of them were subjected to combined bending and direct stress. Figures 5.14 to 5.16 illustrate the test specimens T1 to T3 after they had failed by thread stripping.

5.10 PRYING FORCES

The pressure distribution between the end plate and column flange recorded in the test programme are shown in Figures 5.17 to 5.28. It is very difficult to determine the magnitude of prying forces by experimental means. The prying patterns obtained from the carbon paper show good agreement with analytical results reported in Chapter 7. However, some disagreement was observed in the tension region around column and beam webs. This disagreement was possible due to the weld distortion of the end plate and the imperfections of the connection set up in the tests. If we can eliminate these errors, the prying patterns recorded by carbon paper may be used as a good reference.

5.11 COLUMN WEB DEFORMATION

In an unstiffened connection column web plays an important role and often controls the characteristics of the connection. As most of the previous research only considered the behaviour of stiffened column section, such information are not available. However, the expense incurred and the inconvenience of column stiffening have meant that the role of column web in unstiffened connections be investigated.

In a flush end plate connection, column section is subjected to tensile force acting at the bolt locations in the tension region and compression force acting over some bearing area in the compression region. These forces are resisted by an effective length of column in both regions.

Two strain gauges were mounted on the column web in each test, one at the centre of the column web and the other very close to the column flange. Column web strains recorded in the tests are also given in Chapter 6. Photographs of specimens which failed due to column web buckling are shown in Figure 5.29 to 5.31.

5.12 TYPES OF FAILURE

Two types of failure were recorded (Table 5.1): thread stripping and column web buckling. Bolts manufactured to the British Standard BS 3692[54] are known to fail by thread stripping at a load nearly 10% less than the load required for fracture. The tests carried out by the author (Table 5.2) also confirmed the above fact.

Eurocode 3 does not include thread stripping as a possible failure mode, because the bolts manufactured to European Standards BS EN 24014 etc[55],[56],[57],[58] have different nut dimensions which prevent thread stripping. The author strongly feels that the British Industry should adopt the European Code for bolts at an early date.

5.13 ROTATION CAPACITY

The rotation capacities achieved by the tests are presented in descending order in Table 5.3. Bose and Hughes[6] argued that rotation capacity of 0.03 radians can be considered as adequate for semi-continuous plastic design of frames. If the joints fail to achieve at least 0.02 radians plastic design approach should not be adopted. The range of 0.02 to 0.03 radians represents a grey area. Rotation capacities obtained from the tests clearly indicate that five of them are qualified for semi-continuous plastic design whereas one connection with single row of M20 bolts falls within the grey area.

5.14 MATERIAL TEST

The reliable prediction of the connection behaviour depends on a number of factors including a knowledge of the material properties. Whereas, in the complete structure a local variation, for example in yield stress, may have an insignificant effect in the connection, such a local variation could have serious effects on the structural behaviour. For determining the material properties of the column flange, column web and end plate, test pieces (Figure 5.32) were prepared and tests were conducted in accordance with the specifications of European Standard BS EN 10 002-1[59]. Test pieces were cut from column flange, web and end plate respectively. Tensile testing of M20 and M24 Grade 8.8 bolts were also carried out in compliance with the specifications of British Standard BS 3692[54]. The summary of results obtained from the above tests are given in Table 5.2 and Figures 5.33 and 5.34.

It was noted after these tests had been carried out that the automatic load-extension plot which was used for obtaining the modulus of elasticity, E, for the material did not fully compensate for the stiffness of the machine; it is believed that this is the reason why the values of E obtained from the material tests were much lower than expected. It was therefore decided to ignore these results and assumed a theoretical value of E = 200 kN / mm^2 for all the analysis.

Test	Column	Beam	End plate	Bolts	Failure load kN	Failure moment kNm	Rotation at failure rad	Failure mode
T1	1 No. 254x254 UC89 1200 mm long	2 Nos. 457x191 UB74 1300 mm long	2 Nos. 510x200x12	Single row M20, 8.8	313	187.8	0.025	Thread stripping
T2	1 No. 254x254 UC89 1200 mm long	2 Nos. 457x191 UB74 1300 mm long	2 Nos. 510x200x15	Single row M24, 8.8	459	275.4	0.042	Thread stripping
T3	1 No. 254x254 UC73 1100 mm long	2 Nos. 406x178 UB60 1300 mm long	2 Nos. 460x200x12	Single row M20, 8.8	264	158.4	0.038	Thread stripping
T4	1 No. 254x254 UC89 1200 mm long	2 Nos. 457x191 UB74 1300 mm long	2 Nos. 510x200x12	Double rows M20, 8.8	465	279.0	0.053	Column web buckling
T5	1 No. 254x254 UC73 1100 mm long	2 Nos. 406x178 UB60 1300 mm long	2 Nos. 460x200x12	Double rows M20, 8.8	269	161.4	0.046	Column web buckling
T6	1 No. 254x254 UC73 1100 mm long	2 Nos. 406x178 UB60 1300 mm long	2 Nos. 460x200x15	Double rows M24, 8.8	276	165.6	0.051	Column web buckling

All flange welds 2x10 FW. All web welds 2x8 FW. All material S275.

Table 5.1 Test specimens and results

Specimen	Tensile strength N/mm^2	Young's modulus kN/mm^2	Yield stress N/mm^2	Elongation %
254x254 UC 89 Flange	460	170	344	29.3
254x254 UC 89 Web	479	162	311	26.8
End plate 12 mm	475	157	326	26.8
End plate 15 mm	461	150	307	28.1

(a) Tensile test of column flange, column web and end plates

Specimen	Tensile strength N/mm^2	Elongation %	Failure mode
M20 Grade 8.8 bolt, single nut	882	-	stripping
M20 Grade 8.8 bolt, double nuts to prevent stripping	1086	4.1	fracture
M24 Grade 8.8 bolt single nut	949	17.9	fracture

(b) Tensile test of bolts

Table 5.2 Material test

Test	Detail	Column	Beam	Bolts	Rotation at failure (rad)
T4	W3	254UC89	457UB	M20	0.053
T6	W3	254UC73	406UB	M24	0.051
T5	W3	254UC73	406UB	M20	0.046
T2	W1	254UC89	457UB	M24	0.042
T3	W1	254UC73	406UB	M20	0.038
T1	W1	254UC89	457UB	M20	0.025

Table 5.3 Rotation capacities of standard connections

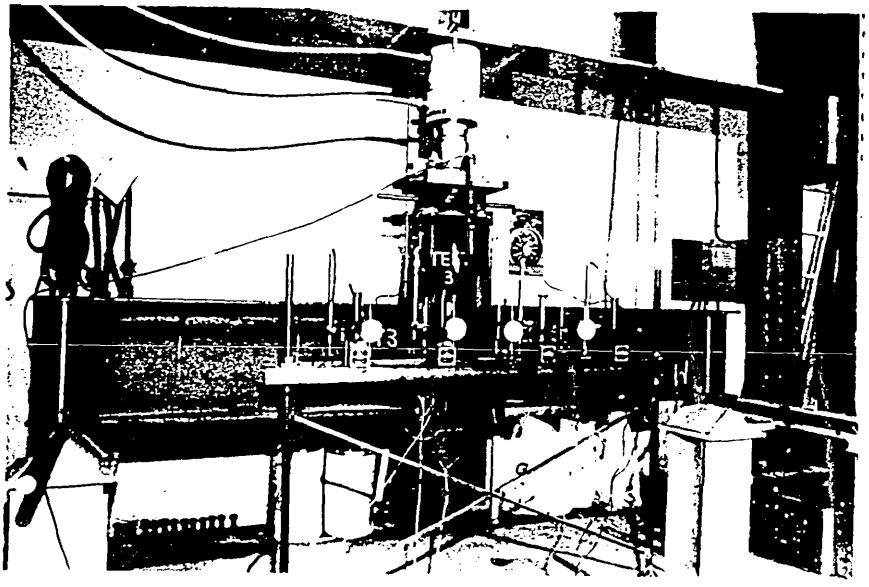

Fig. 5.1 Test set up

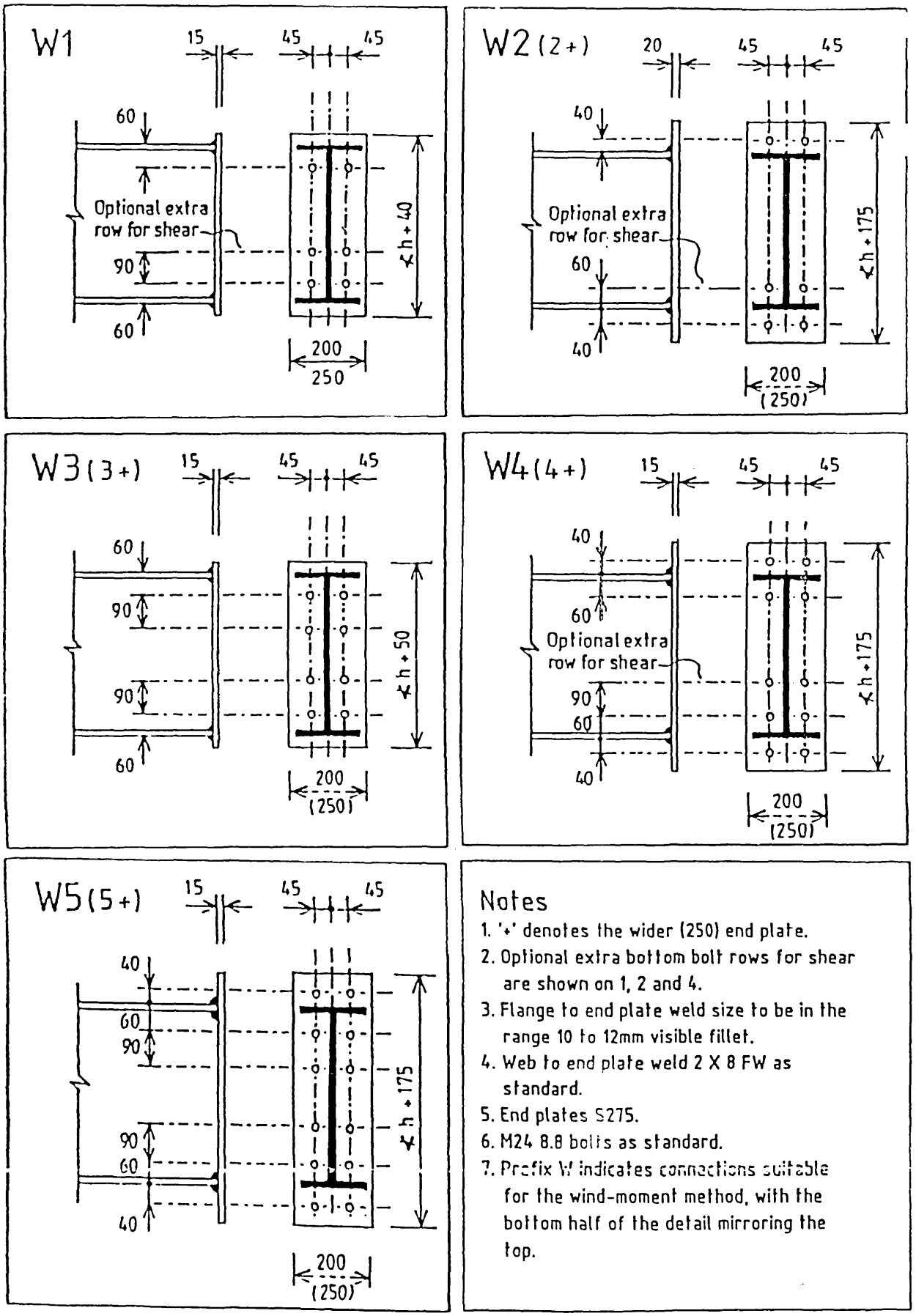

Fig. 5.2 Standard ductile connection

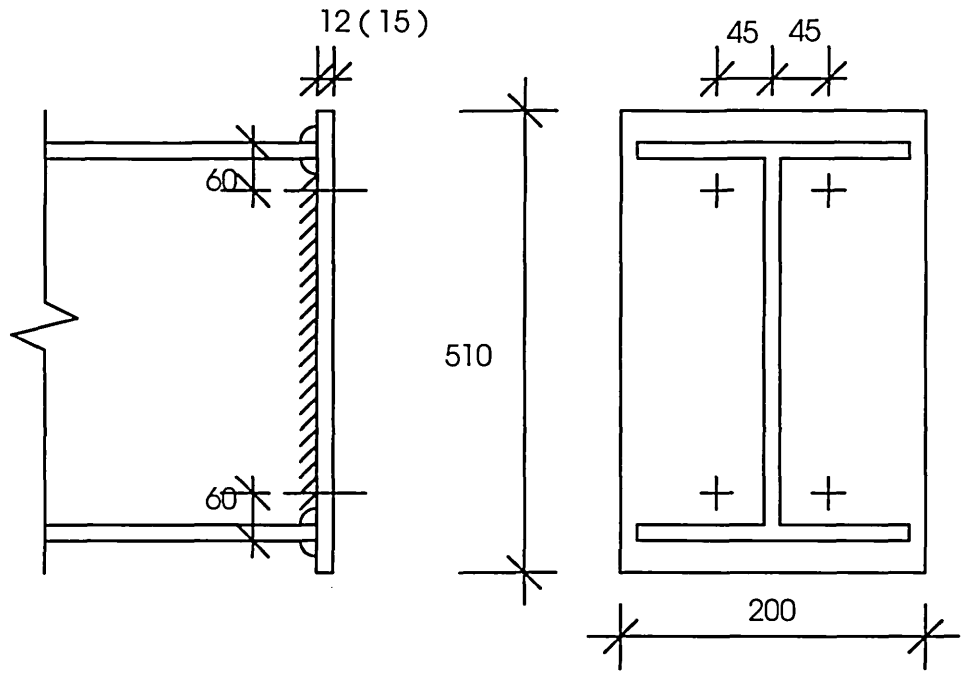

Specimens 1, 2

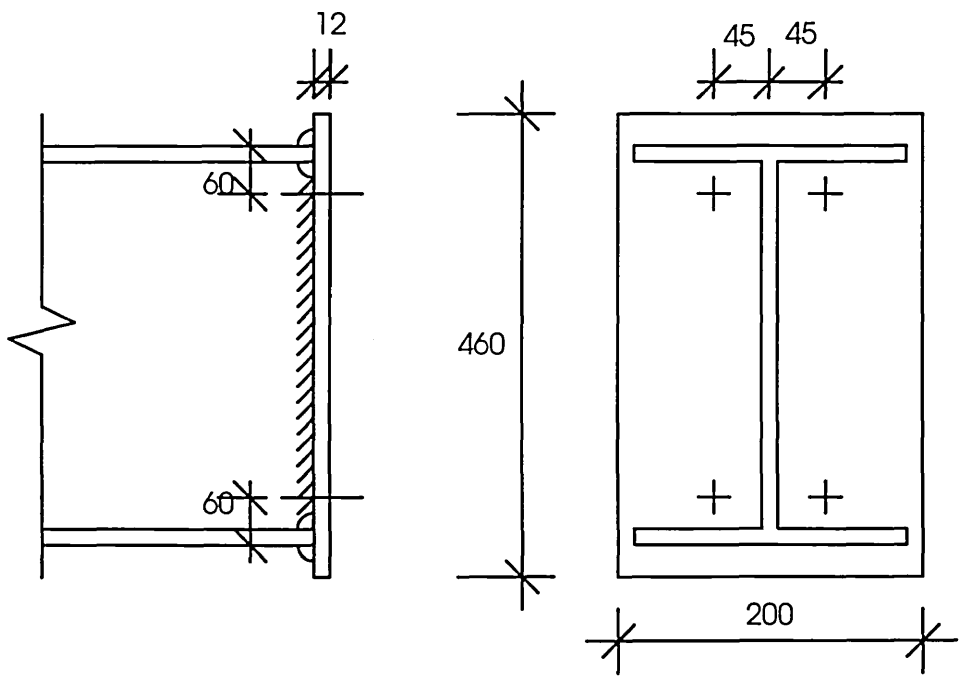

Specimen 3

Fig. 5.3(a) Test specimens

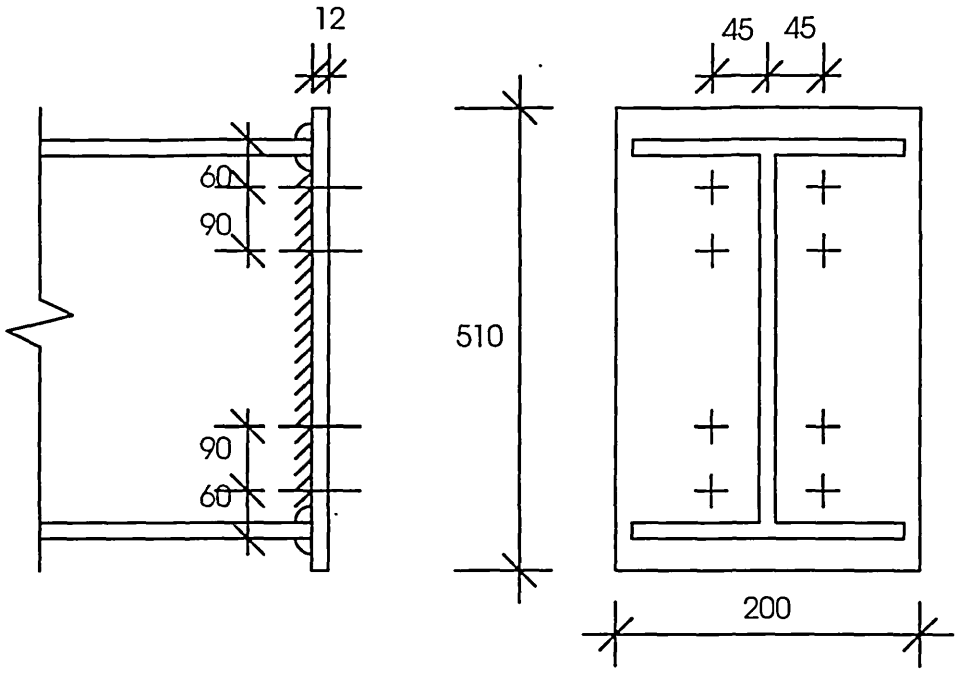

Specimen 4

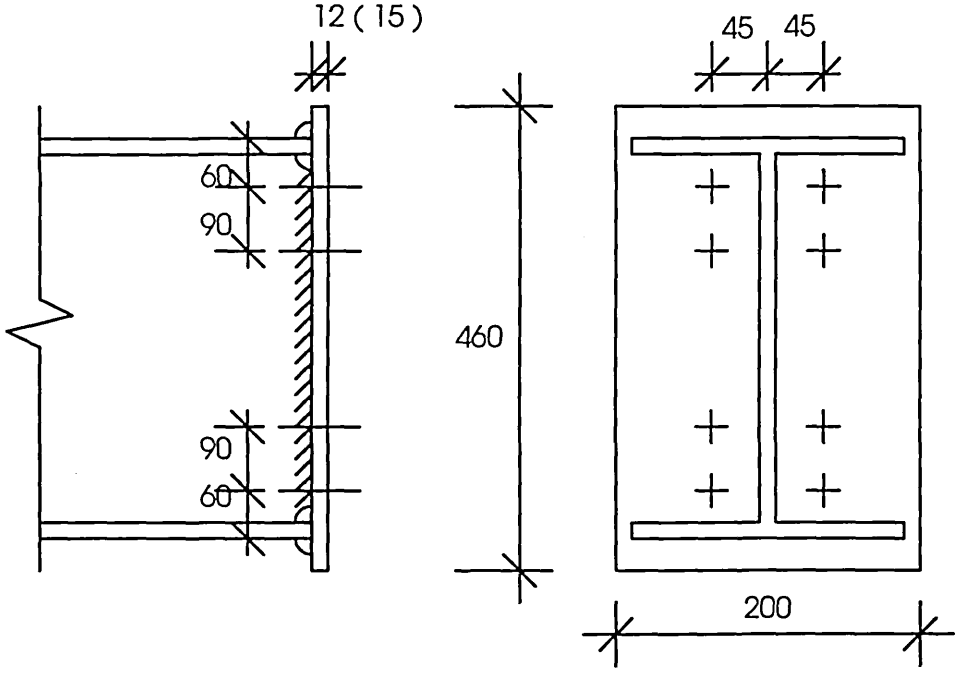

Specimens 5,6

Fig. 5.3(b) Test specimens

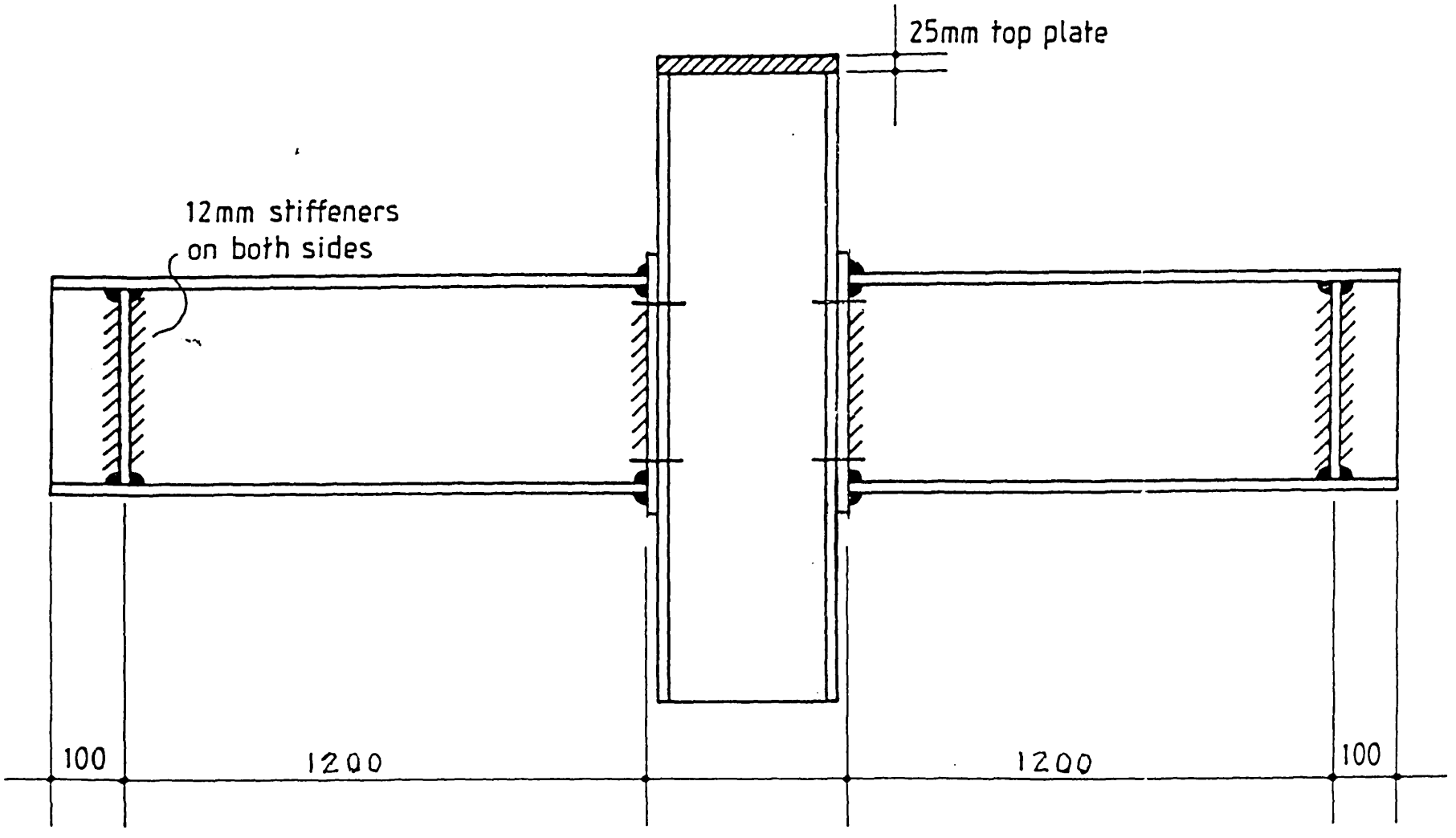

Fig. 5.4 Test specimen

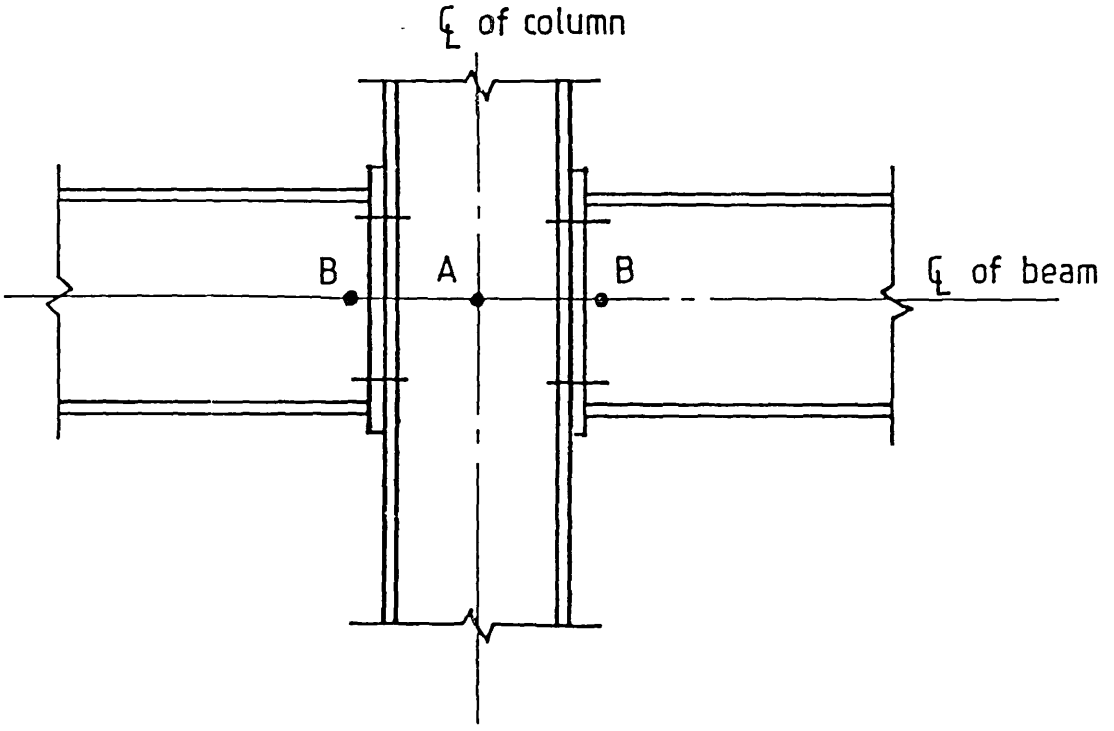

Fig. 5.5 Rotation measurement position

(a) PLAN

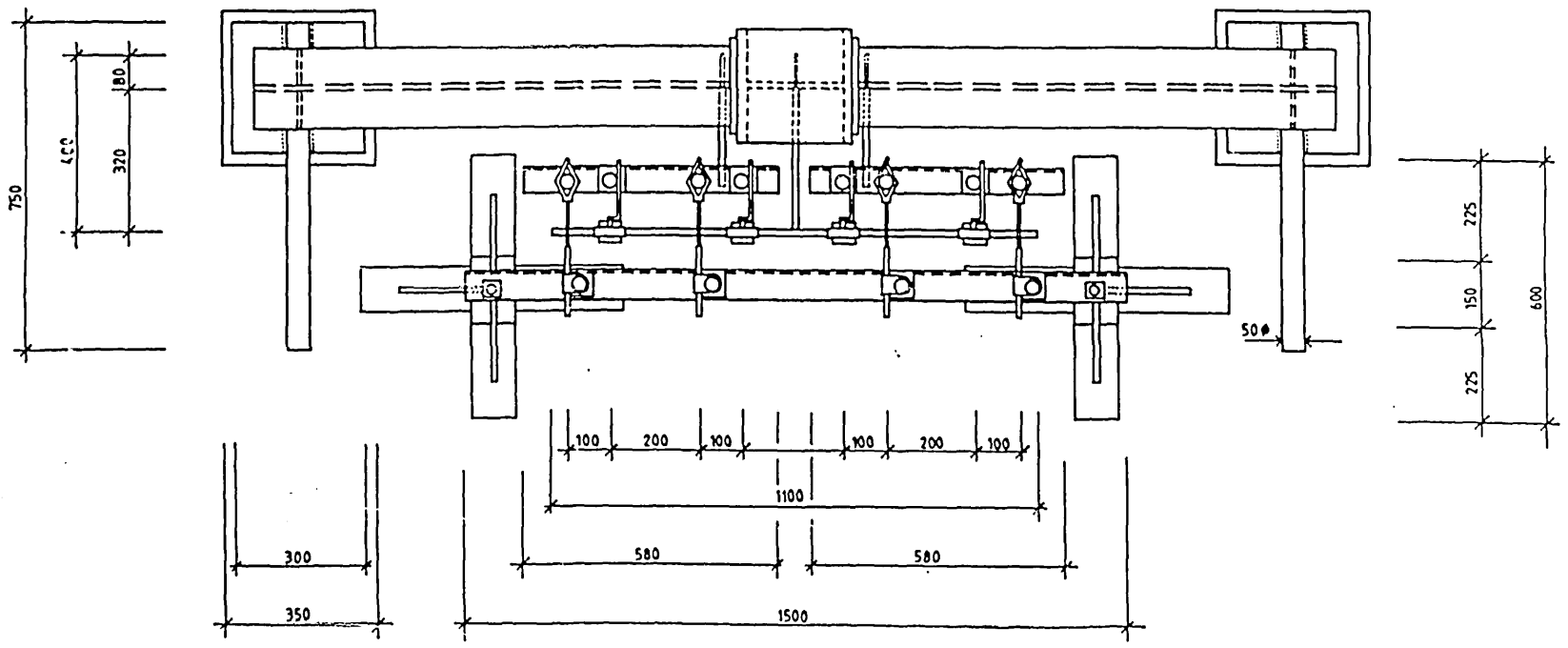

Fig. 5.6 Instrumentation set up

(b) FRONT ELEVATION

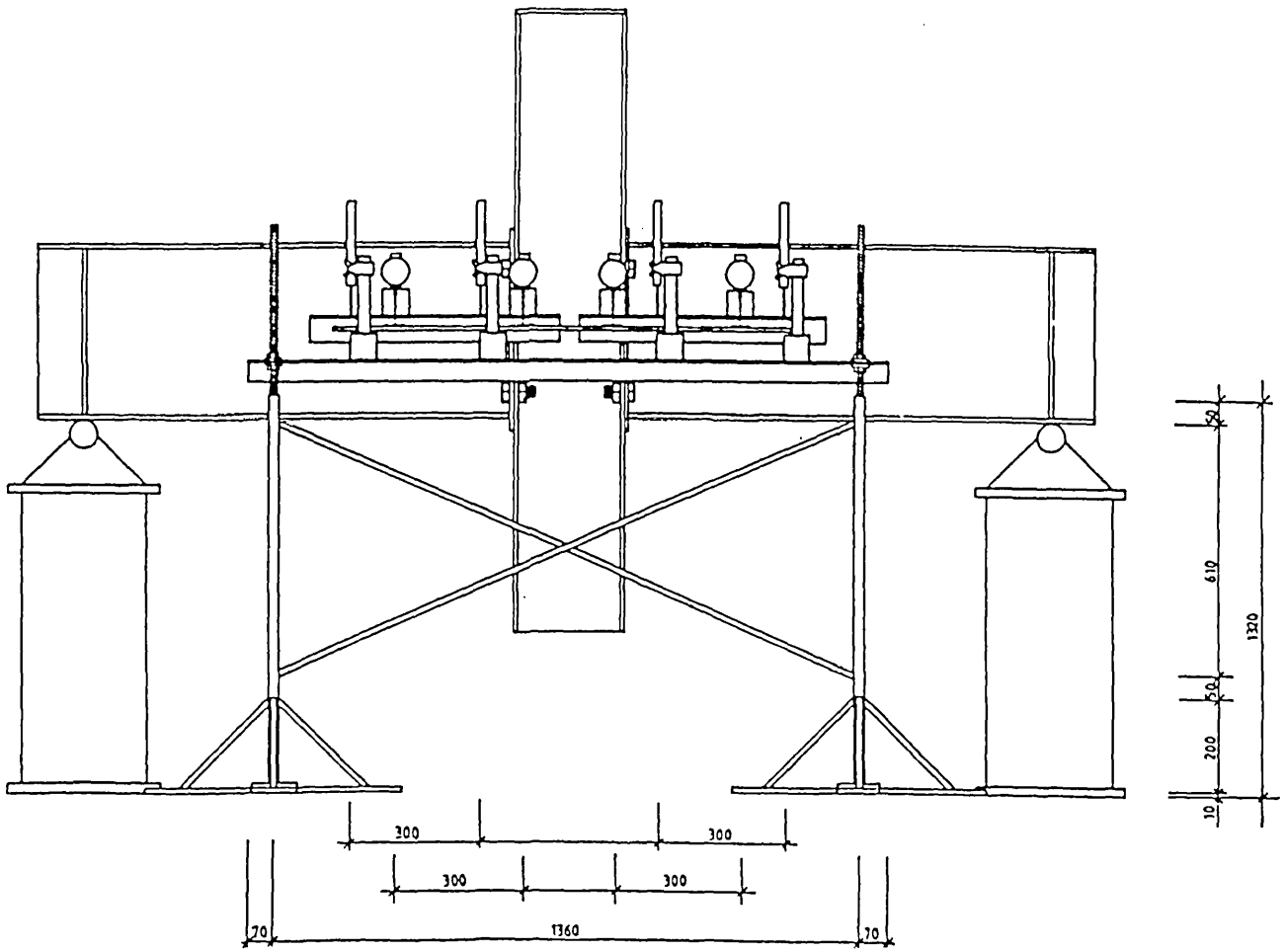

Fig. 5.6 Instrumentation set up

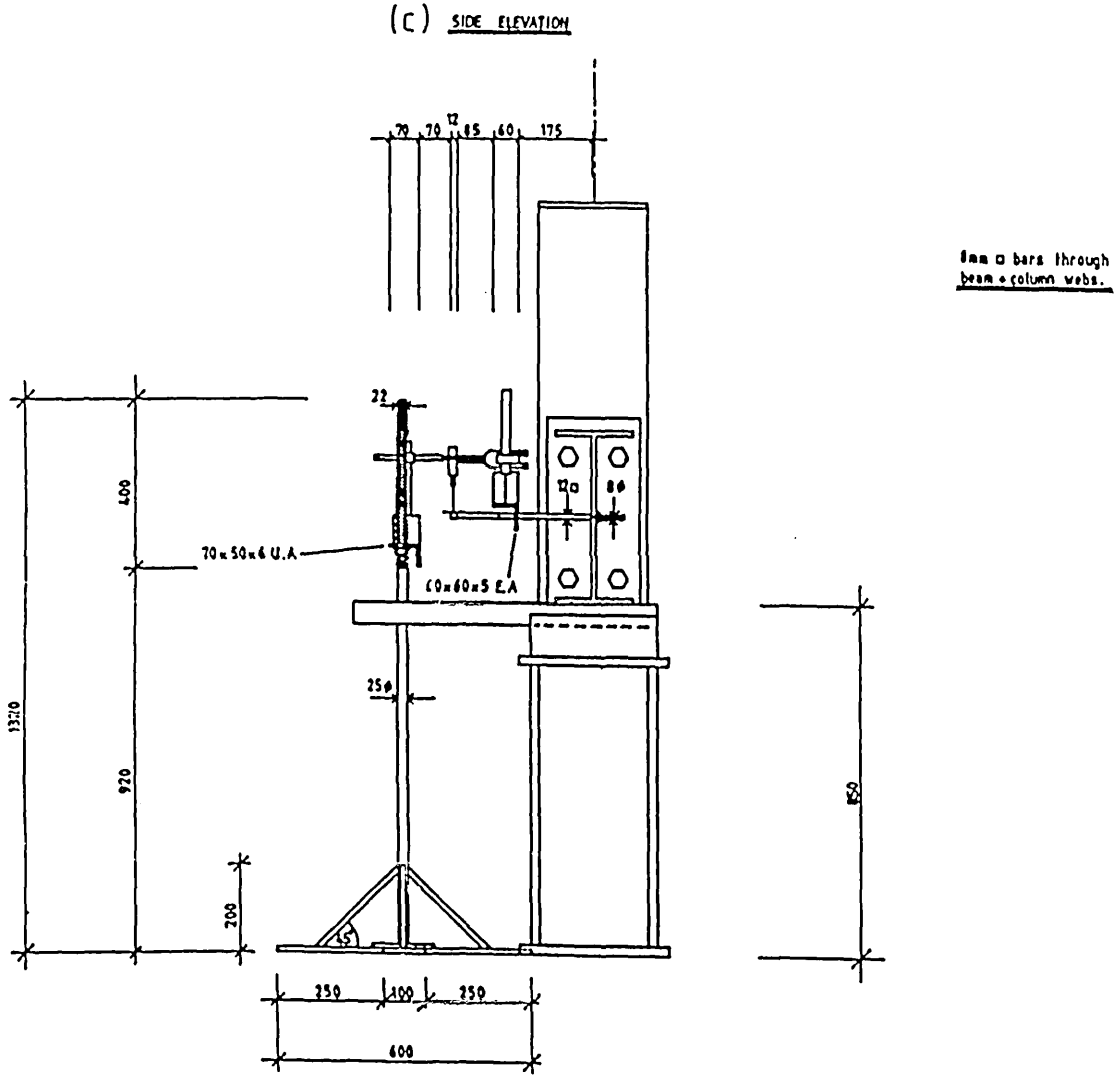

Fig. 5.6 Instrumentation set up

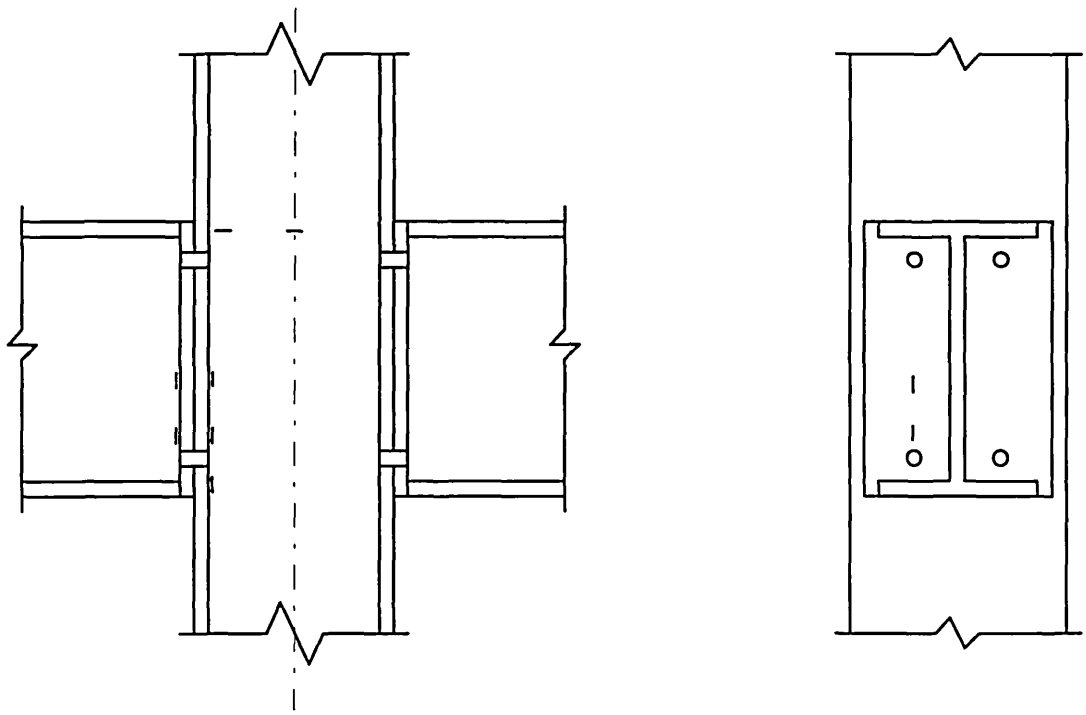

Horizontal strain gauges –

Vertical strain gauges |

Fig. 5.7 Gauge pattern for the test specimens

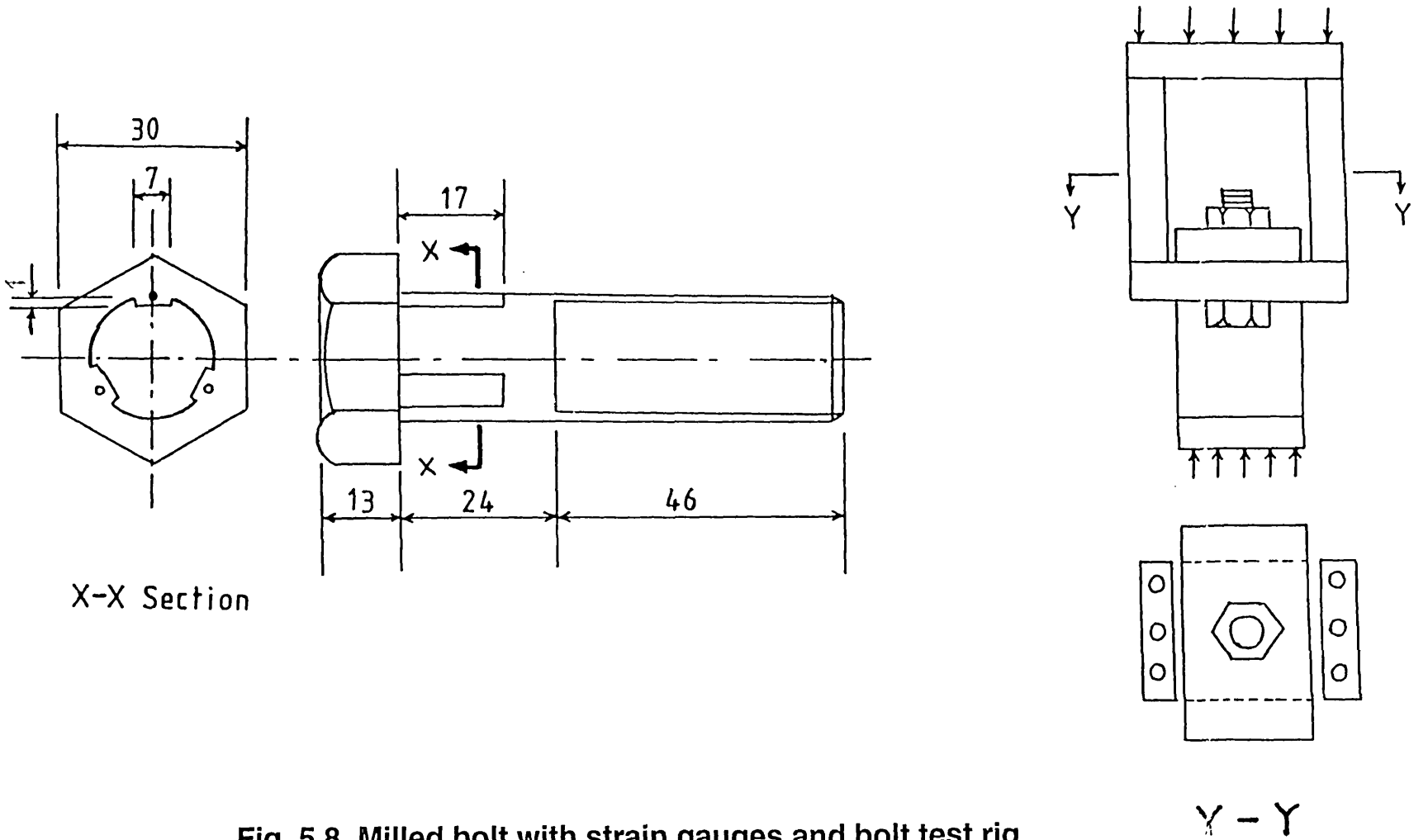

Fig. 5.8 Milled bolt with strain gauges and bolt test rig

Fig. 5.9 Moment-rotation curves for six tests

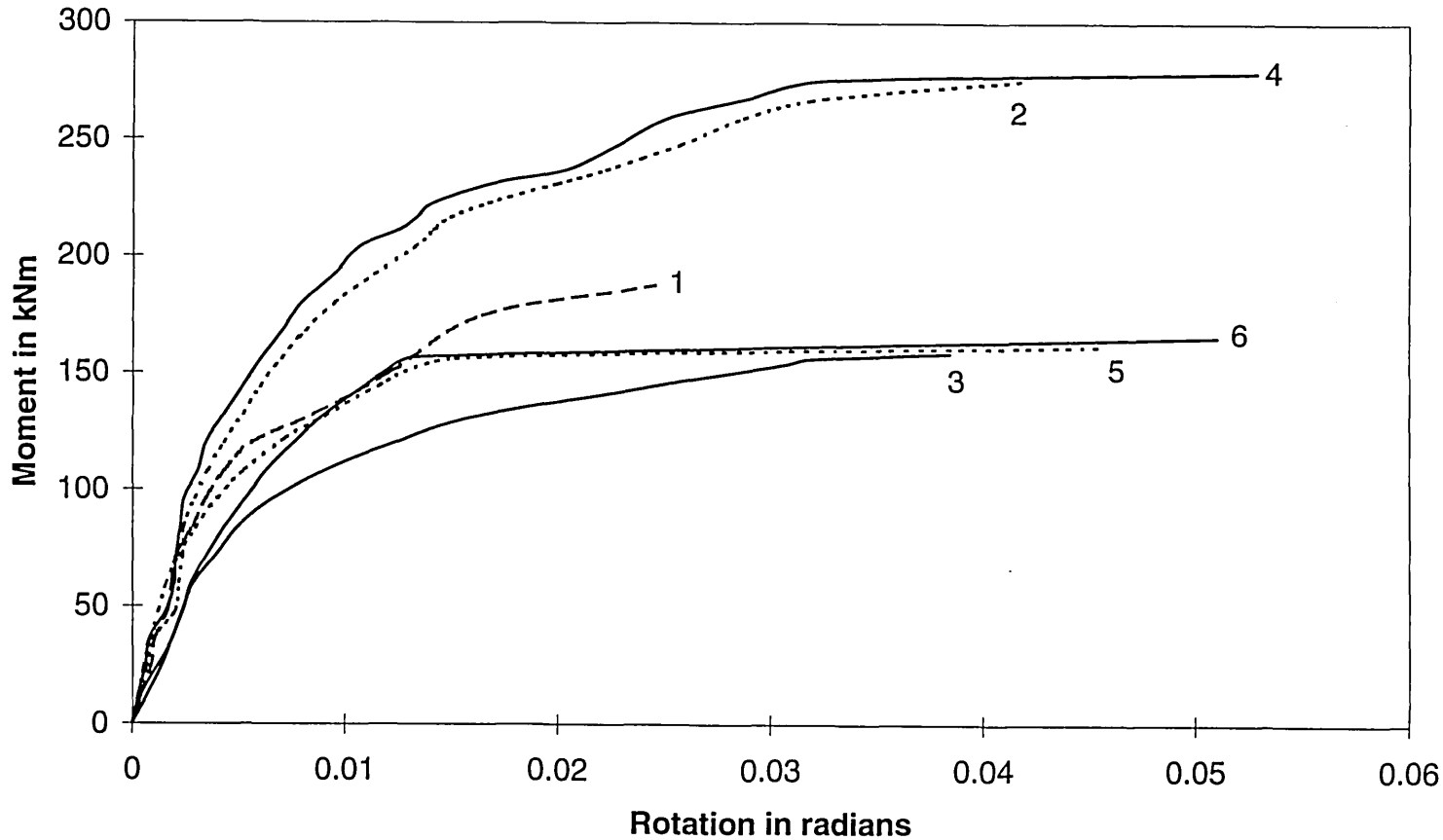

Fig. 5.10 Moment-rotation curves for tests T1 and T2
254x254UC89 column, 457x191UB74 beams

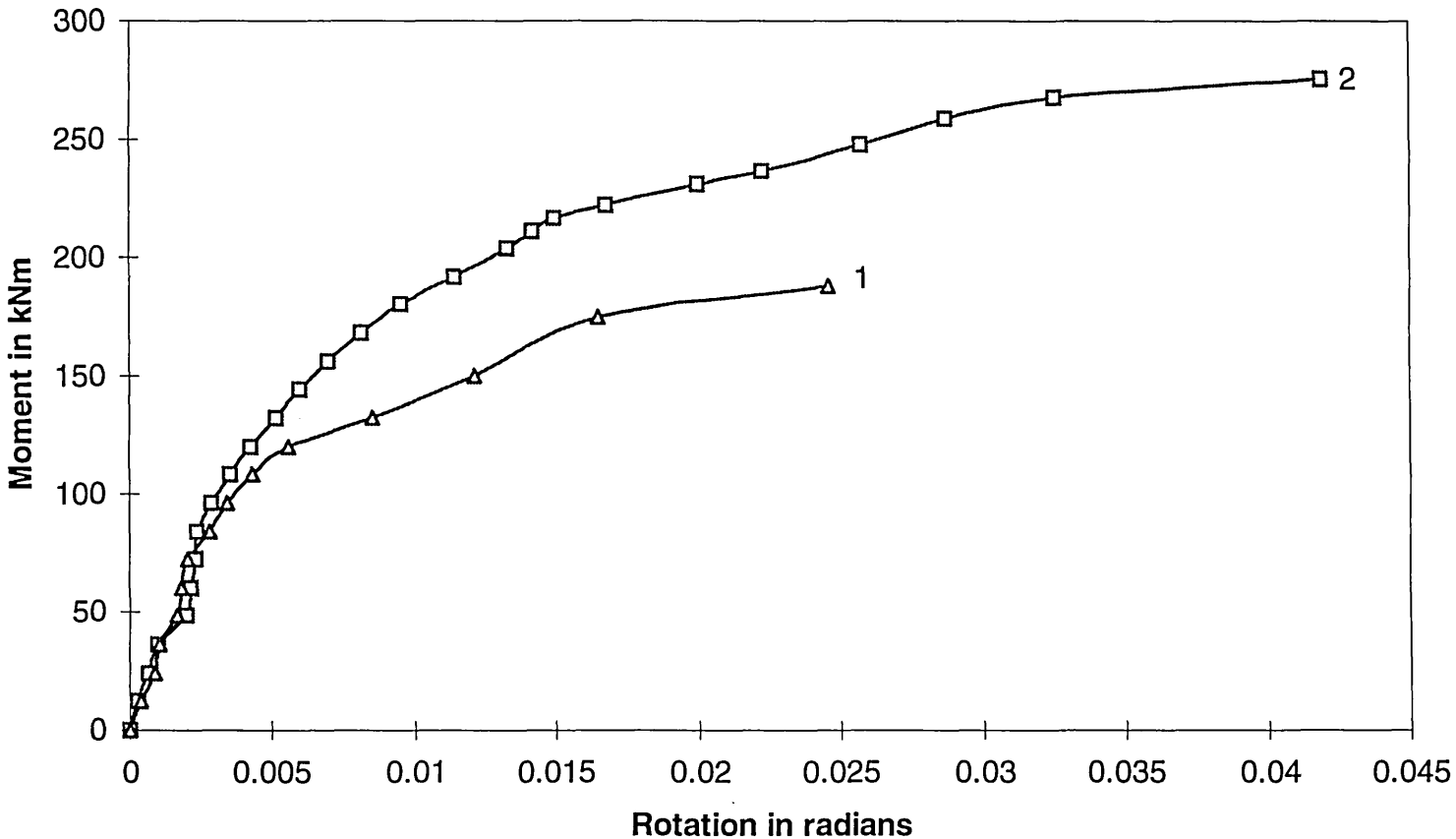

Test T1: End plate 12 mm, single row M20 bolts. Test T2: End plate 15 mm, single row M24 bolts.

Fig. 5.11 Moment-rotation curves for tests T1 and T4
254x254UC89 column, 457x191UB74 beams

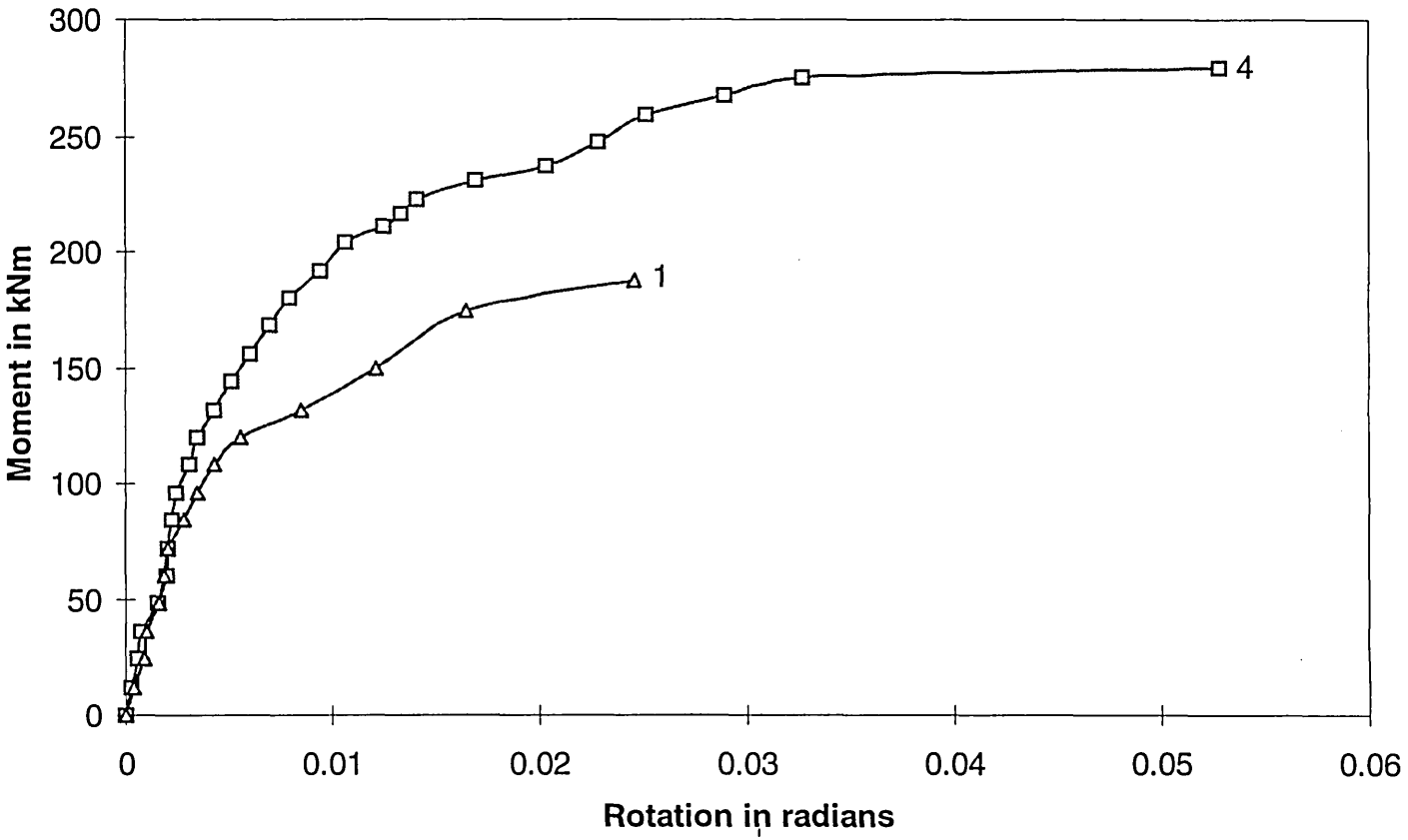

Test T1: Single row M20 bolts. Test T4: Double rows M20 bolts.

Fig. 5.12 Moment-rotation curves for tests T3 and T5
254x254UC73 column, 406x178UB60 beams

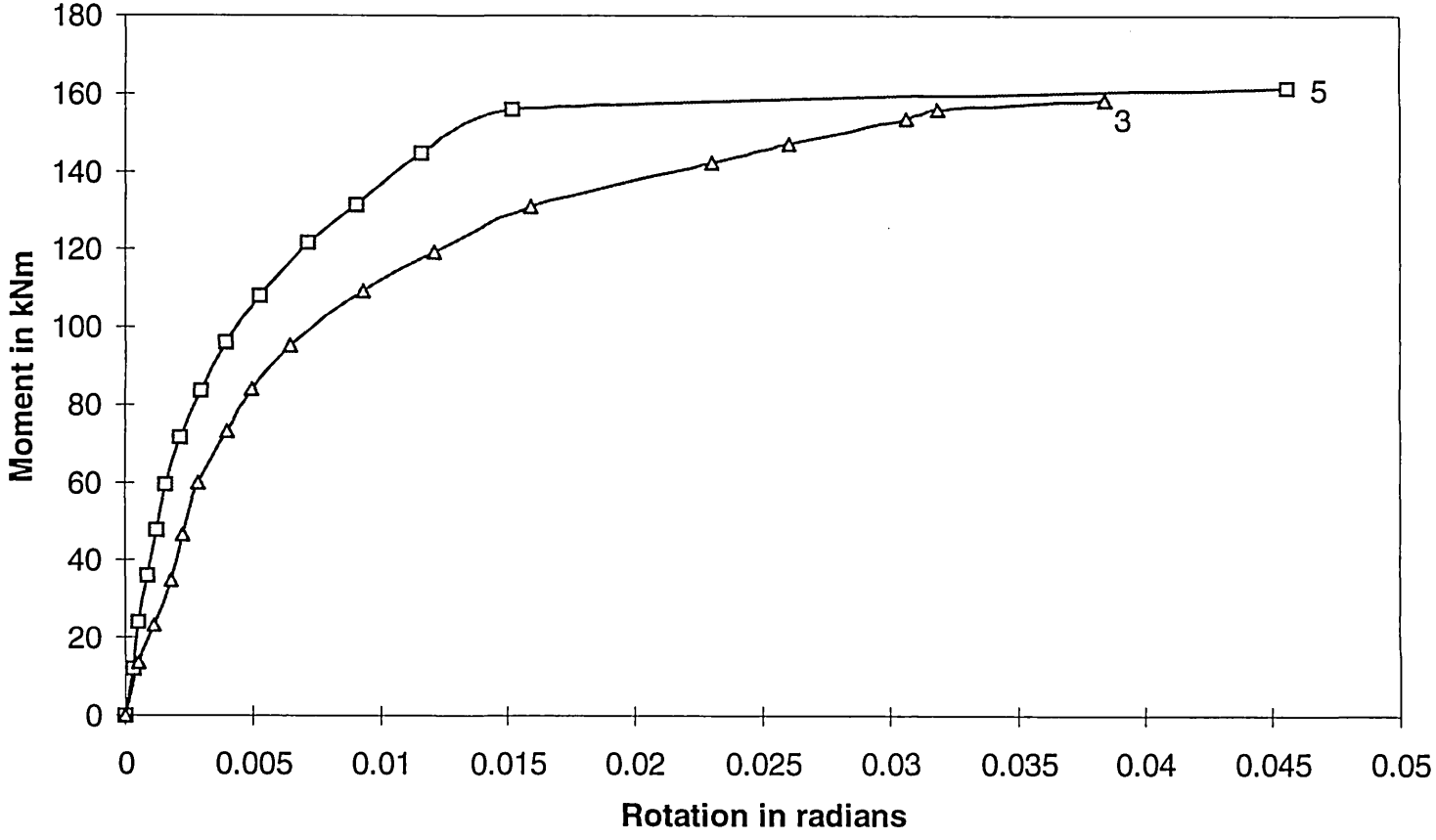

Test T3: Single row M20 bolts. Test T5: Double rows M20 bolts.

Fig. 5.13 Moment-rotation curves for tests T5 and T6
254x254UC73 column, 406x178UB60 beams

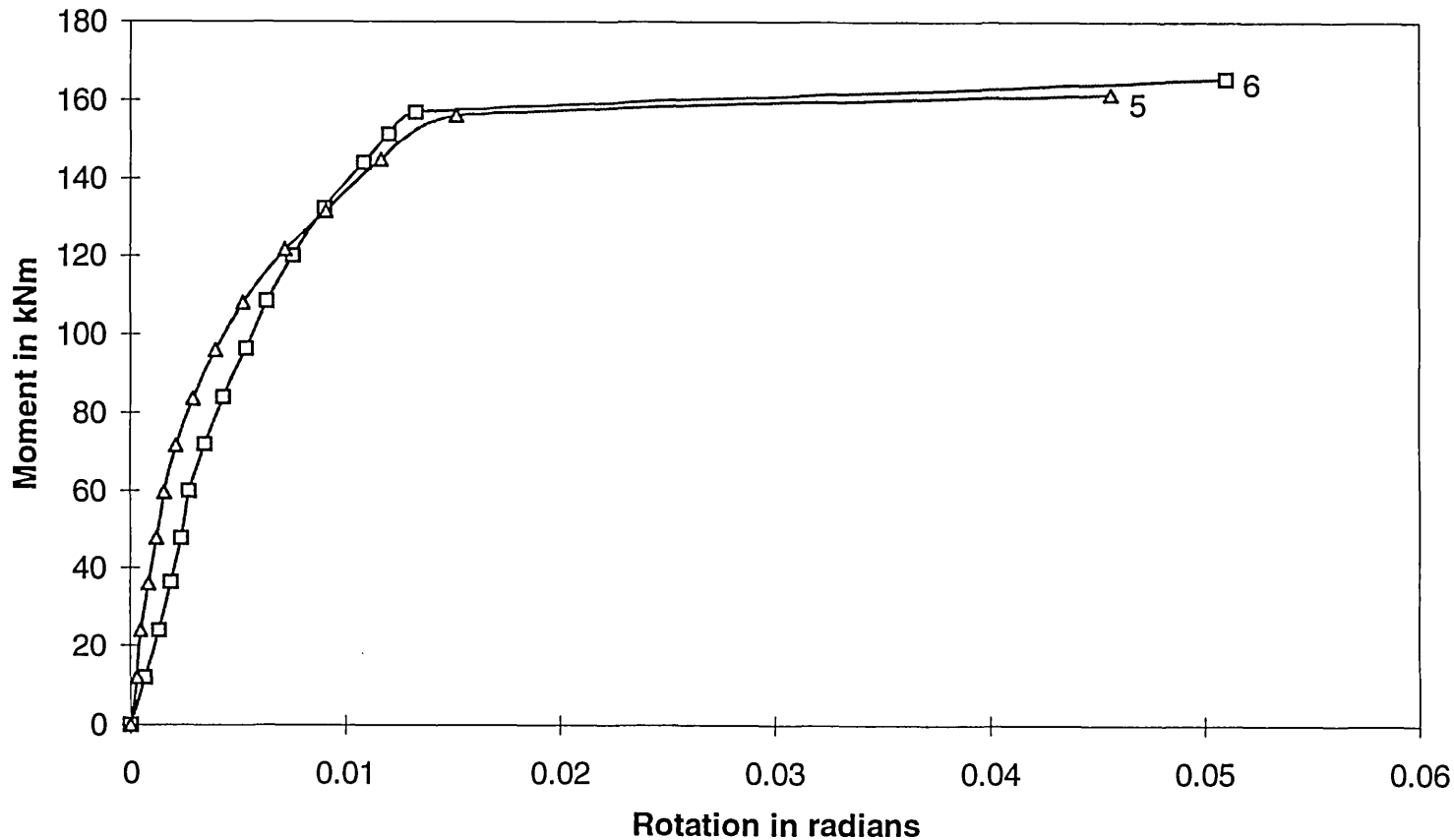

Test T5: End plate 12 mm, double rows M20 bolts. Test T6: End plate 15 mm, double rows of M24 bolts.

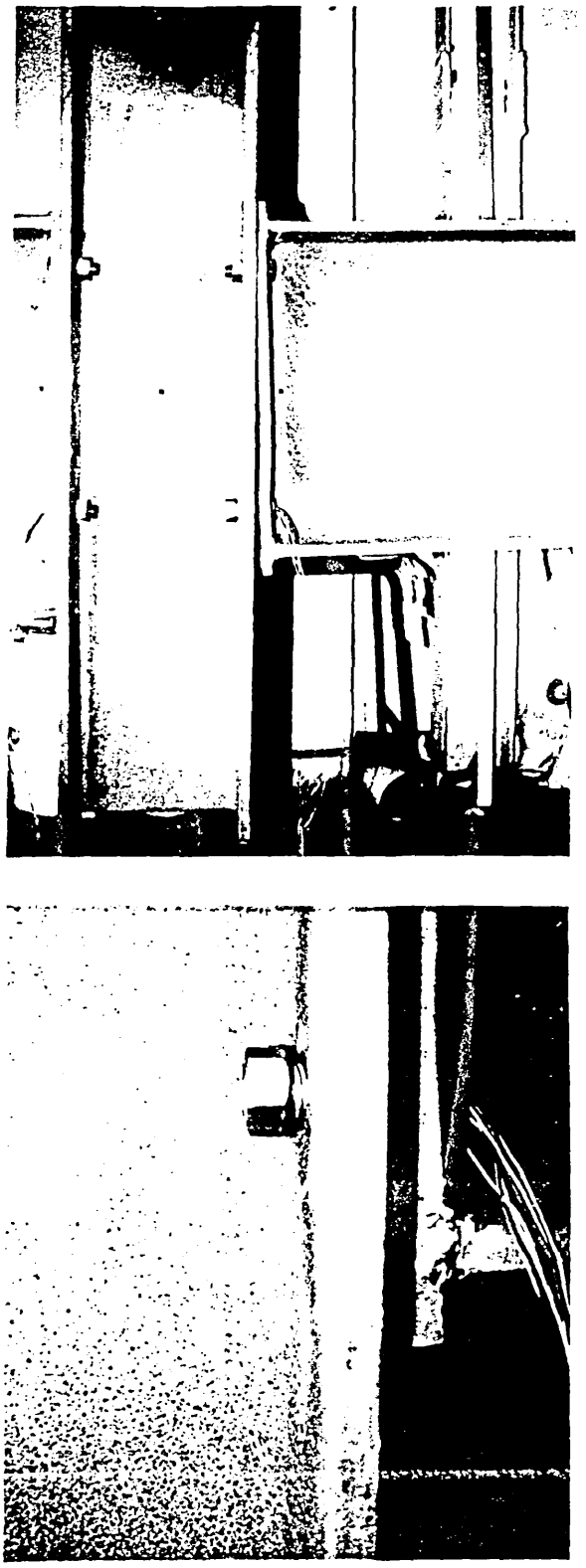

Fig. 5.14 Thread stripping in test T1

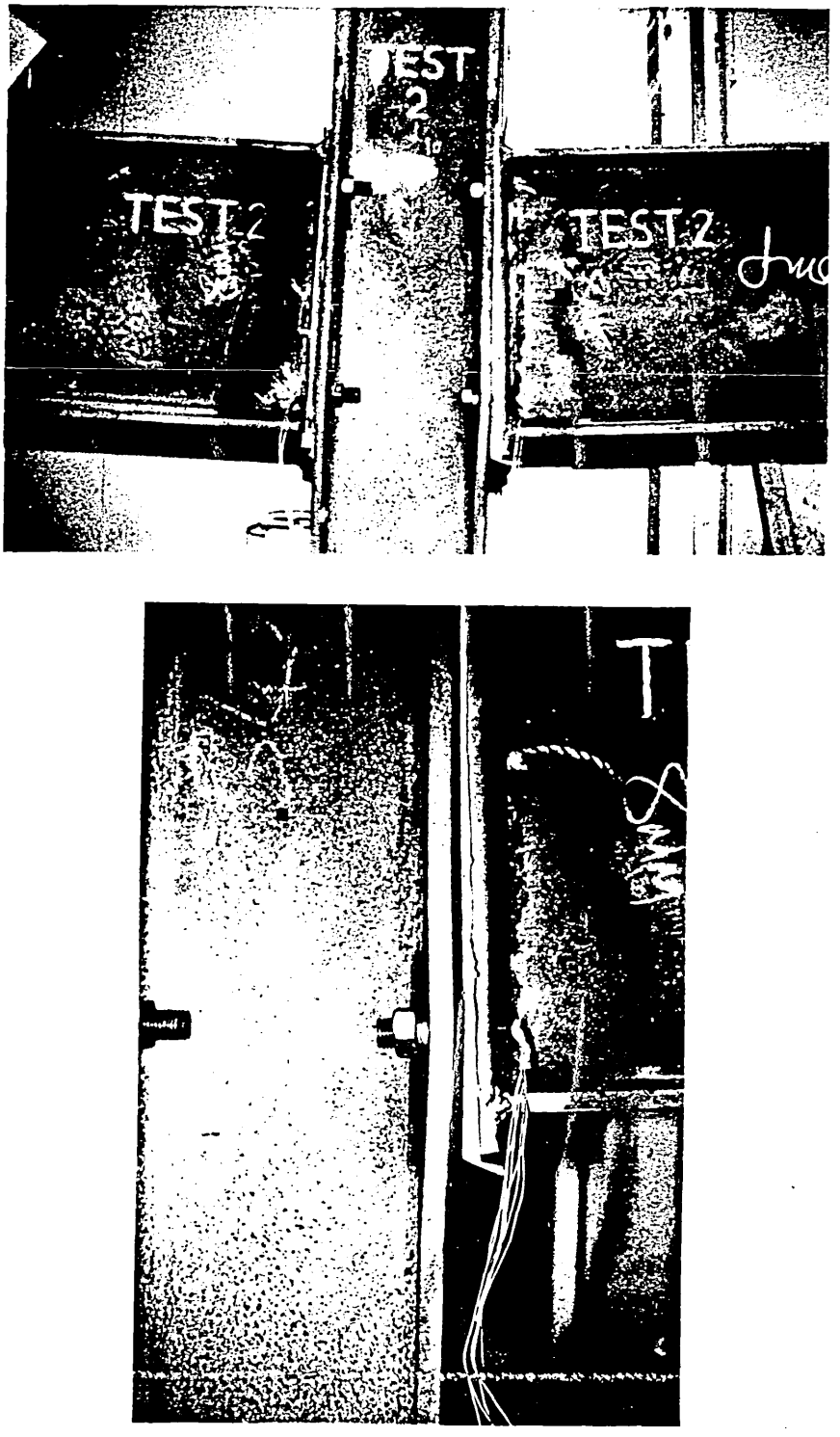

Fig. 5.15 Thread stripping in test T2

Fig. 5.16 Thread stripping in test T3

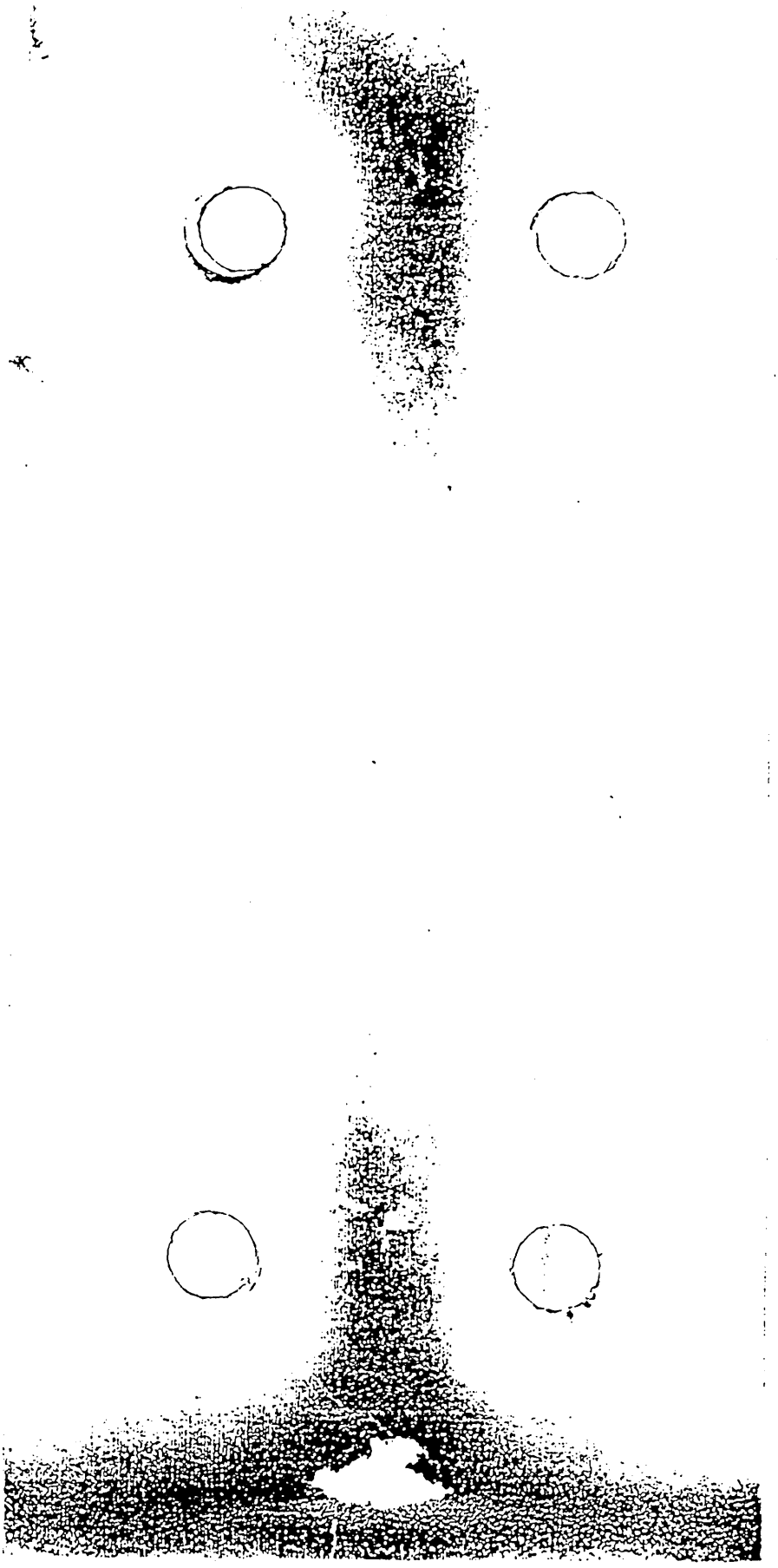

Fig. 5.17 Prying pattern, test T1 (left side)

Fig. 5.18 Prying pattern, test T1 (right side)

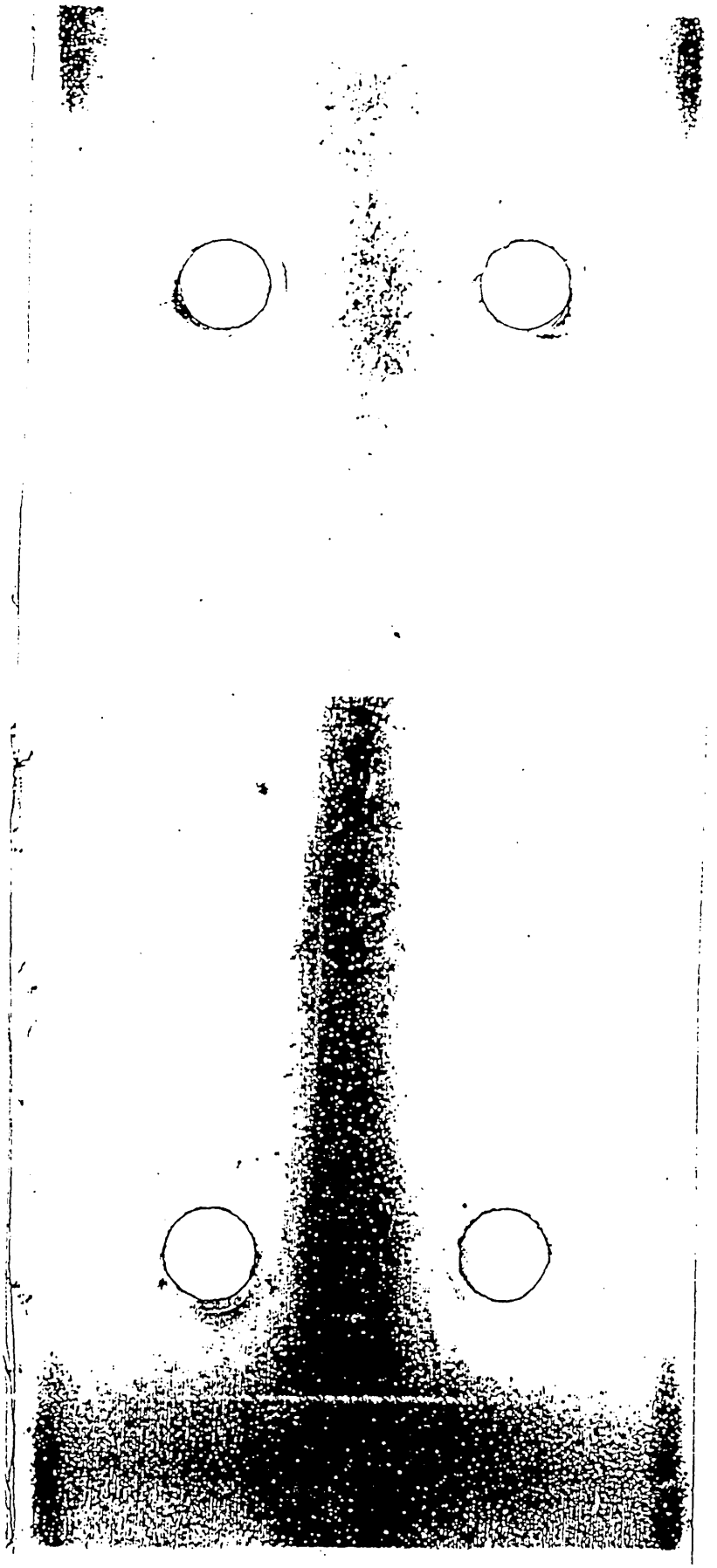

Fig. 5.19 Prying pattern, test T2 (left side)

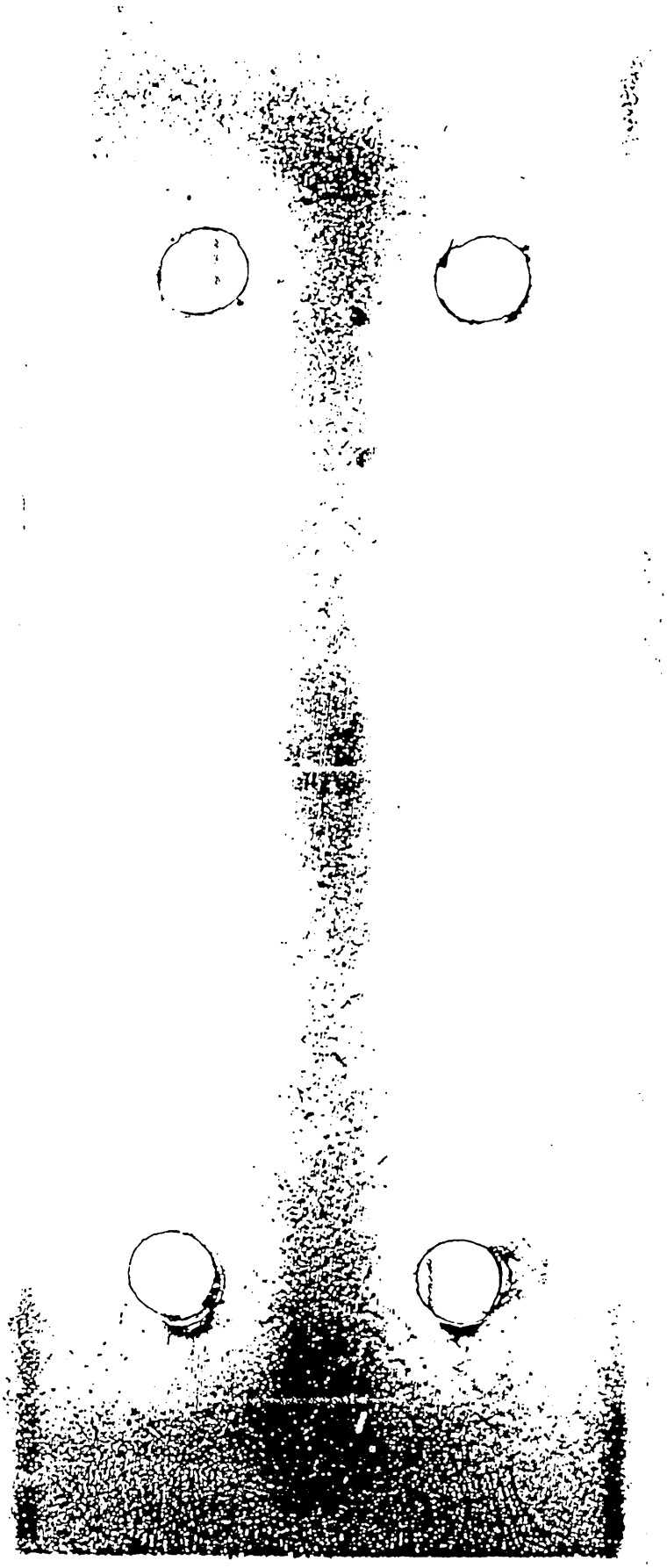

Fig. 5.20 Prying pattern, test T2 (rigth side)

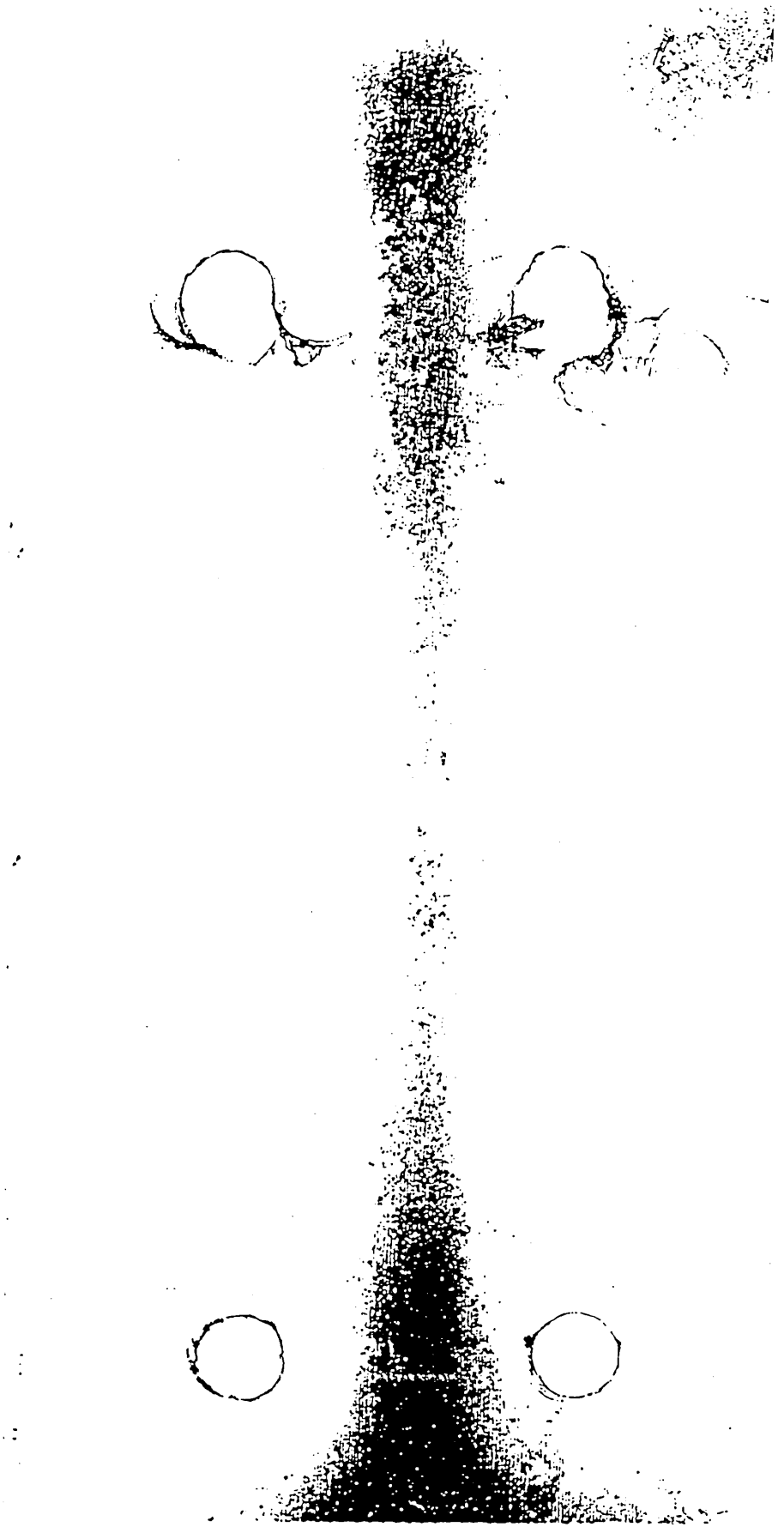

Fig. 5.21 Prying pattern, test T3 (left side)

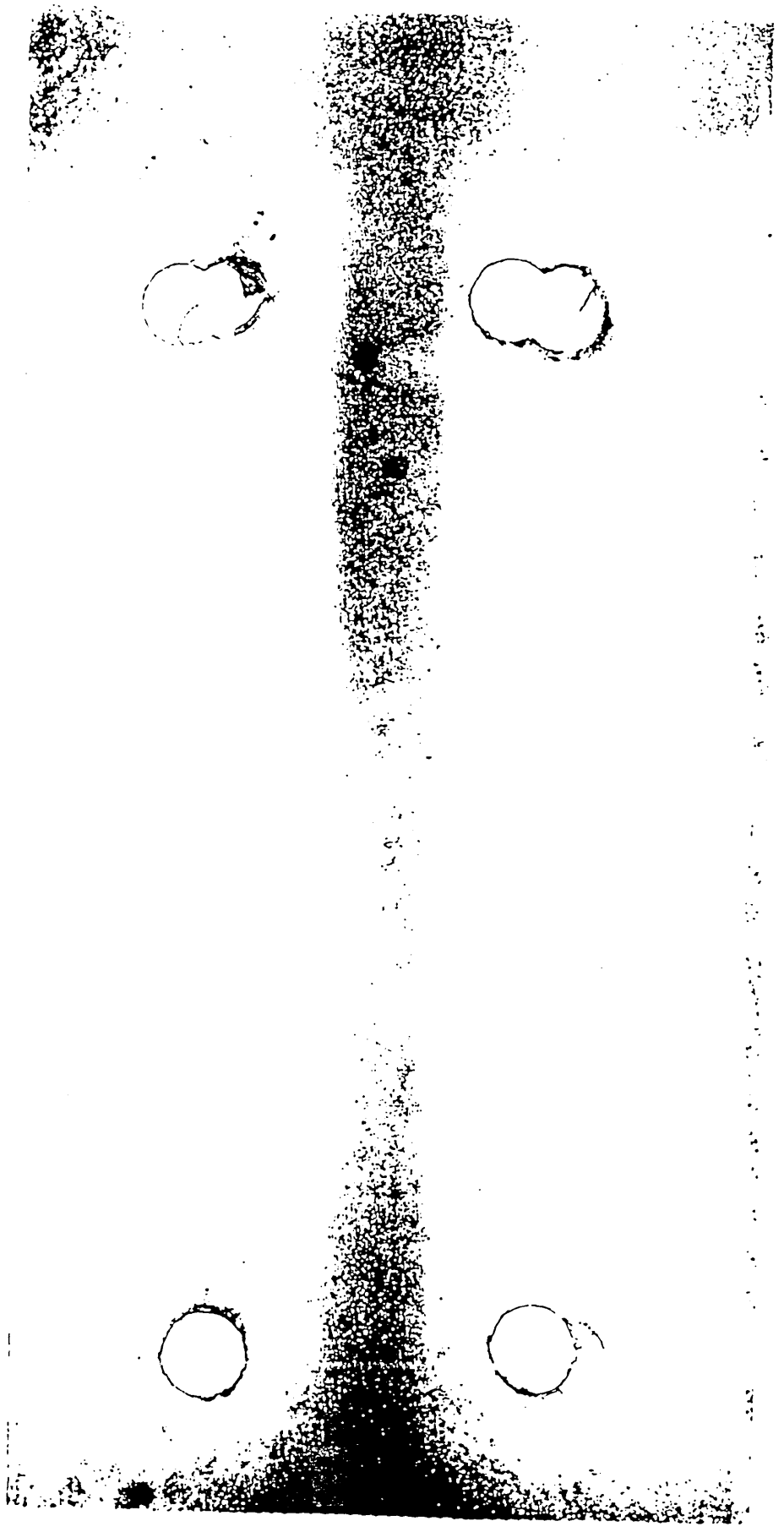

Fig. 5.22 Prying pattern, test T3 (right side)

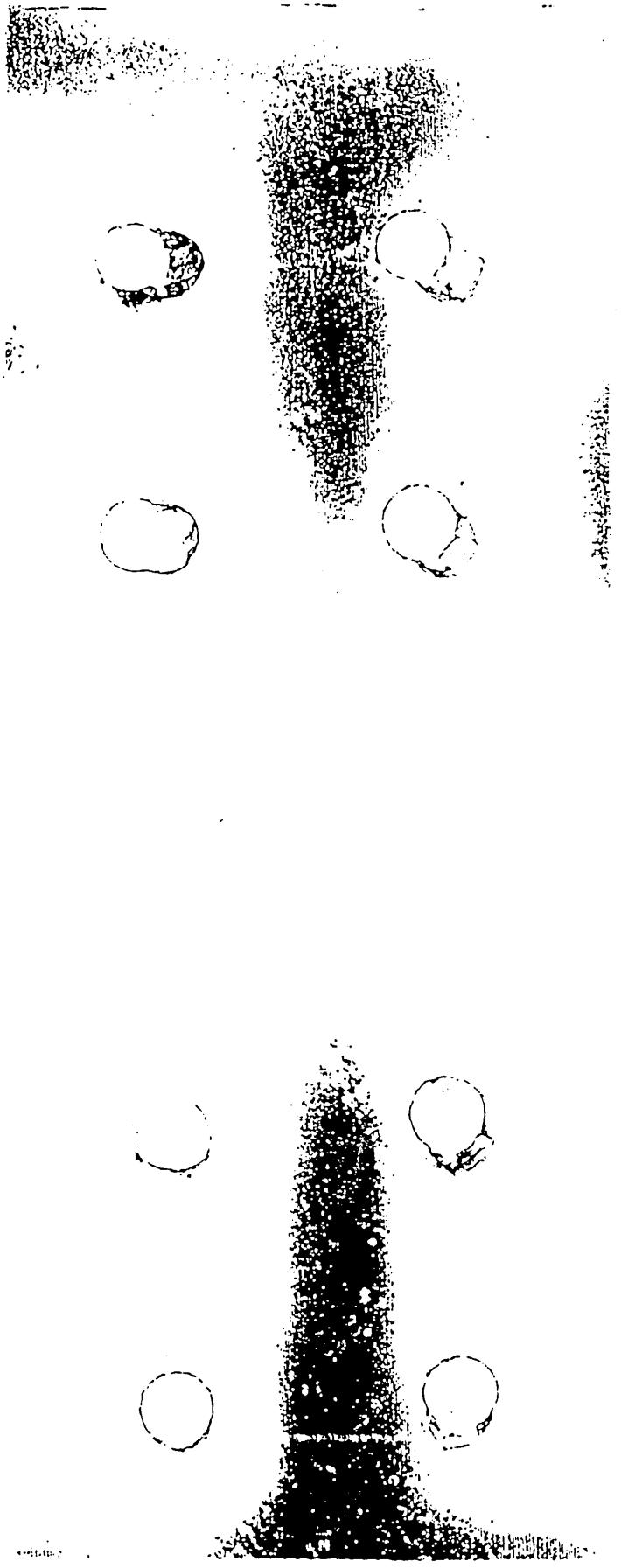

Fig. 5.23 Prying pattern, test T4 (left side)

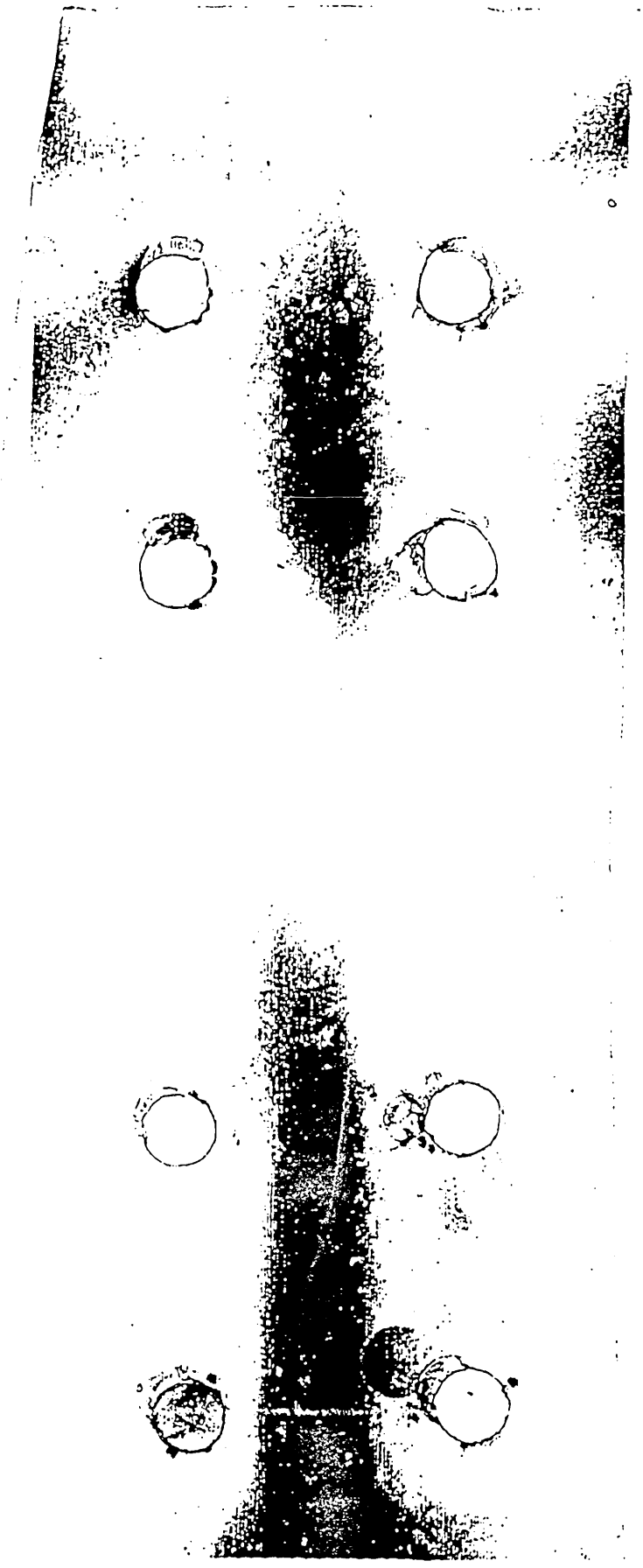

Fig. 5.24 Prying pattern, test T4 (right side)

Fig. 5.25 Prying pattern, test T5 (left side)

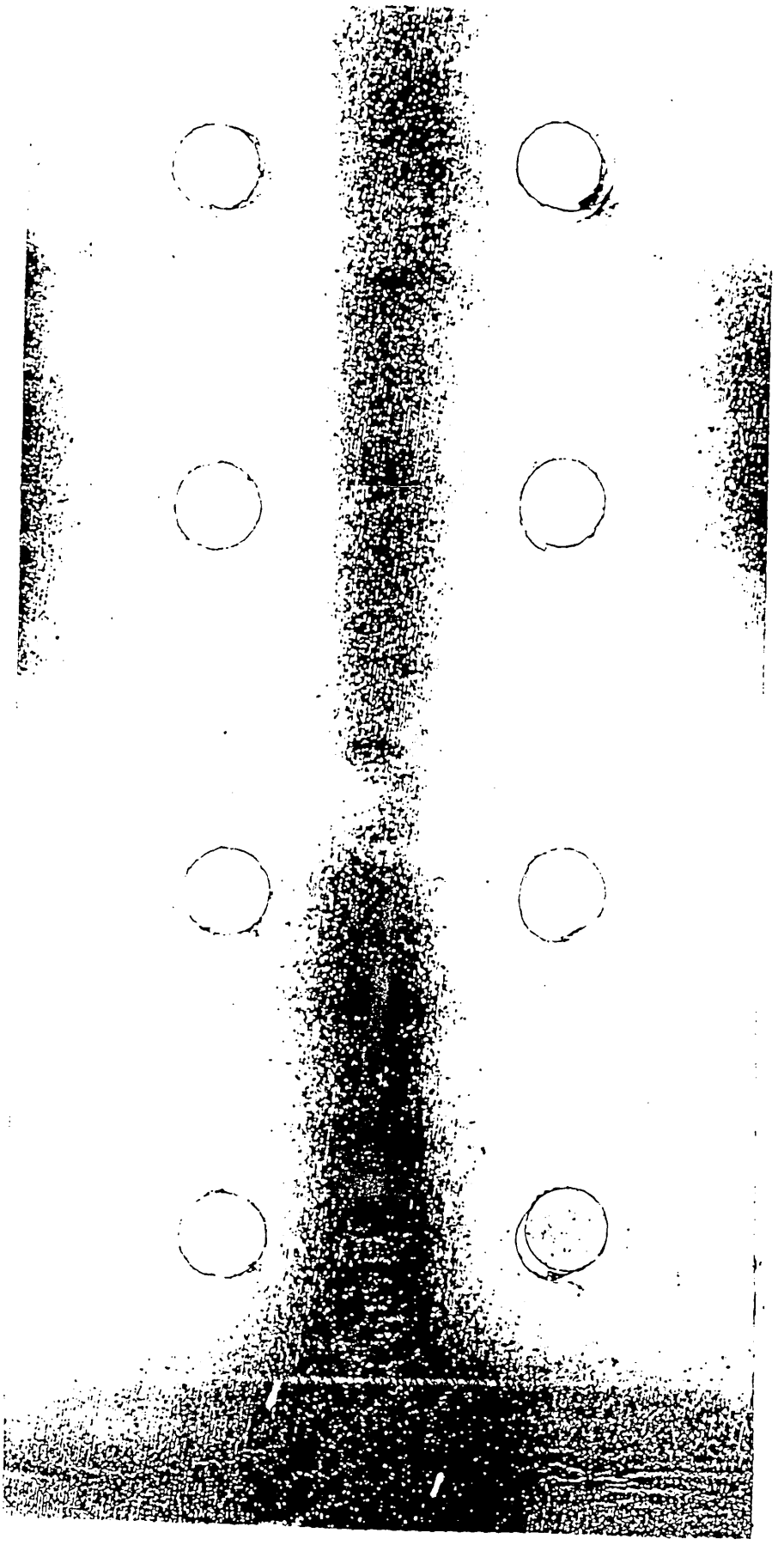

Fig. 5.26 Prying pattern, test T5 (right side)

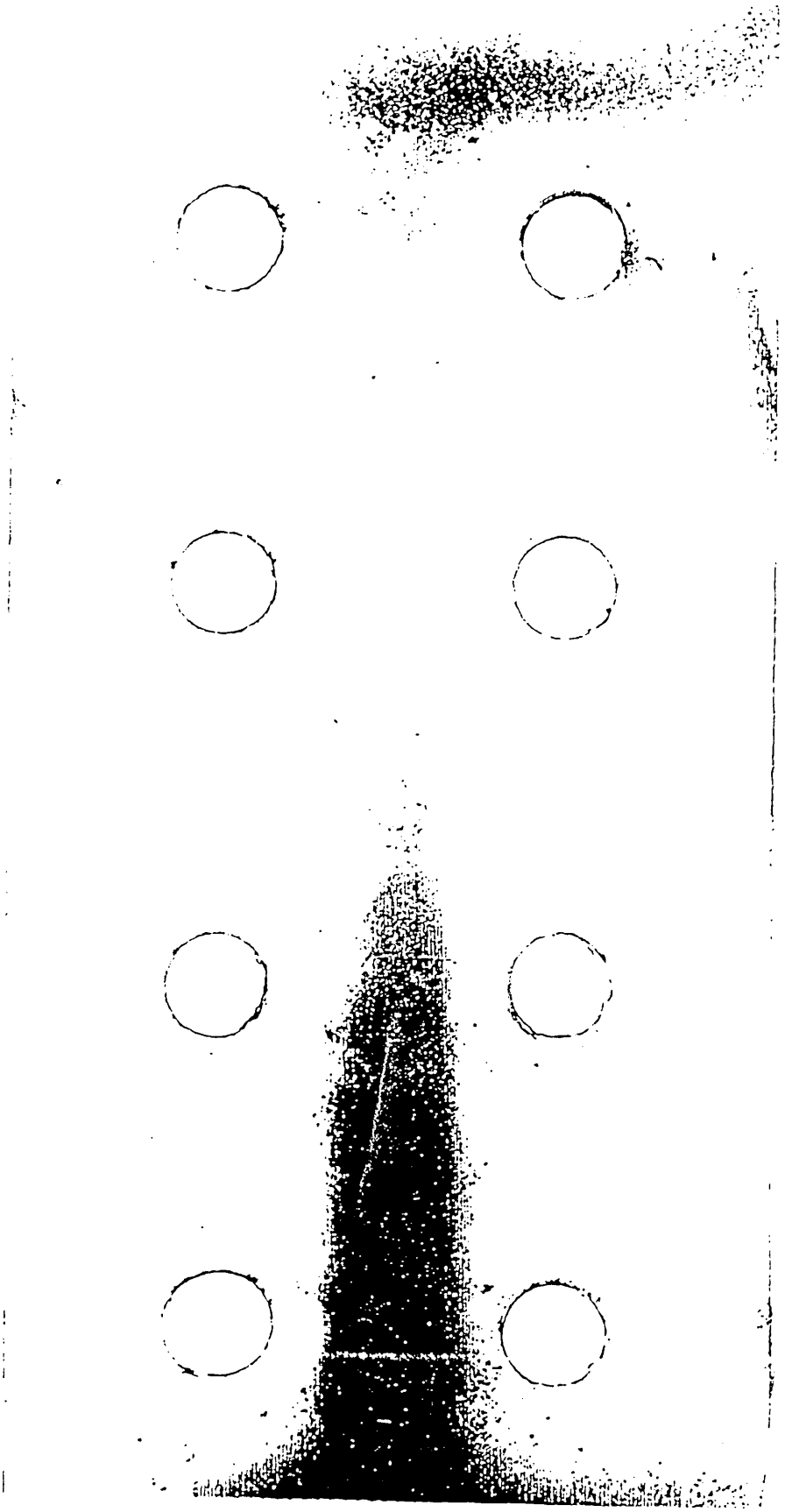

Fig. 5.27 Prying pattern, test T6 (left side)

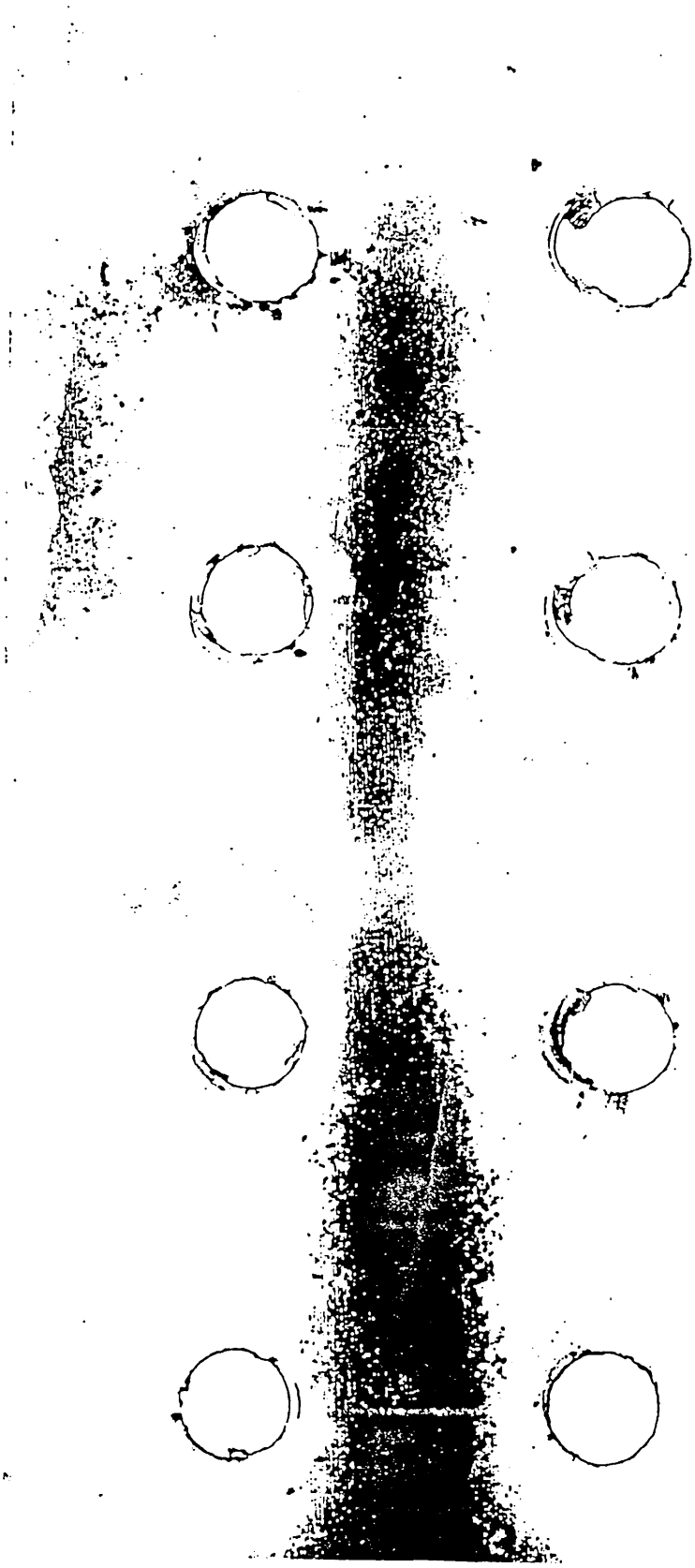

Fig. 5.28 Prying pattern, test T6 (right side)

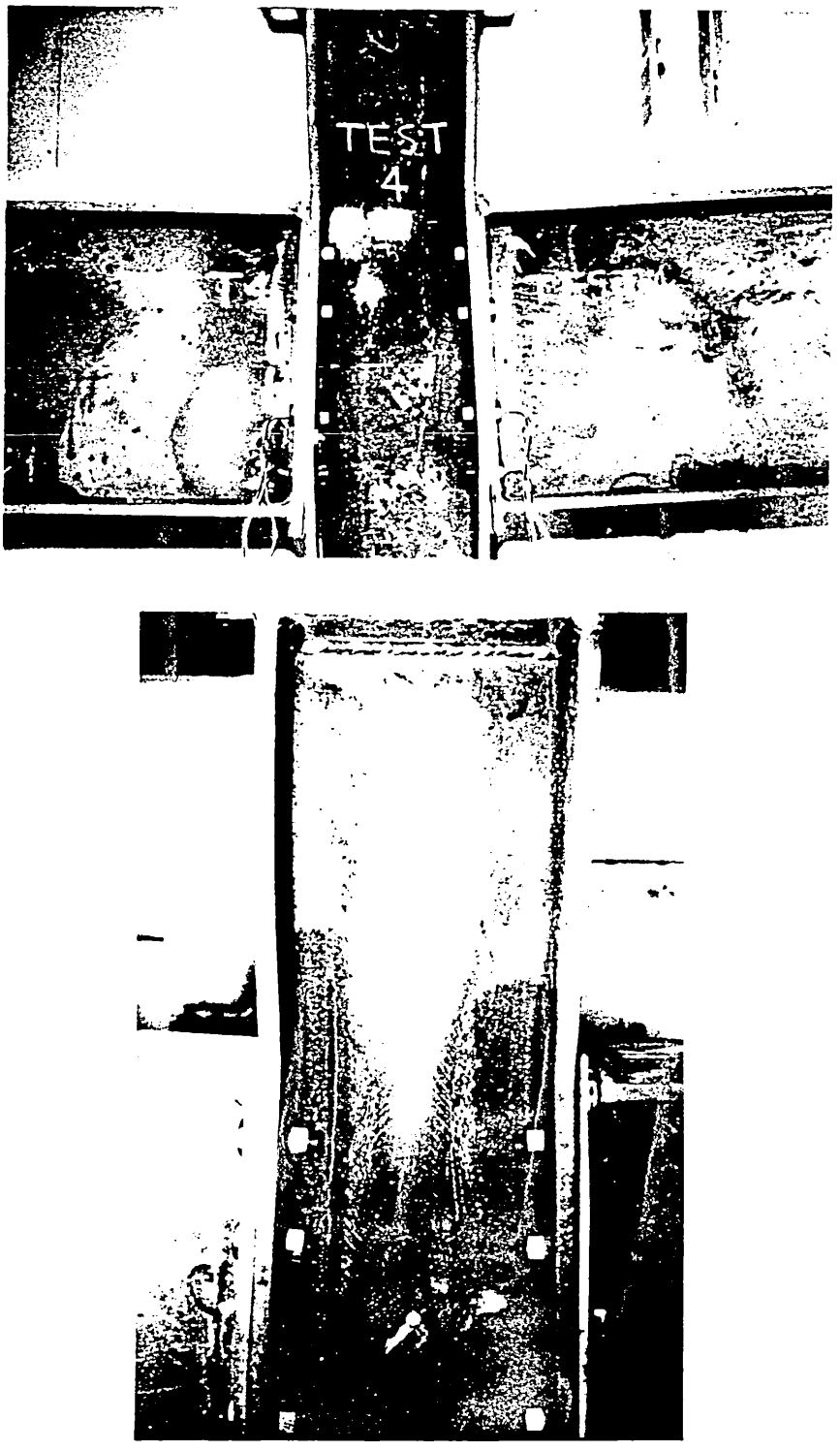

Fig. 5.29 Column web buckling in test T4

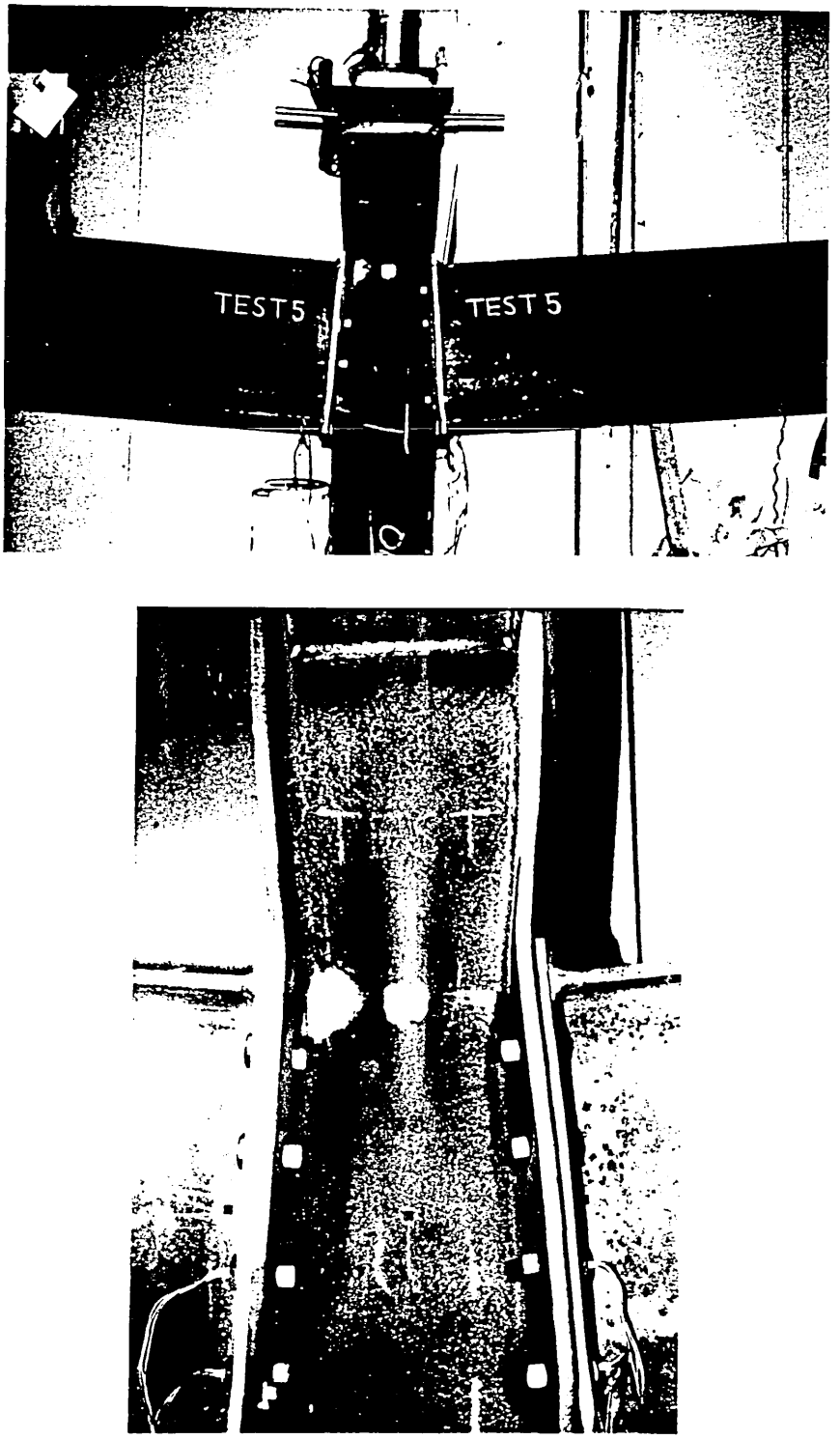

Fig. 5.30 Column web buckling in test T5

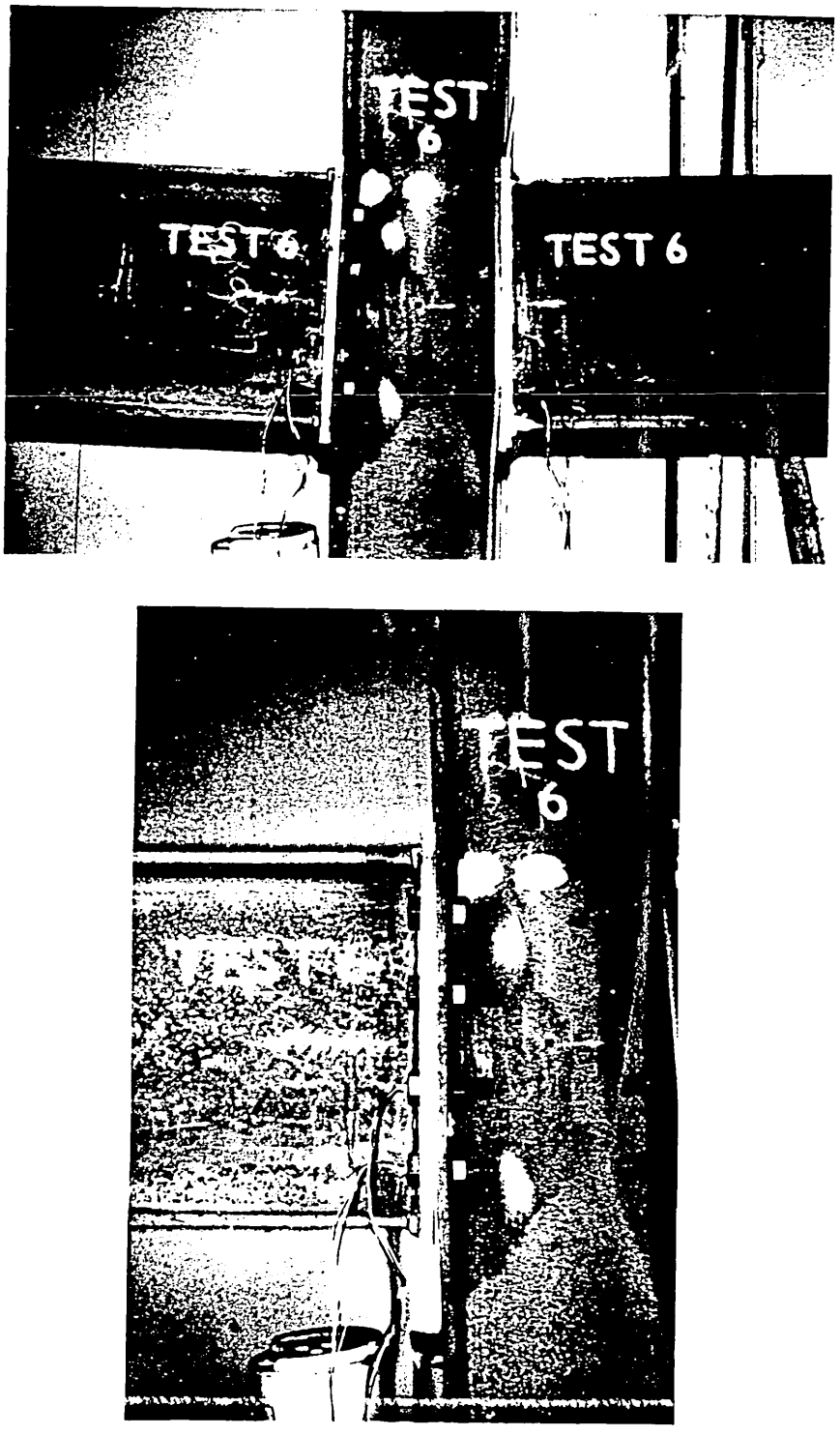

Fig. 5.31 Column web buckling in test T6

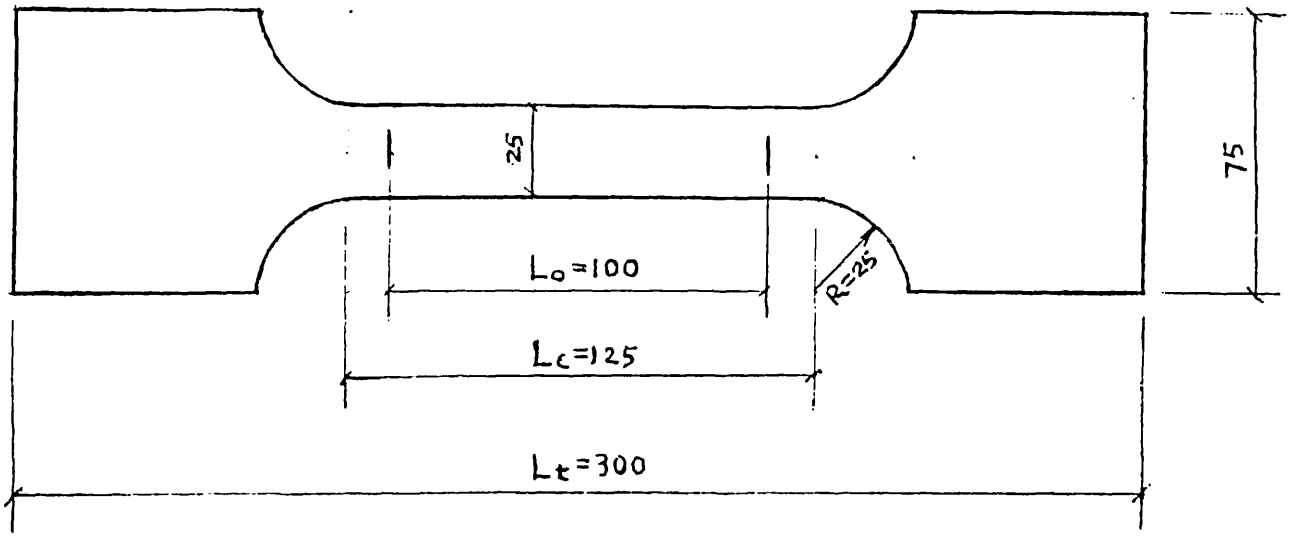

Thickness 5 mm

Fig. 5.32 Test specimen for plates

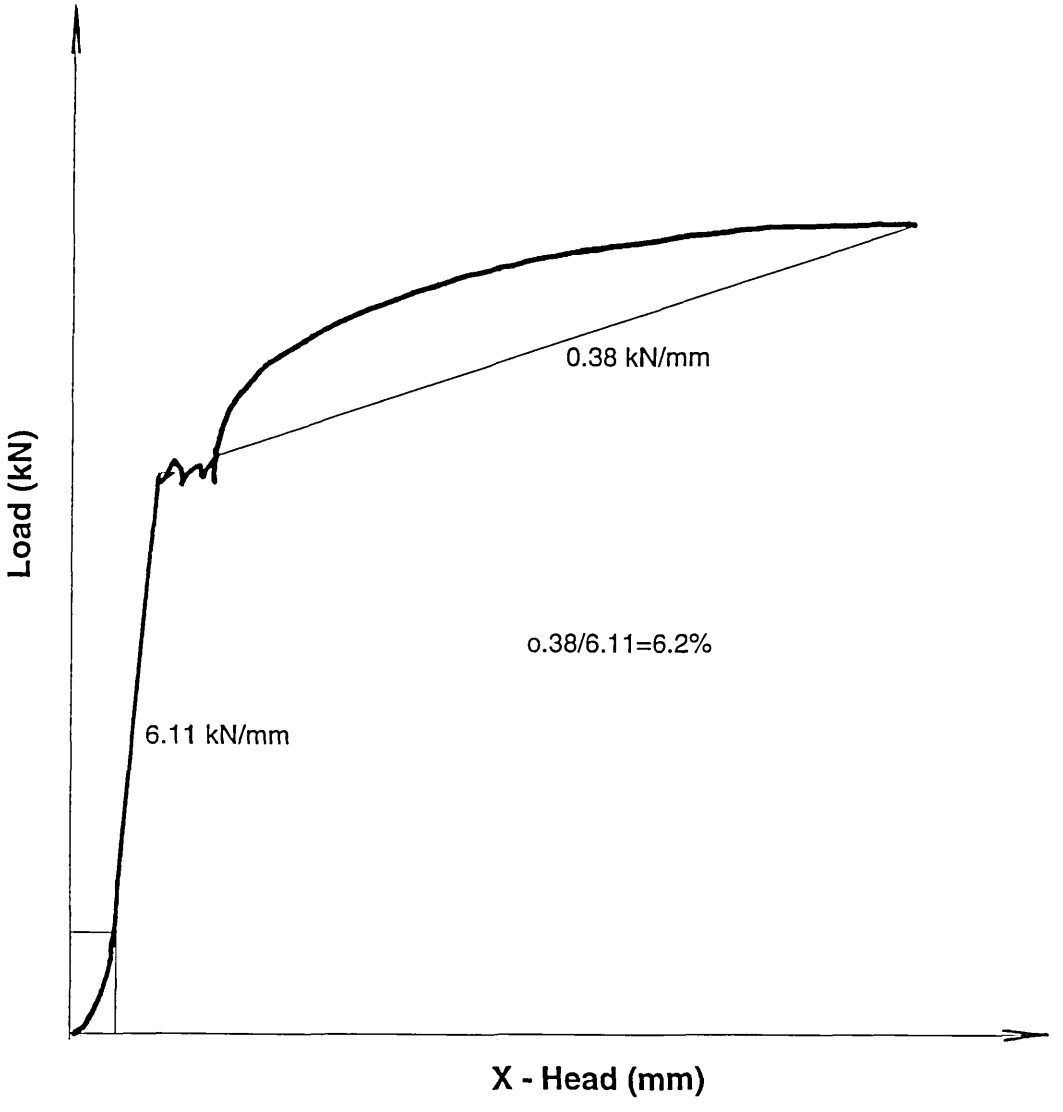

Fig. 5.33 Load elongation curve for end plate

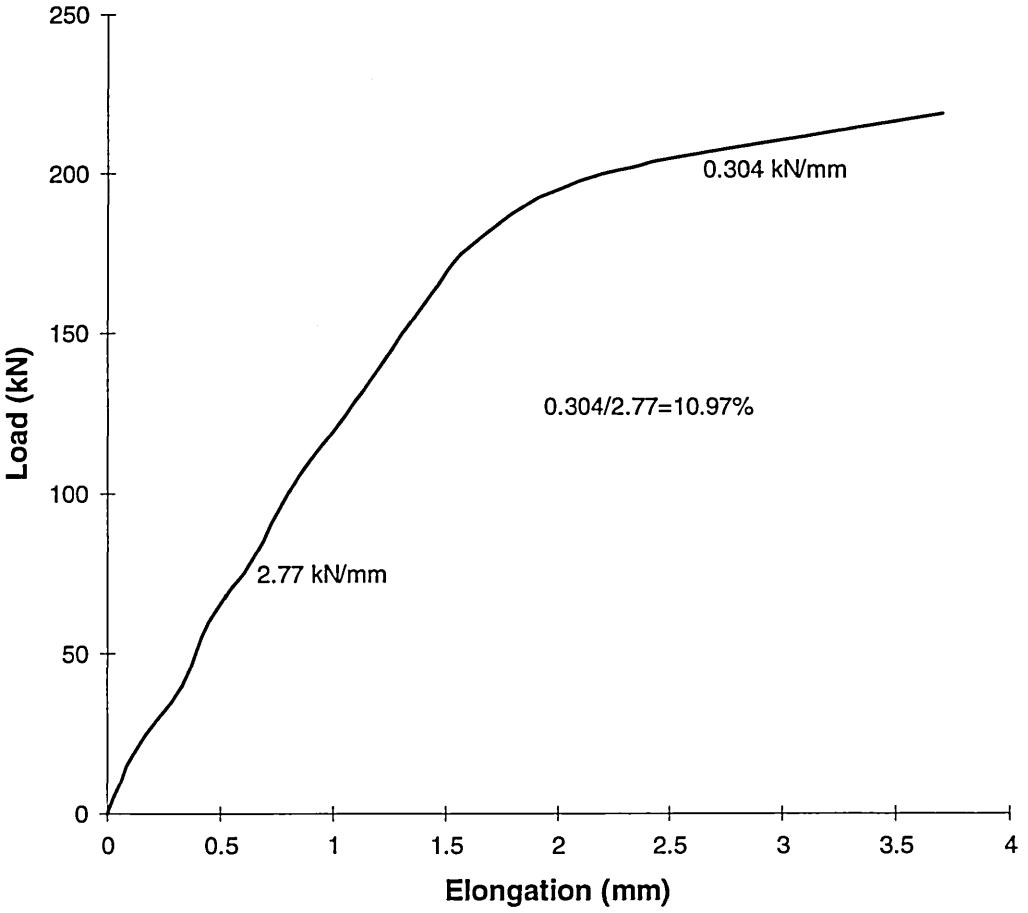

Fig. 5.34 Load elongation curve for M20 bolt

CHAPTER 6

COMPARISON BETWEEN ANALYTICAL AND EXPERIMENTAL RESULTS

6.1 INTRODUCTION

The comparative study was undertaken with the aim of establishing the degree of accuracy with which the finite element method can predict the behaviour of the flush end plate connections. The validity of the non-linear finite element analysis model was established by comparing the following connection properties derived from the analyses with the results obtained from the experimental investigation:

- moment-rotation characteristics
- bolt strains
- strains at preselected locations in the column web
- prying forces at the interface of end plate and column flange

6.2 MOMENT-ROTATION CHARACTERISTICS

The moment-rotation relationship of a connection is a key factor governing the performance of the whole structure. From the moment-rotation curves it is possible to derive the three major properties of the connection, namely the moment resistance, the rotational stiffness and the rotation capacity. The moment-rotation curves for the six connections tested were drawn from the test results. These curves were also obtained from the results of the nonlinear finite element analyses of the connection models. The analytical and experimental moment-rotation curves for each connection were compared.

As stated previously, for the purpose of analysis the moment acting at the beam end is decomposed into a pair of equal and opposite forces acting at the level of the beam flanges. Axial forces transmitted by the web are small and therefore ignored. In the finite element models uniformly distributed loads are considered on

the beam tension and compression flanges. The moment is given by the product of either tensile or compressive forces and the depth of the beam. For computing connection rotation analytically, the centre of rotation is assumed at the bottom edge of the beam compression flange. The prying pattern between the column flange and end plate in the compression region, is known to be triangular with zero force along the free edge of end plate. It is therefore, reasonable to assume that the centre of rotation is above the edge of the end plate and approximately at the edge of the beam compression flange. The connection rotation can, therefore, be computed analytically by dividing the difference in displacements at the centre of tension flange and the edge of the compression flange of the beam by the distance between two points.

The experimental and analytical moment-rotation curves obtained for the six connections are shown in Figures 6.1 to 6.6. In general, there is good agreement between the experimental and analytical results for each connection. However, there is some discrepancy in the initial elastic range and final elastic-plastic range of the curve. Theoretically, moment-rotation curves should be linear in the elastic range. Experimentally, moment-rotation curves exhibit some nonlinearity in the elastic range. Such phenomena are more obvious in tests T1 to T3. This can be attributed to the combination of bolt tightening effect, imperfection in the test set up and lack of fit. It is very difficult to include these factors in the analytical model and hence the curves are linear in the elastic range. The degree of nonlinearity observed in tests T4 to T6 is small.

The moment-rotation curve for test T1, shown in Figure 6.1 exhibits nonlinearity from the very beginning. The curve flattens out near failure which occurs at a moment of 187.8 kNm and rotation of 0.025 radians. However, analytical curve (M1) still shows upward tendency. This can be explained by the fact that the failure occurred due to thread stripping. Such phenomenon can not be modelled in the finite element analysis. If thread stripping could be prevented and

deformation of column flange and/or end plate be allowed, such discrepancy could be avoided. Similar discrepancy was also observed in T2 and M2, T3 and M3, shown in Figures 6.2 and 6.3, which also failed due to thread stripping.

Some discrepancy is also observed in the final stage of the curve, where failure was due to column web buckling (T4 and M4, T5 and M5, T6 and M6). The analytical model M5 was subjected to a maximum load corresponding to the failure moment of 161.4 kNm obtained in the test T5. At that failure moment, the analytical curve reached rotation of 0.017 radians, while a rotation of 0.046 radians was observed in the test T5. This is because of column web buckling which increased the rotation rapidly. Similar variations were also observed in T4 and M4, T6 and M6, as shown in Figures 6.4 and 6.6. In tests T4 to T6 the failure was due to post-yield column web buckling. Unfortunately, LUSAS is incapable of handling post-yield buckling. It is hoped that the LUSAS package will be updated in the near future to cater for such buckling analysis. Alternatively, some other finite element package, eg ABAQUS, which can perform post-yield buckling analysis, may be used. The ABAQUS software was acquired by the University only very recently and therefore it can not be used for the analysis of this work.

6.3 BOLT STRAINS

In bolted end plate connections the applied load is transferred from the beam to the end plate via welds and from the end plate to the column flange via bolts. The bolt response to gradually increasing moment is an important factor controlling the overall behaviour of the connection. The high strength 8.8 bolts are brittle, and as such connection should be designed so that failure of bolts is avoided. Bolt response within a connection is a complex problem which has received scant attention compared with the bolt behaviour under pure tension which has been widely investigated. Bolts in a connection are generally subjected to a combination of axial load, shear force and moment. The prying developed at the interface also affects the performance of the bolts. Lack of reliable information regarding the bolt

performance has forced the designers to assume a large safety factor to prevent any catastrophic failure due to bolt fracture. In the connection model bolts were represented by bar elements. It is important to check that these elements are capable of predicting the bolt behaviour with reasonable accuracy.

As stated previously, the applied moment was resisted by tensile force acting on four bolts in tests T1 to T3 and on eight bolts in tests T4 to T6 together with compressive force acting on a bearing area near the beam compression flange. One half of the total bolts were located near beam tension flange and the other half near the beam compression flange. From the experimental results it was confirmed that the tensile force caused by the beam end moment was carried primarily by the group of bolts near the beam tension flange, while the compressive force was resisted by a bearing area near the beam compression flange. Although the bolts near the beam compression flange carry very small tensile forces, they were included in the finite element model to ensure that the model represents the connection accurately.

A comparative study of strains in the bolts located near the beam tension flange was carried out. The results are shown in Figures 6.7 to 6.12. They indicate good agreement between analytical and experimental results over the entire loading range. However, strain readings in bolts are very sensitive and some discrepancy between the two results are observed. The analytical strains are slightly higher than the experimental results in the early stage of loading. These differences can be attributed to the effect of pretensioning of bolts. Although the pretensioning of bolts was kept to a minimum throughout the test programme, a degree of tightening was necessary to provide a reasonable contact between the end plate and the column flange. This initial force was not considered in the analytical model. Once the pretensioning is overcome, both experimental and theoretical curves follow a similar path. The discrepancy between the two results at high load may have been caused by severe flexural deformation of the bolts induced by large deformation of the plates. The bar elements representing the bolts in the finite element model could not take

account of any bending deformation in the bolts. In the analytical model, eight bar elements represent one bolt and the bolt strain is the average of strains of the eight bar elements. Separate analysis of bar strains gave some indication of the moment acting on the bolts.

6.4 COLUMN WEB STRAINS

The ability of the finite element model to predict the moment-rotation characteristics and bolt strains accurately was demonstrated in Sections 6.2 and 6.3. A comparison between analytical and experimental strains in the column web was also carried out, which are illustrated in Figures 6.13-6.18. Strains at column mid-depth, in line with beam compression flange (Figure 5.7) were considered for the comparative study. In general, close agreement between analytical and experimental results are observed. However, some discrepancies between the results are noticed, which can be attributed to errors associated with any experimental investigation. Very close agreement was achieved in T2 and M2, T3 and M3, as shown in Figures 6.14 and 6.15. The disagreement in the strain results found in other tests is generally small and should not cause any concern.

6.5 COMPARISON OF PRYING FORCES

Some indication of prying forces can be obtained from the test results. However, it is extremely difficult to quantify the prying force by experimental means. Detailed discussion on prying forces are contained in Chapter 7.

6.6 CONCLUDING REMARKS

From the comparative study of finite element analysis and experimental results it is firmly established that the finite element model of the connection is fairly accurate and the connection properties derived from the three-dimensional, non-linear analysis are quite reliable. An in-depth study of the connection, leading to the computation of each component contribution, is the next logical step forward. This will enable better understanding of flush end plate connection behaviour and will lead to the production of design curves and tables for flush end plate connections.

Fig. 6.1 Comparison between analytical and experimental moment-rotation curves, T1 and M1

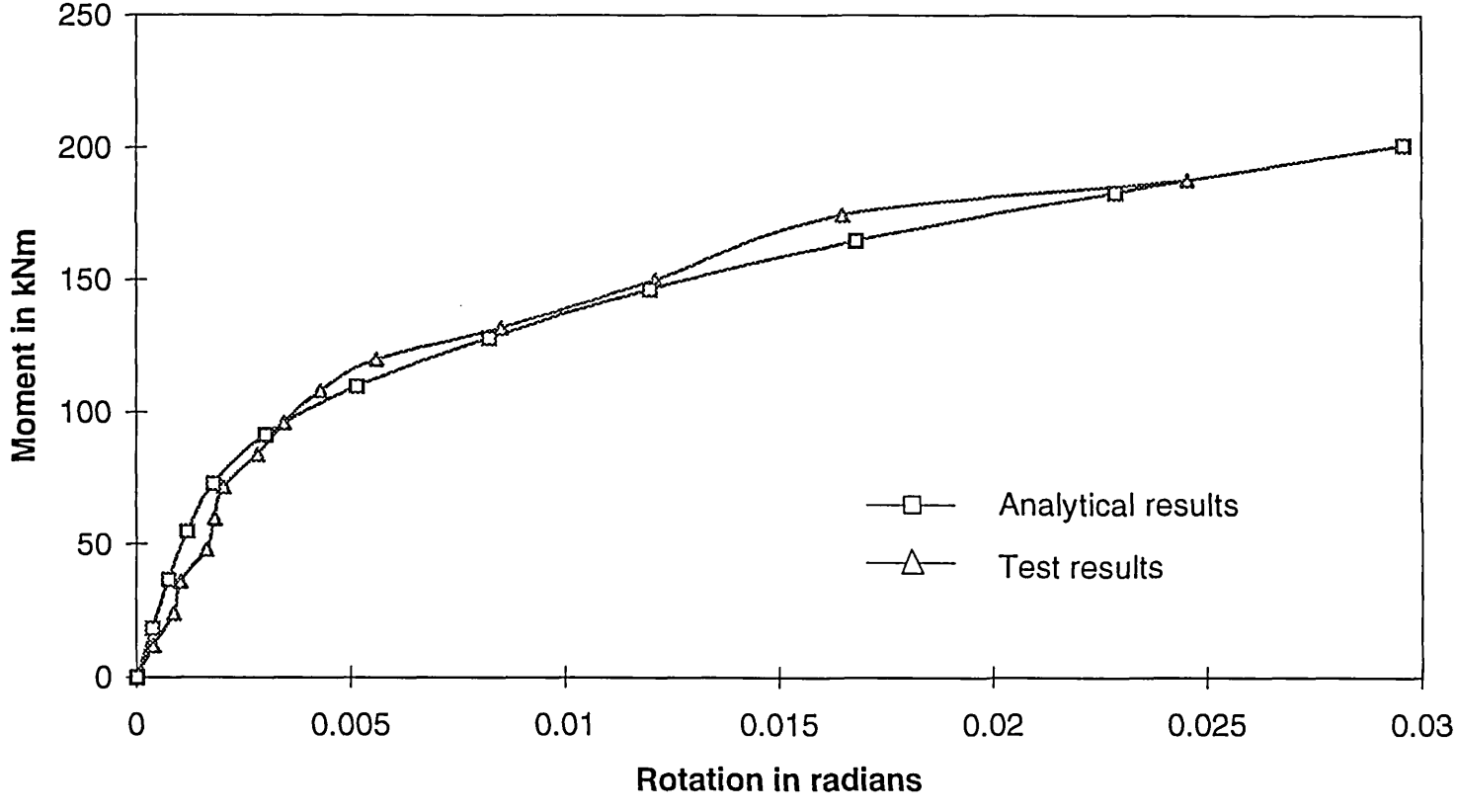

Fig. 6.2 Comparison between analytical and experimental moment-rotation curves, T2 and M2

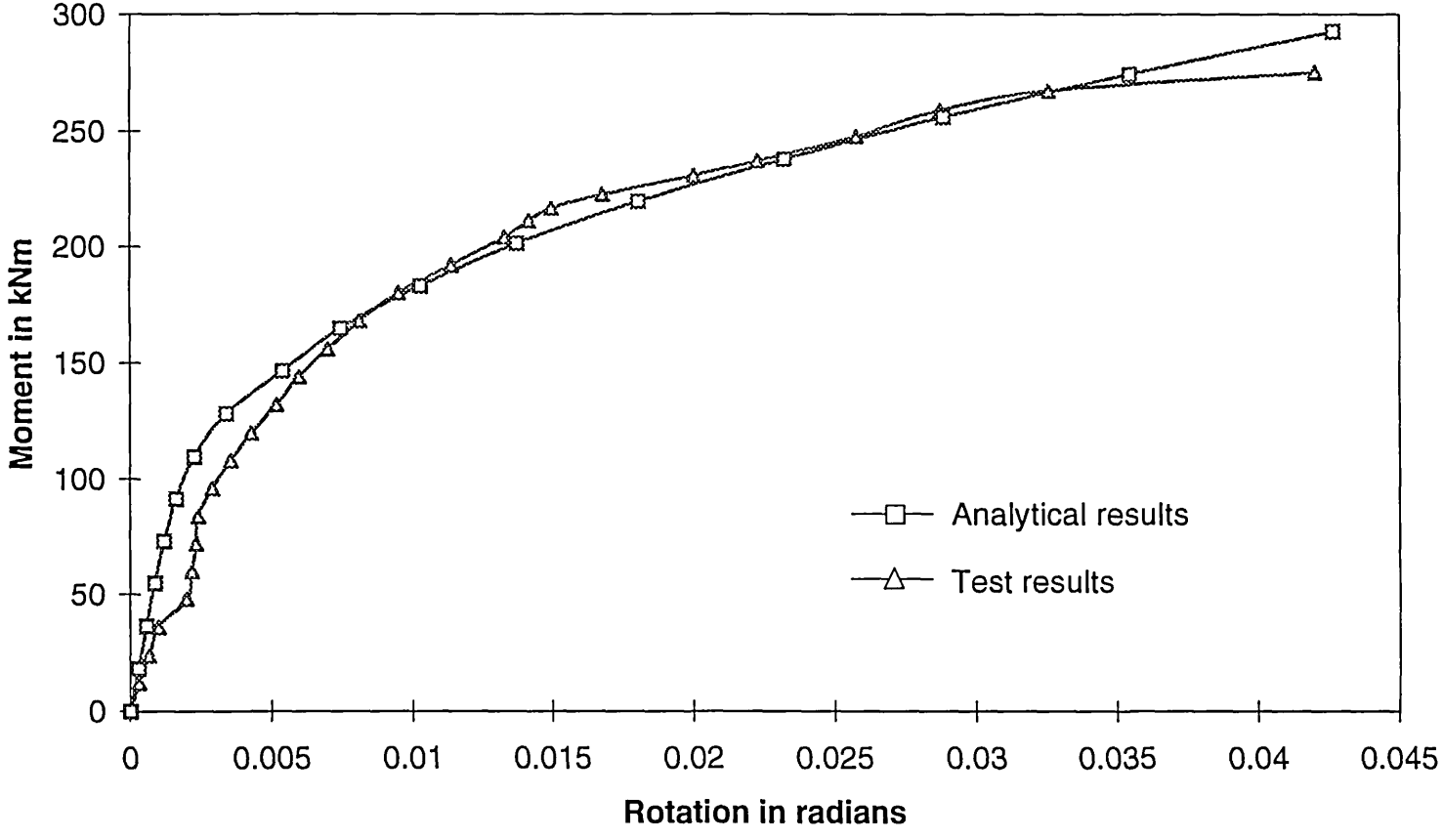

Fig. 6.3 Comparison between analytical and experimental moment-rotation curves, T3 and M3

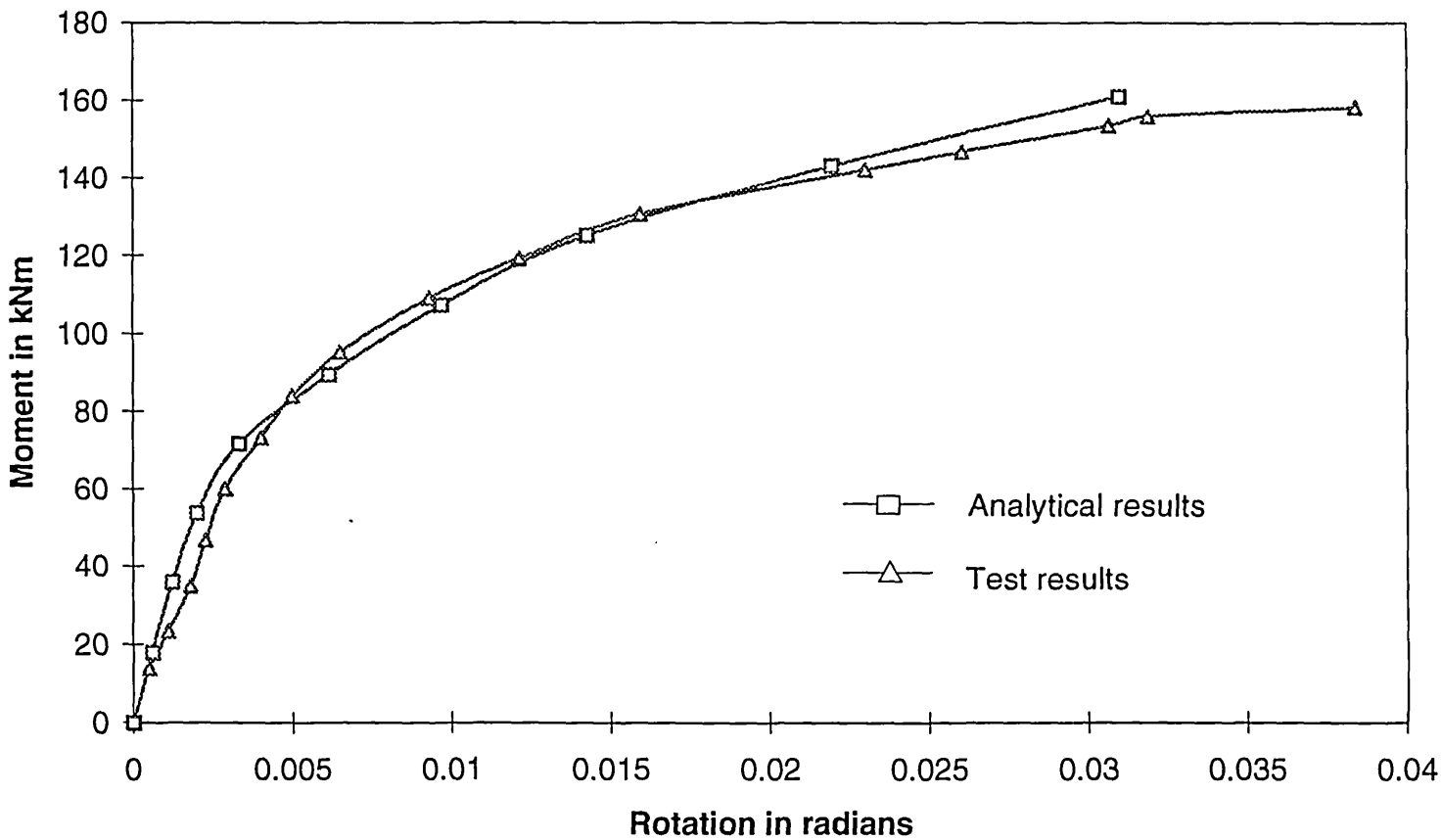

Fig. 6.4 Comparison between analytical and experimental moment-rotation curves, T4 and M4

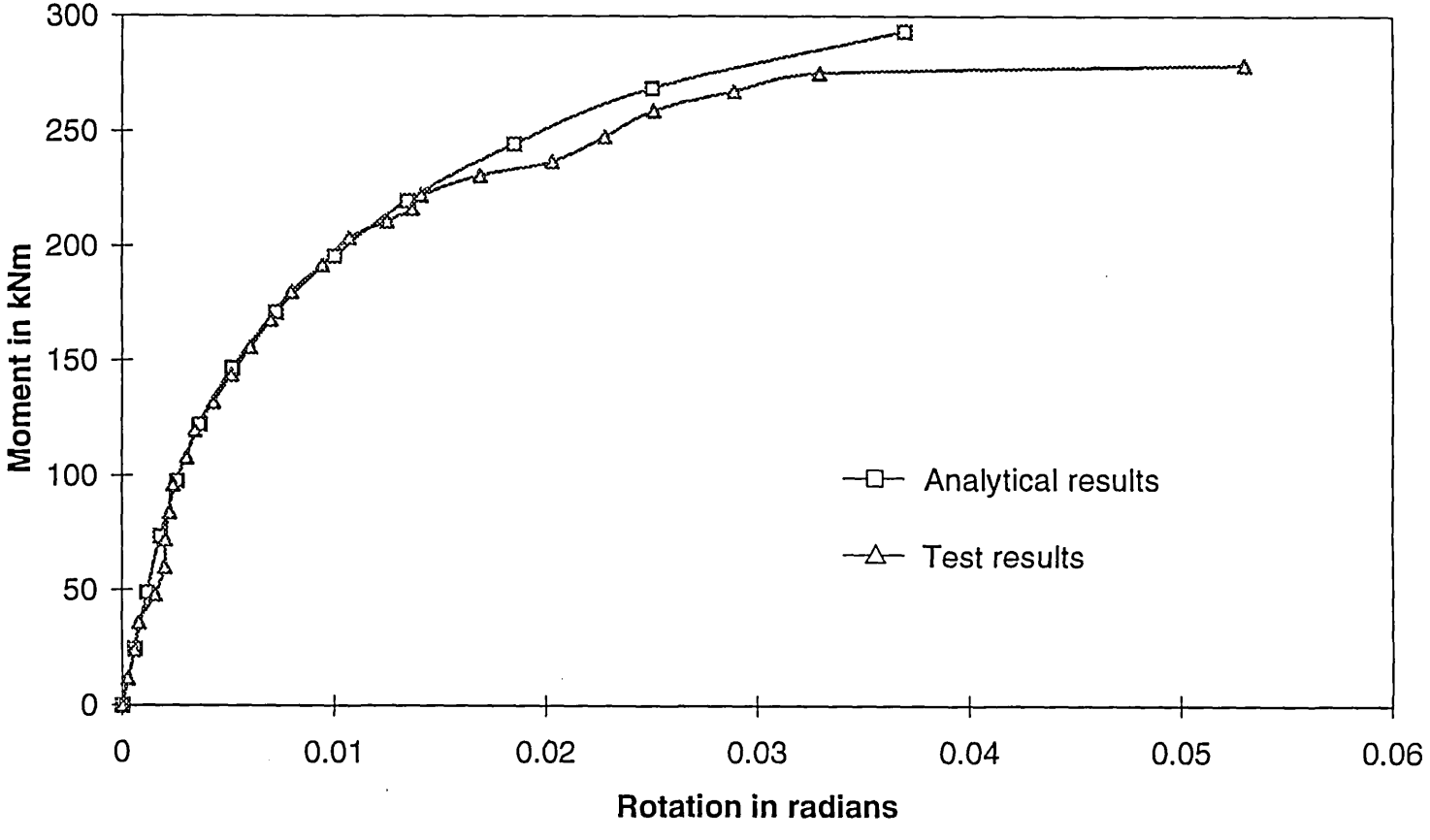

Fig. 6.5 Comparison between analytical and experimental moment-rotation curves, T5 and M5

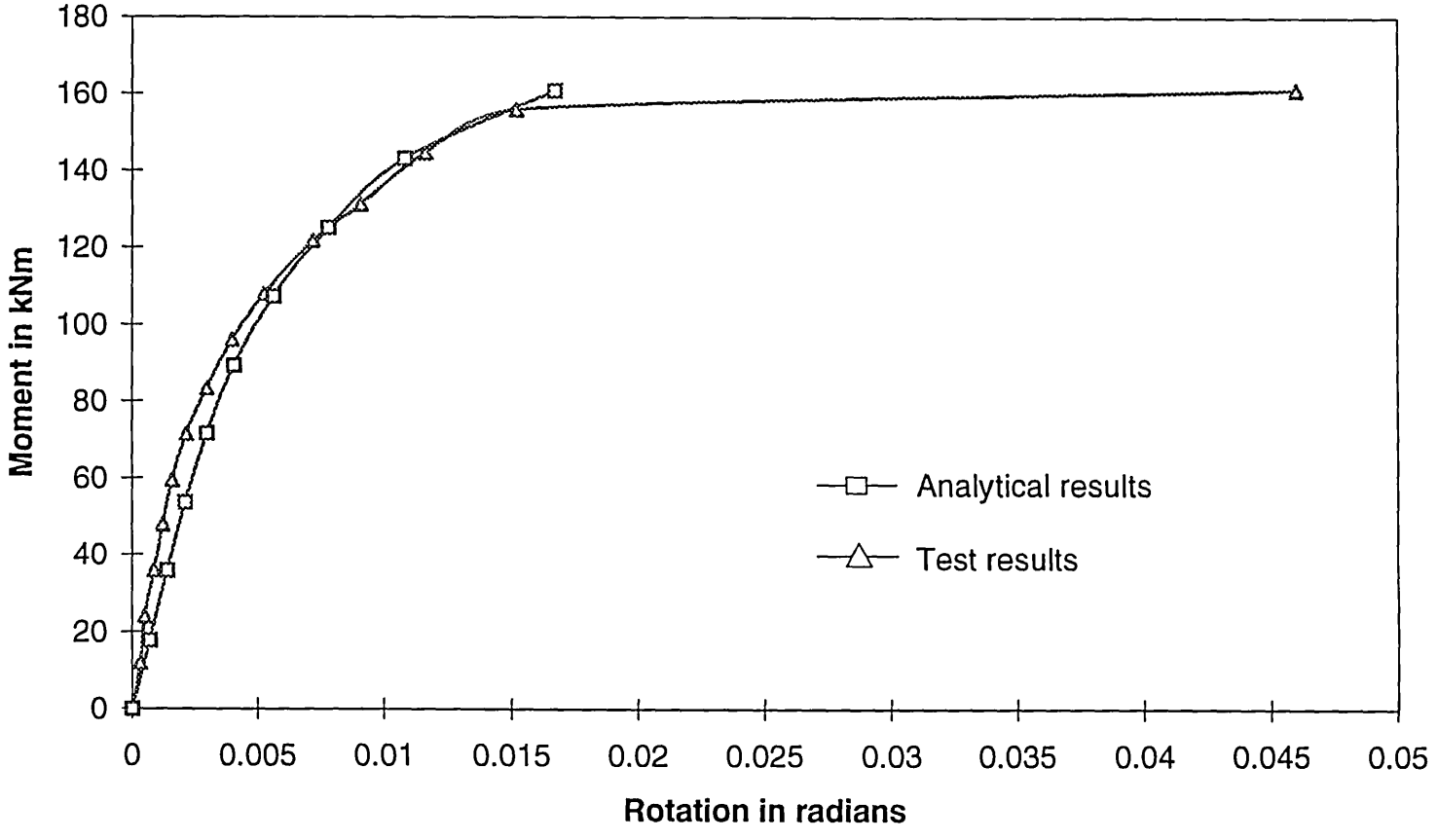

Fig. 6.6 Comparison between analytical and experimental moment-rotation curves, T6 and M6

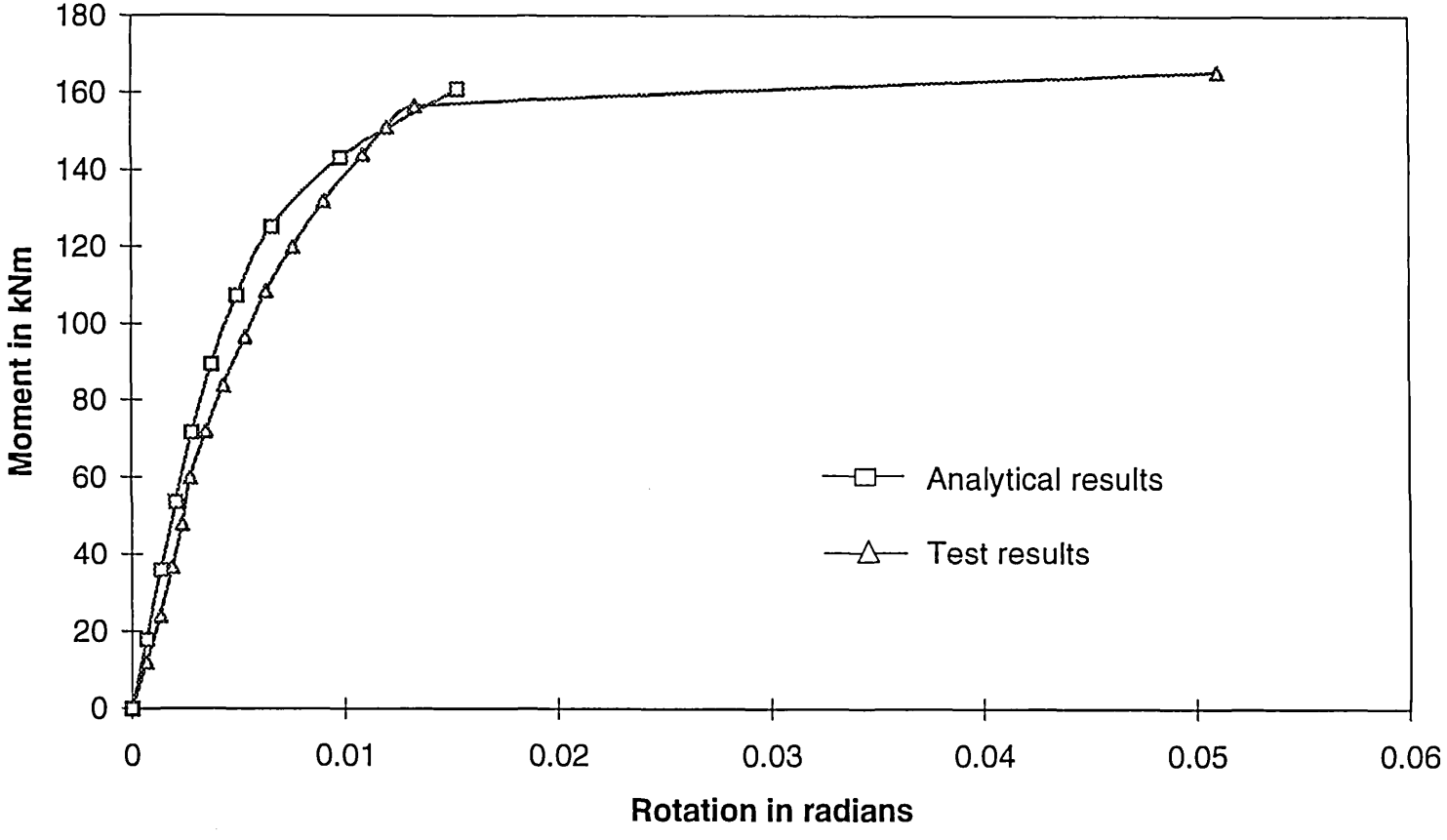

Fig. 6.7 Comparison between analytical and experimental bolt strains, T1 and M1, M20 bolt near the beam tension flange

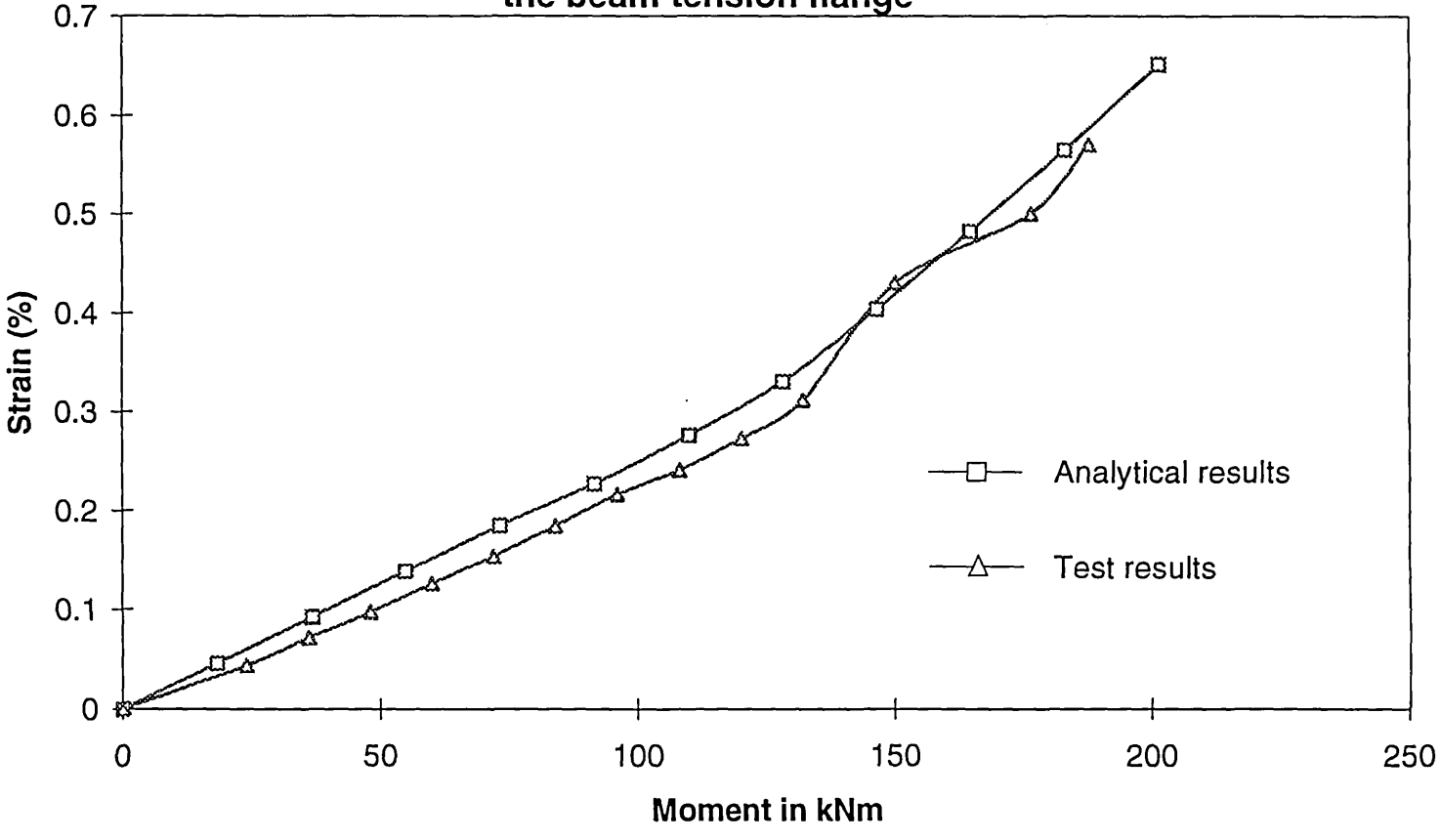

Fig. 6.8 Comparison between analytical and experimental bolt strains, T2 and M2, M24 bolt near the beam tension flange

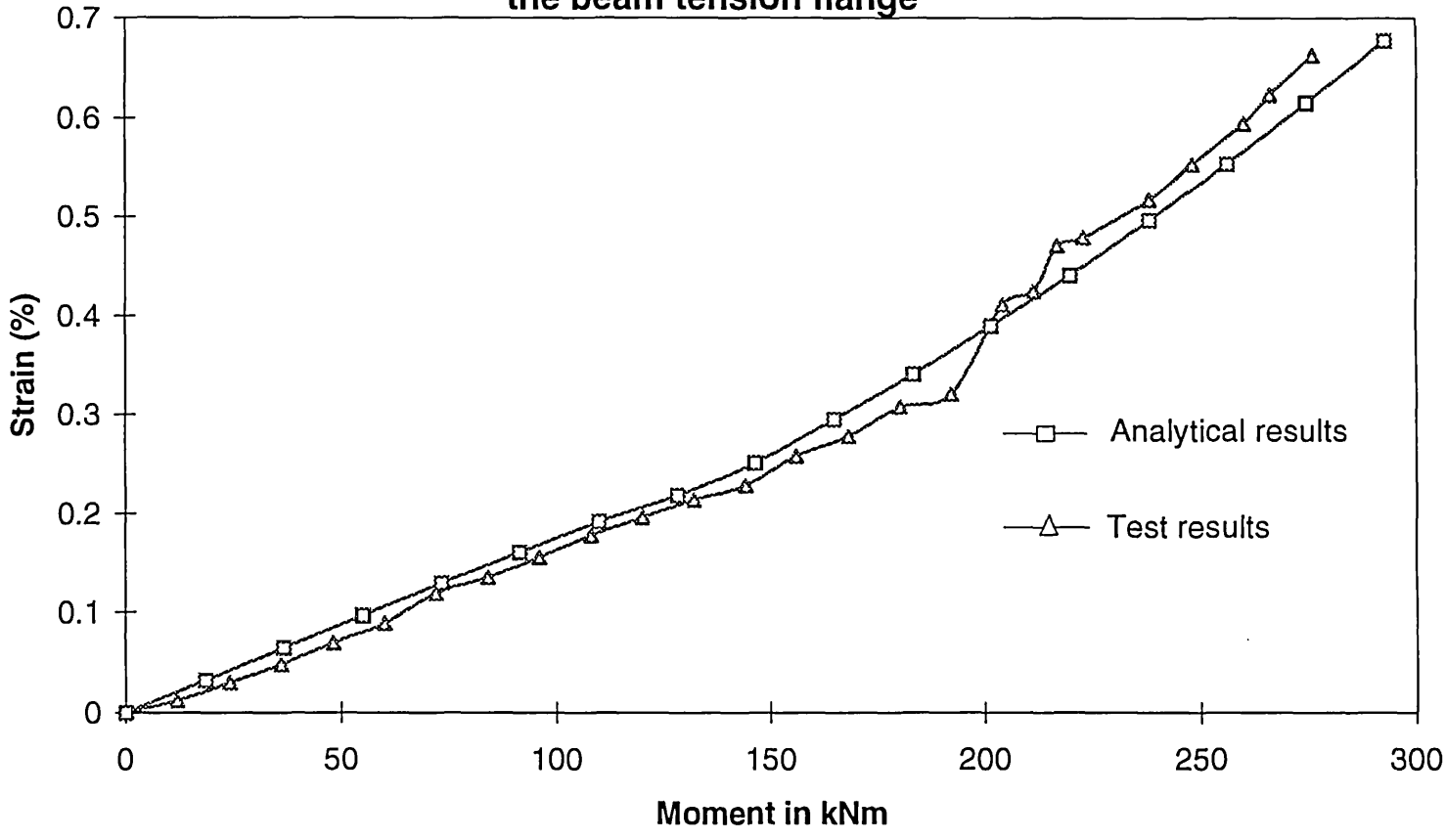

Fig. 6.9 Comparison between analytical and experimental bolt strains, T3 and M3, M20 bolt near the beam tension flange

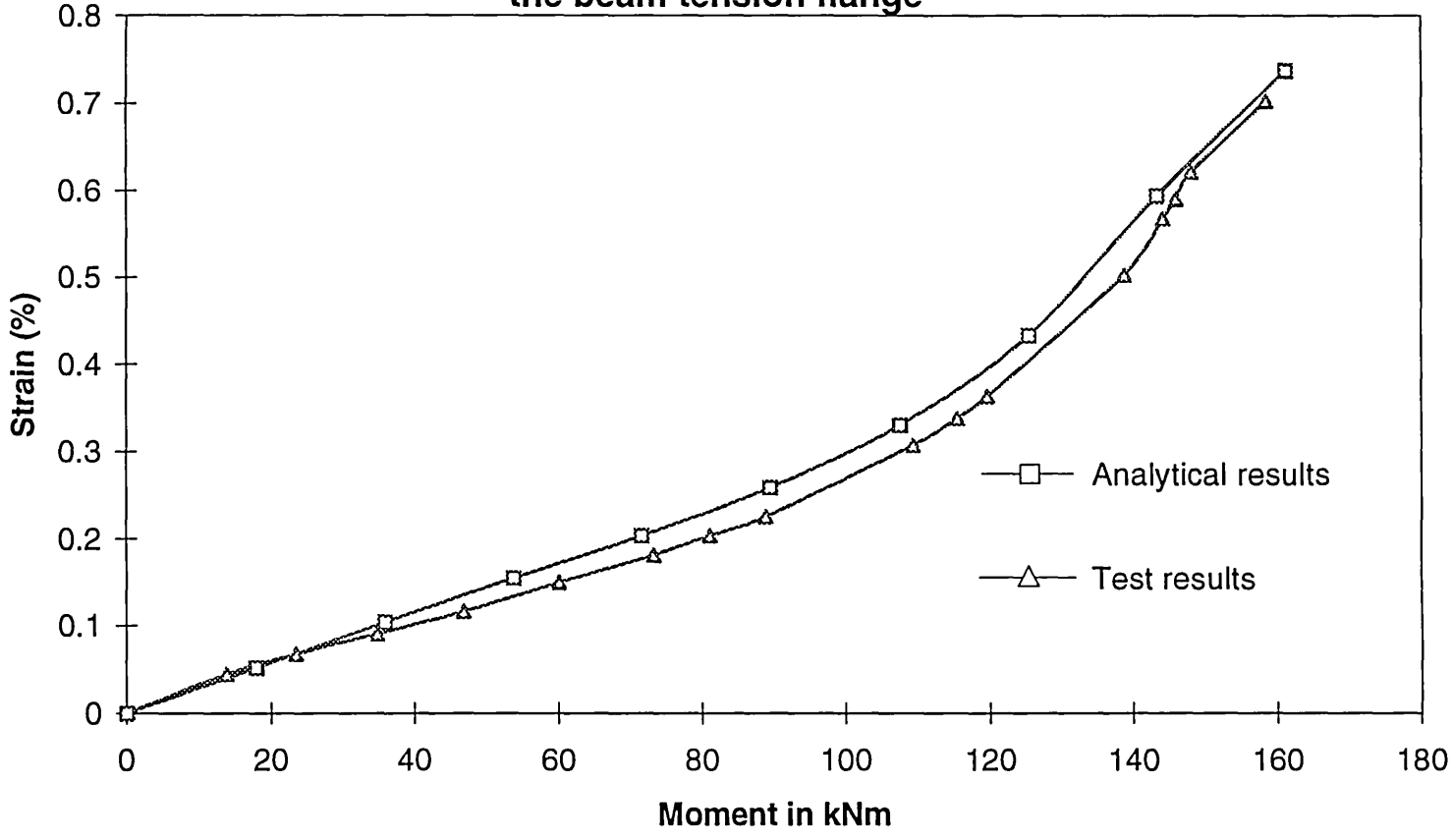

Fig. 6.10 Comparison between analytical and experimental bolt strains, T4 and M4, first row of M20 bolt near the beam tension flange

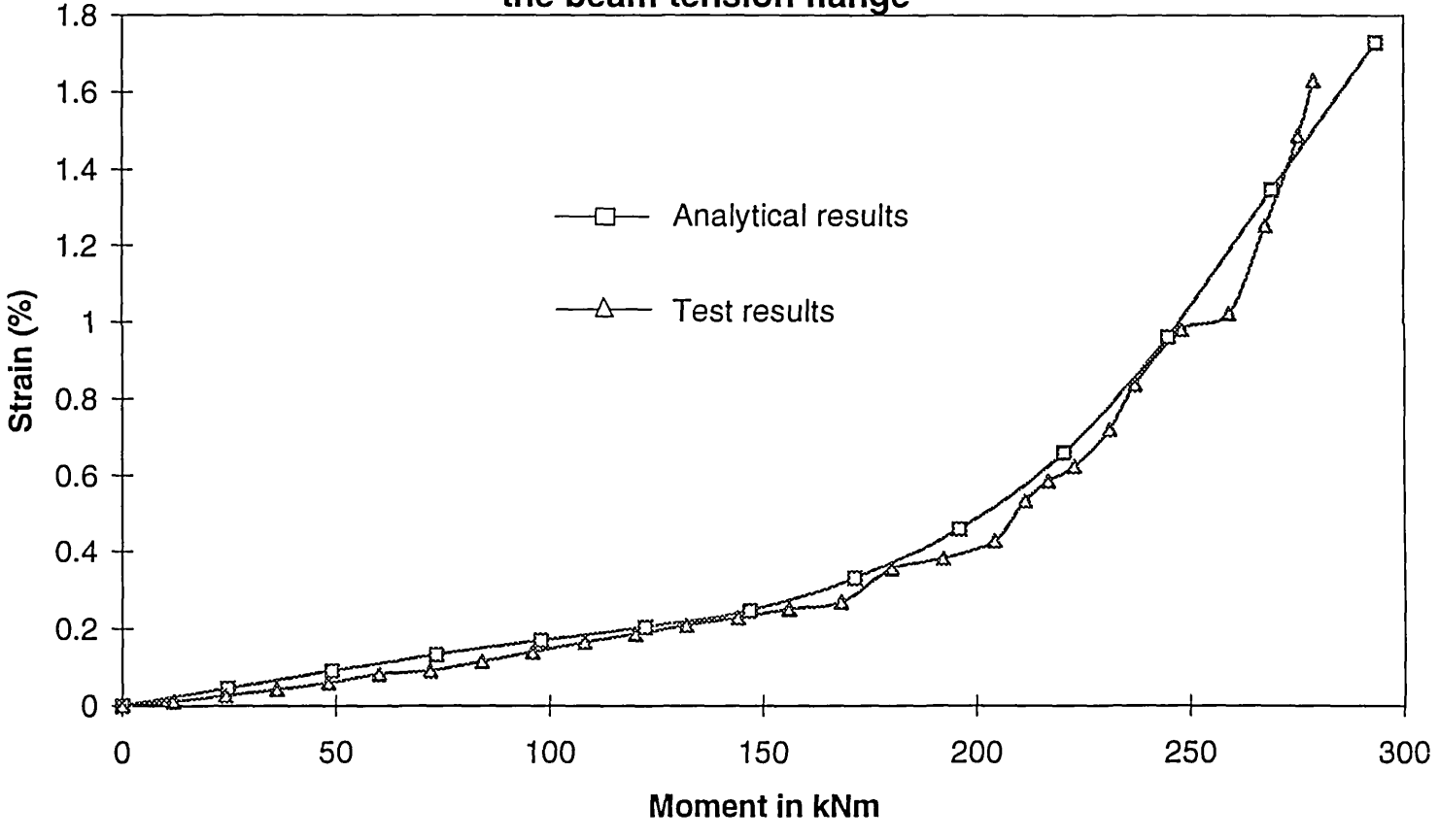

Fig. 6.11 Comparison between analytical and experimental bolt strains, T5 and M5, first row of M20 bolt near the beam tension flange

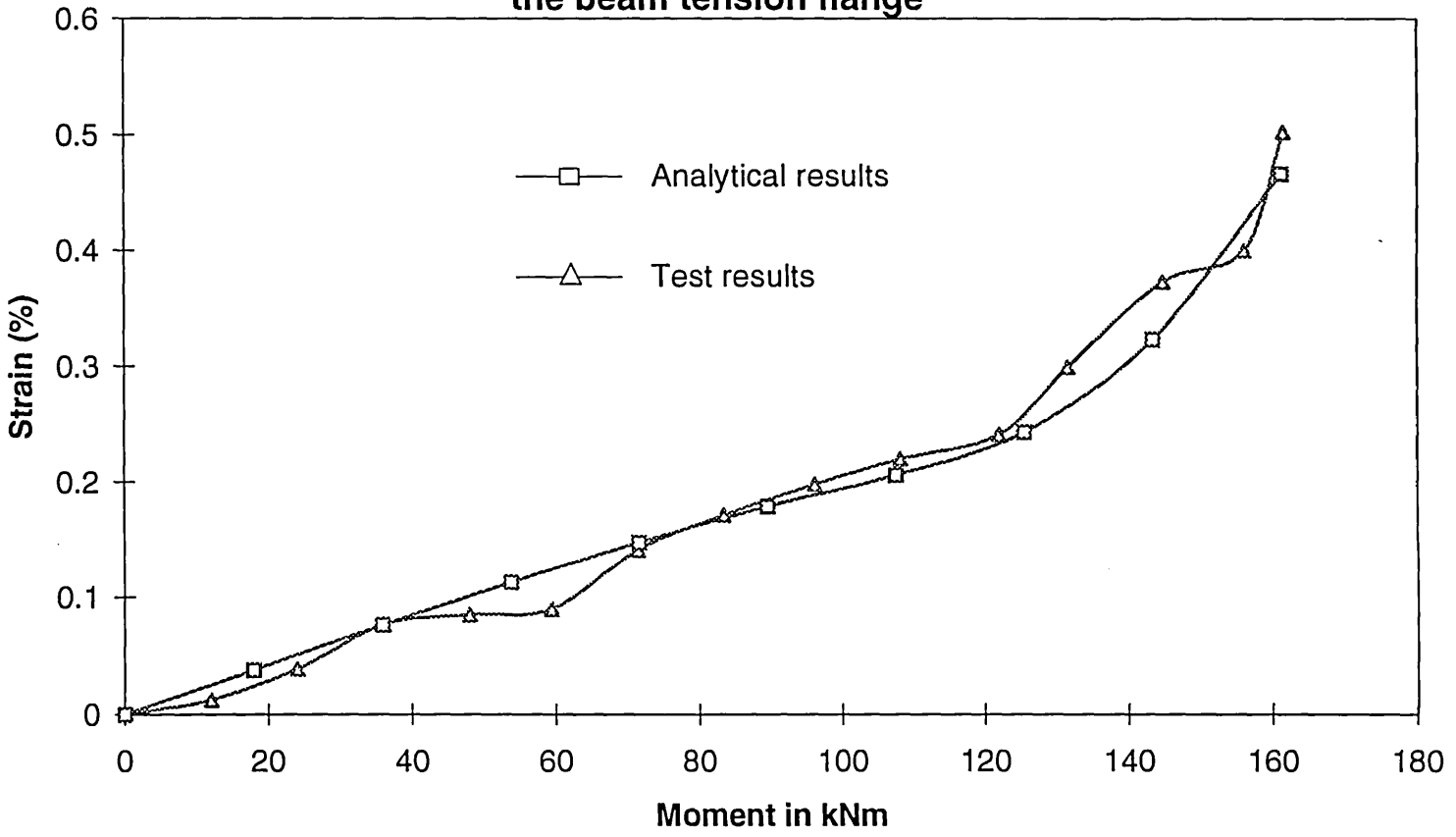

Fig. 6.12 Comparison between analytical and experimental bolt strains, T6 and M6, first row of M24 bolt near the beam tension flange

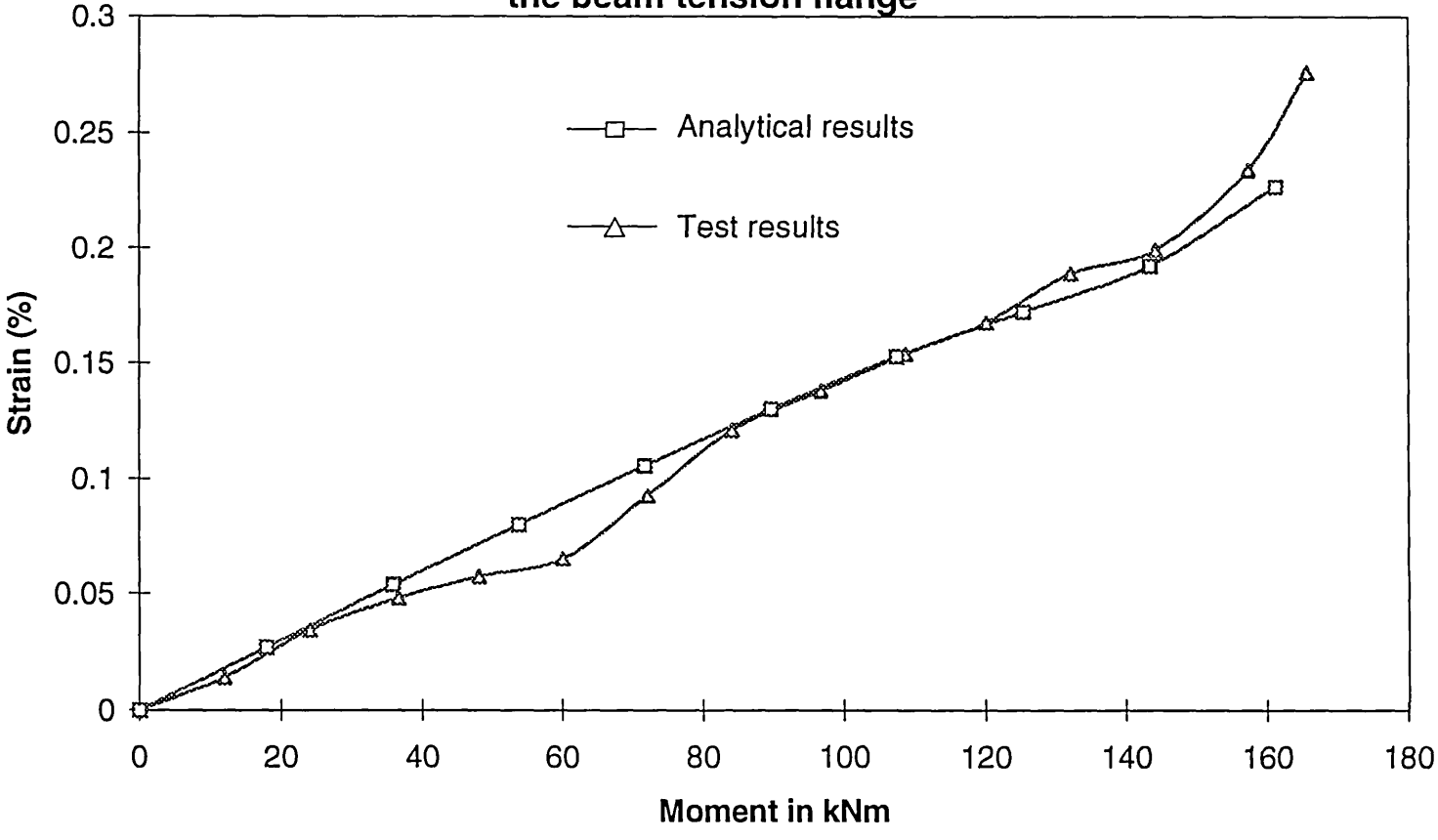

Fig. 6.13 Comparison between analytical and experimental column web strains, T1 and M1, strain at column mid depth, in line with the beam compression flange

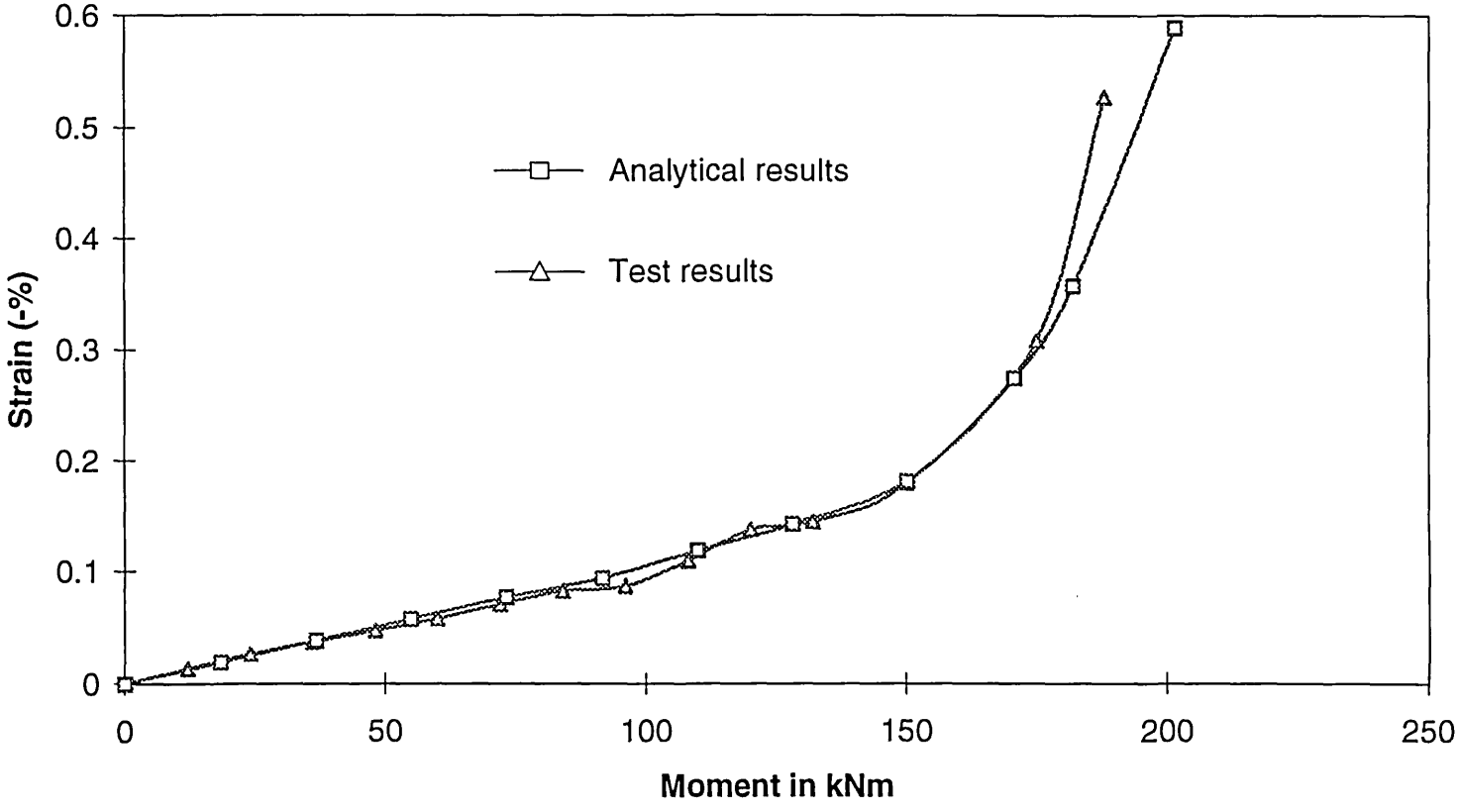

Fig. 6.14 Comparison between analytical and experimental column web strains, T2 and M2, strain at column mid depth, in line with the beam compression flange

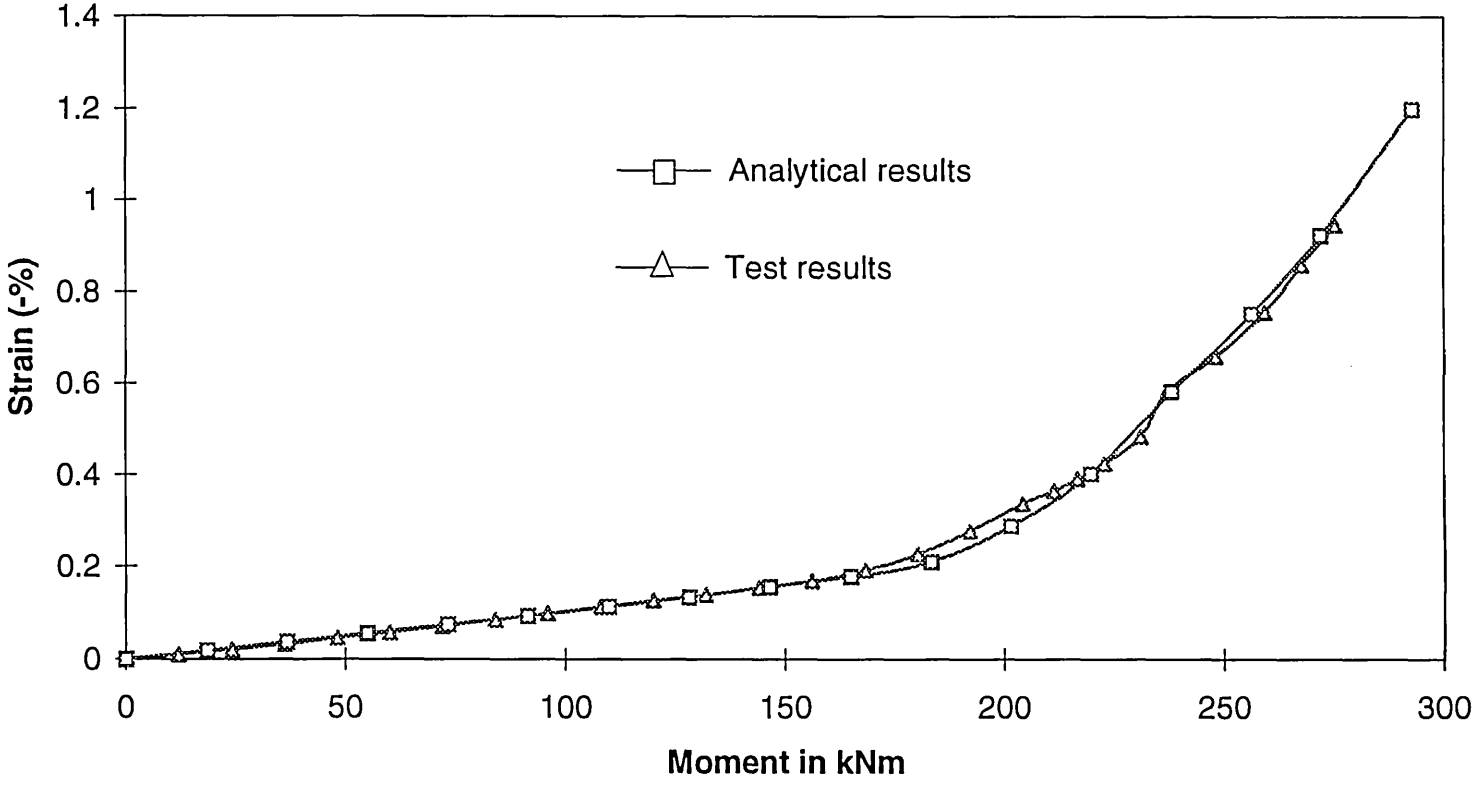

Fig. 6.15 Comparison between analytical and experimental column web strains, T3 and M3, strain at column mid depth, in line with the beam compression flange

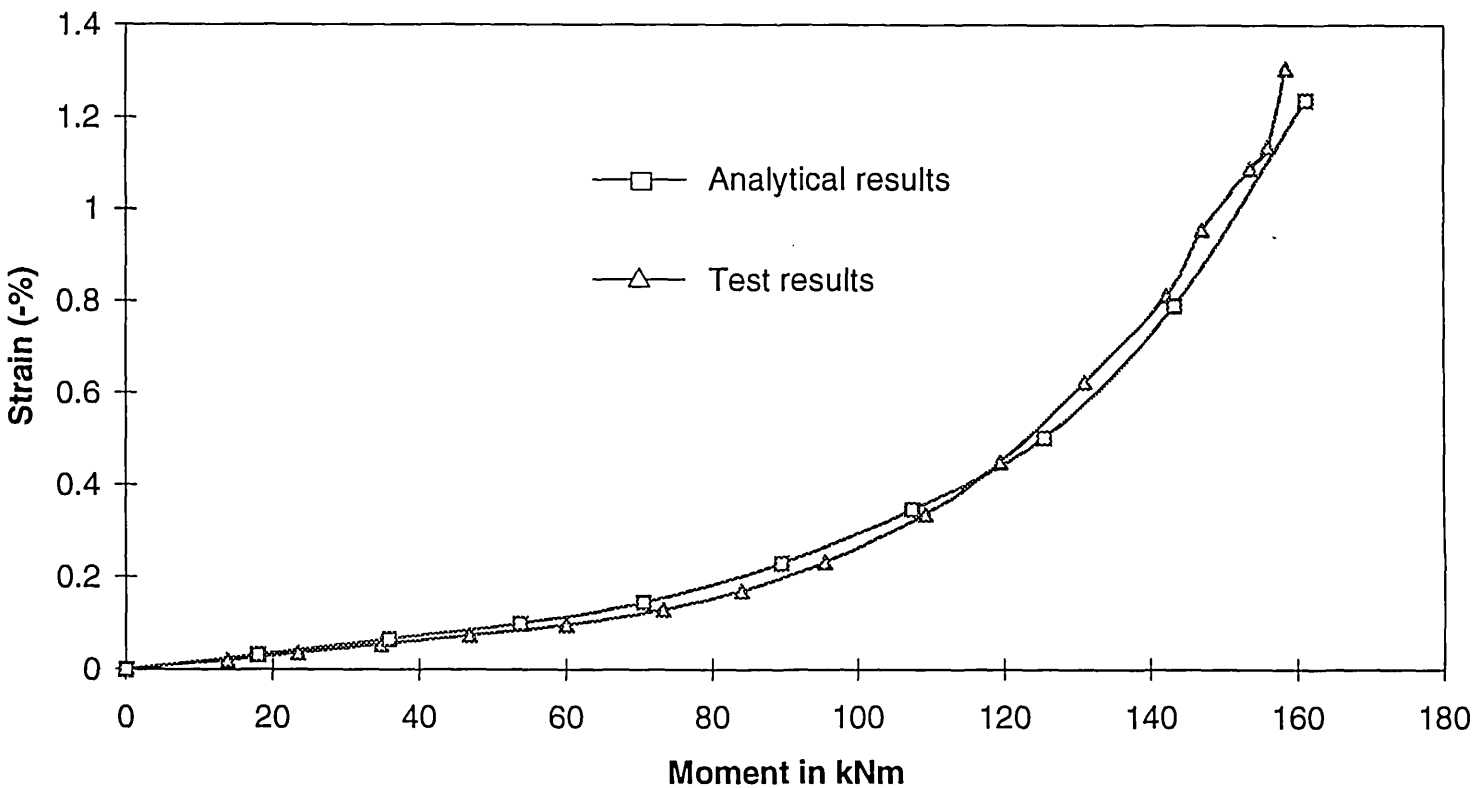

Fig. 6.16 Comparison between analytical and experimental column web strains, T4 and M4, strain at column mid depth, in line with the beam compression flange

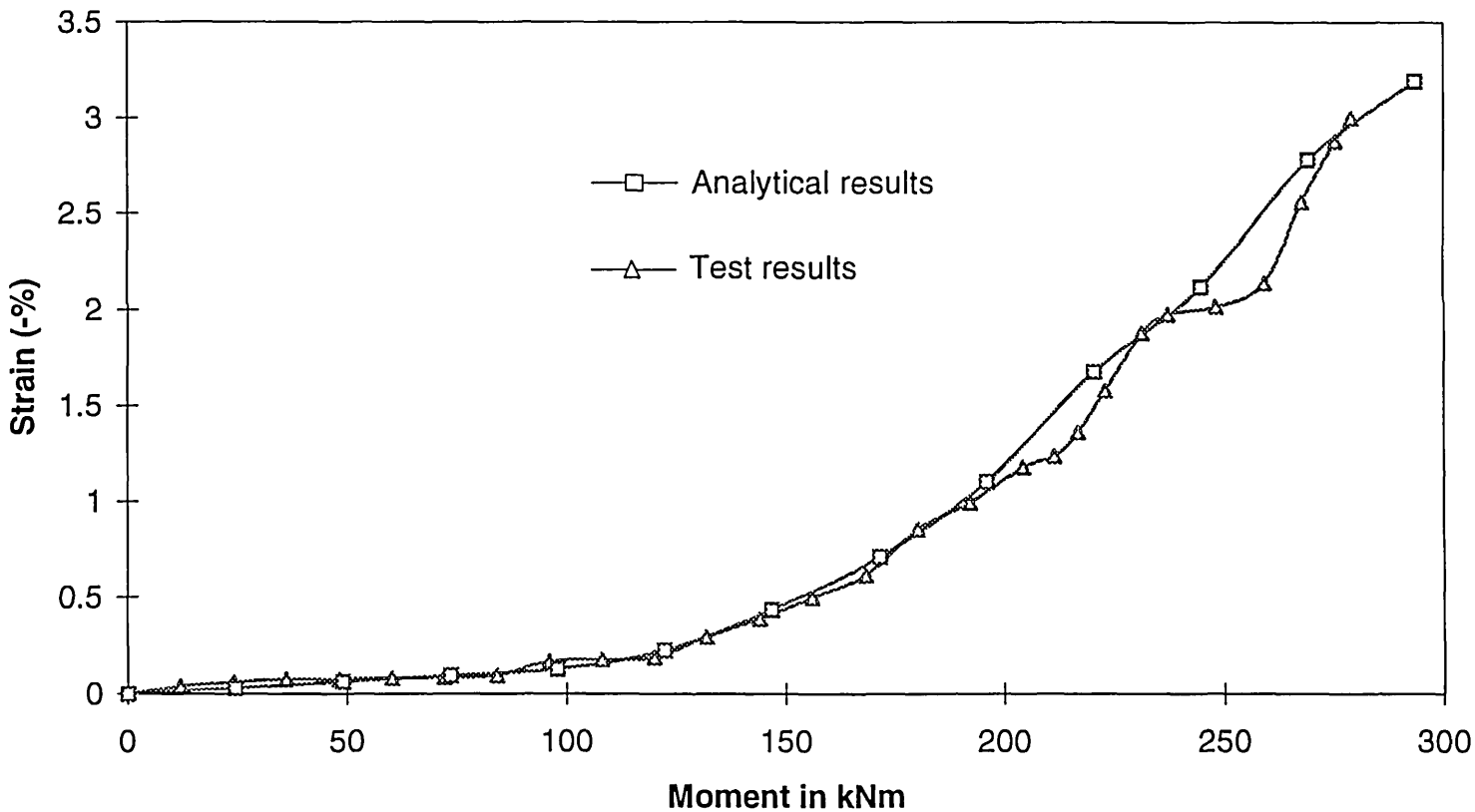

Fig. 6.17 Comparison between analytical and experimental column web strains, T5 and M5, strain at column mid depth, in line with the beam compression flange

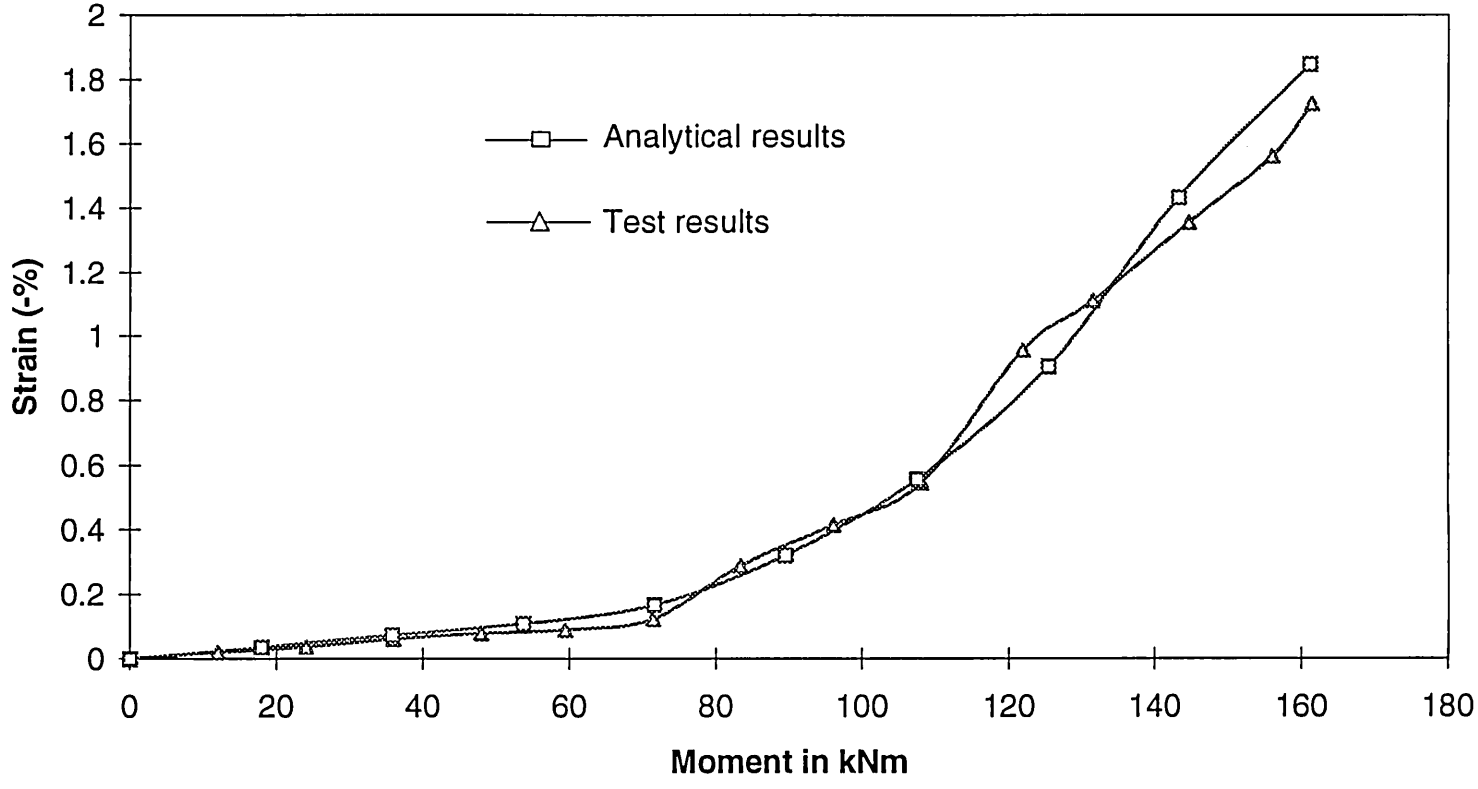

Fig. 6.18 Comparison between analytical and experimental column web strains, T6 and M6, strain at column mid depth, in line with the beam compression flange

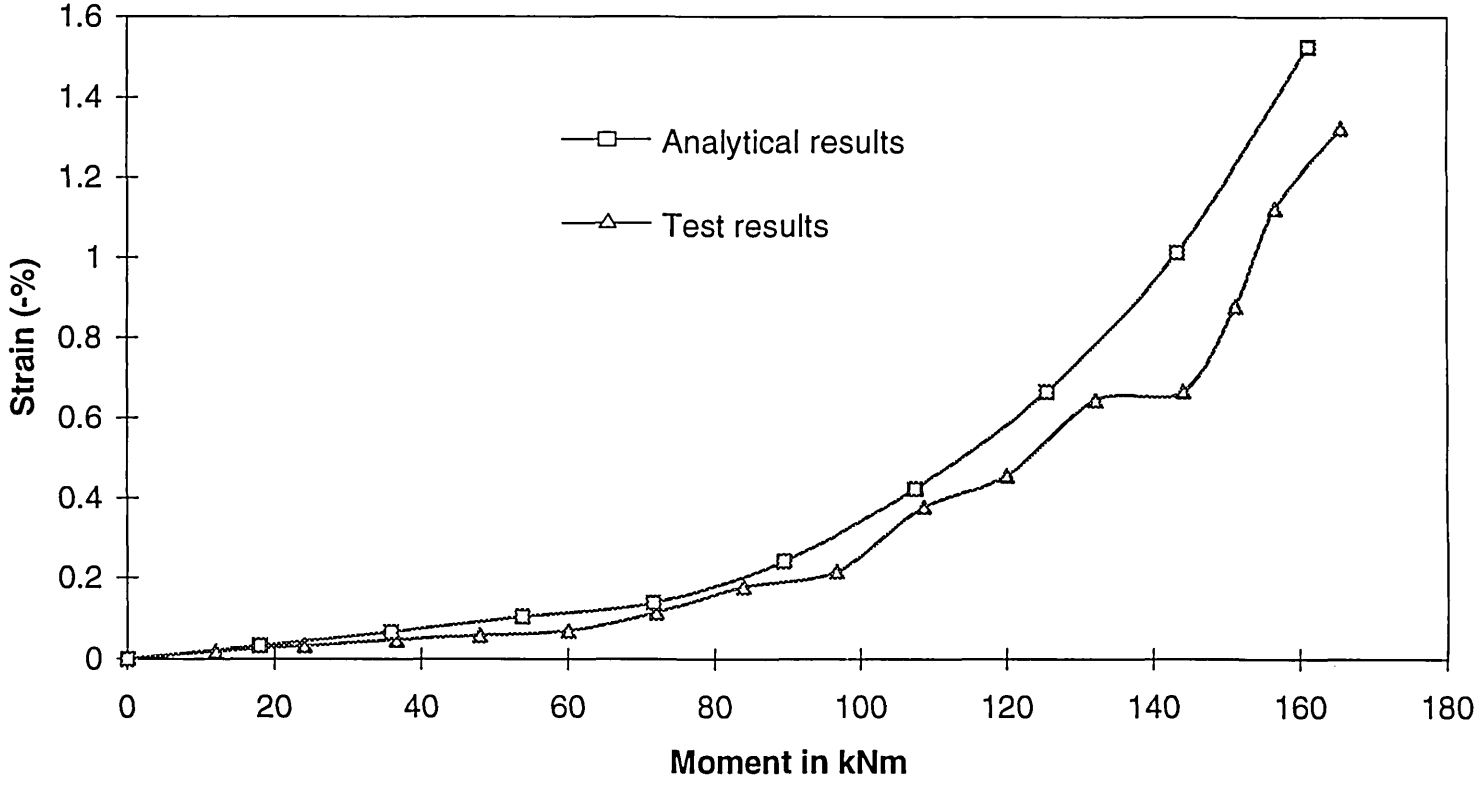

CHAPTER 7

BEHAVIOURAL STUDY OF CONNECTION COMPONENTS

7.1 INTRODUCTION

Based on the comparative study of finite element and experimental results, it was concluded that the finite element model of flush end plate connection was quite accurate and the connection properties derived from the 3-dimensional nonlinear analysis were quite reliable. The finite element technique can, therefore, be applied to develop a design method for these connections. The ability to predict the contribution of each component of the connection is essential for the development of a suitable design method. This enables design curves and tables to be prepared for a rapid design of the flush end plate connections. This chapter includes detailed analytical study of connection components, their performance under loading and the contributions they make towards the overall performance of the connection.

7.2 CONTRIBUTION OF COMPONENTS TO JOINT ROTATION

The rotational stiffness of a connection is composed of the contributions from individual components. For the formulation of a design method it is essential to predict the contribution of each individual component separately. The components which make significant contribution are the column flange, bolts and end plate. As mentioned in Chapter 4 and illustrated in Figures 4.6 and 4.7, the contributions of above components to the total rotation of the connection are given by :

$$\phi = \frac{ab}{D - \frac{T}{2}}$$

$$\phi_{cf} = \frac{a' c'}{D - \frac{T}{2}}$$

$$\phi_{b} = \frac{c' d'}{D - \frac{T}{2}}$$

$$\phi_{ep} = \frac{d' b'}{D - \frac{T}{2}}$$

The total rotation, ϕ, is the aggregate of the three individual rotations and is given by:

$$\phi = \phi_{cf} + \phi_{b} + \phi_{ep}$$

In the linear elastic range, 36% of the total rotation of the analytical model M1 is caused due to bending of end plate, 20% due to bolt elongation and 43% due to column flange deformation, as indicated in Table 7.1 and Figure 7.1. The contribution of a component is variable within the elasto-plastic range. Immediately before failure the contributions of end plate, bolt and column flange of the analytical model M1 are 53%, 28% and 17% respectively. For the six analytical models the contributions of the three components to the connection rotation were determined which are shown in Table 7.1 and Figures 7.1 to 7.6. Modelling and finite element analysis of end plate connection is an extremely time consuming and costly job. Because of the limited data available it is difficult to draw definite conclusions. A lot more computing has to be done to produce sufficient data needed for preparing design tables and charts. From Table 7.1 it can be concluded that end plate and column flange are the main contributors to joint rotation, when the connection configuration is with two rows of bolts in the tension region. It is also obvious that, while the contribution of end plate increases as the connection changes from elastic to elasto-plastic state, the contribution of column flange decreases. No significant

change in bolt contribution is noted. It is further noted that the deformation of end plate is greatly enhanced by two rows of bolts in the tension region.

7.3 BOLT FORCE

In bolted end plate connections the load at the beam end is transferred to the bolts through the end plate. Although the behaviour of the bolts under direct load has been extensively investigated, their response within the confines of a connection has received little attention. In order to bridge the existing gap it was decided to study the bolt response in flush end plate connections.

In practice the bolts in a framed structure are subjected to a combination of forces, such as tensile force, shear force, and bending moment. In order to simplify the complex problem, it is usually assumed that shear force is carried by the bolts which are in the compression side of the connection, while tensile force and bending moment are resisted by the bolts in the tension side of the connection. In the analytical model the shear force is not considered because they are known to have very little effect on the rotational behaviour of the connection.

When the connection reaches the failure load of 187.8 kNm (observed in laboratory experiment), the force in the tension bolts of the analytical model M1 is 217 kN which corresponds to a bolt stress of 886 N/mm^2 , as recorded in Table 7.2. For the three analytical models M1 to M3, with one row of bolts in the tension region, the computed bolt forces are given in Table 7.2 and bolt force-moment curves are shown in Figure 7.7. The bolt stress at failure varied from 854 N/mm^2 to 909 N/mm^2 , which is close to the results of material test (Table 5.2). In the test programme each of these connections failed due to thread stripping. In Figure 7.7 it is also noticed that bolt force is proportioned to the moment until failure. High-strength bolt is a brittle material which undergoes very little elasto-plastic deformation.

For the analytical models M4 to M6, with two rows of bolts in the tension region, the location of the bolt rows and bolt forces in the two rows are recorded in

Table 7.3 and Figures 7.8 to 7.10. The results indicate that bolt forces are generally proportional to the distance of the bolts from the beam compression flange. The absence of any elasto-plastic deformation of bolts is also noticeable.

7.4 BOLT BENDING

In practice the bolts in the tension region of flush end plate connections are not subjected to axial force only. The deformations of end plate and column flange induce moment on the bolts which becomes significant as the load on the connection increases. Fig. 7.11 shows the deformation of the bolt and the elements around that bolt for the analytical model M1 as it approaches failure load. In the finite element model eight bar elements represented one bolt. Significant differences in the elongation of eight bar elements are observed. Generally the bar element 1 in Figure 7.11(a) elongates the most, while bar element 5 elongates the least. The largest and smallest strains in the bar elements representing one bolt is recorded in Table 7.4. It is noticed that the maximum strain is around 4 to 7 times the minimum strain in a bolt. Difference in strains in the eight bar elements can be attributed to bending moment acting on the bolt in addition to direct tensile load. There are both advantages and disadvantages in modelling a bolt by eight bar elements. While bar elements directly output bolt forces and bolt strains, they can model axial force only.

7.5 PRYING FORCE

The development, location and magnitude of prying forces are dependent on the relative stiffnesses of end plate and column flange in the connection. They also depend on the connection details, size of bolts and level of loading. In flush end plate connections prying forces are likely to develop at the free edges of the end plate. It is difficult to quantify prying forces by experimental means. The magnitude and the location of the resultant of prying forces depend on the zones of contact between the connected plates i.e. column flange and end plate, and vary with the nature and magnitude of loading.

By the use of finite element technique it is possible to chart the distribution of prying forces and the changes occurring as the load increases. For the analytical models M1 to M6, the patterns of prying forces at low and high moments are illustrated in Figures 7.12 to 7.17. In the analytical models M1 to M3, with one row of tension bolts, prying force is either totally absent or is very negligible in the tension region. Even the very small prying force disappears at high moment. At small load the prying pattern in the compression region is triangular. However, it gradually changes to a trapezoidal shape with increasing load and the prying forces concentrate towards the bottom edge of the end plate.

The prying patterns for the analytical models M4 to M6, which have two rows of bolts near each of the beam tension and compression flanges, are illustrated in Figures 7.15 to 7.17. These figures show that the prying forces in the tensile region mainly concentrate at the free edge of the end plate near the second row of tensile bolts. They also indicate that some prying forces also scatter at the free edge of end plate near the third row of bolts. At high moment all prying forces in the tensile region disappear in the analytical model M4, while some prying forces still remain in the tensile region in the analytical models M5 and M6. As to the compression region, the prying patterns of these three models are of triangular shape. There are no significant changes in the pattern with increasing load, but there is a tendency for the prying forces to concentrate towards the bottom edge of the end plate.

Comparison of prying patterns recorded experimentally (Figures 5.17 to 5.28 in Chapter 5) and obtained analytically (Figures 7.12 to 7.17) indicates some discrepancy. The main difference is that prying patterns recorded by carbon paper indicate contacts in the region opposite column and beam webs, while no such contacts are shown in finite element analysis. This can be attributed to the distortion of the end plate due to welding. In the rest of the connection prying patterns recorded by carbon paper show good agreement with the analytical results.

The variation of prying force in the tension region with moment in the analytical models M4 to M6 are shown in Figure 7.18. Initially the prying force increases with increasing load; it reaches a maximum value after which it starts decreasing with further increase of load. In the finite element analysis each analytical model was loaded until the maximum load equalled the failure load recorded in the experiment. In the analytical model M4 the prying force was reduced to zero at the maximum load of 244.6 kNm while in the analytical models M5 and M6 significant prying forces acted at failure loads.

The prying force generated at the interface of end plate and column flange increases the bolt force in the tension region. Figures 7.15 to 7.17 indicate that the prying forces in the tension region are mainly concentrated near the second row of tension bolts. It is therefore logical to conclude that prying will mainly affect these bolts. The ratios of prying force in the tension region to the force in the second row of the tension bolts were calculated, which are shown in Figure 7.19 and Table 7.5. These indicate that as the moment acting at the connection increases, the bolt forces are less affected by prying. In the final stage of the analytical model M4 prying vanished and had absolutely no effect on the bolt force. The dominant bolts in terms of bolt strength are the first row of tensile bolts. Analytical results show that prying forces have little effect on the first row of tensile bolts in flush end plate connections.

7.6 DEFORMATION

The deformation of each component of the connection is governed by the system of forces it is resisting. In the present study the moment applied to the connection is replaced by an equivalent couple whose force components act at the level of beam flanges. The contribution of the beam towards joint rotation is negligible and is disregarded in the investigation. However, a short length of the beam with an artificially high modulus of elasticity was included in the connection model. This would ensure that all the nodes common to beam and end plate would remain in one

plane during the analysis. The deformed configurations illustrated in Figures 7.20 to 7.25 confirmed that the above requirement was fulfilled.

The end plate is subjected to tension and compression forces through the respective beam flanges as well as the resisting bolt forces joining end plate to the column flange. This system of forces induces internal forces and stress resultants in the plate and cause deformation. The end plate bends about beam flanges and web which results in its prying into column flange creating another set of forces. The prying action increases forces in the bolts and at the same time it enhances the end plate rigidity by forcing it into double curvature. The bolt bending can be observed through the end plate double curvature.

In Figures 7.20 to 7.25 we can also observe deformation of the column flange and end plate in each of the six analytical models. Indications of prying in the analytical models M5 and M6 are also noticeable in Figures 7.24 and 7.25. In connections with one row of tension bolts large end plate deformations are observed at the level of the tension bolts.

7.7 STRESS AND DISPLACEMENT DISTRIBUTION

Figure 7.26 shows stress (equivalent stress von Mises) and displacement (in z direction) contours of column web of the analytical model M1 at failure load. It is noticed that the stress concentration is high in two areas, one opposite the tension bolt and the other opposite the beam compression flange. Yielding of column web develops at the same locations, as illustrated in Figure 7.27. Figure 7.28 shows stress and displacement contours of column flange of the analytical model M1. High stress concentrations are observed around the two bolt locations, and over an area surrounding the beam compression flange. Displacement contours show that two areas are highly deformed, one (in positive z direction) around tension bolt and the other (in negative z direction) opposite the beam compression flange. Yield patterns of Figure 7.29 highlight three areas which are yielded. It also indicates that the plastification started around tension bolt and along the junction with the web at the

level of beam compression flange. The degree of yield propagation in these regions is limited but increase in load causes the plastification to spread quickly along the line of intersection of the column flange and web at the level of the two beam flanges. Figure 7.30 shows stress and displacement distribution of end plate of the analytical model M1 at failure load. The stress distribution in end plate is similar to that of column flange. There are some areas of high stress concentration along the free edge of the thin end plate. The displacement contours of Figure 7.30 indicate that maximum positive displacement in z direction occurs at the top edge of the end plate while maximum negative displacement happened at the bottom part of the end plate. Figure 7.31 shows that the yield pattern of the end plate at low moment is similar to that of column flange while at high moment the plastification spreads both in the tension and compression regions.

Stress and displacement contours of column web of the analytical model M5 at failure load are illustrated in Figure 7.32. This model contains two rows of bolts in each of the tension and compression regions; as such the stress contours of column web are more complicated than that of the analytical model M1. Two large areas around the tension bolt and beam compression flange are highly stressed. The same two areas are also yielded, as shown in Figure 7.33. In column flange, high stress concentration are found around the two tension bolt locations and over an area near the beam compression flange. The displacement distribution is similar to that of the column flange in the analytical model M1 as shown in Figure 7.34. Yield patterns illustrated in Figure 7.35 are similar to those of the analytical model M1. Stress and displacement contours and yield patterns of the end plate are shown in Figures 7.36 and 7.37. These are similar to those observed in the column flange.

Model	Elastic range (%)			Elasto-plastic range (before failure) (%)		
	Column flange	Bolt	End plate	Column flange	Bolt	End plate
M1	43.7	20.2	36.1	17.9	28.6	53.5
M2	45.1	33.9	21.0	41.9	32.6	25.5
M3	51.6	19.9	28.5	37.0	16.9	46.1
M4	22.4	15.4	62.2	15.8	12.8	71.4
M5	42.9	7.2	49.9	30.7	8.9	60.4
M6	43.2	5.5	51.3	35.5	5.2	59.3

Table 7.1 Contributions of individual components to joint rotation

Model	Failure moment (kNm)	Bolt force (kN)	Bolt stress (N/mm^2)
M1	187.8	217	886
M2	275.4	320	909
M3	158.4	209	854

Table 7.2 Bolt force in models with one row of tension bolts

Model	Distance of bolt (mm)			Bolt force (N)					
				Elastic range			Elasto-plastic range (before failure)		
	1st row	2nd row	Ratio	1st row	2nd row	Ratio	1st row	2nd row	Ratio
M4	397.2	307.2	0.77	99705	70363	0.71	193630	149100	0.77
M5	346.4	256.4	0.74	72372	42338	0.59	139520	110214	0.79
M6	346.4	256.4	0.74	74456	41607	0.56	150660	114923	0.76

Note : Distance of bolt row is measured from the bottom of the compression flange.

Table 7.3 Bolt force in models with two rows of tension bolts

Model	Strain (%) (at failure)		
	Maximum	Minimum	Ratio
M1	1.120	0.293	3.82
M2	1.120	0.237	4.73
M3	1.710	0.248	6.90
M4	2.000	0.288	6.94
M5	1.580	0.209	7.56
M6	0.681	0.130	5.24

Table 7.4 Comparison of bar strains in one bolt model (bolt near beam tension flange)

Model	Ratio of prying to bolt forces (%)	
	Small load	Failure load
M4	17	0
M5	21.6	9.6
M6	21.6	15.2

Table 7.5 Ratio of prying force in the tension region to the force in the second row of tension bolt

Fig. 7.1 Contributions of individual components to joint rotation, model M1

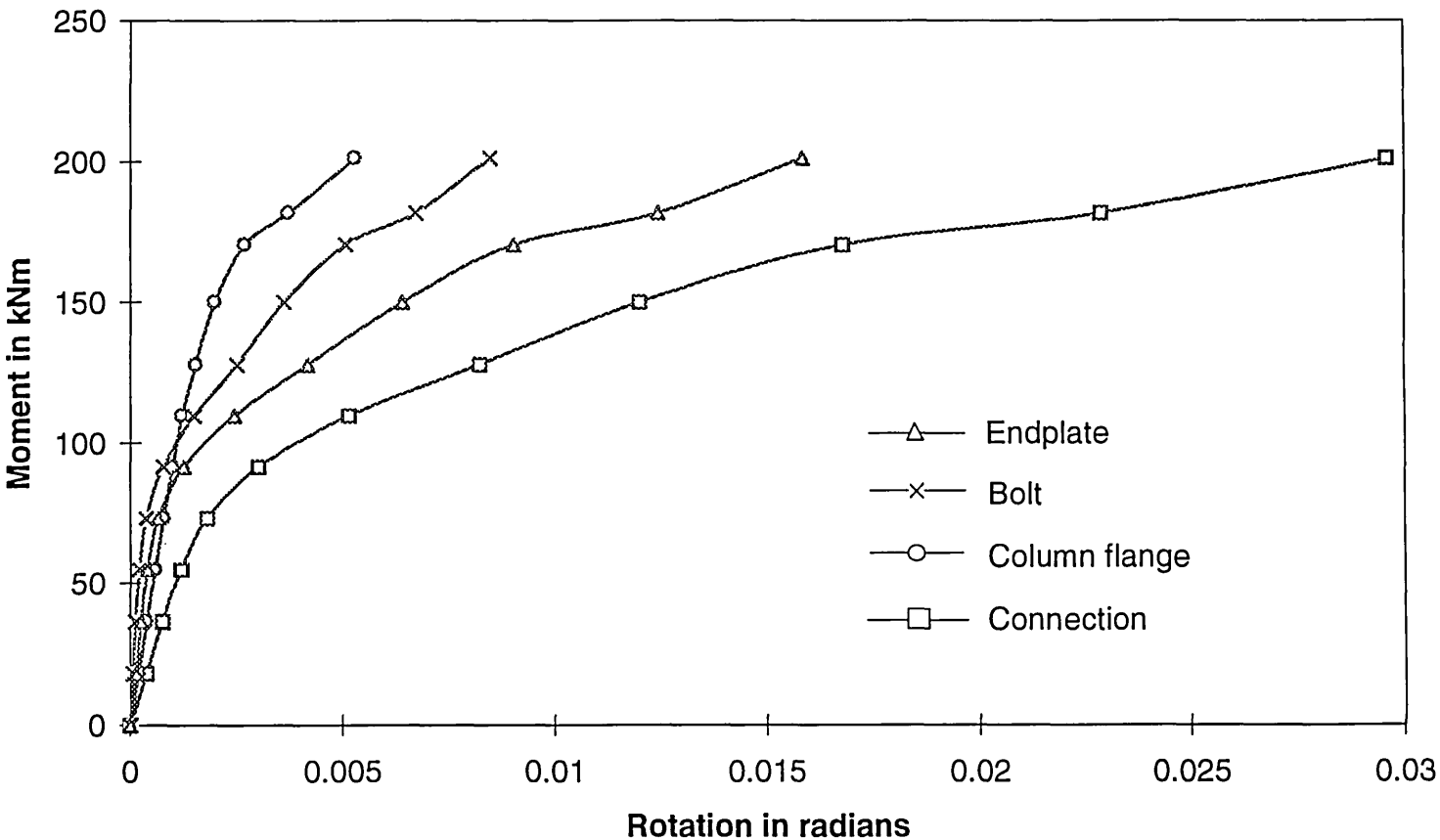

Fig. 7.2 Contributions of individual components to joint rotation, model M2

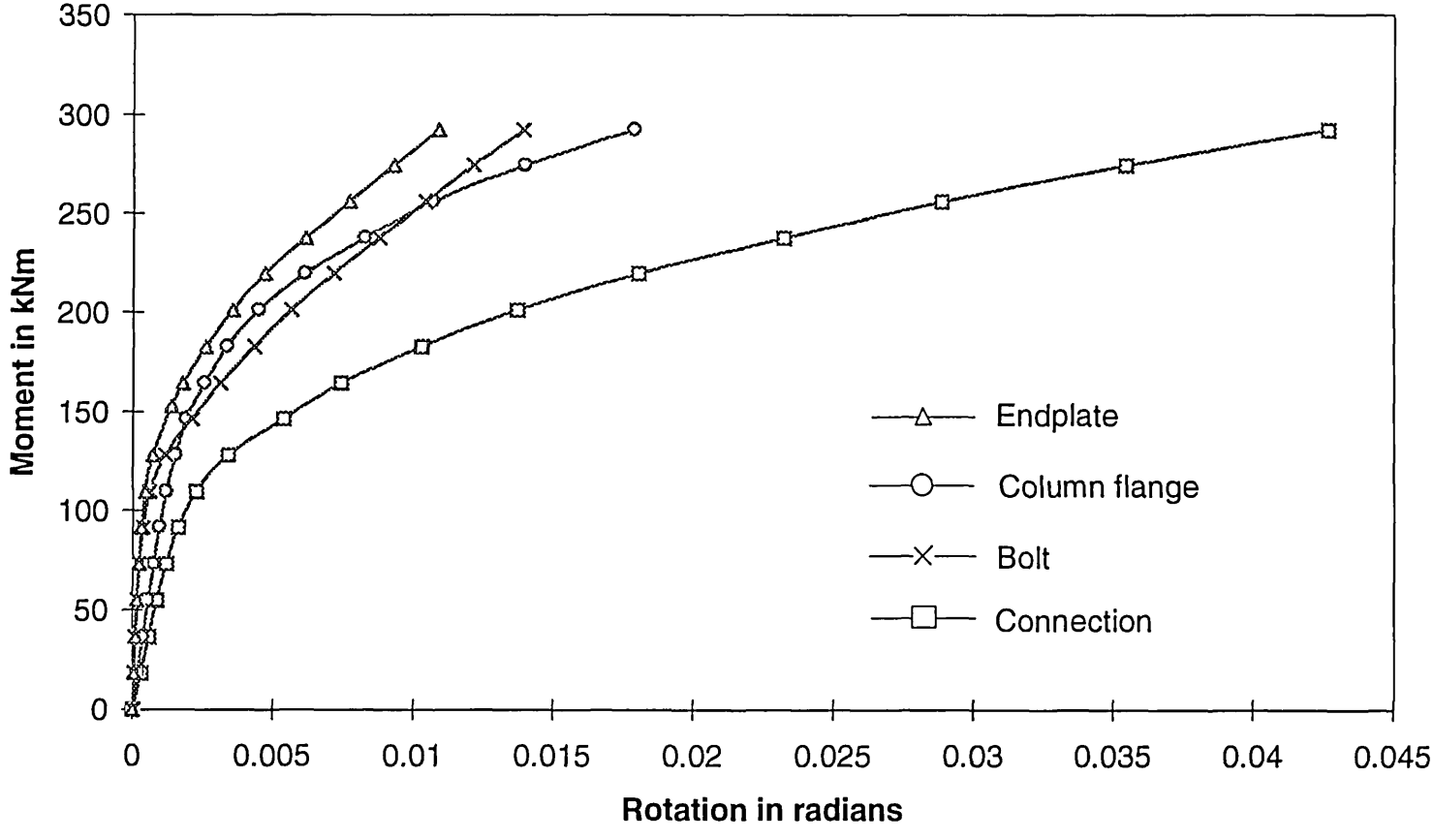

Fig. 7.3 Contributions of individual components to joint rotation, model M3

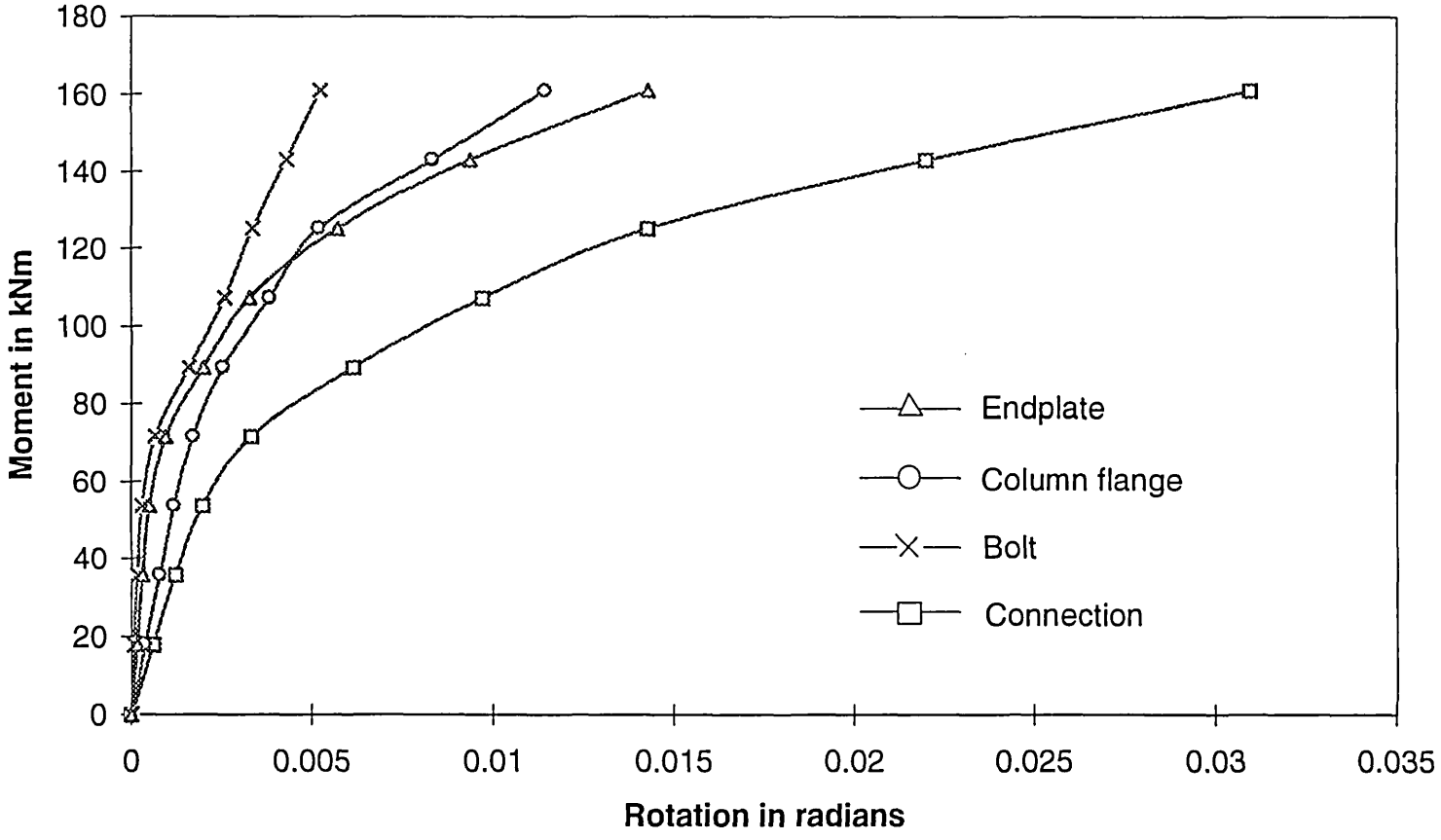

Fig. 7.4 Contributions of individual components to joint rotation, model M4

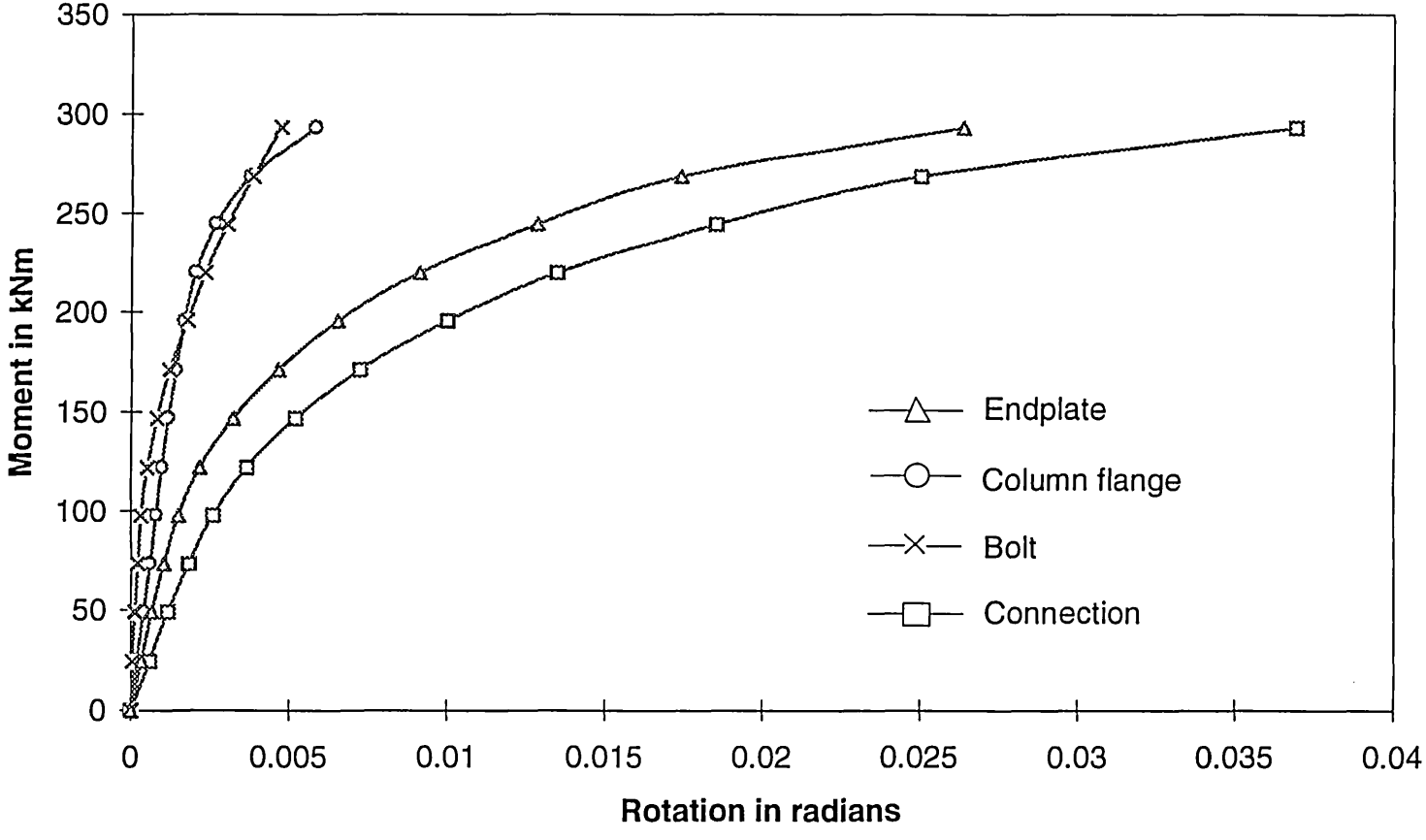

Fig. 7.5 Contributions of individual components to joint rotation, model M5

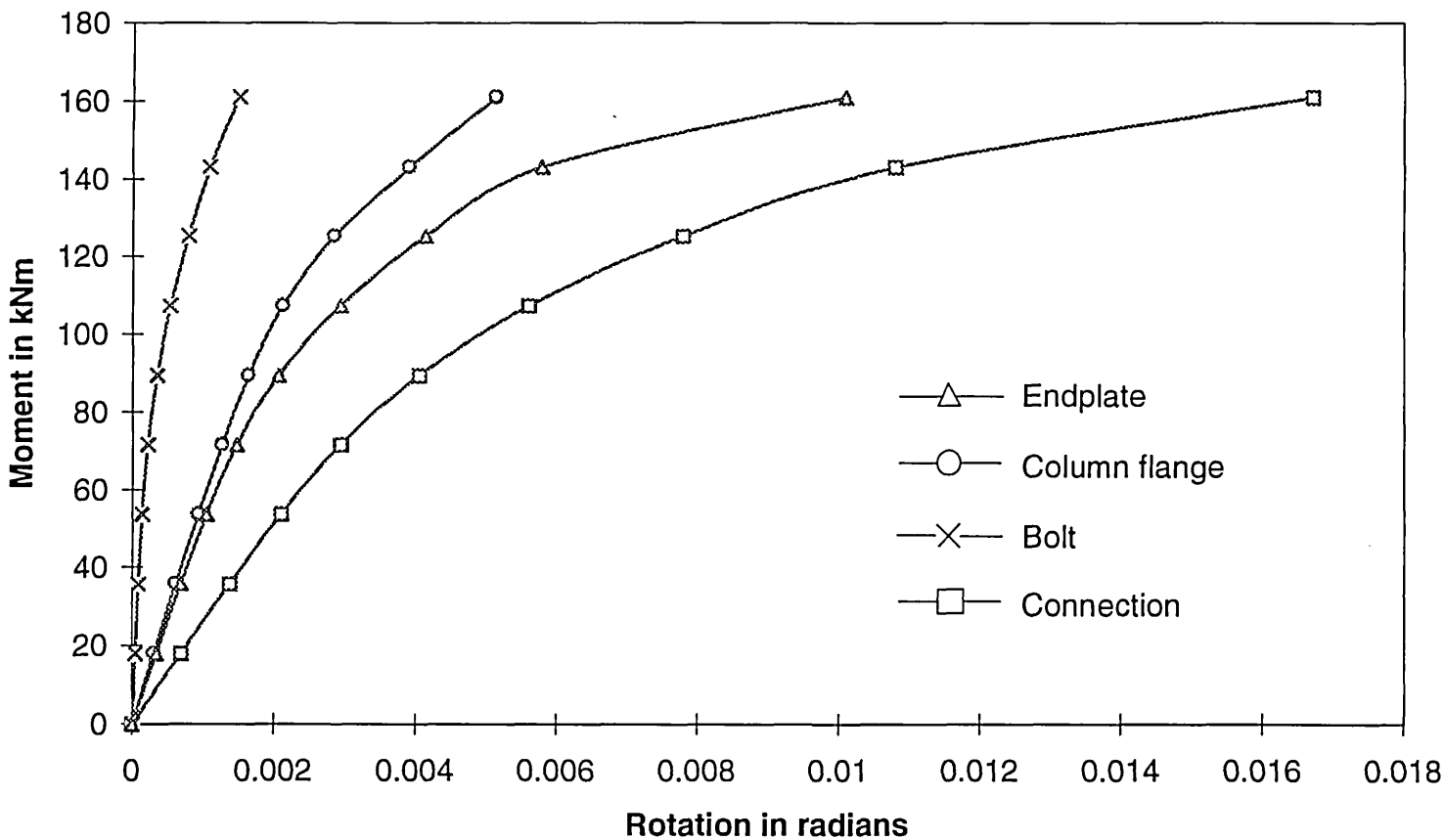

Fig. 7.6 Contributions of individual components to joint rotation, model M6

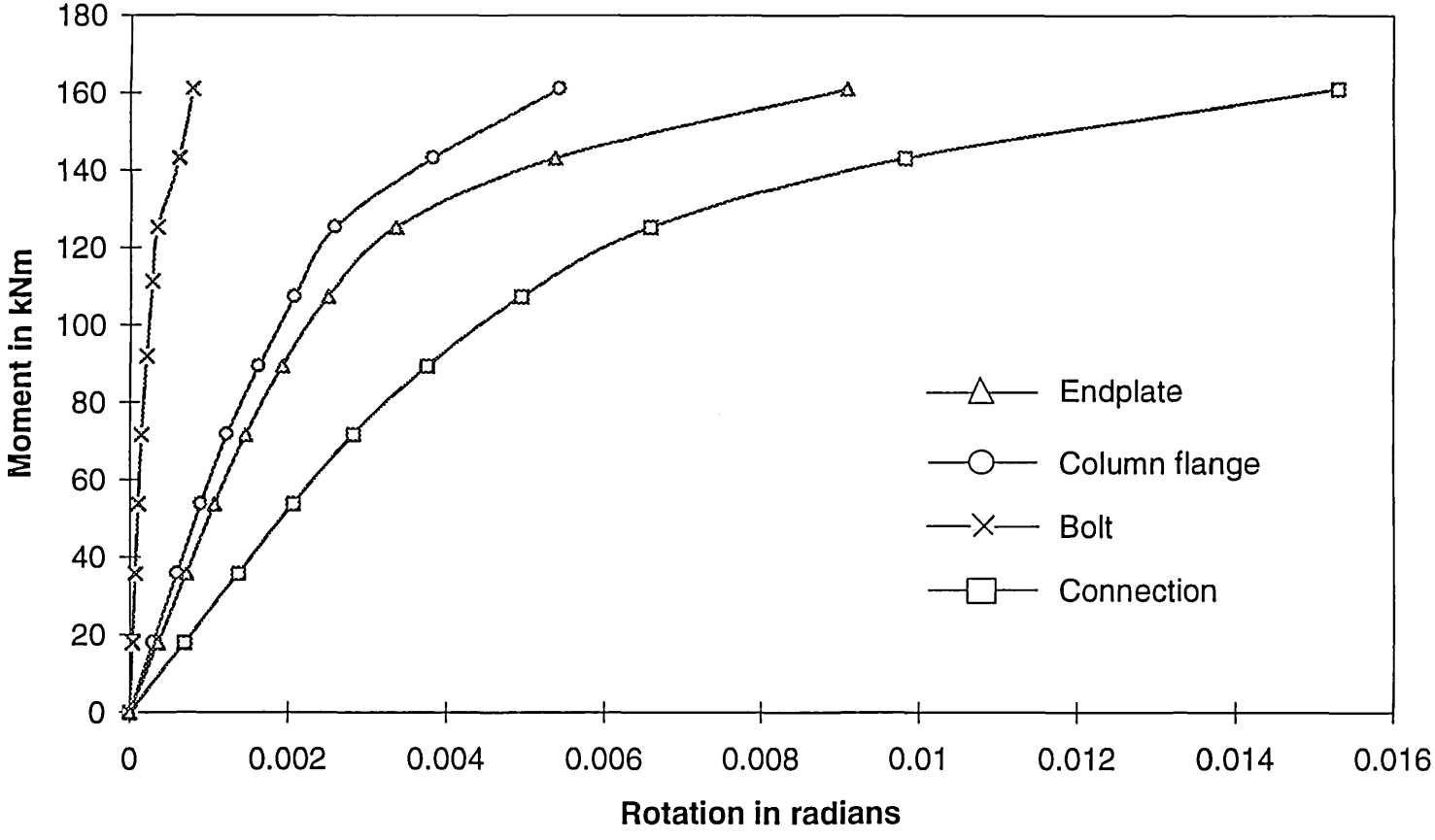

Fig. 7.7 Bolt force-moment curves, models M1 to M3

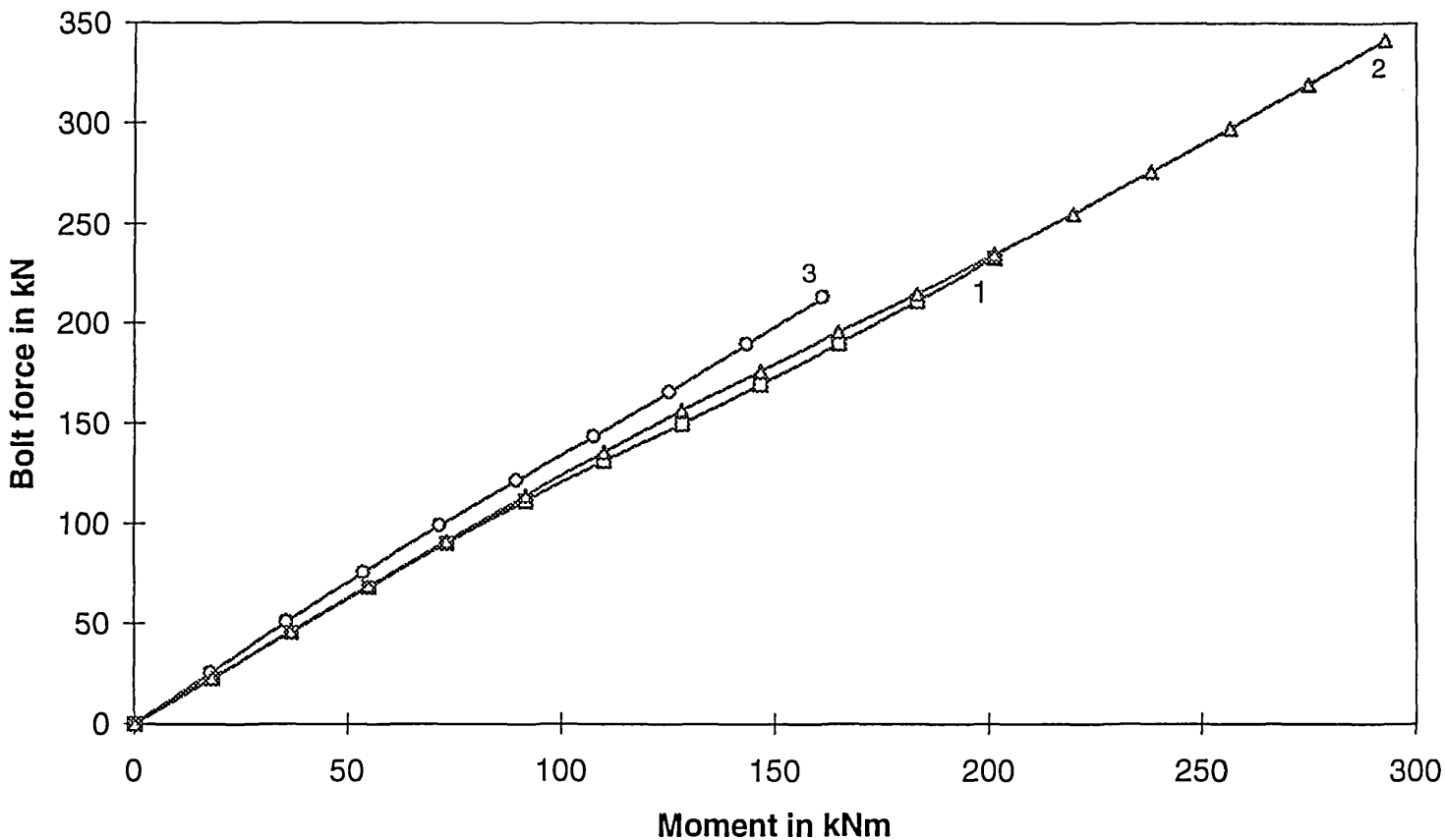

Fig. 7.8 Bolt force-moment curve, model M4

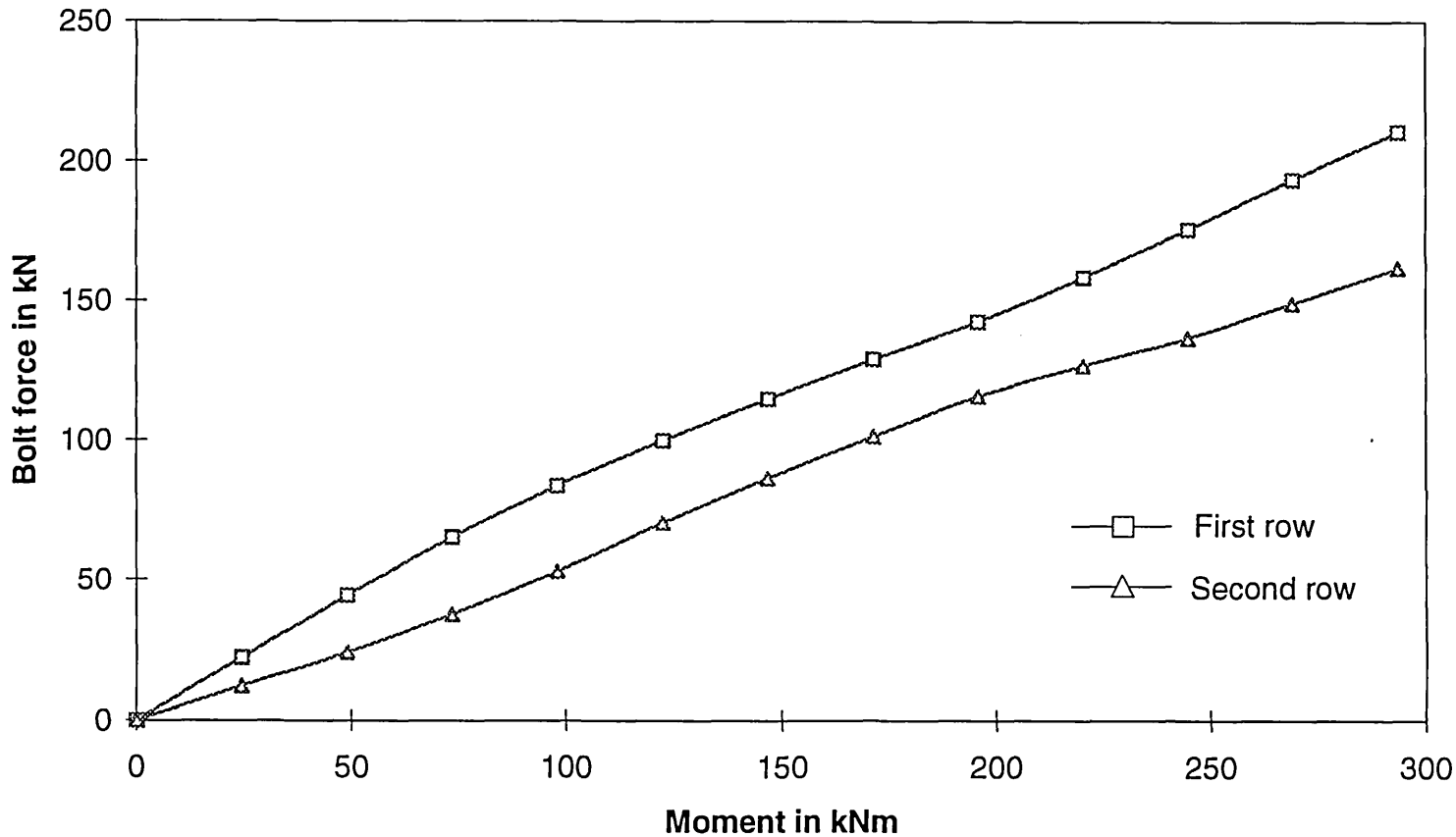

Fig. 7.9 Bolt force-moment curve, model M5

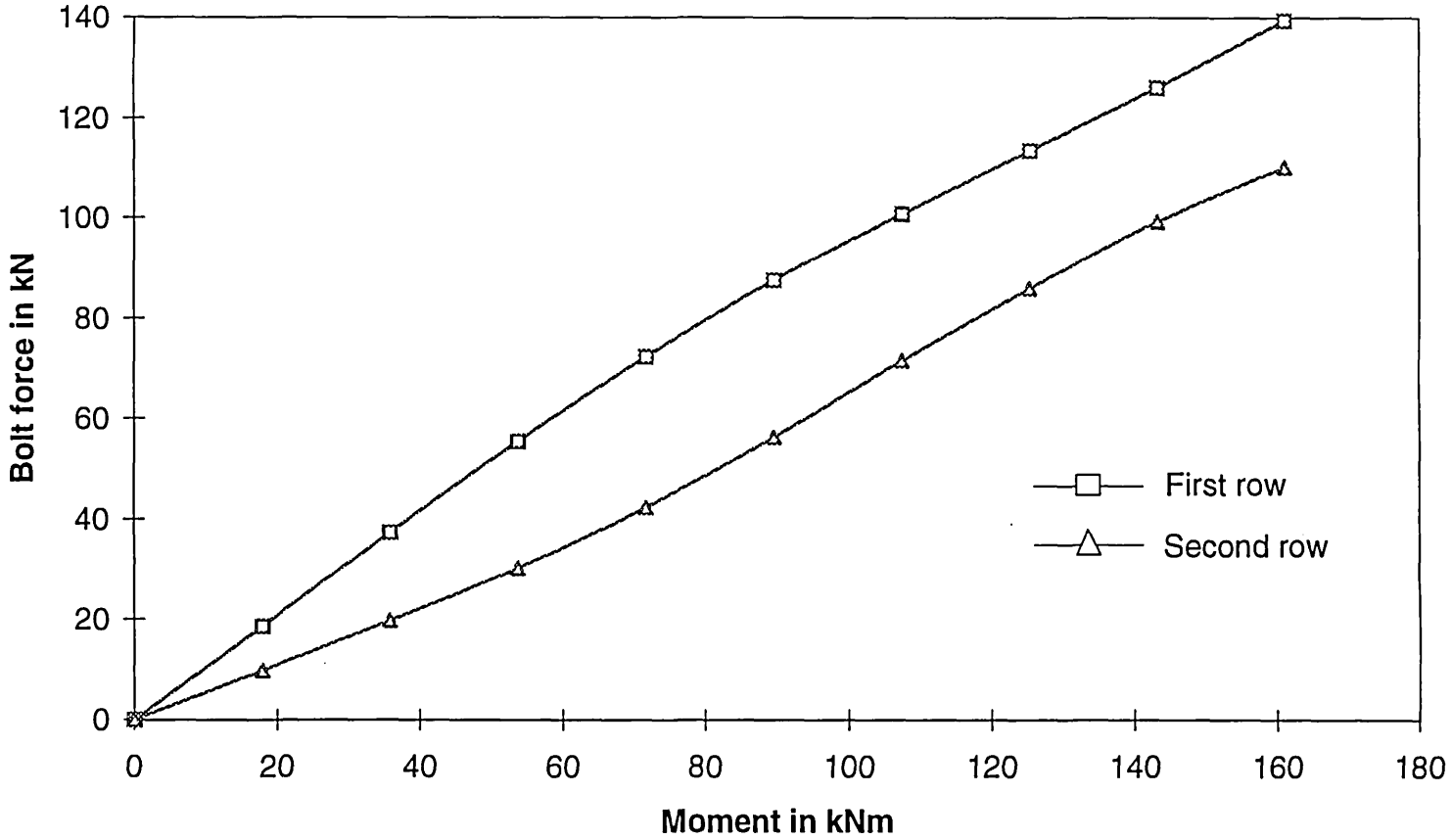

Fig. 7.10 Bolt force-moment curve, model M6

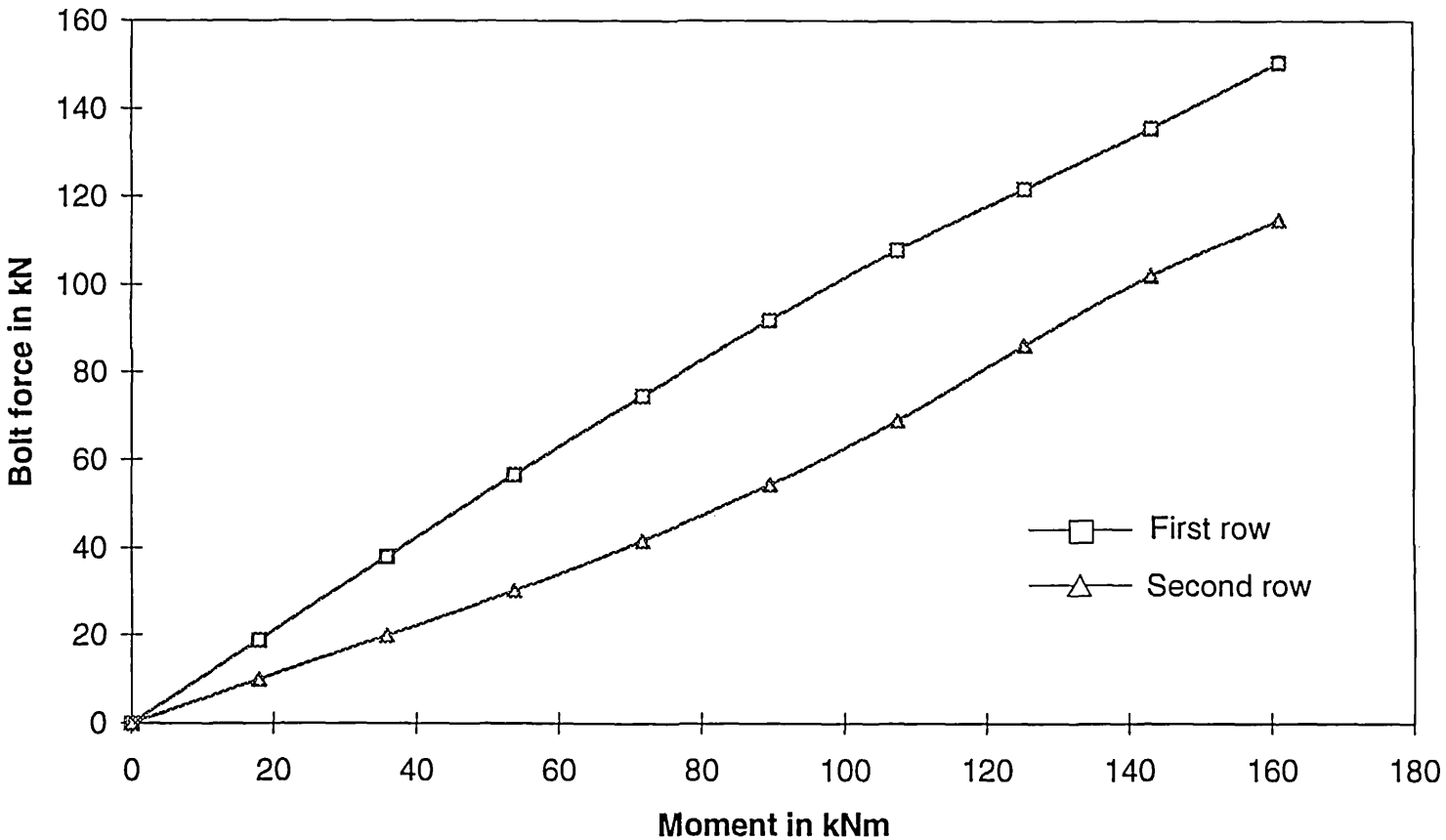

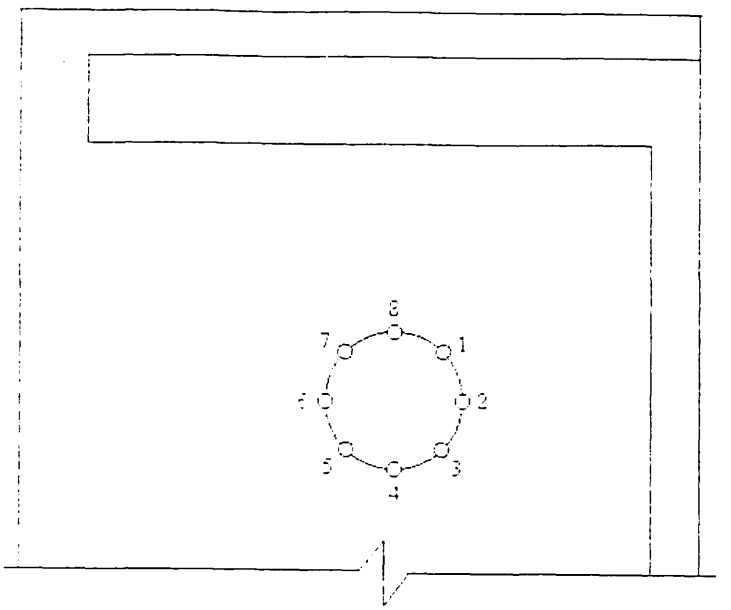

(a)

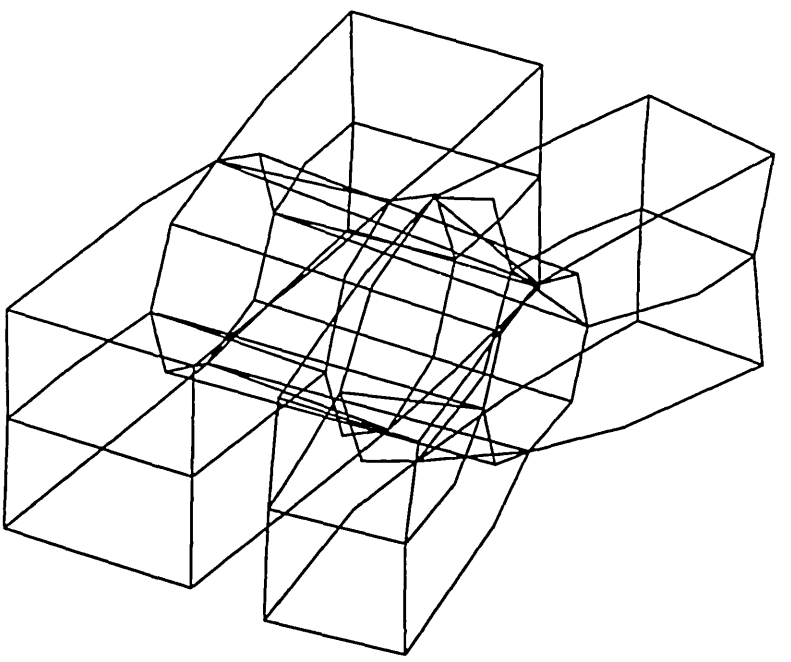

(b)

Fig. 7.11 Deformed bolt and surrounding area

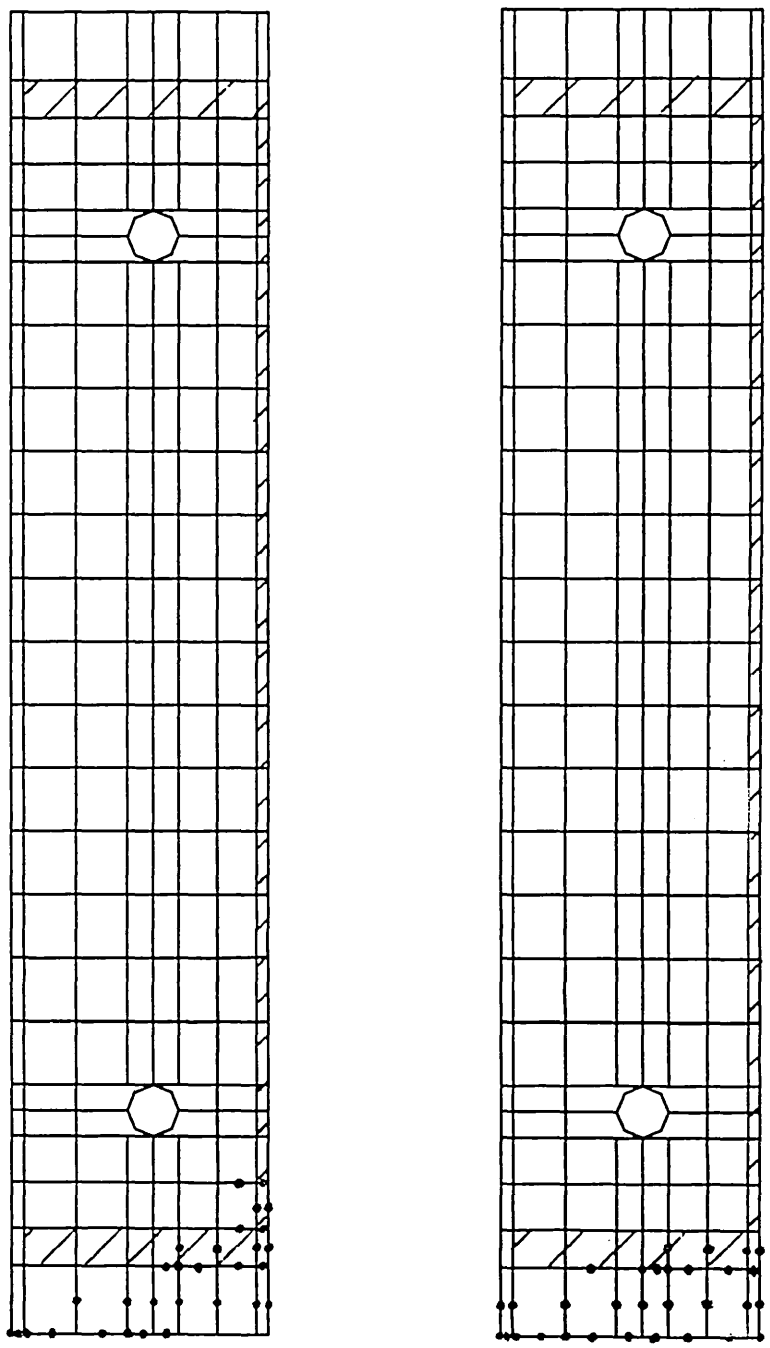

(a) at low moment

(b) at high moment

Fig. 7.12 Prying pattern, model M1

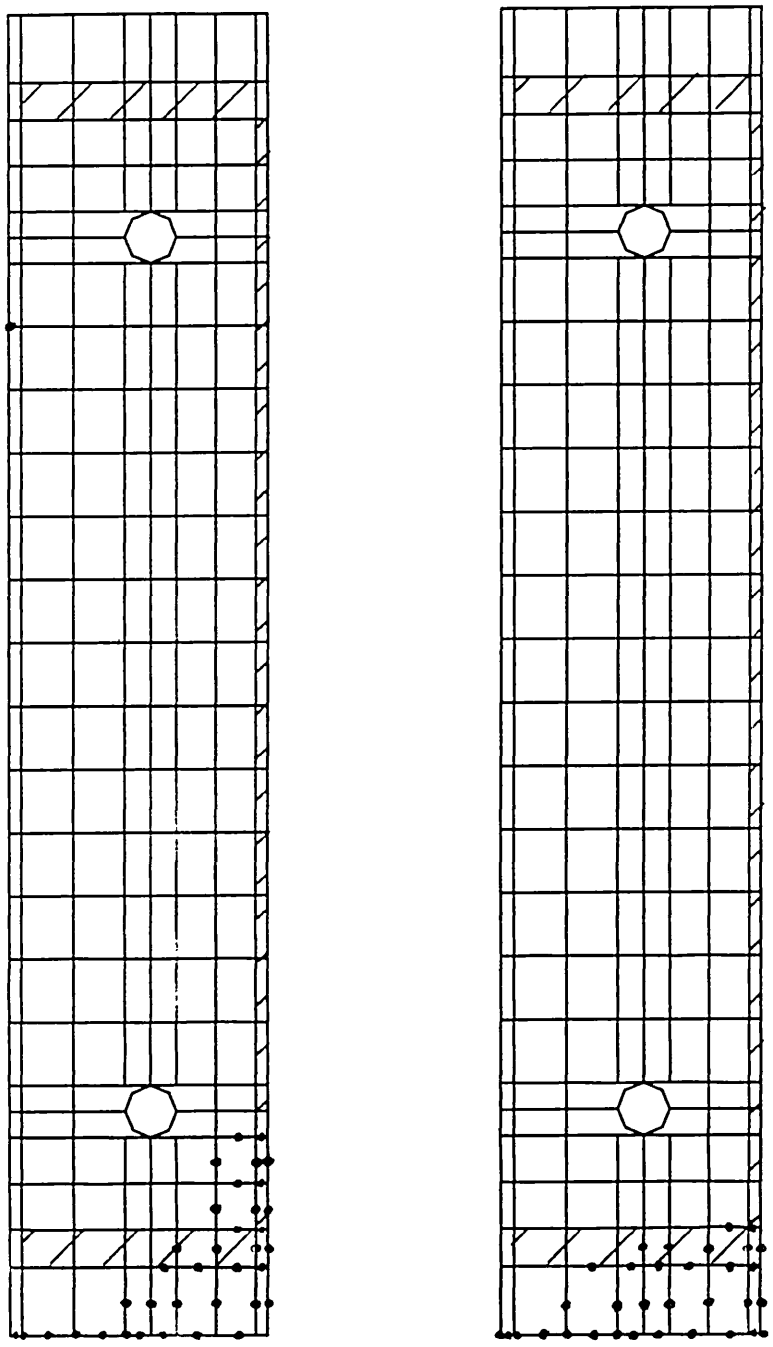

(a) at low moment (b) at high moment

Fig. 7.13 Prying pattern, model M2

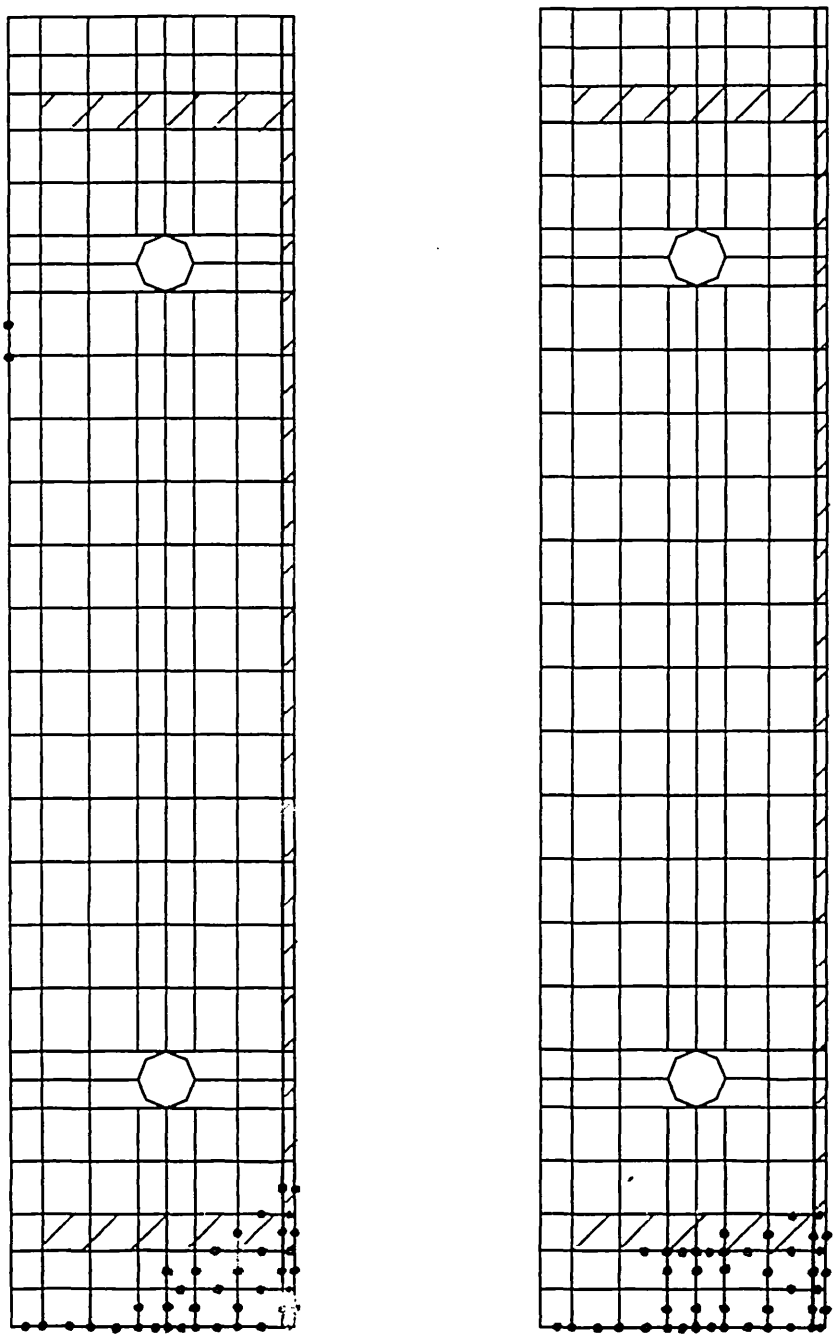

(a) at low moment

(b) at high moment

Fig. 7.14 Prying pattern, model M3

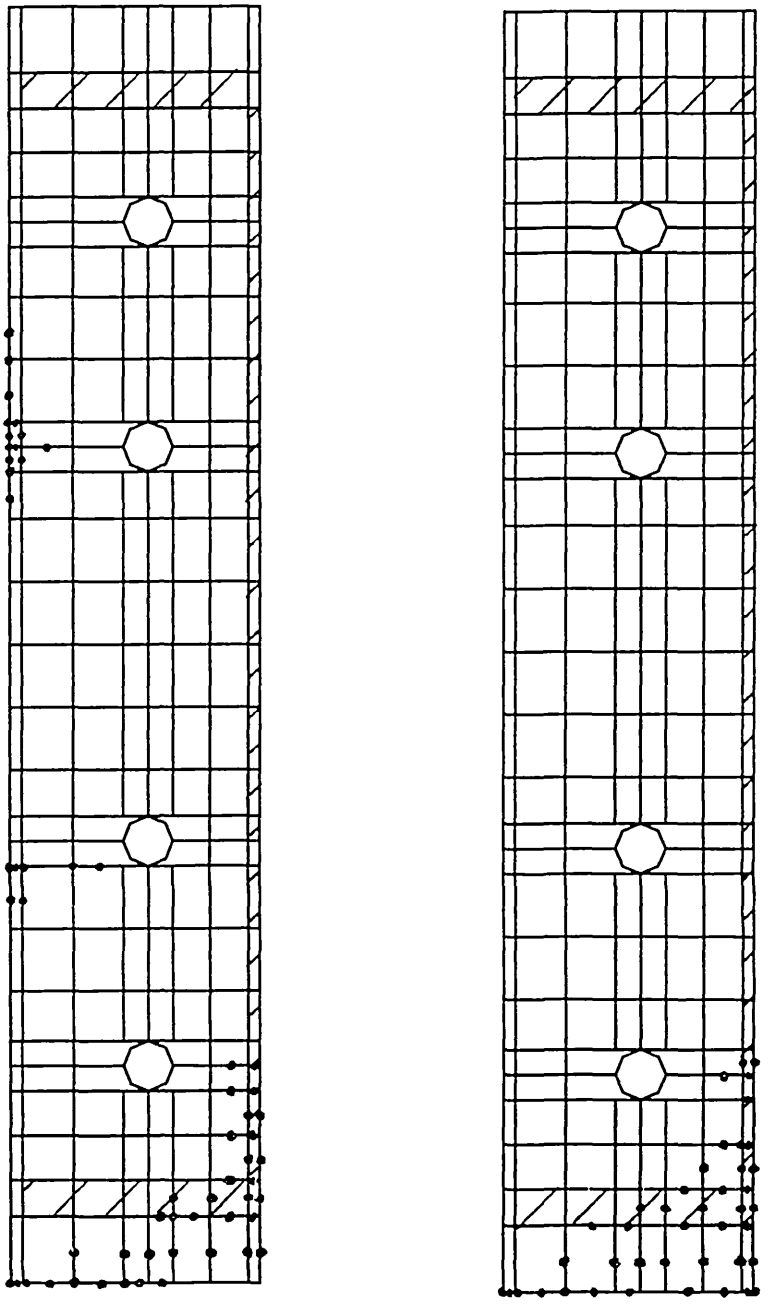

(a) at low moment (b) at high moment

Fig. 7.15 Prying pattern, model M4

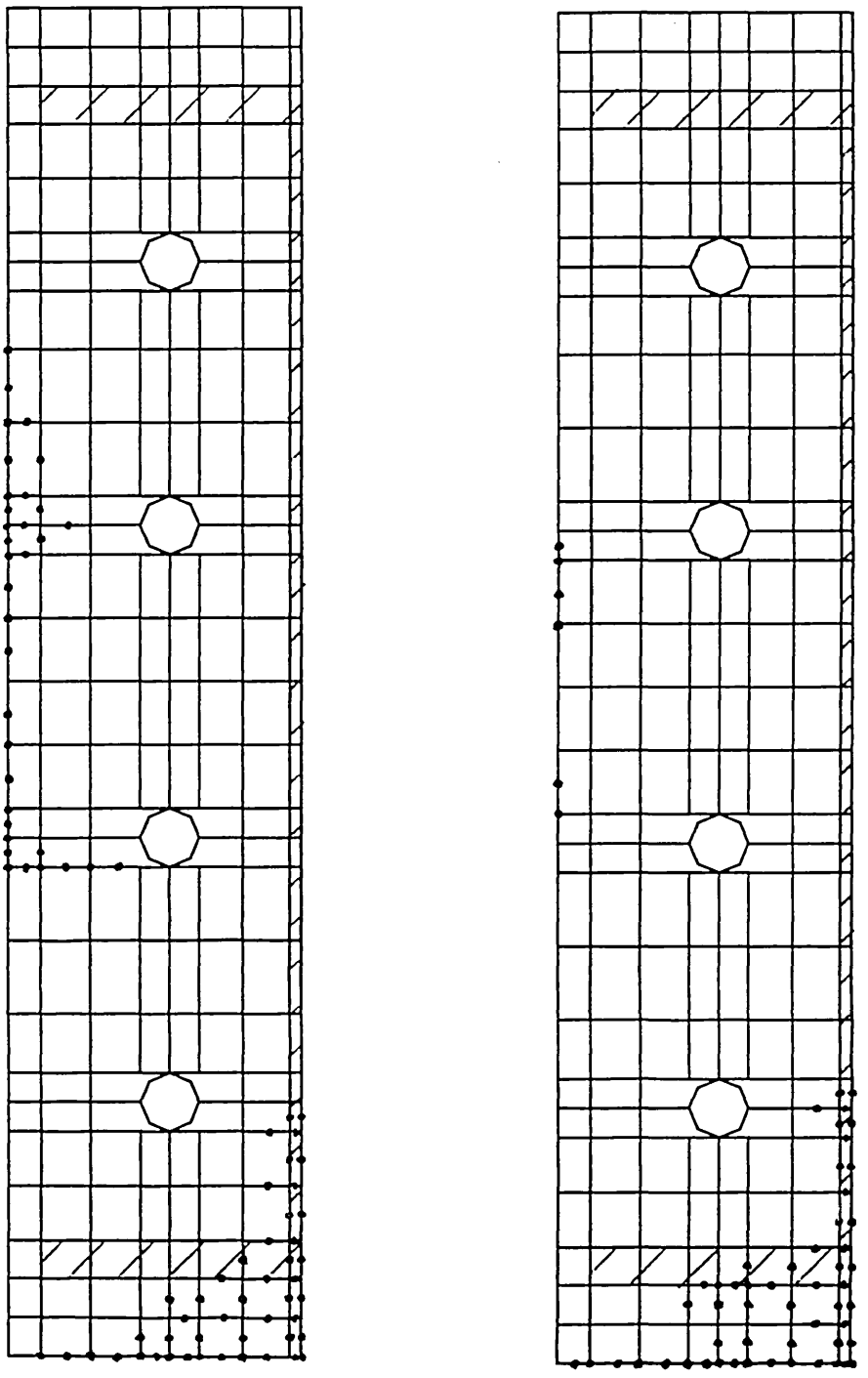

(a) at low moment

(b) at high moment

Fig. 7.16 Prying pattern, model M5

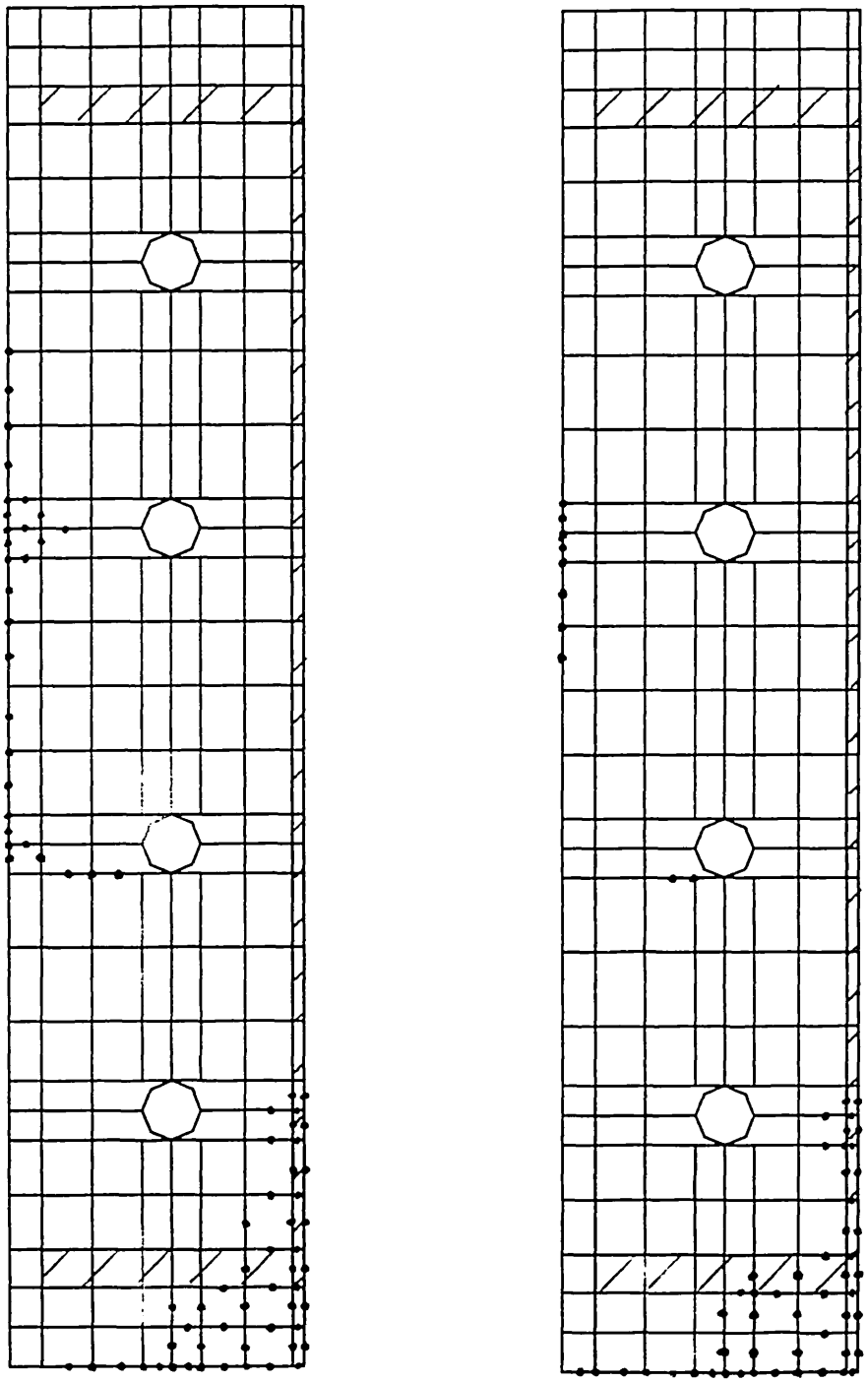

(a) at low moment

(b) at high moment

Fig. 7.17 Prying pattern, model M6

Fig. 7.18 Prying force-moment curves, models M4 to M6

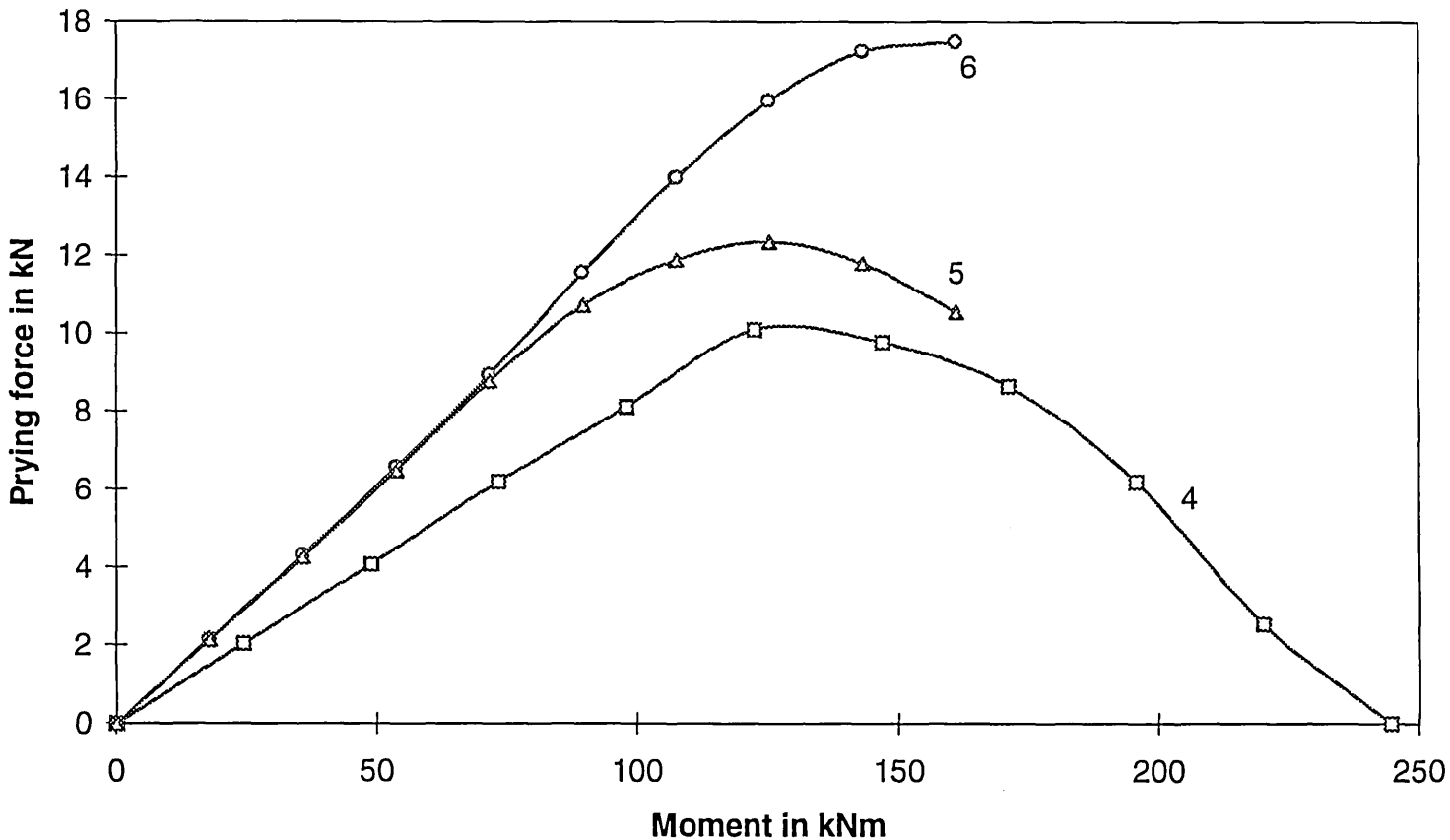

Fig. 7.19 Ratio of prying to bolt forces-moment curves, models M4 to M6

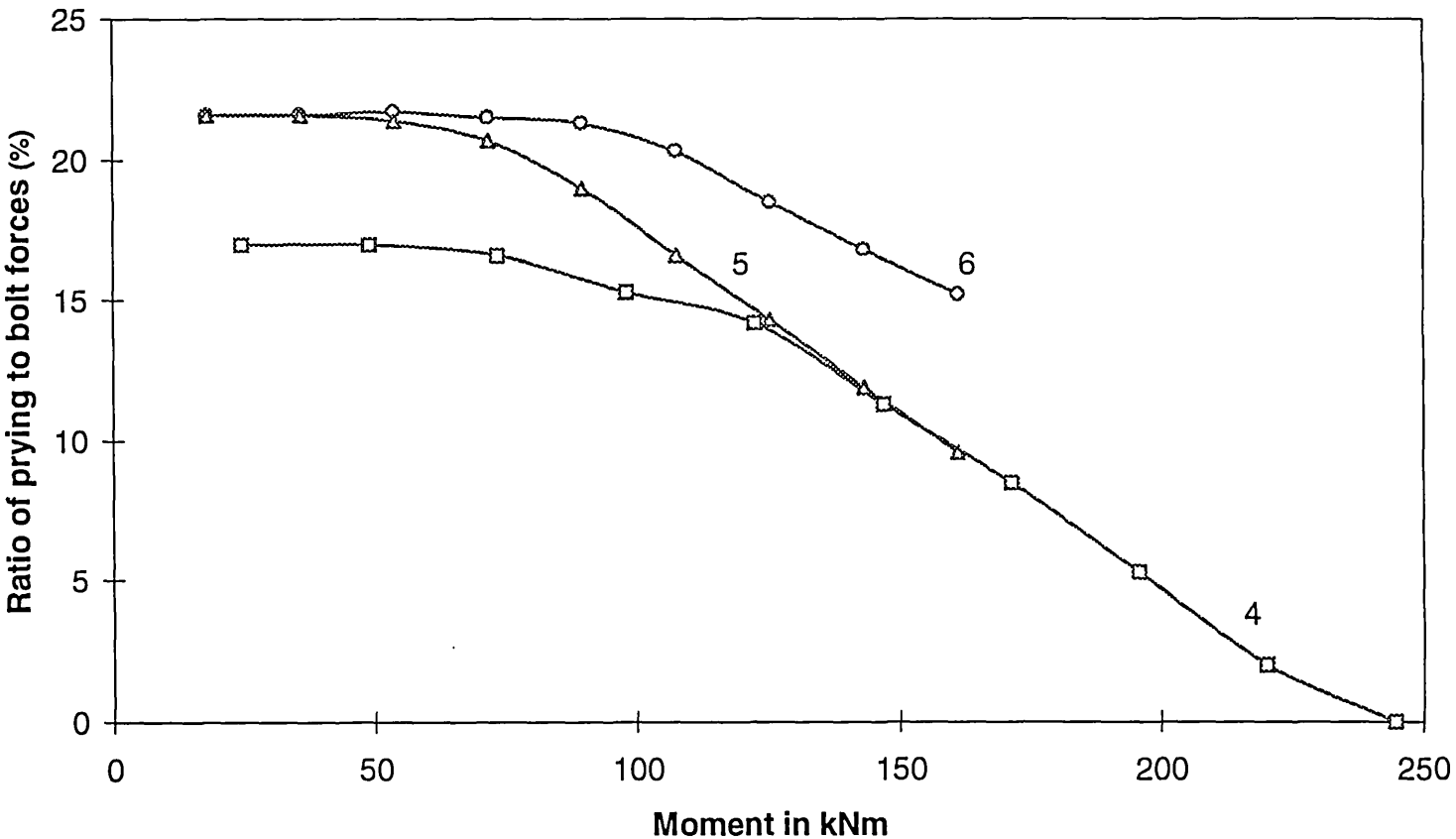

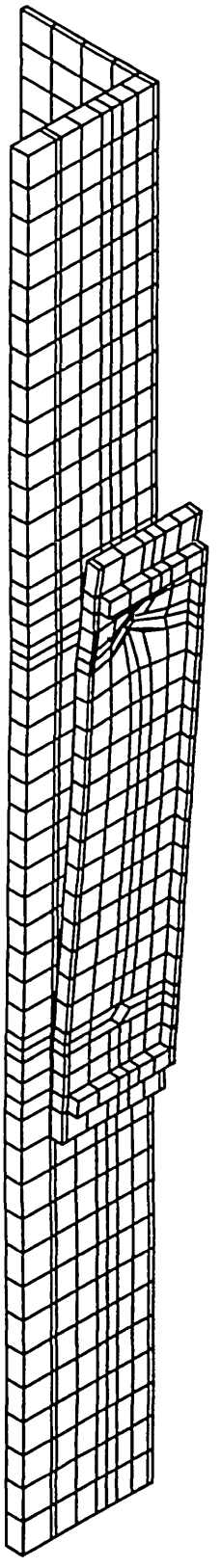

(Exaggeration factor 2)

Fig. 7.20 Deformed mesh, model M1

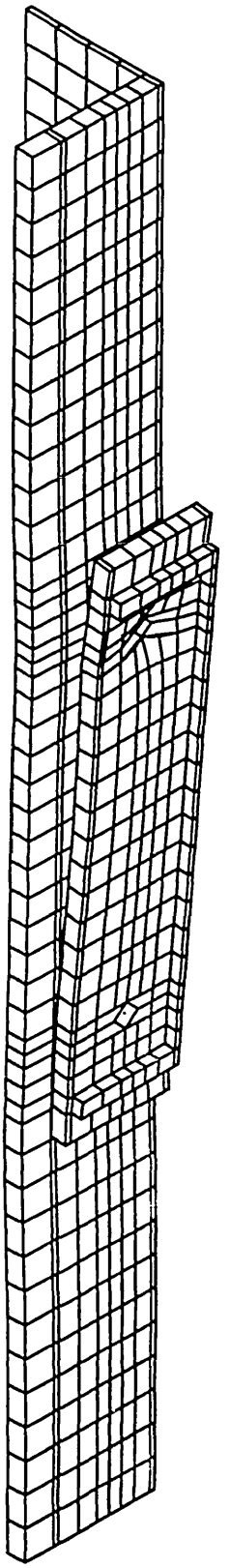

(Exaggeration factor 2)

Fig. 7.21 Deformed mesh, model M2

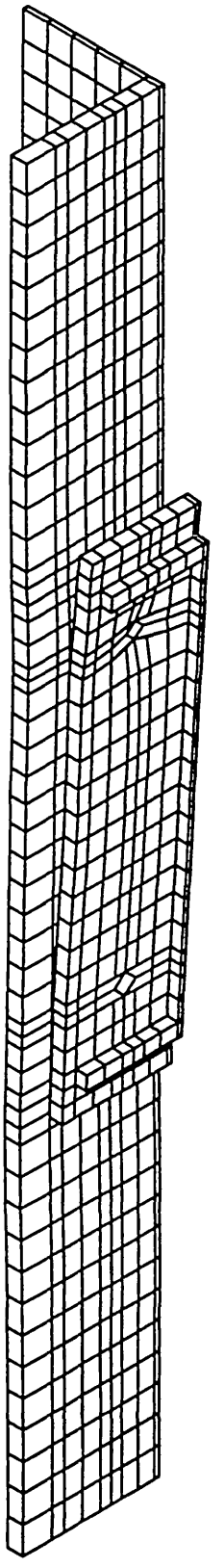

(Exaggeraiion factor 2)

Fig. 7.22 Deformed mesh, model M3

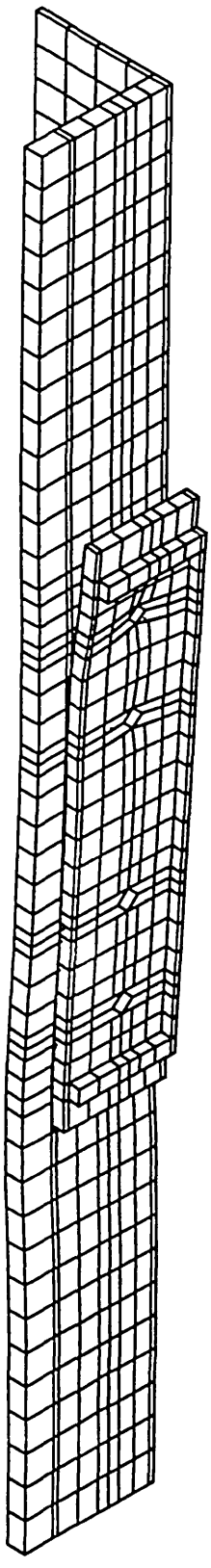

(Exaggeration factor 2)

Fig. 7.23 Deformed mesh, model M4

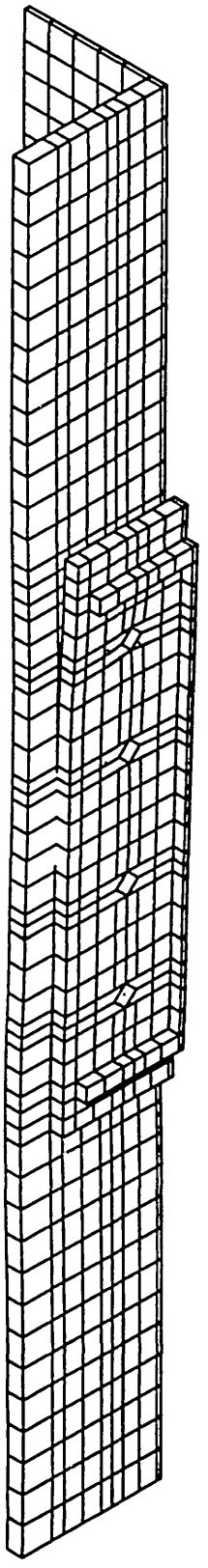

(Exaggeration factor 2)

Fig. 7.24 Deformed mesh, model M5

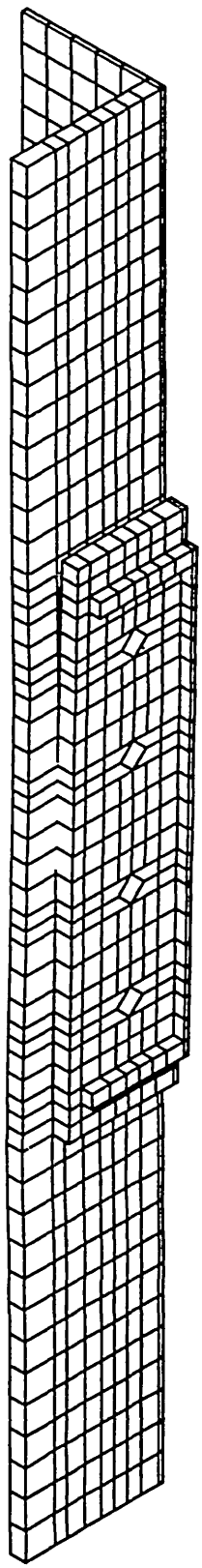

(Exaggeration factor 2)

Fig. 7.25 Deformed mesh, model M6

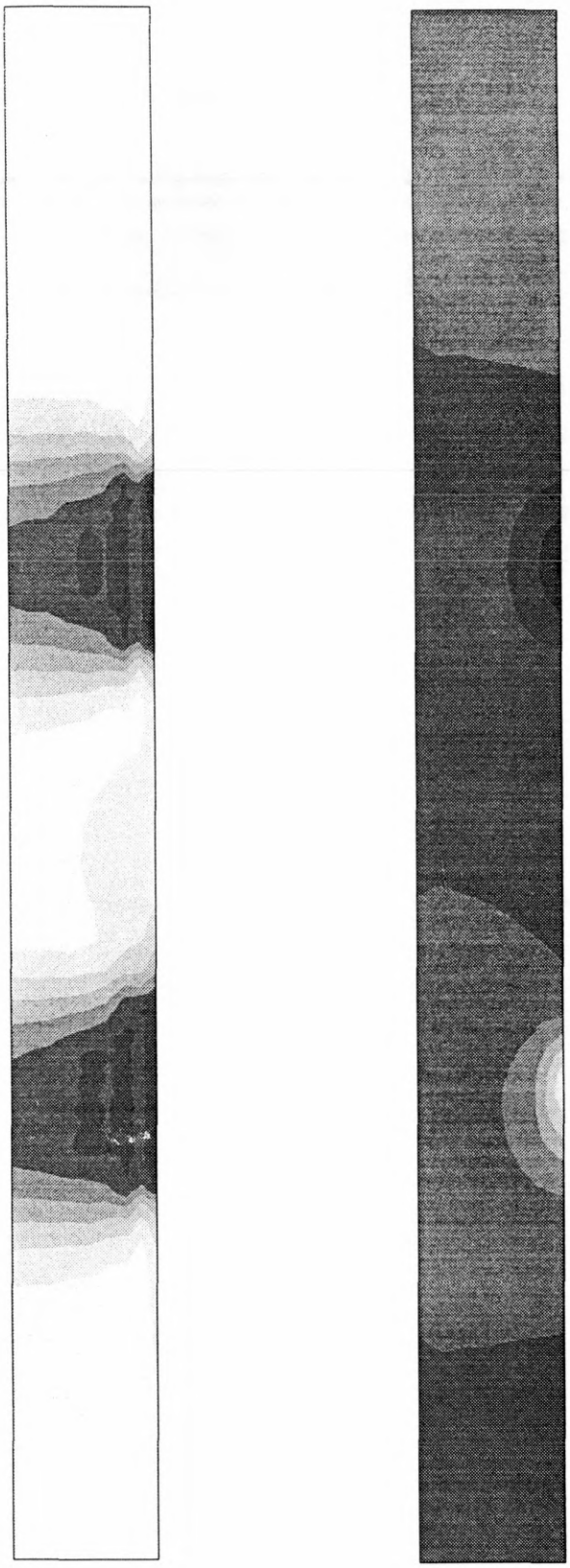

Stress contours Displacement contours

Fig. 7.26 Stress and displacement contours for column web, model M1

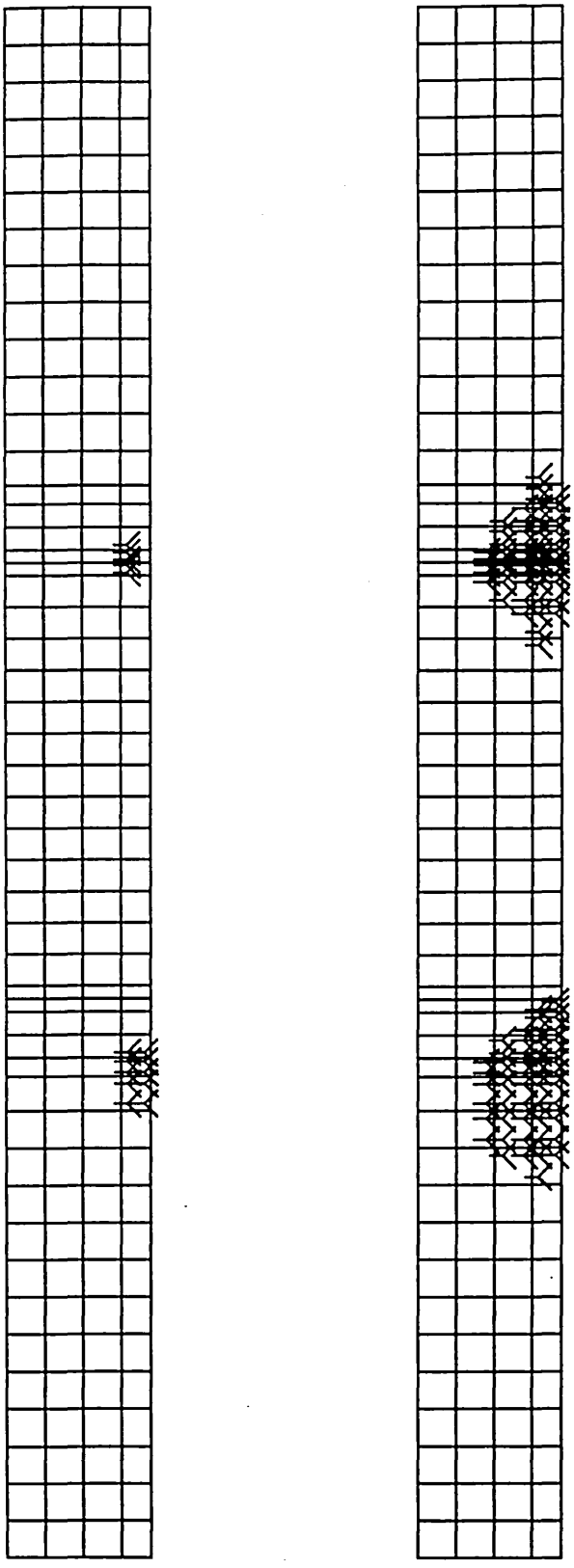

(a) at low moment (b) at high moment

Fig. 7.27 Yield patterns for column web, model M1

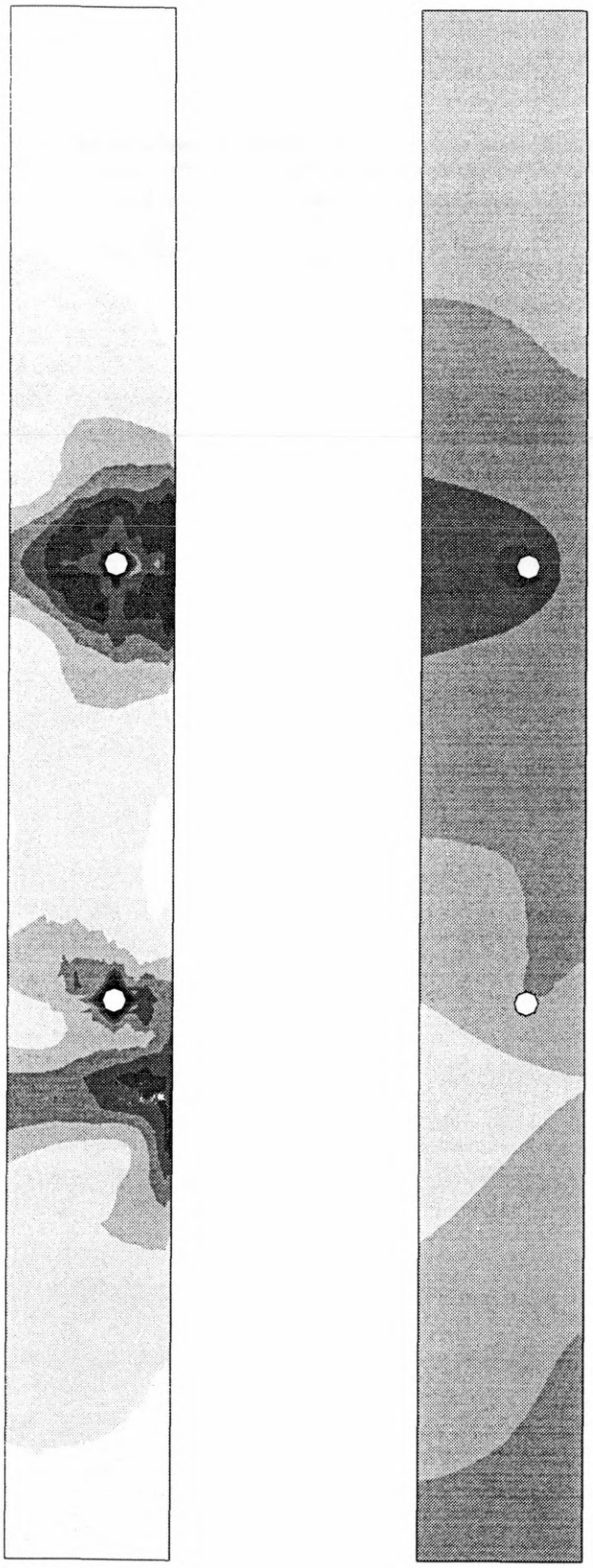

Stress contours

Displacement contours

Fig. 7.28 Stress and displacement contours for column flange, model M1

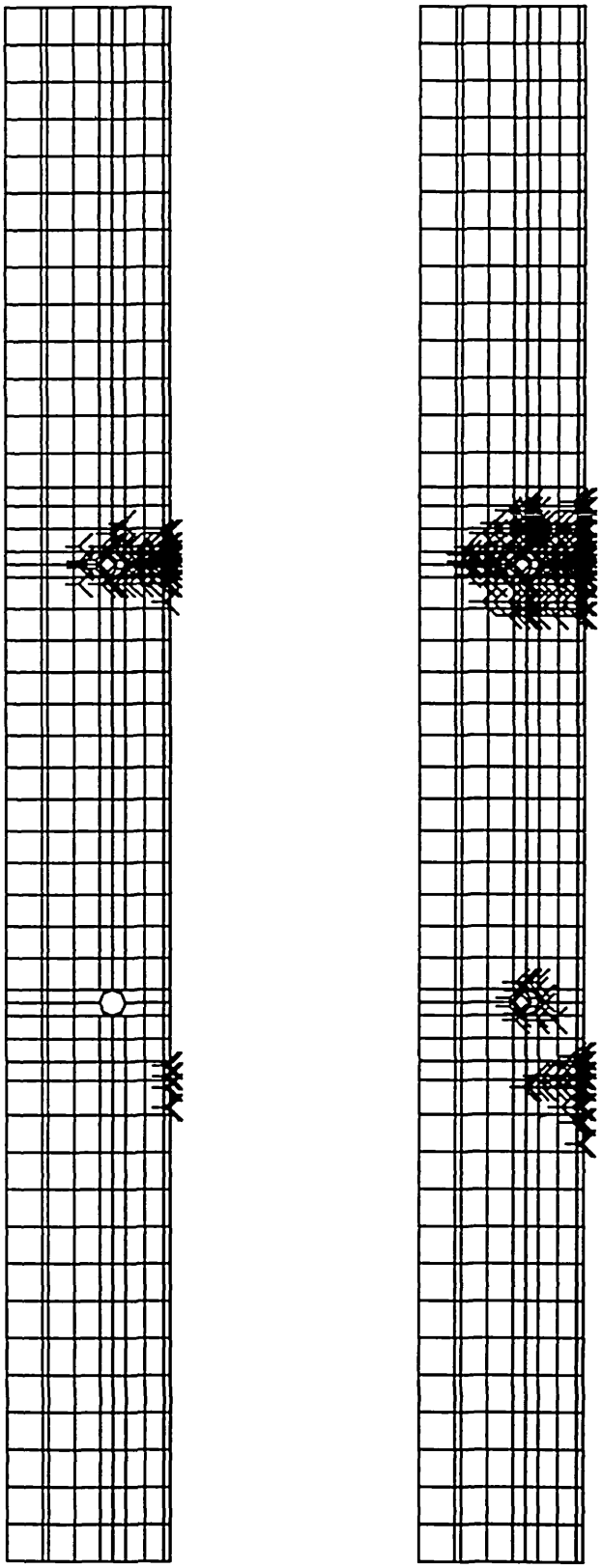

(a) at low moment (b) at high moment

Fig. 7.29 Yield patterns for column flange, model M1

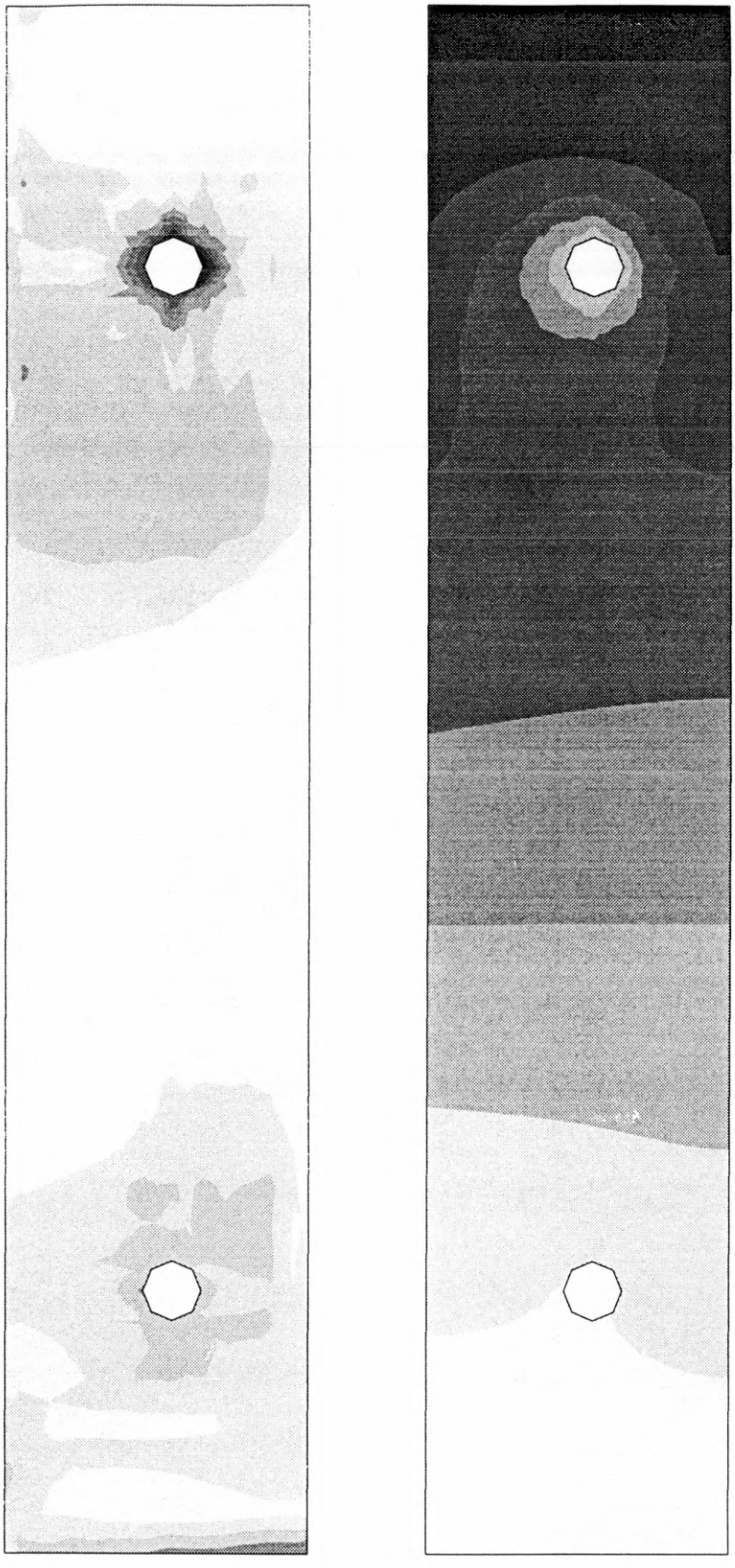

Stress contours

Displacement contours

Fig. 7.30 Stress and displacement contours for end plate, model M1

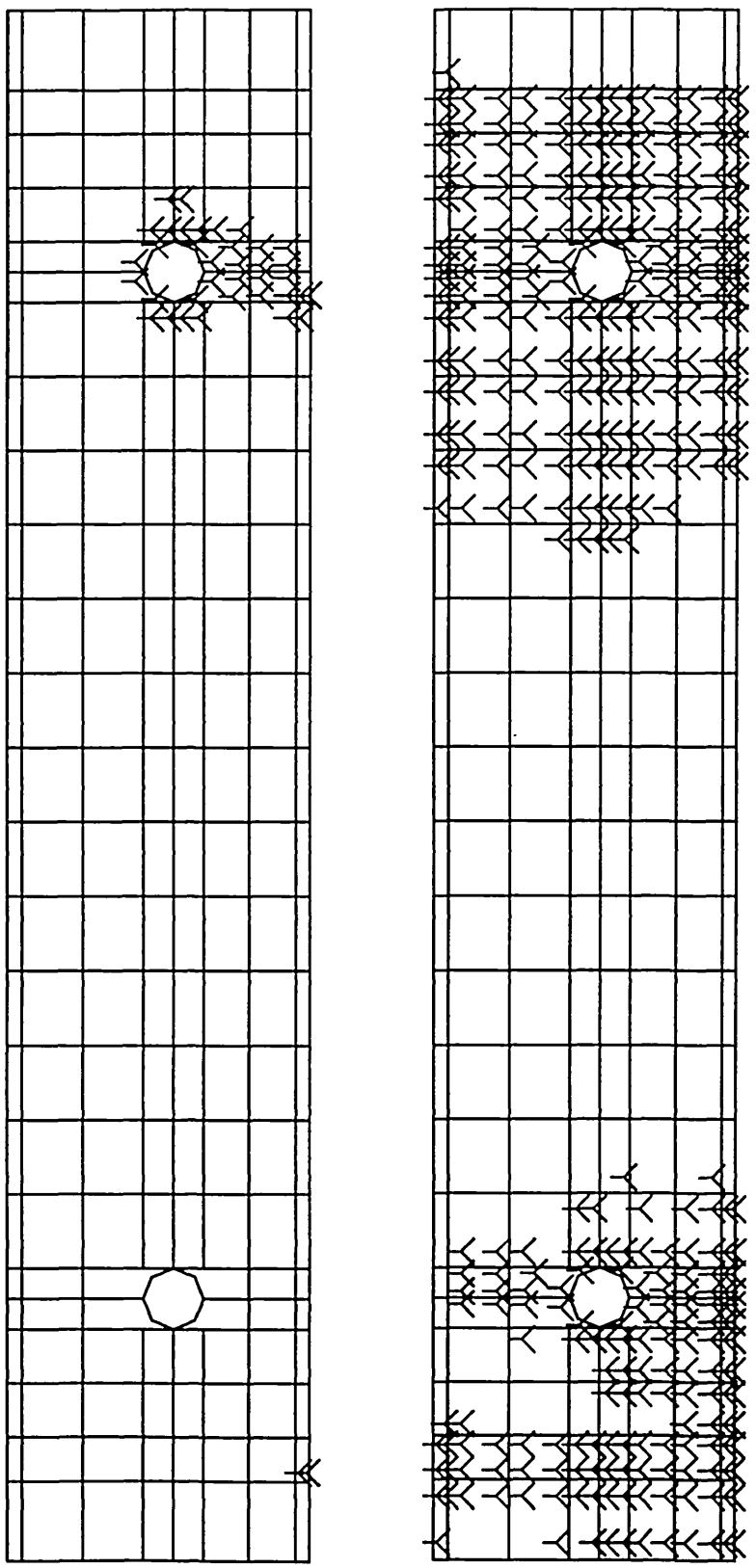

(a) at low moment (b) at high moment

Fig. 7.31 Yield patterns for end plate, model M1

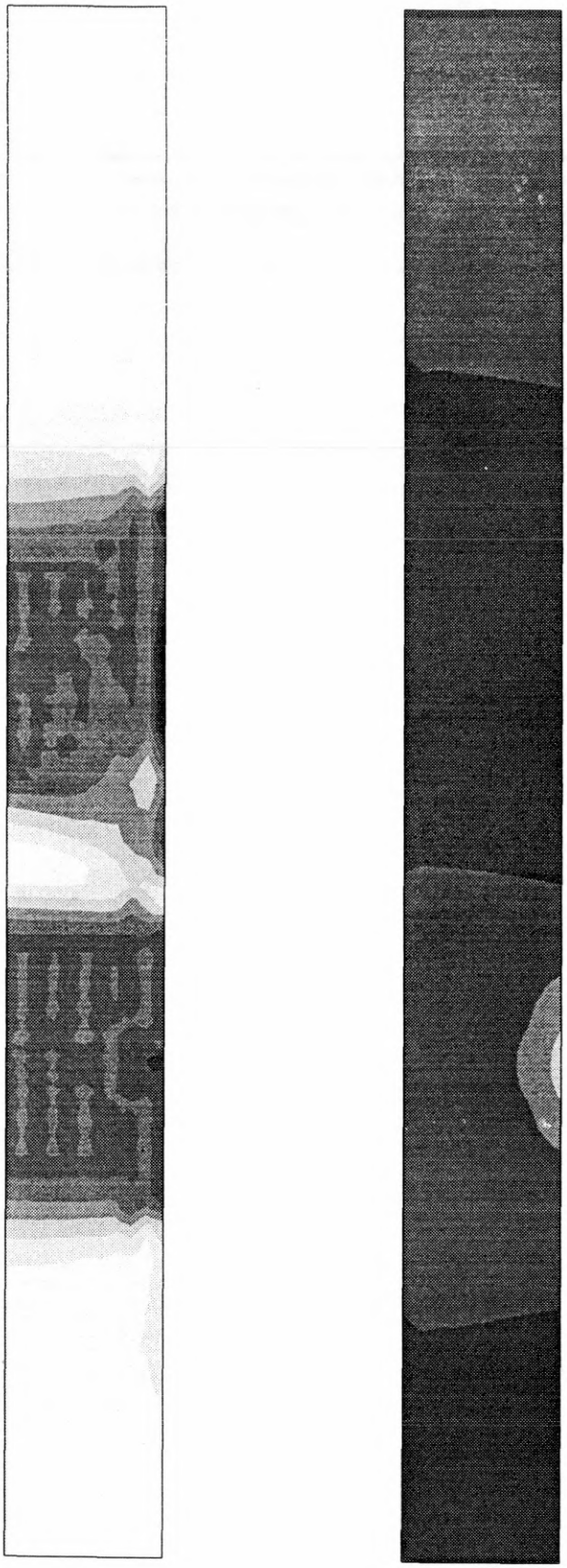

Stress contours Displacement contours

Fig. 7.32 Stress and displacement contours for column web, model M5

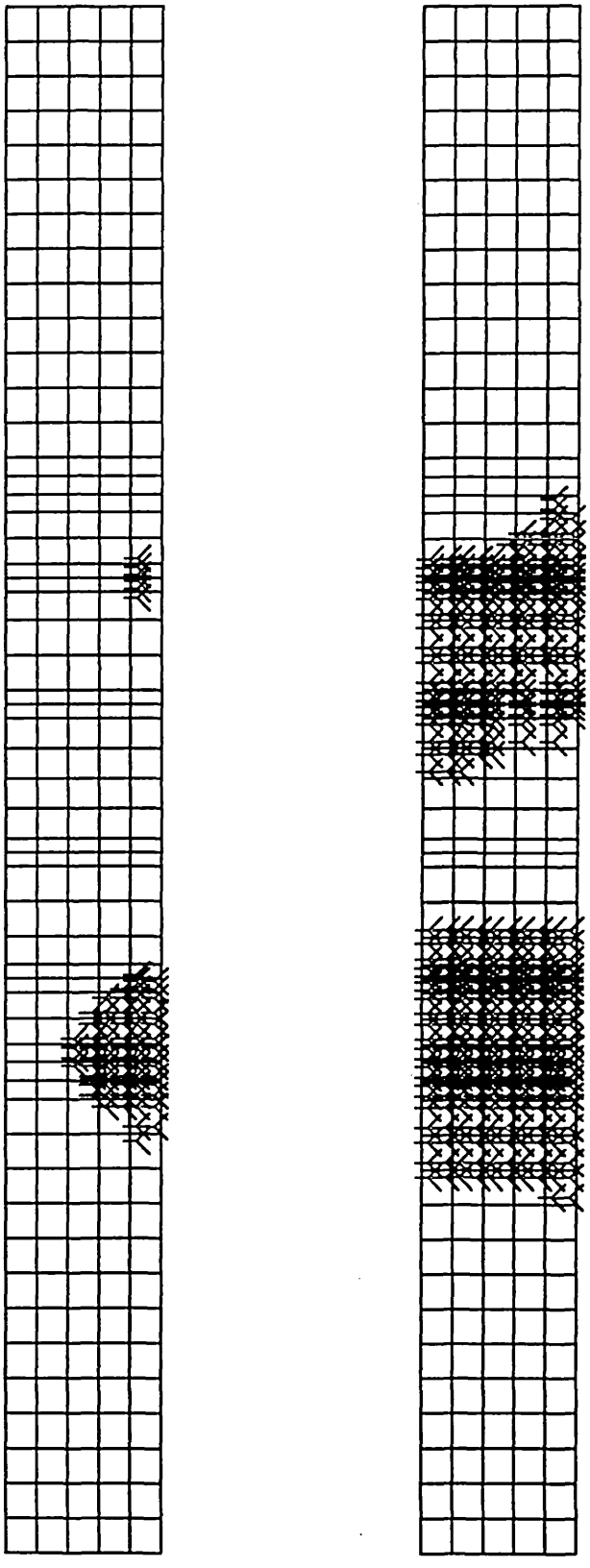

(a) at low moment (b) at high moment

Fig. 7.33 Yield patterns for column web, model M5

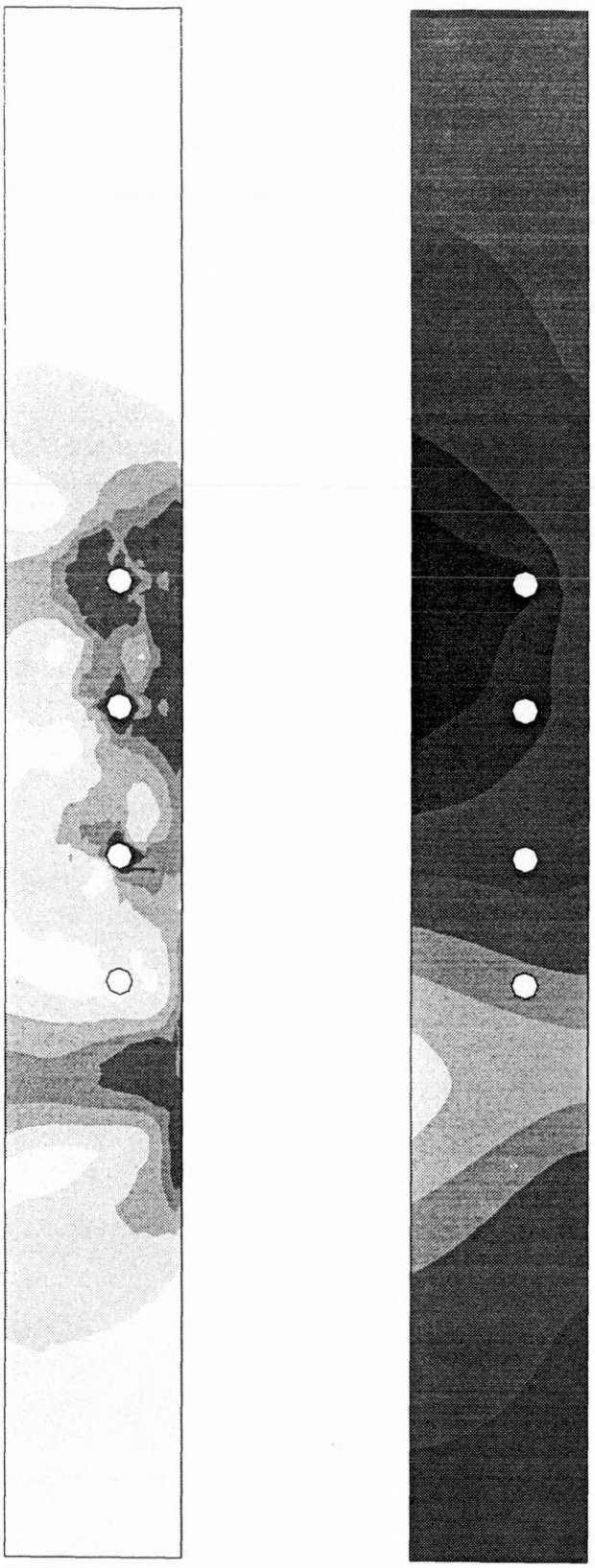

Stress contours

Displacement contours

Fig. 7.34 Stress and displacement contours for column flange, model M5

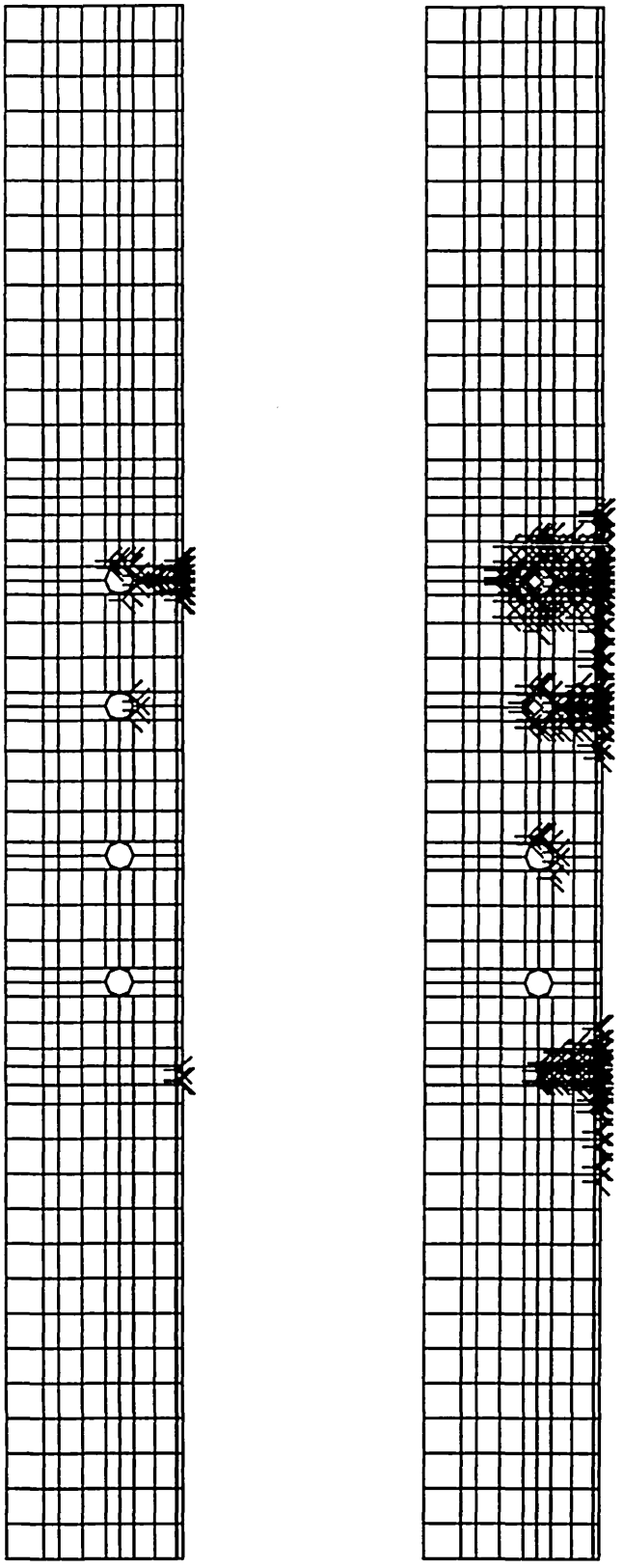

(a) at low moment (b) at high moment

Fig. 7.35 Yield patterns for column flange, model M5

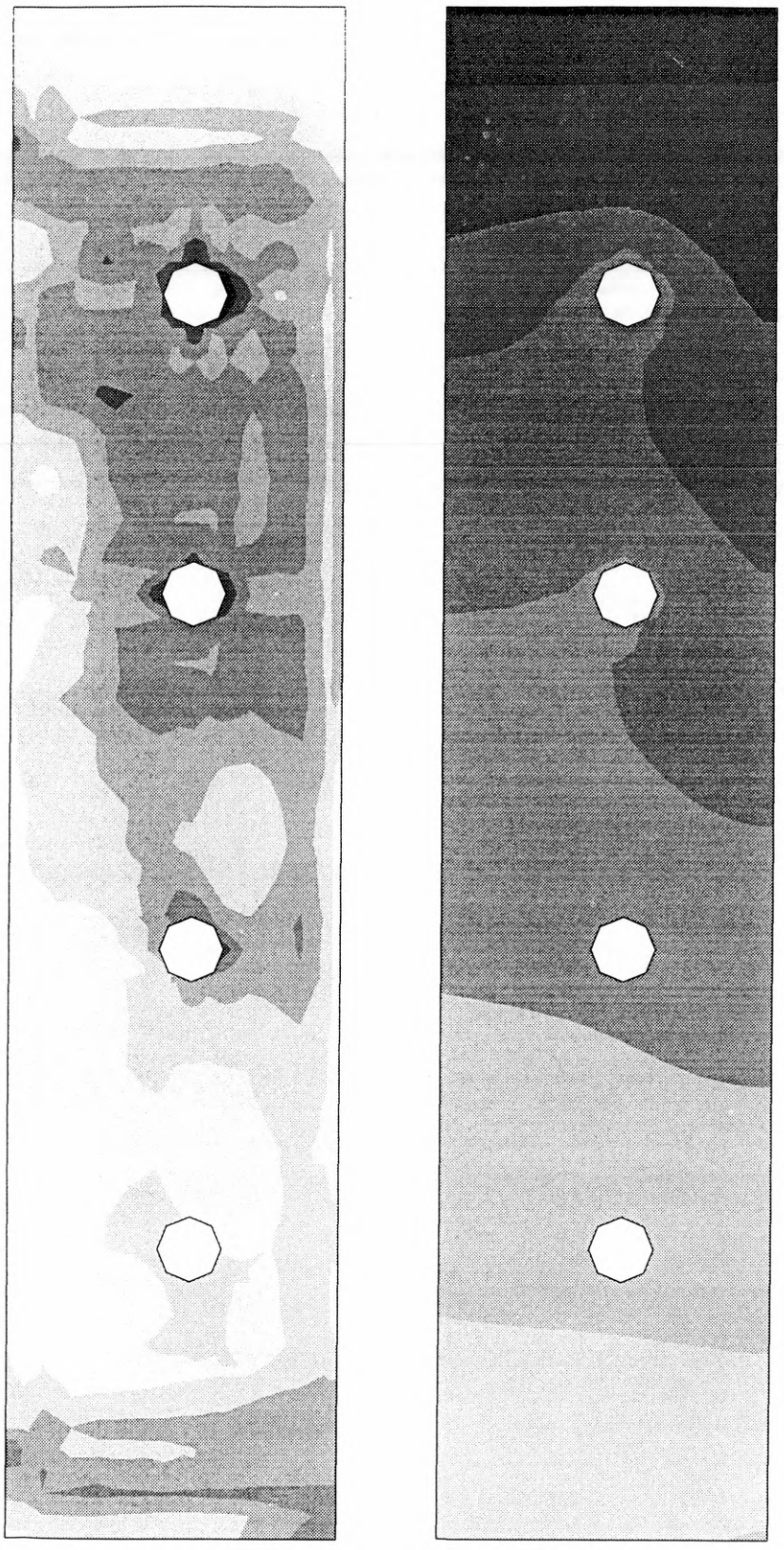

Stress contours

Displacement contours

Fig. 7.36 Stress and displacement contours for end plate, model M5

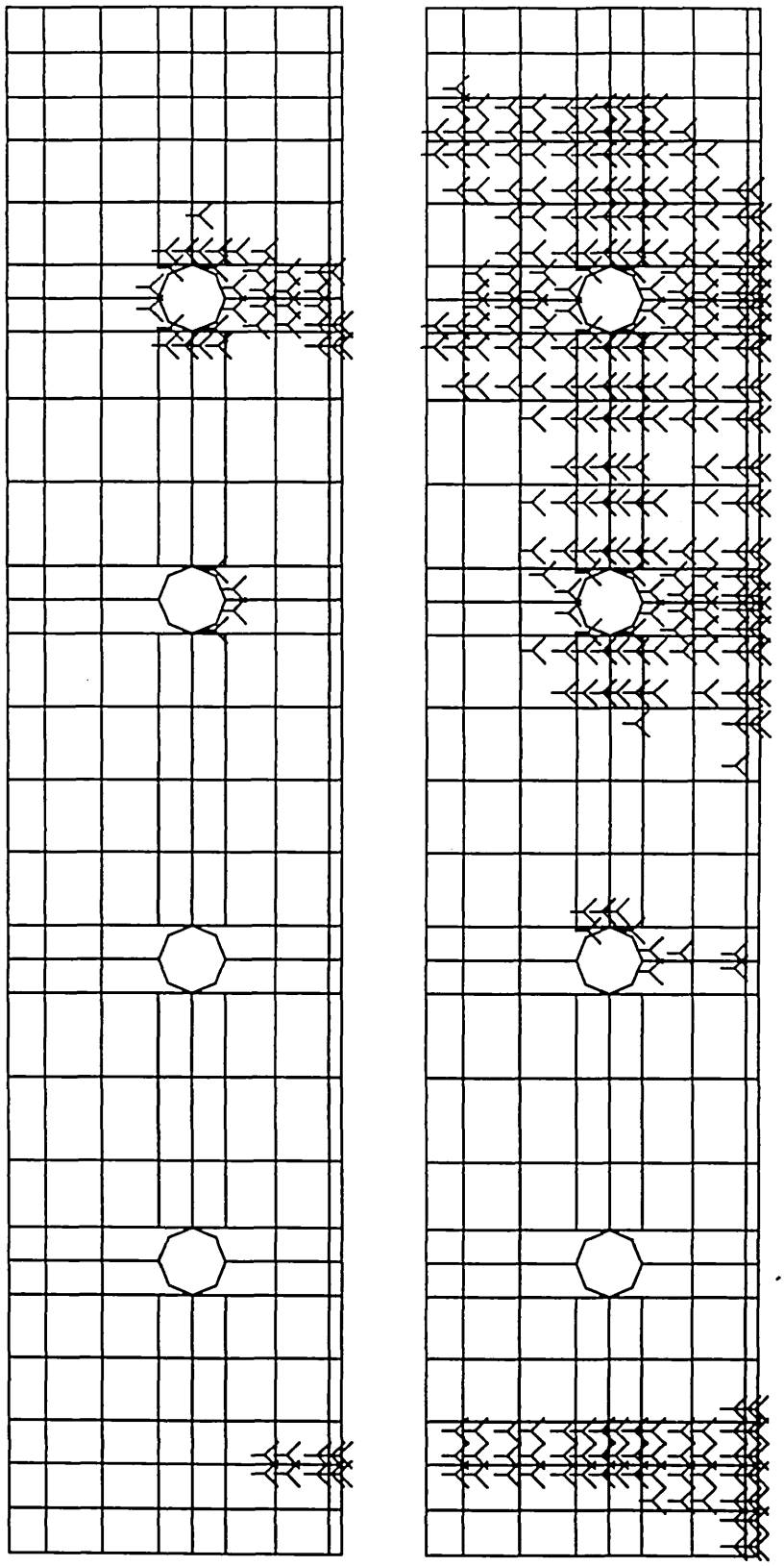

(a) at low moment (b) at high moment

Fig. 7.37 Yield patterns for end plate, model M5

CHAPTER 8

COMPARISON BETWEEN THE DESIGN RULES OF EUROCODE 3, FINITE ELEMENT ANALYSIS AND EXPERIMENTAL RESULTS

8.1 INTRODUCTION

Design methods and application rules for joints in building frames are contained in the revised Annex J[60] of the recently published European Pre-standard, Eurocode 3. These are primarily intended for moment-resisting connections between universal beam and universal column sections in which the beams are connected to the flanges of the columns. Bolted connections with end plates or flange cleats, welded connections and several other specific types are covered.

The typical moment-rotation characteristic of a beam-to-column joint is shown in Figure 8.1 in which the three main structural properties of the joint are defined. These are the moment resistance $M_{j,Rd}$, rotational stiffness $S_{j,ini}$ and rotation capacity ϕ_{Cd} . Methods for determining the moment resistance and rotational stiffness of a joint are given in the revised Annex J.

Joints in a building frame may be classified on the basis of their rigidity or strength. When the classification is by rigidity, a joint may be termed as 'rigid', 'semi-rigid' or 'nominally pinned' by determining its initial rotational stiffness $S_{j,ini}$ and then comparing it with the classification boundaries of Eurocode 3, which are shown in Figure 8.2. On the other hand when the classification is based on strength, the terms 'full strength', 'partial strength' or 'nominally pinned' may be used by computing the moment resistance $M_{j,Rd}$ of the joint and comparing it with the moment resistances of the beam and column members which it joins. The boundaries for strength

classification of a joint at intermediate column height are specified in Annex J, which are explained in Figure 8.3.

On the basis of the above classification bolted flush end plate connections in building frames may be termed as semi-rigid, partial strength joints. The rotational stiffness and moment capacity of these joints are not small enough to be ignored but are insufficiently large to enable them to qualify as rigid, full strength joints.

8.2 ANNEX J OF EUROCODE 3

This section contains the summary of design rules given in the revised Annex J of Eurocode 3.

In the design of a structural element, the three properties which should be taken into consideration are the strength, rigidity and ductility. For a joint in a building frame the terms moment resistance, rotational stiffness and rotation capacity are used to refer to these properties. Eurocode 3 considers any joint as an assemblage of a number of components. The design moment-rotation characteristic of a joint depends on the properties of its basic components. The following basic components of a joint are distinguished in Annex J:

- column web panel in shear;
- column web in compression;
- beam flange and web in compression;
- column flange in bending;
- column web in tension;
- end plate in bending;
- beam web in tension;
- bolts in tension;
- bolts in shear;
- bolts in bearing.

Methods for determining the properties of the individual components and relationship between the properties of components and the structural properties of a joint are given.

8.2.1 MOMENT RESISTANCE

(a) Column web panel in shear

$$V_{wp,Rd} = \frac{0.9 f_{y,wc} A_{vc}}{\sqrt{3}\gamma_{M0}} \qquad (8.1)$$

where:

A_{vc} is the shear area of the column.

γ_{M0} is the safety factor.

(b) Column web in compression

$$F_{c,wc,Rd} = \frac{\rho b_{eff} t_{wc} f_{y,wc}}{\gamma_{M0}} \qquad (8.2)$$

where:

b_{eff} is the effective width of the column web.

ρ is the reduction factor.

(c) Beam flange and web in compression

$$F_{c,fb,Rd} = \frac{M_{c,Rd}}{h_b - t_{fb}} \qquad (8.3)$$

where:

$M_{c,Rd}$ is the design moment resistance of the beam cross section.

(d) Column flange in bending

The design resistance and failure mode of an unstiffened column flange in bending, together with the associated bolts in tension, should be considered as similar to those of an equivalent T-stub flange. The design tension resistance of a T-stub flange $F_{t,Rd}$ should be taken as the smallest value for the three possible failure modes, as shown in Figure 8.4:

Mode 1: Complete yielding of the flange

$$F_{t,Rd} = \frac{4M_{pl1,Rd}}{m} \qquad (8.4)$$

Mode 2: Bolt failure with yielding of the flange

$$F_{t,Rd} = \frac{2M_{pl2,Rd} + n\Sigma B_{t,Rd}}{m+n} \qquad (8.5)$$

Mode 3: Bolt failure

$$F_{t,Rd} = \Sigma B_{t,Rd} \qquad (8.6)$$

in which:

$$M_{pl1,Rd} = \frac{0.25\Sigma l_{eff,1} t_f^2 f_y}{\gamma_{M0}} \qquad (8.7)$$

$$M_{pl2,Rd} = \frac{0.25\Sigma l_{eff,2} t_f^2 f_y}{\gamma_{M0}} \qquad (8.8)$$

$$n = e_{\min} \quad \text{but} \quad n \leq 1.25m \qquad (8.9)$$

where:

$B_{t,Rd}$ is the design tension resistance of a bolt-plate assembly;

$\Sigma B_{t,Rd}$ is the total value of $B_{t,Rd}$ for all the bolts in the T-stub;

$\Sigma l_{eff,1}$ is the value of Σl_{eff} for mode 1;

$\Sigma l_{eff,2}$ is the value of Σl_{eff} for mode 2.

(e) Column web in tension

$$F_{t,wc,Rd} = \frac{\rho b_{eff} t_{wc} f_{y,wc}}{\gamma_{M0}} \qquad (8.10)$$

(f) End plate in bending

The design resistance and failure mode of an end plate in bending, together with associated bolts in tension, should be considered as similar to those of an equivalent T-stub flange. The calculation of the design tension resistance of a T-stub flange $F_{t,Rd}$ takes the same forms as column flange in bending. The only difference is in determining coefficients in these formulas, such as $m, n, e_{\min}, \Sigma l_{eff,1}$ and $\Sigma l_{eff,2}$.

(g) Beam web in tension

$$F_{t,wb,Rd} = \frac{b_{eff} t_{wb} f_{y,wb}}{\gamma_{M0}} \qquad (8.11)$$

8.2.2 ROTATIONAL STIFFNESS

The rotational stiffness of a joint may be determined from the flexibility of its basic components.

$$S_j = \frac{Ez^2}{\mu \sum_i \frac{1}{k_i}} \qquad (8.12)$$

where:

k_i is the stiffness coefficient representing component i ;

z is the lever arm;

μ is the stiffness ratio $S_{j,ini} / S_j$;

$S_{j,ini}$ is the value of S_j when the moment $M_{j,Sd}$ is zero.

in which

$$\mu = \left[\frac{1.5 M_{j,Sd}}{M_{j,Rd}} \right]^{\psi} \qquad (8.13)$$

where:

for bolted end plate $\psi = 2.7$;

The stiffness coefficients k_i representing the basic components used in a joint should be determined as follow:

(a) Column web panel in shear

$$k_1 = \frac{0.38 A_{ve}}{\beta z} \qquad (8.14)$$

where:

β is the transformation parameter.

(b) Column web in compression

$$k_2 = \frac{0.7 b_{eff} t_{wc}}{d_c} \qquad (8.15)$$

where:

d_c is the clear depth of the column web.

(c) Column flange, single bolt row in tension:

$$k_3 = \frac{0.85 l_{eff} t_{fc}^3}{m^3} \qquad (8.16)$$

(d) Column web in tension

$$k_4 = \frac{0.7 b_{eff} t_{wc}}{d_c} \qquad (8.17)$$

(e) End plate, single bolt row in tension

$$k_5 = \frac{0.85 l_{eff} t_p^3}{m^3} \qquad (8.18)$$

(g) Bolts, single bolt row in tension

$$k_7 = \frac{1.6A_s}{L_b} \qquad (8.19)$$

where:

L_b is the elongation length of the bolt.

For end plate connections with more than one bolt row in tension, the stiffness coefficients (k_3, k_4, k_5, k_7) for basic components related to all of these bolts rows should be represented by a single equivalent stiffness coefficient k_{eq} determined from:

$$k_{eq} = \frac{\sum_r k_{eff,r} h_r}{z} \qquad (8.20)$$

where:

h_r is the distance between bolt row r and the centre of compression;

$k_{eff,r}$ is the effective stiffness coefficient for bolt row r taking into account the stiffness coefficients k_i for the basic components mentioned above;

z is the lever arm.

in which:

$$k_{eff,r} = \frac{1}{\sum_i \frac{1}{k_{ir}}} \qquad (8.21)$$

where:

k_{ir} is the stiffness coefficient representing component i relative to bolt row r.

The lever arm z should be determined from:

$$z = \frac{\sum_r k_{eff,r} h_r^2}{\sum_r k_{eff,r} h_r} \qquad (8.22)$$

8.2.3 ROTATION CAPACITY

A joint with a bolted connection with end plates may be assumed to have sufficient rotation capacity for plastic analysis if both the following conditions are satisfied:

(a) the design moment resistance of the joint is governed by the resistance of either :

- the column flange; or,
- the beam end plate.

(b) the thickness t of either the column flange or the beam end plate (not necessarily the same component as in (a)) satisfies:

$$t \leq 0.36d\sqrt{f_{ub} / f_y} \qquad (8.23)$$

where:

f_{ub} is the ultimate tensile strength of the bolts;

f_y is the yield strength of the relevant basic component.

8.3 COMPARISON BETWEEN ANNEX J OF EUROCODE 3, FINITE ELEMENT ANALYSIS AND TEST RESULTS

8.3.1 MOMENT RESISTANCE

The predicted (Annex J) and actual failure moments of six joints are given in Table 8.1. As expected the actual failure moments observed in the tests are always higher than the moment resistances predicted by Eurocode 3. For the purpose of calculating moment resistances by Annex J method, the material properties of the joint components, given in Table 5.2, were used. The ratio of test to predicted (Annex J) value varies between 1.09 and 1.96. The large discrepancy and

inconsistency between the test and predicted (Annex J) values should be investigated.

8.3.1.1 Types of failure

In the tests performed on flush end plate connections, failure of joints occurred due to either of the two factors, column web buckling and thread stripping. Thread stripping is not considered in Eurocode 3. In the revised Annex J (Clause J.3.5.3) column web buckling has been ignored for the purpose of computing the moment resistance of a joint. Only column web crushing is considered.

8.3.1.2 Column web buckling

Column web buckling governed the failure moment of each of the three flush end plate connections with two rows of bolts. Crushing of column web was never observed. For the universal column sections tested, the crushing and buckling resistances of column webs differ little, as shown in Table 8.2. However, universal beam sections are often used as columns. For such a section, the buckling strength of column web can be considerably lower than its crushing strength. Consider, for example, a joint with a 20 mm thick end plate which connects a 356x171UB51 beam to a 406x178UB60 column. Assuming the yield strength of 275 N/mm^2, the crushing and buckling strengths of the column web are 363.7 kN and 299.2 kN respectively. It is hoped that any future revision of Annex J would correct this serious omission.

It is worth commenting on the effective breadth of column web specified in Eurocode 3 and BS 5950 for determining its buckling resistance. These are based on the same design principles, but different effective width of a column web is specified. In Eurocode 3, the effective width is taken as $b_{eff} = (h^2 + s_s^2)^{0.5}$, in which h is the depth of the column section and s_s is the length of stiff bearing. A larger effective width, $b_{eff} = (b_1 + n_1)$ is considered in BS 5950, in which b_1 and n_1 are synonymous with s_s and h respectively. The effective breadths specified in Eurocode 3 and BS 5950 are explained in Figures 8.5 and 8.6. The buckling resistance of column web

predicted by BS 5950 is always higher than Eurocode 3. The buckling loads observed in tests and the predicted buckling resistances are given in Table 8.3. From the comparison it is concluded that the provision of Eurocode 3 for column web buckling resistance is satisfactory. The rule contained in BS 5950 may lead to unsafe prediction.

8.3.1.3 Bolt failure

Bolts were responsible for the failure of half of the joints tested. Each of the three joints which failed due to thread stripping had one row of M20 or M24 bolts.

Stripping of threads prior to bolt fracture occurs if either the nut material is weaker than the bolt material or the thread interlock is less than specified because of some deviation from the permitted tolerances. Bolts made to British Standard BS 3692[54] are susceptible to thread stripping. Tensile tests performed on M20 and M24 bolts are reported in Table 5.2, which indicate that thread stripping occurred at a load 7% less than bolt fracture. In Eurocode 3 bolts are specified to Standard BS EN 24014 etc[55],[56],[57],[58]. These have different specification from the nuts used in the British construction industry. Premature failure due to thread stripping is unlikely in these bolts. It is strongly recommended that British industry should adopt the European Standards on bolts and nuts without delay. This will minimise the risk associated with bolt stripping.

8.3.1.4 Strength classification

The classifications of the six joints based on the test results and the specifications of Eurocode 3 are shown in Table 8.4. Except one joint which can be designated as nominally pinned according to Annex J, all joints can be classified as partial strength.

8.3.2 ROTATIONAL STIFFNESS

For elastic analysis of frames it is necessary to classify joints on the basis of their rotational stiffnesses. If the joints are semi-rigid their rotational stiffness needs to be known before the analysis can be attempted. The rotational stiffnesses of the six joints were determined from test results, finite element analysis and Eurocode 3.

These are recorded in Table 8.5. The moment-rotation characteristics of some joints were affected by bolt slip and/or lack of fit, consequently the M-ϕ curves in the initial stages were not very regular from which the rotational stiffness could be predicted accurately. However, one fact is clear from the results; Eurocode 3 generally overestimates the rotational stiffnesses of joints. The formulae for computing the stiffness coefficients of various joint components should be improved by calibration with reference to more experimental results.

8.3.2.1 Boundaries for stiffness classification

Compared with BS 5950, Annex J of Eurocode 3 is more stringent and requires joints to be a lot stiffer before they can be termed as rigid. No distinction between braced and unbraced frames is made in BS 5950 and a joint may be considered as rigid if its rotational stiffness is greater than the stiffness of the members it joins. Depending on whether the support condition at the other end is free or fixed it can be 2EI/L, 3EI/L, 4EI/L, 6EI/L .... Annex J treats rigid joints in braced and unbraced frames differently. For a rigid joint in braced frames, stiffness greater than 8EI/L of the beam is required, whereas, for unbraced frames, a joint stiffness greater than 25EI/L is demanded. For a joint to be treated as nominally pinned its rotational stiffness has to be less than 0.5EI/L of the beam, irrespective of whether the frame is braced or unbraced.

For a beam the term EI/L varies inversely with its length. Therefore, the classification of joints in a building frame depends on the length of beams they join. A joint which may be termed as rigid for a long beam with small stiffness, will be deemed as semi-rigid or even nominally pinned for a short beam with large stiffness. For the purpose of this investigation, a length of beam equal to 25 times its depth is assumed. Table 8.6 gives the stiffness requirement for the two beams used in the test programme.

Of the various parameters which affect the rotational stiffness of a joint, including column flange/web thickness, end plate thickness, bolt size and lever arm, it is the lever arm of the joint which makes the most significant contribution.

8.3.2.2 Stiffness classification

Lines representing 0.5EI/L, 8EI/L and 25EI/L are superimposed on the moment-rotation graphs of the two beams, as shown in Figures 8.7 and 8.8. The stiffness classification of the six joints may be based on the above figures. Alternatively, joints may be classified by comparing the rotational stiffnesses of the joints (Table 8.5) with the stiffness classification boundaries of the beams (Table 8.6). If the frames are unbraced all the joints can be treated as semi-rigid. According to test results and Eurocode 3 some of the joints in braced frames may be termed as rigid.

8.3.3 ROTATION CAPACITY

Bose and Hughes[6] argued that a rotation capacity of 0.03 radians can be considered as adequate for the plastic design of frames. If the joints fail to achieve at least 0.02 radians plastic design approach should not be adopted. The range 0.02 to 0.03 radians should be treated as a grey area. The rotation capacities achieved by the six joints are given in Table 8.1. It indicates that five of them are definitely qualified for plastic design whereas one joint with single row of M20 bolts falls within the grey area. Had it not failed prematurely due to thread stripping, this joint would possibly have developed at least 0.03 radian rotation.

The predicted (Annex J) moment resistances of five joints are governed by the resistances of the end plate (Table 8.7). This meets one of the requirements for sufficient rotation capacity. However, in one joint a combination of column web in compression and end plate governs the moment resistance. Another requirement (Equation 8.23) limits the thickness of either column flange or end plate relative to the bolt diameter. Assuming the yield strength of end plate and column flange as 275 N/mm^2 and the ultimate strength of grade 8.8 bolts as 800 N/mm^2 , the thickness of either end plate or column flange must be less than 0.6d, where d is the nominal

diameter of the bolts, which means end plate/column flange thickness of 14.4 mm for M24 and 12 mm for M20 bolts respectively. Among the five joints which achieved adequate rotation capacities three used M20 bolts with 12 mm end plates and two employed M24 bolts with 15 mm end plates which satisfy the above conditions.

Test	Column	Beam	End plate	Failure moment kNm	Predicted moment resistance kNm	Ratio= actual / predicted	Rotation at failure rad	Observed failure mode
1	254x254UC89	457x191UB74	510x200x12	187.8	104.6	1.80	0.025	Thread stripping
2	254x254UC89	457x191UB74	510x200x15	275.4	140.4	1.96	0.042	Thread stripping
3	254x254UC73	406x178UB60	460x200x12	158.4	91.2	1.74	0.038	Thread stripping
4	254x254UC89	457x191UB74	510x200x12	279.0	142.5	1.96	0.053	Column web buckling
5	254x254UC73	406x178UB60	460x200x12	161.4	121.2	1.33	0.046	Column web buckling
6	254x254UC73	406x178UB60	460x200x15	165.6	152.3	1.09	0.051	Column web buckling

All flange welds 2x10 FW; all web welds 2x8 FW. All material S275. All bolts 8.8.

Table 8.1 Comparison between predicted (Annex J) moment resistance and actual (test) results

Test	Failure type (according to Annex J)	Force in each bolt row kN	Total force acting on bolts kN	Column web in compression $F_{c,wc,Rd}$ kN	Buckling resistance kN	Force required to induce bolt failure in each row kN
1	End plate in mode 1	268.1	268.1	619.2	618.1	532.1
2	End plate in mode 2	360.1	360.1	637.0	620.3	670.0
3	End plate in mode 1	268.1	268.1	465.3	445.5	532.1
4	Row 1 - End plate in mode 2 Row 2 - End plate in mode 1 (group failure)	268.1 126.5	394.6	619.2	618.1	532.1
5	Row 1 - End plate in mode 2 Row 2 - End plate in mode 1 (group failure)	268.1 120.1	388.2	465.3	445.5	532.1
6	Row 1 - End plate in mode 2 Row 2 - Column web in compression	358.7 121.2	479.9	479.9	447.1	670.0

Table 8.2 Component forces for moment resistance

Test	Column	Experimental buckling load kN	Buckling resistance		Predicted buckling resistance / Experimental buckling load	
			BS 5950 kN	Eurocode 3 kN	BS 5950	Eurocode 3
4	254x254 UC 89	808.7	784.6	618.0	0.97	0.76
5	254x254 UC 73	547.1	565.2	445.5	1.03	0.81
6	254x254 UC 73	561.4	576.9	447.1	1.03	0.80

Note: Unsafe predictions are underlined.

Table 8.3 Buckling resistance of unstiffened column web

Test	Column	Beam	$M_{c,pl}$ kNm	$M_{b,pl}$ kNm	Moment required for full strength appellation kNm	Failure moment kNm	Predicted moment resistance kNm	Strength classification	
								Actual (Test)	Predicted (Annex J)
1	254x254UC89	457x191UB74	326	456	456	187.8	104.6	PS	NP
2	254x254UC89	457x191UB74	326	456	456	275.4	140.4	PS	PS
3	254x254UC73	406x178UB60	272	327	327	158.4	91.2	PS	PS
4	254x254UC89	457x191UB74	326	456	456	279.0	142.5	PS	PS
5	254x254UC73	406x178UB60	272	327	327	161.4	121.2	PS	PS
6	254x254UC73	406x178UB60	272	327	327	165.6	152.3	PS	PS

PS - Partial strength ; NP - Nominally pinned.

Table 8.4 Strength classification

Test	Initial rotational stiffness MNm/rad			Ratio= Test / FE model	Ratio= Test / Annex J	Stiffness classification					
						Test		FE model		Annex J	
	Test	FE model	Annex J			Braced	Unbraced	Braced	Unbraced	Braced	Unbraced
1	30.4	37.5	46.1	0.81	0.66	SR	SR	SR	SR	SR	SR
2	36.0	48.0	55.2	0.75	0.65	SR	SR	SR	SR	R	SR
3	21.3	25.3	29.8	0.84	0.71	SR	SR	SR	SR	SR	SR
4	46.7	47.8	53.6	0.98	0.87	SR	SR	SR	SR	R	SR
5	40.0	26.7	32.6	1.50	1.23	R	SR	SR	SR	SR	SR
6	21.3	29.0	37.6	0.73	0.57	SR	SR	SR	SR	R	SR

SR - Semi rigid ; R - Rigid .

Table 8.5 Stiffness classification

Beam	Assumed beam length L_b m	Flexural rigidity EI_b MNm^2	Nominally pinned $0.5EI_b/L_b$ MNm/rad	Rigid	
				Braced $8EI_b/L_b$ MNm/rad	Unbraced $25EI_b/L_b$ MNm/rad
406x178UB60	10	45.2	2.3	36.2	113.0
457x191UB74	11	70.1	3.2	51.0	159.3

Table 8.6 Boundaries for stiffness classification

Test	Failure Type	
	Actual (Test)	Predicted (Annex J)
1	Thread stripping	End plate in mode 1
2	Thread stripping	End plate in mode 2
3	Thread stripping	End plate in mode 1
4	Column web buckling	Row 1 - End plate in mode 2 Row 2 - End plate in mode1 (group failure)
5	Column web buckling	Row 1 - End plate in mode 2 Row 2 - End plate in mode1 (group failure)
6	Column web buckling	Row 1 - End plate in mode 2 Row 2 - Column web in compression

Mode 1 - Complete yielding of flange
Mode 2 - Bolt failure with yielding of flange

Table 8.7 Failure types

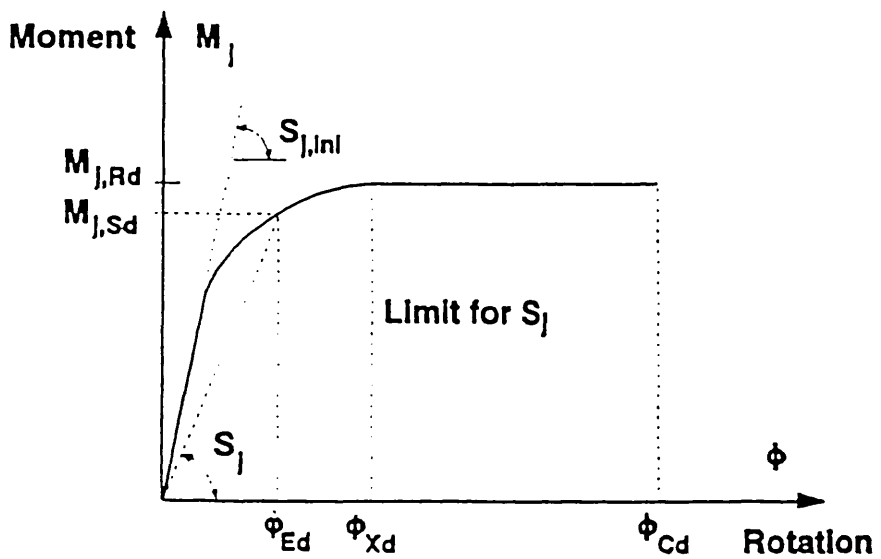

Fig. 8.1 Design moment-rotation characteristic

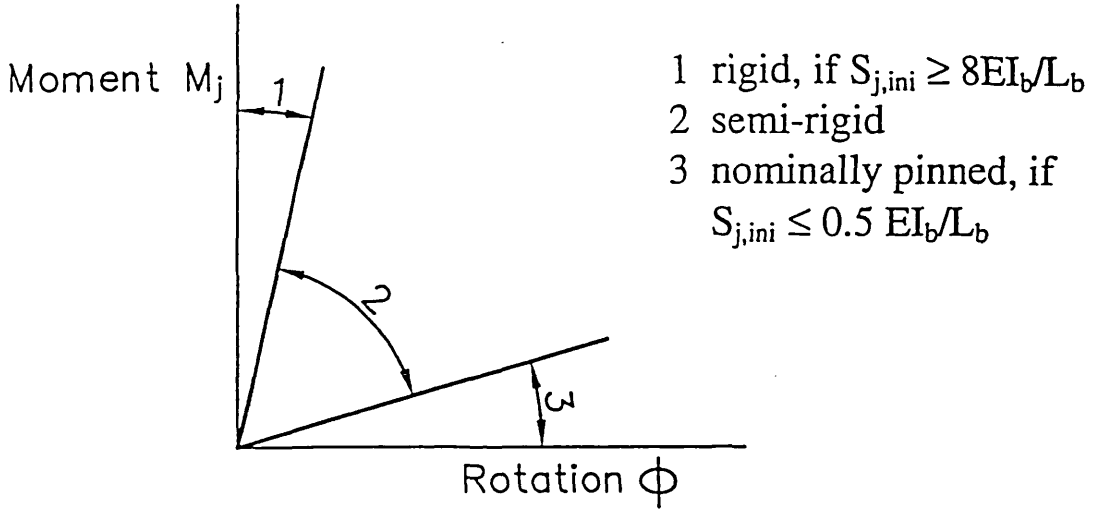

(a) Braced frames

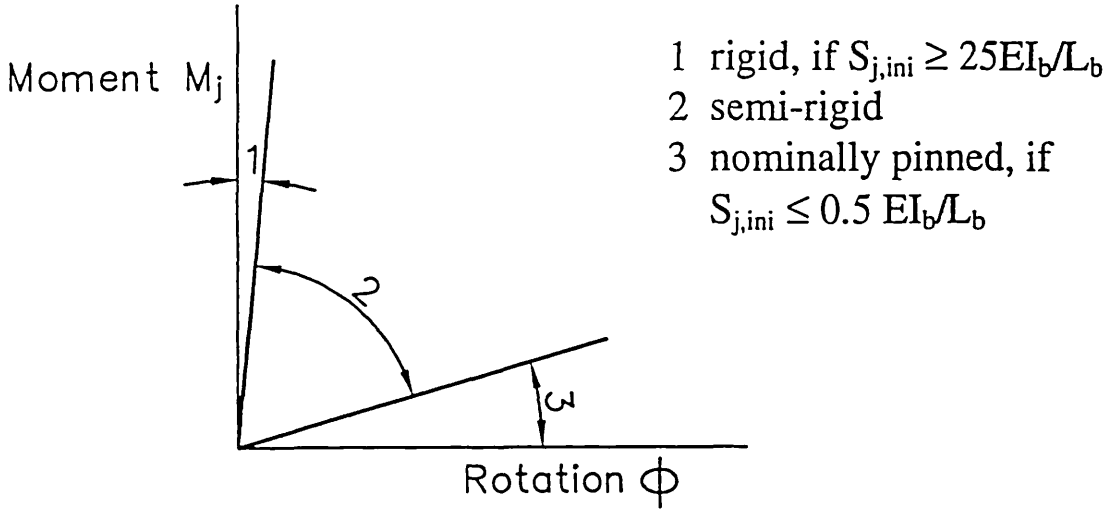

(b) Unbraced frames

Fig. 8.2 Stiffness boundary classification

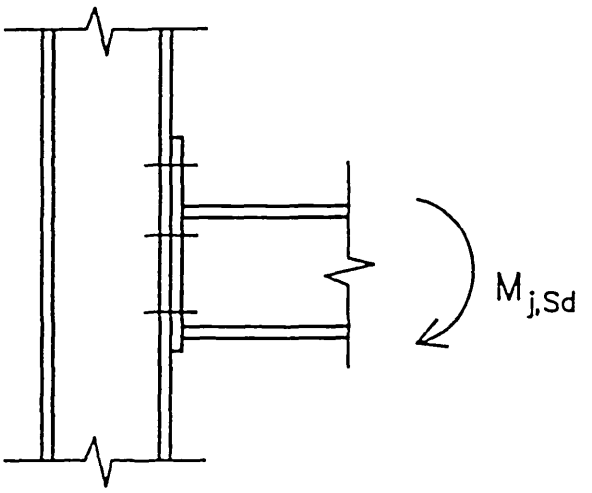

Full strength, if either $M_{j,Rd} \geq M_{b,pl,Rd}$

or $M_{j,Rd} \geq 2M_{c,pl,Rd}$

Nominally pinned, if $M_{j,Rd} < 0.25$ times the moment resistance required for a full strength joint

Fig. 8.3 Strength boundary classification

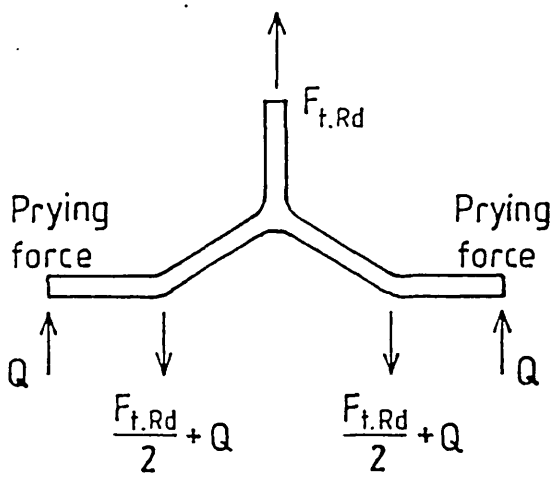

Mode 1: Complete flange yielding

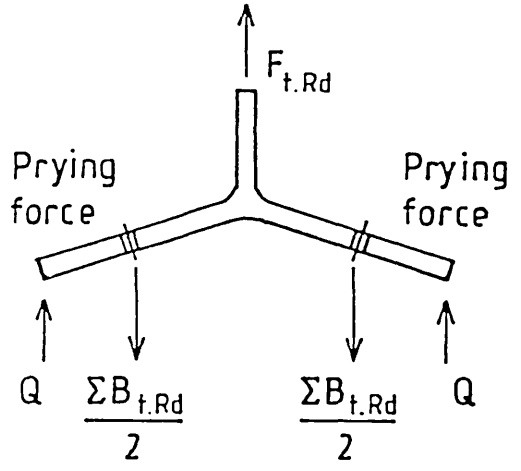

Mode 2: Bolt failure with flange yielding

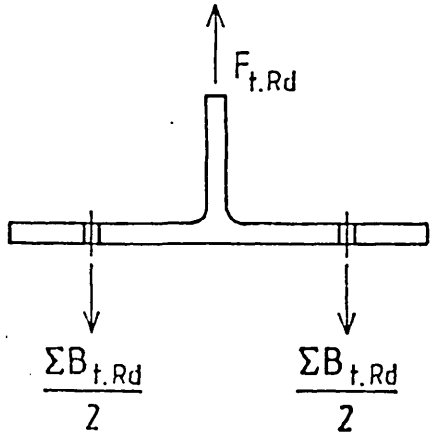

Mode 3: Bolt failure

Fig. 8.4 Failure modes

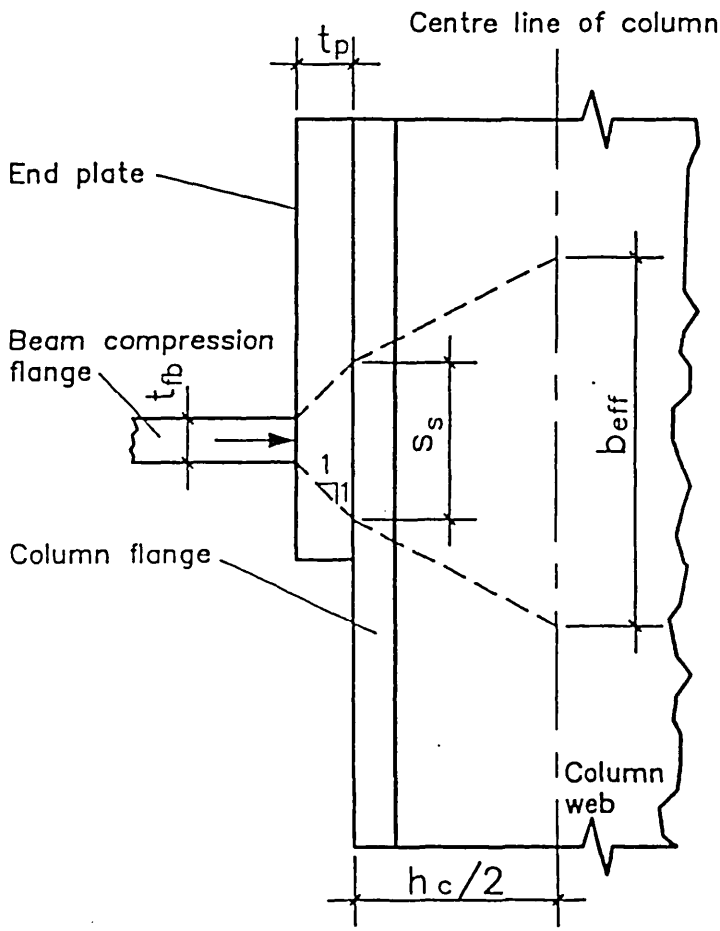

Fig. 8.5 Effective breadth for web buckling resistance in Eurocode 3

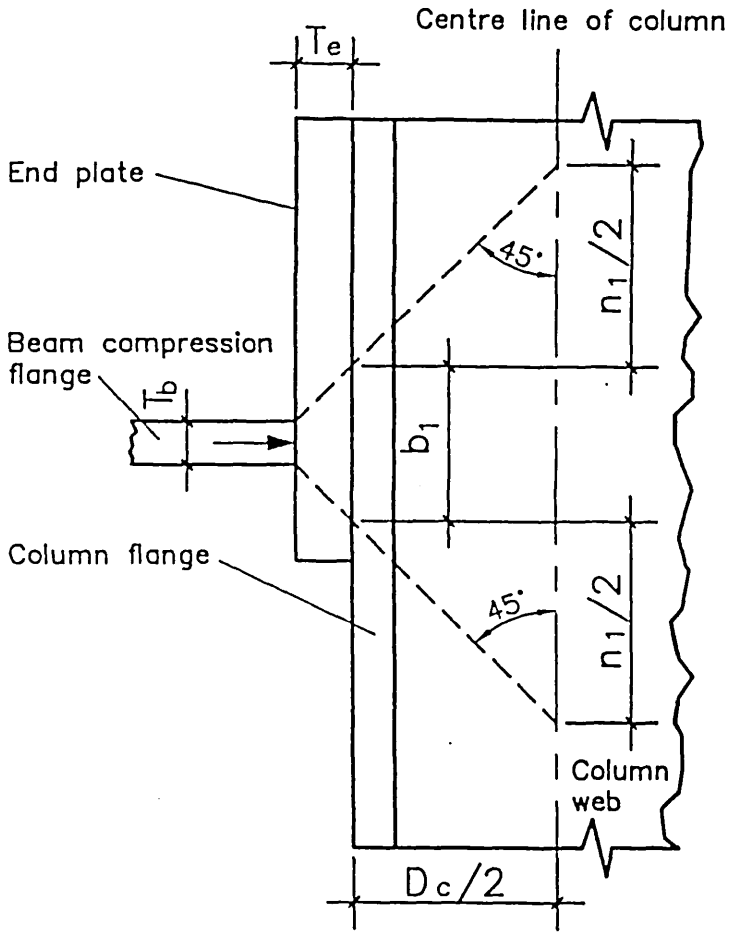

Fig. 8.6 Effective breadth for web buckling resistance in BS 5950

Fig. 8.7 406x178UB60
Test 3, 5, 6

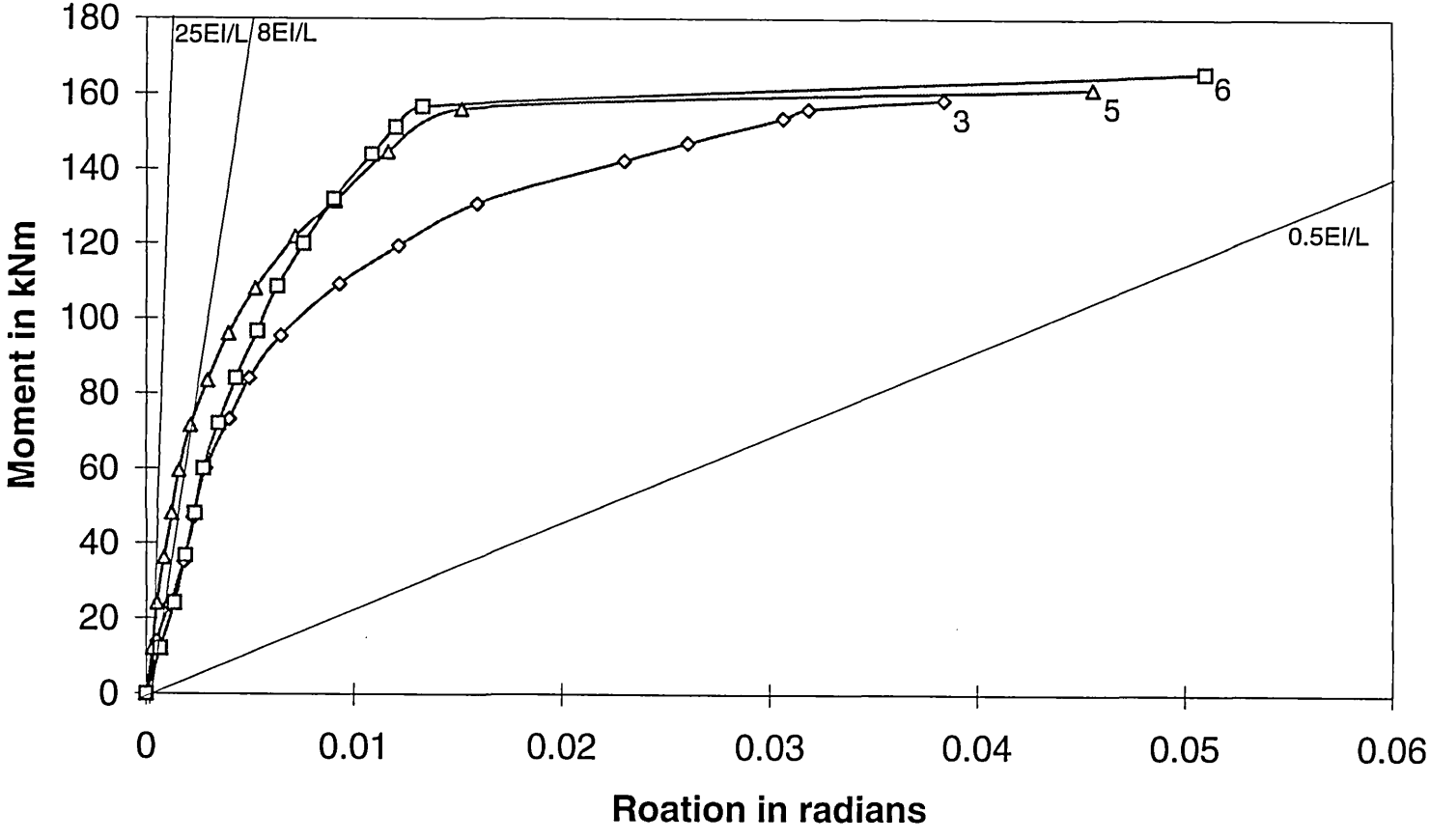

Fig. 8.8 457x191UB74
Test 1, 2, 4

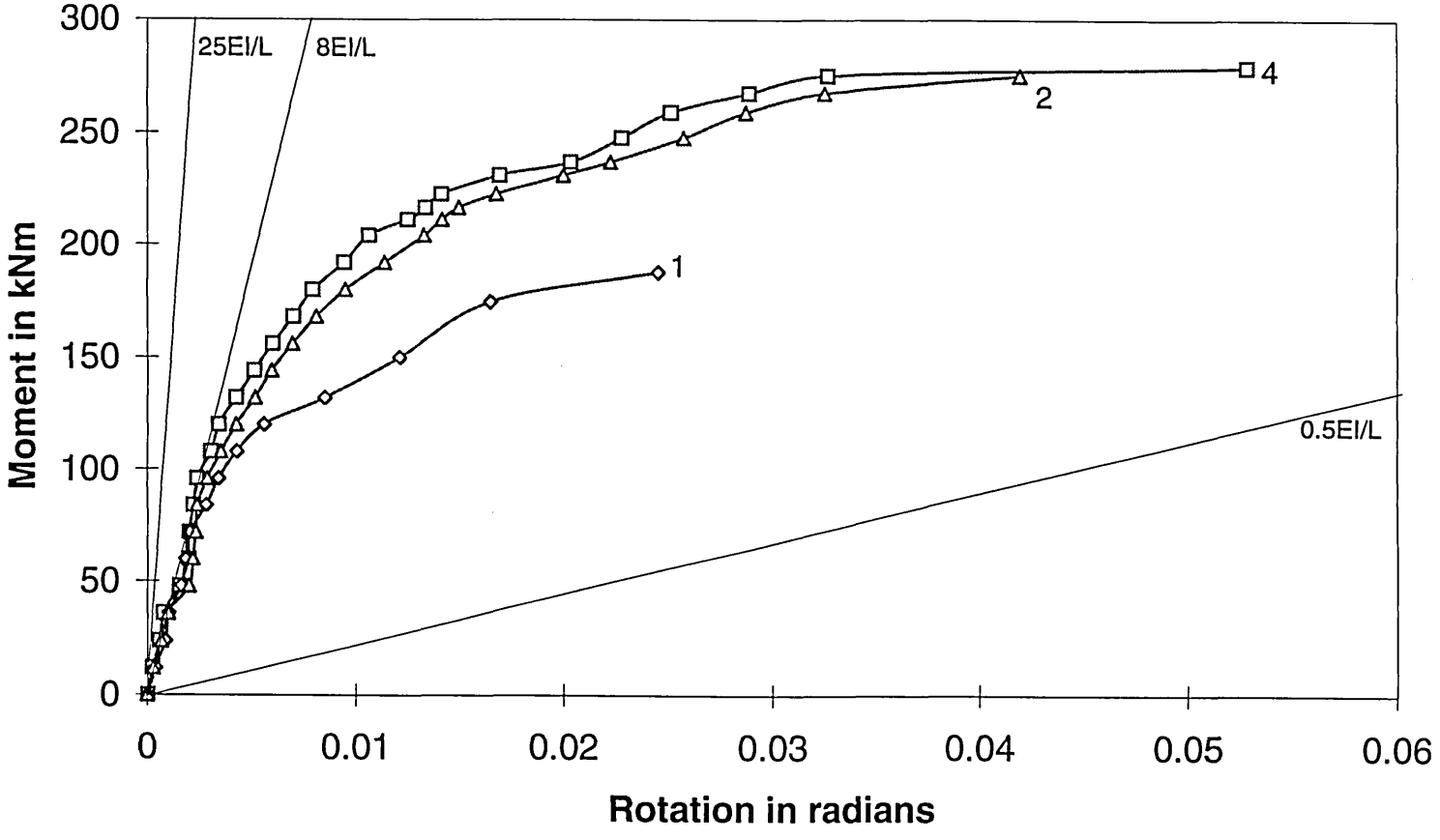

CHAPTER 9

DISCUSSION AND CONCLUSIONS

9.1 STANDARD CONNECTIONS AND CONNECTION DATABASE

The concept of connection standardization[61] is widely accepted. In today's construction industry an important element in cost reduction is the more economic use of manpower. Connections in a typical steel frame account for 50% of the installed cost and handling is the single largest factor. Standardisation of the connection will reduce manpower requirement and increase the productivity, which is achieved by means of repetition or computerised automated and semi-automated procedures. Standardization of the connection not only reduces the number of parameters involved in any connection design but also allows the designers to choose between a range of connections once the beam and column sections have been decided.

It is a good idea to set up a database of marketable standardized connections. Once such standardized connection details are available, computer model can be used to provide structural properties of the connections, which can be tabulated by beam size. Tables 9.1 and 9.2 give typical examples of the design tables[7]. Also moment-rotation curves of the connections can be drawn if needed by the designers, as shown in previous chapters. From the design tables and moment-rotation curves, the designer can choose suitable connection to suit the design of structural steel frame.

Setting up connection database is a daunting task. Large amount of data has to be collected and an appropriate data bank has to be created. The European Research Project COSTC1 has created a database called SERICON for semi-rigid connections. The test results of 18 full scale tests of connections performed at the

University of Abertay Dundee, including the 6 performed by the author, was submitted for storage in the SERICON database.

9.2 CONCLUSIONS

I. Survey of British Structural Steelwork Industry

End plate connections are extensively used as moment resistant connections between members in steel frames. Surveys of the English and Scottish Steelwork Industry carried out by Hatfield Polytechnic and University of Abertay Dundee (formerly Dundee Institute of Technology) clearly indicate that the flush end plate connection is the most popular type of beam-to-column connection in steel-framed structures. The surveys indicated that the flush end plate connection was being used frequently by 83% and 91% of the suppliers in England and Scotland respectively. Extended end plate connection is also a popular type of connection and frequently used in pitched roof portal frames. The popularity of these connections can be attributed to the simplicity of the connection detail and economy associated with their fabrication and erection. Flush end plate connection is less rigid and has a lower moment capacity than that of an extended end plate connection. If a rigid joint is aimed, extended end plate connection should be used, whereas if a semi-rigid joint is needed flush end plate connection can be employed. Column stiffeners may be provided at the level of beam flanges; however this involves costly fabrication and may interfere with the connection of cross beams to the web of the column. It may therefore be preferable to use a heavier column section in order to avoid stiffening. At present, the construction industry seems to favour the use of stiffeners.

II. Review of Previous Research Work

The flush end plate connection represents an extremely complex and highly indeterminate problem with a large number of parameters affecting its structural behaviour. Early attempts to solve the problem by classical structural principles involved many simplifying assumptions and resulted in simple but conservative design formulae. In recent years efforts have been made to carry out a thorough

investigation of the connection with the aim of predicting its behaviour more accurately and formulating a rational and economic design procedure. Two advanced techniques which have been frequently used in the investigation are the yield line and the finite element method. Each method has some advantages and disadvantages as mention in Chapter 1. With the development of high speed computers and powerful finite element softwares, finite element method offers an ideal means for tackling complex structural engineering problems. Early attempts to analyse the end plate connections using finite element technique were generally based on two dimensional analysis. Three dimensional finite element technique was first applied at the University of Abertay Dundee to investigate the behaviour of unstiffened end plate connection[8].

It should be recognised that a flush end plate connection is essentially a three dimensional problem. The author has been successful in building a sophisticated model of the unstiffened flush end plate connection and in applying finite element technique to carry out a three dimensional elasto-plastic analysis of the connection. It was originally hoped that a suitable design method would be developed in the final stage of the investigation, but this could not be achieved due to lack of enough data.

III. Finite Element Model

In Chapter 4, a finite element model of the unstiffened flush end plate connection was presented. The finite element package, LUSAS was employed for the analytical study of the connection. Solid elements were used for the plates, bar elements for the bolts and joint elements for the interaction generated between the end plate and column flange. The joint elements had non-linear properties with infinite (very large) stiffness in compression and zero stiffness in tension. This ensured displacement compatibility at nodes where end plate and column flange were in contact but allowed separation at all other nodes. The contribution of the beam towards the rotational stiffness of the connection is small and was not considered. However, its contribution towards the bending behaviour of the end plate was recognised and

included in the model. A short length of the beam was incorporated in the model with fictitiously very high modulus of elasticity to ensure that the boundary of the end plate, where it was connected to the beam flanges and web, remained in a plane at all time during the loading cycle. A length of column equal to two and half times the depth of the beam was considered in the model. The loads on the connection were modelled as distributed loads acting at beam flanges. They formed a couple which was equivalent to the moment transmitted by the connection.

Some simplifying assumptions were made in modelling the connection in order to save the cost of computing and disk space. Welds, bolt heads/nuts and column fillets were not included in the model; it was assumed that their contributions to the moment-rotation characteristics were insignificant.

IV. Comparison Between Experimental And Analytical Results

Six full scale destructive tests were conducted and data obtained from the tests were analysed. Material tests were also carried out in order to provide appropriate material properties to the prediction model. Test results were compared with the results obtained from the finite element analysis and the validity of the assumptions made and the accuracy of the three dimensional finite element model were assessed. The analytical moment-rotation curves, bolt strains, strains at preseleted locations in column web and prying patterns were compared with their corresponding experimental values.

Experimental investigation on flush end plate connections and comparison between analytical and experimental results are reported in Chapter 5 and 6 respectively. The comparative study of the six connections which were tested demonstrated that there was good agreement between the experimental and analytical results. However, there was some disagreement in the initial elastic range and in the final range before failure occurred. Analytical moment-rotation curves were linear in the elastic range whereas the experiment responses were not. This can be attributed to the combination of tightening effect, imperfection in set up and lack

of fit. There was some discrepancy also in the final range. This happened because premature failure (thread stripping and column web buckling) occurred in all six tests. The finite element package used could not model these phenomena. Thread stripping will be avoided when the European Standard on bolts are adopted, It is hoped that the future version of LUSAS will be able to handle material nonlinear buckling. A comparative study of bolt strains also show good agreement between analytical and experimental results. Some differences were observed in the early stage and in the final stage. These can be attributed to the effect of pretensioning of the bolts in the early stage and complex stress acting on the bolts in the final stage. Pretensioning of bolts and complex stresses were not considered in the analytical model. Comparison of column web strains also show good agreement between analytical and experimental results.

V. In-depth Investigation Of The Connection

(i) Contribution of various components

The analytical investigation into the contribution of the various connection components toward the moment rotation characteristics indicates that the contribution of the end plate towards rotation increases as the material of the end plate reaches plastic range, while the contribution of the column flange decreases; the contribution of the bolts changes very little. End plate contributes much more when the connection contains two rows of tension bolts compared with one row.

(ii) Bolt force

If the connection contains two rows of bolts in tension region, the bolt forces in the two rows are not proportional to their distances from the beam compression flange in the elastic range; in the final stage of the elasto-plastic range they tend to be proportional. Bending of the bolt was analysed using analytical results. Big difference was observed between the smallest and largest strains within one bolt; the largest strains were 4 to 7 times the smallest strains.

(iii) Prying force

One difference was observed between prying patterns recorded by the carbon paper and obtained from the analytical results. Prying patterns recorded by the carbon paper indicate contacts adjacent to the column and beam webs, while no such contacts are shown by the finite element analysis. This can be attributed to the distortion of end plate due to welding at the time of fabrication. Apart from this difference, prying patterns show good agreement. There is very little prying force in the tension region if the connection contains one row of tension bolts. Prying forces generally scatter near the second row of tension bolts if the connection contains two rows of tension bolts. This indicates that prying forces in these connections mainly affect the second row of tension bolts at the service load. As the load increases such effect decreases.

(iv) Deformation

Double curvatures and prying effects were observed in the figures illustrating deformed meshes of the connections. End plate deformed greatly in the region surrounding the tension bolt if the connection contained one row of tension bolts. Analytical stress contours show that high stresses concentrate in the areas around tension bolts and surrounding the beam compression flange. Yielding also happened at the same locations.

VI. Failure Mode And Failure Load

Very frequently, bolted end plate joints fail due to column web buckling, but the Annex J of Eurocode 3 considers only the crushing resistance of column web for the purpose of evaluating the moment resistance of joints. For many UB and some UC sections, buckling resistance is smaller than crushing resistance. The Annex J of Eurocode 3 significantly underestimates the moment resistance of many joints and predicts the failure type incorrectly. Large discrepancies between test and predicted values of rotational stiffness are also detected. There is scope for improving the stiffness formulae by calibration of the component stiffness coefficients. Premature

failure due to thread stripping occurred in many joints. This can be prevented by using bolts which comply with European Standards.

The investigation has indicated that the flush end plate connection represents a semi-rigid connection in steel-framed structures and exhibits a nonlinear moment-rotation relationship over the entire loading range.

9.3 RECOMMENDATIONS FOR FUTURE WORK

The behaviour of the end plate connection depends on a large number of parameters including the thickness of column flange and web, depth of beam, thickness of end plate, size and grade of bolt and connection details. The three-dimensional finite element model developed was found to be capable of predicting the complex behaviour of the connection with a high degree of accuracy. In modelling of the connection some simplifying assumptions were made. It would be appropriate to investigate the effects of these assumptions on the performance of the model. The author recommends that the following investigations be carried out in the future:

i. Column web buckling or collapse analysis should be carried out. This would require either one half or the entire connection be modelled. The ABAQUS finite element software, recently acquired by the University can be employed for the analysis.

ii. The effect of bolt heads and nuts on the moment-rotational performance of the end plate connection should be investigated.

iii. Welds, the effect of welding in the heat affected zone (HAZ) and column fillet were ignored in author's model. Investigation of their effects on the behaviour of the connection should be carried out.

iv. Detailed parametric study of the connection should be carried out in order to separate the contribution of various components towards the moment-rotation characteristics.

v. A range of standard flush end plate connections should be developed. The various connection properties for different column and beam sizes should then be

tabulated. This can be achieved with the aid of the 3-dimensional finite element model of the connection.

No.	Detail	Column	End plate	Failure moment kNm	Rotation at failure rad	Failure mode	Strength classification	Initial rotational stiffness MNm/rad	Stiffness classification	
									Braced	Unbraced
1	W1/20	254x254UC73	460x200x12	158.4	0.038	Bolt stripping	PS	21.3	SR	SR
2	W1/20	254x254UC89	450x200x12	125.4	0.036	Bolt stripping	PS	21.6	SR	SR
3	W1/24	254x254UC89	450x200x15	231.0	0.050	Bolt stripping	PS	37.5	R	SR
4	W3/20	254x254UC73	460x200x12	161.4	0.046	Column web buckling	PS	26.7	SR	SR
5	W3/24	254x254UC73	460x200x15	165.6	0.051	Column web buckling	PS	29.0	SR	SR

All flange welds 2x10 FW; all web welds 2x8 FW. All material S275. All bolts 8.8

Table 9.1 Connection property for beam 406x178 UB 60

No.	Detail	Column	End plate	Failure moment kNm	Rotation at failure rad	Failure mode	Strength classification	Initial rotational stiffness MNm/rad	Stiffness classification	
									Braced	Unbraced
1	W1/20	254x254UC89	510x200x12	187.8	0.025	Bolt stripping	PS	30.4	SR	SR
2	W1/24	254x254UC89	510x200x15	275.4	0.042	Bolt stripping	PS	36.0	SR	SR
3	W3/20	254x254UC89	510x200x12	279.0	0.053	Column web buckling	PS	46.7	SR	SR

All flange welds 2x10 FW; all web welds 2x8 FW. All material S275. All bolts 8.8

Table 9.2 Connection property for beam 457x191 UB 74

REFERENCES

1. The Hatfield Polytechnic. Interim report on local failures in steelwork structures, No.1 and No.2. 1983 and 1984.

2. Dundee Institute of Technology. Connection types survey of structural steelwork in Scotland. 1993.

3. DISQUE R. O. End plate connections. National Engineering Conference proceedings, American Institute of Steel Construction, pp 30-37. 1962.

4. BS5950 : Structural Use of Steelwork in Building, Part 1. Code of practice for design in simple and continuous construction : hot rolled sections. British Standards Institution. 1985.

5. Eurocode 3 : Design of Steel Structure, Part 1.1 General rules and rules for buildings. British Standards Institution. 1992.

6. BOSE B. and HUGHES A. F. Verifying the performance of standard ductile connections for semi-continuous steel frames. Proceeding of the Institution of Civil Engineers, Structures and Buildings, pp 441-457. November 1995.

7. BOSE B., YOUNGSON G. K. and WANG Z. M. An appraisal of the design rules in Eurocode 3 for bolted end plate connections by comparison with experimental results. Accepted for publication in the Proceeding of the Institution of Civil Engineers, Structures and Buildings .

8. BAHRAMI, M. Behaviour of beam-to-column end plate connections in structural steelwork. PhD thesis, Dundee Institute of Technology. 1991.

9. LUSAS : Finite element analysis system, Version 11, User manual. Finite Element Analysis Ltd. 1993.

10. MAXWELL S M, HOWLETT J H, JENKINS W M and BOSE B. A realistic approach to the performance and application of semi-rigid joints in steel structures. International Conference on Joints in Structural Steelwork, Teesside Polytechnic, Pentech Press Ltd. 1981.

11. TONG C S. The elastic behaviour of semi-rigid connections in steel structures. PhD Thesis, Hatfield Polytechnic, Hatfield. 1985.

12. PRESCOTT A T. The performance of end plate connections in steel structures and their influence on overall structural behaviour. PhD Thesis, Hatfield Polytechnic, Hatfield. 1987.

13. PASK J W. Manual on connections for beam and column construction. BCSA Publication, No. 9/82. 1982.

14. HIGGINS T R and RUBLES. Structural uses of High Strength bolts. Transactions ASCE, Vol. 120. 1955.

15. WILSON W M and MOORE H F. Tests to determine the riveted joints of steel structures. University of Illinois, Engineering Experiment Station, Bulletin 104. 1917

16. Steel Structures Research Committee. 1st, 2nd and 3rd reports. Dept of Scientific and Industrial Research, HMSO, London. 1931, 1934 and 1936.

17. YOUNG C R and JACKSON K B. The relative rigidity of welded and riveted connections. Canadian Journal of Research, Vol 11, No 1 and No 2. 1934.

18. HECHTMAN R A and JOHNSON B G. Riveted semi-rigid beam-to-column building connections. Progress Report No 1, Committee of Steel Structures Research, AISC. Nov 1947.

19. SCHUTZ F W. Strength of moment connections using high tensile strength bolts. Proc Nat Eng Conf, AISC. 1959.

20. DOUTY R T and McGUIRE W. High strength bolted moment connections. Journal of Structural Division, ASCE, Vol 91. April 1965.

21. NAIR R S, BIRKEMOE P C and MUNSE W H. High strength bolts subjected to prying. Journal of Structural Division, ASCE, Vol 100, 1-3. 1974.

22. AGERKOV H. High strength bolted connections subject to prying. Journal of Structural Division, ASCE, Vol 102. Jan 1976.

23. AGERKOV H. Analysis of bolted connections subject to prying. Journal of Structural Division, ASCE, Vol 103. Nov 1977.

24. SHERBOURNE A N. Bolted beam to column connections. The Structural Engineer, Vol 39. June 1961.

25. ZOETEMEIJER P. A design method for the tension side of statically loaded, bolted beam-to-column connections. Heron 20, No 1, Delft University, The Netherlands. 1974.

26. PACKER J A and MORRIS C J. A limit state design method for the tension region of bolted beam-to-column connections. The Structural Engineering, London. 1977.

27. SURTEES J O and MANN A P. End plate connections in plastically designed structures. Conference in Joints in Structures, Vol 1, Papre 5, University of Sheffied. 1970.

28. HOWLETT J H, JENKINS W M and STRINSBY R (Editors). Joints in structural steelwork. International Conference, Teesside Polytechnic, Pentech Press Ltd. 1981.

29. ZEOTERMEIJER P. Semi-rigid bolted beam-to-column connections with stiffened column flanges and flush end plates. International Conference on Joints in Structural Steelwork, Teesside Polytechnic, Pentech Press Ltd. 1981.

30. PHILLIPS J and PACKER J A. The effect of plate thickness on flush end plate connections. International Conference on Joints in Structural Steelwork, Teesside Polytechnic, Pentech Press Ltd. 1981.

31. AGGARWAL A. K.. Behaviour of flexible end plate beam-to-column joints. Journal of Constructional Steel Research, Elsevier Science Publishers Ltd, pp 111-132. 1990.

32. BOSE B. Tests to verify the performance of standard ductile connections. Dundee Institute of Technology, Consultancy Report C1/93. December 1993.

33. BOSE B. Additional tests of standardised ductile connections. University of Abertay Dundee, Consultancy Report C1/94. December 1994.

34. KRISHNAMURTHY N and GRADDY D E. Correlation between 2 and 3 dimensional finite element analysis of steel bolted end plate connections. Computers and Structures, Vol. 6, No. 415, pp 381-389. August 1976.

35. KRISHNAMURTHY N. Steel bolted end plate connections. Proceedings of International Conference on Finite Element Methods in Engineering, Adelaide, Australia, pp 23.1-23.16. December 1976.

36. KRISHNAMURHTY N. Fresh look at bolted end plate behaviour and design. Engineering Journal of Structural Division, ASCE, Vol. 15, Part 2, pp 39-49. 1978.

37. KRISHNAMURHTY N, HUANG H, JEFFERY P K and AVERY L K. Analytical M-θ curves for the end plate connections. Journal of Structural Division, ASCE, Vol. 105, ST1, pp 133-145. January 1979.

38. KRISHNAMURHTY N and OSWALT R E. Bolt head and weld effects in steel connection behaviour. International Conference on Joints in Structural Steelwork, Teesside Polytechnic, Pentech Press Ltd. 1981.

39. TARPY T S and CARDINAL J W. Behaviour of Semi-rigid Beam-to-Column End-Plate Connection. Joint in Structural Steelwork. Proceedings of The International Conference on Joints in Steelwork. Held at Middlesbrough, Cleveland, United Kingdom Pentach Press, London, pp.2.3-2.25. 1981.

40. MAXWELL S M, JENKINS W M and HOWLETT J H. A theoretical approach to the analysis of connection behaviour. Joints in Structural Steelwork. Pentech Press. 1981.

41. PATEL K V and CHEN W F. Nonlinear analysis of steel moment connections. Journal of Structural Engineering, ASCE, Vol. 110, No. 8, pp 1861-75. 1984.

42. PATEL K V and CHEN W F. Analysis of fully bolted connection using NONSAP. Computers and Structures, Vol. 21, No. 3, pp 505-11. 1985.

43. JENKINS W M, TONG C S and PRESCOTT A T. Moment-transmitting end plate connections in steel construction and a proposed basis for flush end plate design. The Structural Engineer, Vol. 64A, No. 5, pp 121-132. May 1985.

44. JENKINS W M. Moment-transmitting bolted end plate connections. Structural connections: stability and strength, ed. Narayanam, Elsevier Science Publishers, pp 219-251. 1989.

45. GENDRON G, BEAULIEU D and DHAAT G. Finite element modelling of bolted connections. Canadian Journal of Civil Engineering, Vol. 16, pp 172-181. 1989.

46. BOSE B, SARKAR S and BAHRAMI M. Finite element analysis of unstiffened extended endplate connections. Structural Engineering Review, Chapman and Hall. 1991.

47. BOSE B, SARKAR S and BAHRAMI M. Behaviour of extended endplate connections : Comparison between finite element analyses and experimental results. The 2nd International Conference on ' Computational Structures Technology ', Athens. August 1994.

48. SHERBOURNE A N and BAHAARI M R. 3D simulation of end-plate bolted connections. Journal of Structural Engineering, Vol. 120, No. 11. November 1994.

49. ZIENKIEWICZ O C. Finite element method. Fourth Edition, McGraw-Hill. 1989.

50. OWEN D R J and HINTON E. Finite element in plasticity (Theory and Pratice). Pineridge Press. 1980.

51. RAO S S. The finite element method in engineering. Pergamon Press. 1982.

52. ROWE G W, STURGESS C E N, HARTLEY P and PILLINGER I. Finite-element plasticity and metalforming analysis. Cambrige University Press. 1991.

53. ROCKEY K C, EVANS H R, GRIFFITHS D W and NETHERCOT D A. The Finite Element Method. Second Edition. Granada Publishing, 1983.

54. BS 3692: 1967. Specification for ISO Metric Precision Hexagon bolts, screws and nuts. British Standards Institution.

55. BS EN 24014:1992. Hexagon head bolts. Product Grades A and B. British Standards Institution.

56. BS EN 24016:1992. Hexagon head bolts. Product Grade C. British Standards Institution.

57. BS EN 24032:1992. Hexagon nuts style 1. Product Grades A and B. British Standards Institution.

58. BS EN 24034:1992. Hexagon nuts. Product Grade C. British Standards Institution.

59. BS EN 10 002-1:1990. Tensile testing of metallic materials, Part 1. Method of test at ambient temperature. British Standards Institute.

60. Eurocode 3, Part 1.1 Revised Annex J: Joint in building frames. European Committee for standardization (CEN). 1994.

61. FEWSTER S. M. C., GIRARDIER E. V. and OWENS G. W. Economic design and the importance of standardised connections. Proceedings of the First World Conference on Constructional Steel Design, Acapulco. 1992.

Publication

An appraisal of the design rules in Eurocode 3 for bolted end plate connections by comparison with experimental results.

(Accepted for publication in the Proceeding of the Institution of Civil Engineers, Structures and Buildings)

AN APPRAISAL OF THE DESIGN RULES IN EUROCODE 3 FOR BOLTED END PLATE JOINTS BY COMPARISON WITH EXPERIMENTAL RESULTS

B Bose, BSc(Eng), PhD, CEng, MIStructE
Lecturer in Civil Engineering, University of Abertay Dundee

G K Youngson, B Eng
Research Officer, University of Abertay Dundee

Z M Wang, B Eng
Research Student, University of Abertay Dundee

SYNOPSIS

The summary of a large number of full scale tests carried out on bolted end plate joints is reported in this paper. The three main properties of the joints, namely the moment resistance, rotational stiffness and rotation capacity are determined and compared with values obtained by the design rules of Eurocode 3. Technical content of Eurocode 3 concerning joint design is examined and discrepancies between test results and Eurocode 3 predictions are analysed.

NOTATION

A_s	tensile stress area of a bolt
d	diameter of bolt
E	modulus of elasticity
f_{ub}	ultimate tensile strength of bolts
f_y	yield strength
I_b	second moment of area of a beam
L_b	span of a beam
$M_{b,pl,Rd}$	plastic moment resistance of a beam
$M_{c,pl,Rd}$	plastic moment resistance of a column
$M_{j,Rd}$	moment resistance of a joint
$M_{j,Sd}$	bending moment applied at the joint
$S_{j,ini}$	initial rotational stiffness of a joint
t	thickness
ϕ_{Cd}	rotation capacity of a joint

1 INTRODUCTION

Design methods and application rules for joints in building frames are contained in Eurocode 3[1] Annex J [2]. These are primarily intended for moment-resisting joints between universal beam and universal column sections in which the beams are connected to the flanges of the columns. Bolted connections with end plates or flange cleats, welded connections and several other specific types are covered.

The typical moment-rotation characteristic of a beam-to-column joint is shown in Fig.1, in which the three main structural properties of the joint are defined. These are the

moment resistance $M_{j,Rd}$, rotational stiffness $S_{j,ini}$ and rotation capacity ϕ_{Cd}. Methods for determining the moment resistance and rotational stiffness of a joint are given in the revised Annex J.

Joints in a building frame may be classified on the basis of their rigidity or strength. When the classification is by rigidity a joint may be termed as 'rigid', 'semi-rigid' or 'nominally pinned'. For this the initial rotational stiffness $S_{j,ini}$ of the joint is determined and compared with the classification boundaries of Annex J, which are reproduced in Fig.2. On the other hand, if the classification is by strength, the terms 'full strength', 'partial strength' or 'nominally pinned' may be used. The moment resistance $M_{J,Rd}$ of the joint is computed and compared with the moment resistances of the beam and column members which it joins. Fig.3 illustrates the boundaries, specified in Annex J, for strength classification of a joint at intermediate column height.

In general, bolted end plate joints in a building frame represent semi-rigid, partial strength joints. The rotational stiffness and moment capacity of these joints are not small enough to be ignored but are insufficiently large to enable them to qualify as rigid, full strength joints.

'Semi-continuous design' is an umbrella term which has been adopted by Eurocode 3. It embraces both semi-rigid (elastic) and partial strength (plastic) approaches to the analysis of moment resisting frames. For both elastic and plastic analysis of semi-continuous frames it is necessary to check the rotation capacity of the joints. Unfortunately, Eurocode 3 does not specify any method for determining the rotation capacity of a joint. It merely states that a beam-to-column joint may be assumed to have adequate rotation capacity for plastic analysis if the moment resistance of the joint is governed by the resistance of the column web

panel in shear. If it is a bolted end plate joint, it may also be deemed to possess sufficient rotation capacity if the two following conditions are satisfied :

(i) the moment resistance of the joint is governed by the flexural resistance of either the column flange or the end plate, and

(ii) the thickness of either the column flange or the end plate satisfies the condition $t \leq 0.36\, d\sqrt{f_{ub}/f_y}$, where f_y is the yield strength of the relevant component.

Eurocode 3 does not specify any value for the rotation capacity which may be considered as sufficient.

A range of standard ductile joints has been developed by the SCI/BCSA Connections Group in collaboration with the University of Warwick. These connections have been designed with reference to Eurocode 3 Annex J. A large number of representative connections from the range were subjected to experimental verification of their performance. The tests, which are reported here, were performed at the University of Abertay, Dundee in connection with two consultancies commissioned by the Steel Construction Institute[3,4] and a PhD study[5] on end plate joints.

2 TESTS OF END PLATE JOINTS

2.1 Joint details

The range of standard ductile joints developed at the Steel Construction Institute was originally based around five different bolt configurations, with either flush or extended end plates in two standard widths. Bolts are M24 or M20, Grade 8.8. Fig.4 illustrates the range for M24 bolts; for M20 bolts the geometry is the same, except that the end plate thickness is one size smaller, 12 mm in place of 15 mm and 15 mm in place of 20 mm.

2.2 Test programme

In all, 18 full scale tests were performed which embraced the following :

- Four beam depths
- Four connection details (W1, W2, W3 and W4)
- Two bolt sizes (M20 and M24, both grade 8.8)
- One column size of three different masses (73, 89 and 132 kg/m)
- Three non-standard details

The test specimens were supplied by two local steel fabricators. No attempt was made to control the material or workmanship, except that punched (not drilled) holes were specified. In practice, the holes in the end plate were punched, whereas holes in the column flange were drilled.

The test specimens, shown in Fig.5, were assembled on the strong floor of the Heavy Structures Laboratory at the University of Abertay Dundee, using a podger spanner to tighten the bolts. A sheet of carbon paper sandwiched between two sheets of cartridge paper was interposed between the end plate and column flange on each side to map the contact pressure. Ordinary bolts for general building construction were used in the first series of tests (Table 2); for the second and third series, fully threaded bolts were employed. No washers were used.

Standard cruciform beam-to-column joint tests were performed in a loading frame. The load was applied by a 1000 kN capacity hydraulic jack which was monitored by a load cell of similar capacity.

Joint rotation is defined as the change in angle between the centre lines of beam and column induced by the load at the joint. A simple but reliable instrumentation configuration, illustrated in Fig.6, was employed to measure the joint rotation. Straight arms

were connected to the column at location A and to the beam at location B, as shown in Fig.7. Point A was located in the column web at the intersection of column and beam centre lines, whereas point B was located on the beam centre line very close to the welded end plate. A portable rigid frame was erected in front of the test specimen. Two independent sets of measurements were taken to compute the joint rotation on each side of the column. For the first set, two dial gauges were supported on the beam arm with their pointers resting on the column arm at 300 mm apart. For the second set, two displacement transducers were supported on the rigid frame with their pointers resting on top of the beam arm at 300 mm apart. Similar arrangements were made on either side of the column so that two values of joint rotation were determined for either side. The load cell and the displacement transducers were connected to a datalogger. At any applied load, the joint rotation was given by the difference of the two dial gauge or displacement transducer readings divided by 300 mm. The moment resisted by the joint was determined by multiplying the support reaction (half of the applied load) by the distance between the support and the face of the column flange.

2.3 Test results

In an earlier paper[6], the results of 12 tests commissioned by the Steel Constructiion Institute were reported. Subsequently, 6 additional tests of flush end plate connections, conforming to the standard details W1 and W3, were conducted in connection with a PhD study[5]. The summary of 18 test results is compiled in Table 1. All tests were performed until failure occurred. Failure was due to a number of factors, namely column web buckling, bolt failure and end plate fracture. Failure of bolts occurred in 8 tests, 6 due to thread stripping and 2 due to fracture. Buckling of column web was responsible for 6 failures and fracture of end plate for a further 1. A combination of column web buckling, end plate fracture and bolt failure occurred in the remaining 3 tests. Three typical failure types are illustrated in Figures 8 and 9.

The test data were analysed and moment-rotation characteristics (M - ϕ curves) of the joints were plotted, which are shown in Figs. 10 - 13 for the four standard details and in Figs. 14 - 17 for the four beam depths. The material properties of column flange, column web, end plate and bolts were determined by standard tensile tests which are summarised in Table 2.

3 COMPARISON BETWEEN PREDICTED AND TEST RESULTS

The design of a structural element should consider the three main properties which are strength, rigidity and ductility. For a joint in a building frame the terms moment resistance, rotational stiffness and rotation capacity are used to refer to these properties. In Eurocode 3, a joint is treated as an assemblage of a number of components. Methods for determining the properties of the individual components and relationships between the properties of components and the structural properties of a joint are given. The aim of this investigation is to examine critically, the design rules of Eurocode 3 Annex J for bolted end plate connections and to detect any discrepancies or anomalies. To achieve this, the moment resistance, initial rotational stiffness and rotation capacity of each of the 18 end plate joints predicted by Eurocode 3 Annex J are ascertained. These are then compared with the results of full scale tests.

3.1 Moment resistance

In the case of the 18 end plate joints described earlier, the moment resistances predicted by Annex J and failure moments observed in the tests are given in Table 1. For the purpose of calculating the moment resistances by the Annex J method, material properties of the joint components, given in Table 2, were used. The test values were, in all cases, higher than the predicted values with the ratio of test to predicted value ranging between 1.09 and

1.96. The large discrepancy between the test and predicted values in the case of a large number of joints is disconcerting.

3.1.1 *Types of failure*

The types of joint failure predicted by the design method of Annex J are given in Table 3. These are generally not in agreement with those observed in tests. Each of the 6 flush end plate joints with a single row of M20 or M24 bolts (Tests 1 to 6) failed due to thread stripping or bolt fracture. Extended end plate joints with a single row of M24 bolts in the plate extension (Tests 7 and 16) failed due to end plate fracture. Buckling of column web was generally responsible for failure of both flush and extended end plate joints with 2 or more rows of M24 bolts. There were 2 exceptions. The extended end plate joints 14 and 15 connected beams to heavy column sections with relatively thick web thickness (t = 15.6 mm). These joints failed due to bolt fracture. The non-standard extended end plate joint 17 used M20 bolts and failed due to thread stripping. Welds performed satisfactorily and no weld failure was observed in any test.

Failure of end plate in mode 1 (complete yielding of flange) or mode 2 (bolt failure with yielding of flange) are predicted by Annex J for 15 of the 18 end plate joints subjected to testing. One joint (Test 11) connected 15 mm thick end plate to 14.2 mm thick column flange (254 UC 73). Strength of column flange in mode 1 governs the force in bolt row 2. In Clause J.3.5.3 of Annex J, crushing of column web in compression has been considered for determining the strength of the joint; buckling of column web is disregarded. Crushing of column web is predicted for 2 joints (tests 10 and 18). Only 1 extended end plate joint with 3 rows of bolts was included in the test programme (Test 18). The force in bolt row 3 is found to be zero according to Annex J. For the design of joints to Eurocode 3, the designer has to comply with the requirements of European Standards for bolts and nuts (Ref. 9 to 12). No thread stripping is encountered in these bolts.

3.1.2 *Column web buckling*

It is evident from the test results that buckling of column webs governs the failure moments of many bolted end plate joints, especially those with 2 or more rows of bolts. Buckling of column web in compression is ignored in Annex J (Clause J.3.5.3) and only column web crushing is considered. For many universal column sections, the crushing and buckling resistances of column webs differ little, as shown in Table 4. However, universal beam sections are often used as columns. For such a section, the buckling strength of column web can be considerably lower than its crushing strength. Consider, for example, a joint with a 20 mm thick end plate which connects a 356 x 171 UB 51 beam to a 406 x 178 UB 60 column. Assuming the yield strength of 275 N/mm^2, the crushing and buckling strengths of the column web are 363.7 kN and 299.2 kN respectively. It is to be hoped that any future revision of Annex J would correct this serious omission.

At this stage, it would be useful to comment briefly on the design methods of Eurocode 3 and BS 5950 for determining the buckling resistance of column webs. These are based on the same design principles, but different effective width of a column web is specified. In Eurocode 3, the effective width is taken as $b_{eff} = (h^2 + s_s^2)^{0.5}$, in which h is the depth of the column section and s_s is the length of stiff bearing. A larger effective width, $b_{eff} = (b_1 + n_1)$ is considered in BS 5950, in which b_1 and n_1 are synonymous with s_s and h respectively, resulting in a higher buckling resistance compared with Eurocode 3. In a forthcoming paper[13], a comparative study of buckling load of column web obtained from tests and the two codes will be reported. This reveals that the BS 5950 predictions are not always safe, and that the reduced effective width of column web specified in Eurocode 3 produces satisfactory results.

3.1.3 *Bolt failure*

Bolt fracture and thread stripping caused a large number of failures. Stripping of threads prior to bolt fracture happens if either the nut material is weaker than the bolt material, or the thread interlock is less than specified because of some deviation from the permitted tolerances. Bolts complying with the British Standard BS 3692[8] are susceptible to thread stripping. Tensile tests performed on M20 and M24 bolts are reported in Table 2 which indicates that thread stripping occurred at a load 5 % less than bolt fracture. In Eurocode 3, bolts and nuts are specified to Standards BS EN 24014 etc[9,10,11,12]. These have different specifications from the nuts used in the British construction industry. Premature failure due to thread stripping is unlikely in these bolts. It is strongly recommended that the British industry should adopt the European Standards on bolts and nuts without delay. This will minimise the risk associated with bolt stripping.

Bolt force in each row was determined, as shown in Table 4, for the purpose of computing the moment resistance of the joints. The force required to cause tensile failure of bolts in each row is also given in Table 4. This is given by $2f_{ub}A_s$, in which f_{ub} is the tensile strength of bolts (Table 2) and A_s is the tensile stress area of a bolt. It is noticeable that Annex J greatly underestimates the bolt forces.

3.1.4 *Strength classification*

On the basis of strength, the 18 joints are classified as shown in Table 5. With very few exceptions these may be termed as partial strength joints. If test results of failure moments are considered, all joints except one will earn the partial strength appellation. The extended end plate joint (Test 13), which connected a deep beam possessing high plastic moment of resistance to a column possessing relatively low plastic moment of resistance, may be termed as full strength.

If the predicted moment resistances are considered for joint classification, only two (Tests 3 and 16) fail to achieve partial strength status. One flush end plate joint with a single row of M20 bolts (Test 3) and one extended end plate joint with single row of M24 bolts in the extension plate (test 16) have very low moment resistances and qualify as nominally pinned.

3.2 Rotational stiffness

Only after the joints have been classified on the basis of their stiffnesses is it possible to perform an elastic analysis of a steel frame. If the joint happens to be semi-rigid, it is essential to know its rotational stiffness before any analysis can be attempted. The M - ϕ curves (Figures 10 to 17) were the source from which the initial rotational stiffnesses of the joints were determined. Annex J also contains a method for computing the stiffness of a joint. The initial rotational stiffnesses of the 18 joints are compiled in Table 6. The M - ϕ curves of many joints were not very smooth in the initial stage, due to slip of bolts or a lack of fit and it was difficult to determine the stiffness very accurately. However, this cannot account for the large discrepancy between the test and predicted results. The formulae for computing the stiffness coefficients of various joint components should be improved by calibration with reference to more experimental results.

3.2.1 *Boundaries for stiffness classification*

Compared with BS 5950, Annex J is more stringent and requires rigid joints to be stiffer. No distinction between braced and unbraced frames is made in BS 5950 and a joint is treated as rigid if its rotational stiffness is greater than the stiffnesses of the members it joins. This can mean 2EI/L, 3EI/L, 4EI/L, 6EI/L ... of the member depending on the support condition at the other end. Annex J treats rigid joints in braced and unbraced frames differently. For a joint in a braced frame, stiffness greater than 8EI/L of the beam is required, whereas, for an unbraced frame, a joint stiffness greater than 25EI/L is demanded. If the

stiffness of a joint in any braced or unbraced frame is less than 0.5EI/L of the beam, it may be treated as nominally pinned.

Classification of a beam-to-column joint in a building frame is influenced by the length of beam connected at the joint. A joint which is classified as rigid when the beam length is large may change to semi-rigid or even nominally pinned if the beam length is small. For the purpose of this investigation, beam length equal to 25 times its depth is assumed. For the four beams used in the test programme the stiffness requirements are given in Table 7.

Various parameters which affect the rotational stiffness of a joint include column flange and web thicknesses, end plate thickness, bolt size and lever arm. It is, however, the lever arm of the joint which makes the most significant contribution and, from the tabulated results, it is concluded that the rotational stiffness of a joint is proportional to the square of its lever arm.

3.2.2 *Stiffness classification*

Lines representing 0.5EI/L, 8EI/L and 25EI/L are drawn on the M - ϕ graphs (Figures 14 to 17) of joints involving the four beams. For the purpose of joint classification (Table 6) the rotation stiffnesses of joints are compared with the classification boundaries given in Table 7. It is noticeable that the joints will generally perform as semi-rigid in unbraced frames. Only two joints (Tests 14 and 15), both involving relatively heavy column sections, can be considered as rigid according to Annex J. In braced frames, many of the joints may be treated as rigid, including all the extended end plate joints with two or more rows of bolts (Details W4 and W5).

3.3 Rotation capacity

In an earlier paper[6], it was argued that joints achieving 0.03 radians rotation capacity can be confidently promoted for plastic design of frames. If the joints fail to achieve 0.02 radians rotation capacity, plastic design should not be employed. The 0.02 to 0.03 radians range represents the grey area. For detailed information, readers should consult the paper.

Joint rotations at failure are presented in descending order in Table 8. It is concluded that 13 joints definitely qualify for plastic design. One flush end plate joint with a single row of M20 bolts (Test 3) would probably have achieved 0.03 radians rotation if thread stripping had not terminated the test prematurely. The obvious conclusion to draw is that all the standard joints with beams up to and including 686x254UB125 are admirably suited for the purpose of plastic design. The two standard joints with 762x267UB147 beams (Tests 13 and 15) and the two non-standard joints with thicker end plates (Tests 17 and 18) are unacceptable.

It is reassuring to observe that the same joints which did not achieve 0.02 radians rotation (Tests 13, 15, 17 and 18) also fail to fulfill Annex J requirements of rotation capacity for plastic design. The thickness of either end plate or column flange exceeds the maximum thickness ($0.36d\sqrt{f_{ub}/f_y}$) specified in Annex J. However, a number of joints which had achieved 0.03 radians rotation are found to be unacceptable according to Annex J. These include three joints (Tests 12, 10 and 4) which had developed large rotation at failure.

4 CONCLUSIONS

(i) Very frequently, bolted end plate joints fail due to column web buckling, but, unfortunately, Annex J considers only crushing resistance of column web for evaluating the moment resistance of joints. For many UB and some UC sections, buckling resistance is smaller than crushing resistance. It is, therefore, recommended that Clause J.3.5.3 of Annex J, which deals with column web in compression, be revised to take account of column web buckling.

(ii) Annex J greatly underestimates the moment resistance of many joints and predicts the failure type incorrectly. Failure of column web in compression is predicted for two joints (Tests 10 and 18), whereas six failures due to column web buckling, including the above two, were observed in tests. Moment resistances of these two joints are predicted more accurately than others for which failure of end plate in mode 1 or 2 is predicted. It is quite obvious that moment resistance of end plate is generally underestimated in Annex J.

(iii) Large discrepancies between test and predicted values of rotational stiffness are detected. There is scope for improving the stiffness formulae by calibration of the component stiffness coefficients.

(iv) Many joints which do not meet the requirements of Annex J for sufficient rotation capacity, achieved rotation which may be deemed as adequate for plastic design.

(v) Premature failure due to thread stripping occurred in many joints. This can be prevented by using bolts which comply with European Standards.

ACKNOWLEDGEMENTS

This investigation into the provision made in Eurocode 3 for the design of end plate connections is supported by a grant from the Institution of Civil Engineers Research and Development Enabling Fund and a research contract awarded by the UK Department of Environment. The test programme was financed by the British Steel Market Development Fund, Steel Construction Industry Federation and the University of Abertay Dundee.

The authors would like to express thanks to many individuals for their support and encouragement. Special mention is due to Dr R M Lawson, Messrs J C Taylor, D G Brown and A S Malik at the Steel Construction Institute, Mr A F Hughes at Ove Arup & Partners, Dr D B Moore at the Building Research Establishment, Professor W M Jenkins at University of Leeds, Dr J P Jaspart at the University of Liege, and Professor S Sarkar and Dr J R Underwood at the University of Abertay Dundee.

REFERENCES

1. DD ENV 1993-1-1:1992, Eurocode 3 : Design of Steel Structures, Part 1.1 General rules and rules for buildings. British Standards Institution.

2. ENV 1993-1-1:1992/prA2:1994, Eurocode 3, Part 1.1 Revised Annex J : Joints in building frames. European Committee for Standardization (CEN).

3. Bose B. Tests to verify the performance of standard ductile connections. Dundee Institute of Technology, Consultancy Report C1/93, 1993, December.

4. Bose B. Additional tests of standardised ductile connections. University of Abertay Dundee, Consultancy Report C1/94, 1994, December.

5. Wang Z.M. Behaviour of beam-to-column flush end plate connections in structural steelwork. PhD thesis to be submitted in 1995, University of Abertay Dundee.

6. Bose B. and Hughes A.F. Verifying the performance of standard ductile connections for semi-continuous steel frames. Accepted for publication in the Proceedings of the Institution of Civil Engineers, Structures and Buildings.

7. BS 5950:Part 1:1985, Structural use of steelwork in building, Part 1, Code of practice for design in simple and continuous construction : hot rolled sections. British Standards Institution.

8. BS 3692:1967, Specification for ISO Metric Precision Hexagon Bolts, Screws and Nuts. British Standards Institution.

9. BS EN 24014:1992, Hexagon head bolts. Product grades A and B. British Standards Institution.

10. BS EN 24016:1992, Hexagon head bolts. Product Grade C. British Standards Institution.

11. BS EN 24032:1992, Hexagon nuts, style 1. Product Grades A and B. British Standards Institution.

12. BS EN 24034:1992, Hexagon nuts. Product Grade C. British Standards Institution.

13. Bose B. and Youngson G.K. Behaviour of column webs in bolted beam-to-column connections. To be presented at the International colloquium on 'Semi-Rigid Structural Connections' sponsored by the International Association for Bridge and Structural Engineering, Istanbul, Turkey, 25 - 27 September, 1996.

Test	Detail	Column	Beam	End plate	Failure load kN	Failure moment kNm	Predicted moment resistance kNm	Ratio = Test/ Predicted	Rotation at failure rad	Failure mode
1	W1/20	254 x 254 UC 73	406 x 178 UB 60	460 x 200 x 12	264	158.4	91.2	1.74	0.038	Thread stripping
2	W1/20	254 x 254 UC 89	406 x 178 UB 60	450 x 200 x 12	209	125.4	85.2	1.47	0.036	Thread stripping
3	W1/20	254 x 254 UC 89	457 x 191 UB 74	510 x 200 x 12	313	187.8	104.6	1.80	0.025	Thread stripping
4	W1/24	254 x 254 UC 89	406 x 178 UB 60	450 x 200 x 15	385	231.0	119.7	1.93	0.050	Thread stripping
5	W1/24	254 x 254 UC 89	457 x 191 UB 74	510 x 200 x 15	459	275.4	140.4	1.96	0.042	Thread stripping
6	W1/24	254 x 254 UC 89	686 x 254 UB 125	720 x 250 x 15	709	425.4	228.4	1.86	0.034	Bolt fracture
7	W2/24	254 x 254 UC 89	457 x 191 UB 74	640 x 200 x 20	417	250.2	164.9	1.52	0.031	End plate fracture
8	W3/20	254 x 254 UC 73	406 x 178 UB 60	460 x 200 x 12	269	161.4	121.2	1.33	0.046	Column web buckling
9	W3/20	254 x 254 UC 89	457 x 191 UB 74	510 x 200 x 12	465	279.0	142.5	1.96	0.053	Column web buckling
10	W3/24	254 x 254 UC 73	406 x 178 UB 60	460 x 200 x 15	276	165.6	152.3	1.09	0.051	Column web buckling
11	W4/24	254 x 254 UC 73	457 x 191 UB 74	640 x 200 x 15	470	282.0	223.4	1.26	0.033	Column web buckling
12	W4/24	254 x 254 UC 89	457 x 191 UB 74	640 x 200 x 15	688	412.8	235.0	1.76	0.061	Column web buckling & end plate fracture
13	W4/24	254 x 254 UC 89	762 x 267 UB 147	930 x 250 x 15	574	688.8	462.3	1.49	0.019	Column web buckling
14	W4/24	254 x 254 UC 132	457 x 191 UB 74	640 x 200 x 15	689	413.4	240.7	1.72	0.039	Bolt fracture
15	W4/24	254 x 254 UC 132	762 x 267 UB 147	930 x 250 x 15	554	664.8	462.3	1.44	0.009	Bolt fracture, thread stripping and end plate fracture
16	Note (i)	254 x 254 UC 89	457 x 191 UB 74	640 x 200 x 15	308	184.8	102.5	1.80	0.034	Bolt fracture and end plate fracture
17	Note (ii)	254 x 254 UC 89	457 x 191 UB 74	640 x 200 x 15	412	247.2	208.6	1.18	0.013	Thread stripping
18	Note (iii)	254 x 254 UC 89	686 x 254 UB 125	860 x 250 x 20	929	557.4	444.7	1.25	0.007	Column web buckling

All flange welds 2 x 10 FW; all web welds 2 x 8 FW. All material S275. All bolts 8.8

(i) As detail W2/24 except that end plate is 15 (not 20) thick

(ii) As detail W4/20 except that end plate is 15 (not 12) thick

(iii) As detail W5/24 except that end plate is 20 (not 15) thick

Table 1 Summary of test results

	Component	Yield strength N/mm^2	Tensile strength N/mm^2	Modulus of elasticity kN/mm^2	Elongation %
FIRST SERIES Tests 1, 3, 5, 8, 9 and 10	Column flange (254 UC 89)	344	460	170	29.3
	Column web (254 UC 89)	311	479	162	26.8
	12 mm end plate	326	475	157	26.8
	15 mm end plate	307	461	150	28.1
	M20 8.8 bolt with single nut	-	882*	-	-
	M20 8.8 bolt with two nuts	-	1086	-	4.1
	M24 8.8 bolt with single nut	-	949	-	17.9
SECOND SERIES Tests 4, 6, 7, 11 and 12	Column flange (254 UC 89)	281	441	207	31.3
	Column web (254 UC 89)	355	469	209	24.3
	15 mm end plate	310	511	225	18.3
	20 mm end plate	301	486	217	23.4
	M24 8.8 bolt with single nut	-	876*	-	12.4
	M24 8.8 bolt with two nuts	-	922	-	13.0
THIRD SERIES Tests 2, 13, 14, 15, 16, 17 and 18	Column flange (254 UC 89)	344	477	205	31.6
	Column web (254 UC 89)	311	484	201	34.1
	Column flange (254 UC 132)	328	483	207	29.9
	Column web (254 UC 132)	350	478	194	32.0
	12 mm end plate	405	551	165	28.0
	15 mm end plate	327	489	213	35.0
	20 mm end plate	300	464	154	35.0
	M20 8.8 bolt with single nut	-	845*	-	-
	M20 8.8 bolt with two nuts	-	888	-	18.8
	M24 8.8 bolt with single nut	-	907	-	19.1

* premature failure by thread stripping

Table 2 Material properties

Test	Detail	Failure type	
		Test	Predicted
1	W1/20	Thread stripping	End plate in mode 1
2	W1/20	Thread stripping	End plate in mode 2
3	W1/20	Thread stripping	End plate in mode 1
4	W1/24	Thread stripping	End plate in mode 2
5	W1/24	Thread stripping	End plate in mode 2
6	W1/24	Bolt fracture	End plate in mode 2
7	W2/24	End plate fracture	End plate in mode 2
8	W3/20	Column web buckling	Row 1- End plate in mode 2 Row 2- End plate in mode 1 (group failure)
9	W3/20	Column web buckling	Row 1- End plate in mode 2 Row 2- End plate in mode 1 (group failure)
10	W3/24	Column web buckling	Row 1- End plate in mode 2 Row 2- Column web in compression
11	W4/24	Column web buckling	Row 1- End plate in mode 1 Row 2- Column flange in mode 1
12	W4/24	Column web buckling and end plate fracture	Row 1- End plate in mode 1 Row 2- End plate in mode 2
13	W4/24	Column web buckling	Row 1- End plate in mode 1 Row 2- End plate in mode 2
14	W4/24	Bolt fracture	Row 1- End plate in mode 1 Row 2- End plate in mode 2
15	W4/24	Bolt fracture, thread stripping and end plate fracture	Row 1- End plate in mode 1 Row 2- End plate in mode 2
16	NON-STANDARD	Bolt fracture and end plate fracture	End plate in mode 1
17		Thread stripping	Row 1- End plate in mode 1 Row 2- End plate in mode 2
18		Column web buckling	Row 1- End plate in mode 2 Row 2- Column web in compression Row 3- Zero force

Mode 1 - complete yielding of flange
Mode 2 - bolt failure with yielding of flange

Table 3 Failure types

Test	Detail	Failure type	Force in each bolt row kN	Total force acting on bolts kN	Column web in compression $F_{c,wc,Rd}$ kN	Buckling resistance kN	Force required to induce bolt failure in each row kN
1	W1/20	End plate in mode 1		268.1	465.3	445.5	532.1
2	W1/20	End plate in mode 2		250.6	614.2	617.5	435.1
3	W1/20	End plate in mode 1		268.1	619.2	618.1	532.1
4	W1/24	End plate in mode 2		352.0	721.4	687.7	650.9
5	W1/24	End plate in mode 2		360.1	637.0	620.3	670.0
6	W1/24	End plate in mode 2		374.5	732.9	689.2	650.9
7	W2/24	End plate in mode 2		336.5	761.0	693.3	650.9
8	W3/20	Row 1 - End plate in mode 2	268.1	388.2	465.3	445.5	532.1
		Row 2 - End plate in mode 1 (group failure)	120.1				532.1
9	W3/20	Row 1 - End plate in mode 2	268.1	394.6	619.2	618.1	532.1
		Row 2 - End plate in mode 1 (group failure)	126.5				532.1
10	W3/24	Row 1 - End plate in mode 2	358.7	479.9	479.9	447.1	670.0
		Row 2 - Column web in compression	121.2				670.0
11	W4/24	Row 1 - End plate in mode 1	198.4	522.1	552.5	491.9	650.9
		Row 2 - Column flange in mode 1	323.7				650.9
12	W4/24	Row 1 - End plate in mode 1	191.4	544.8	727.1	688.4	650.9
		Row 2 - End plate in mode 2	353.4				650.9
13	W4/24	Row 1 - End plate in mode 1	261.5	636.5	645.9	621.6	640.3
		Row 2 - End plate in mode 2	375.0				640.3
14	W4/24	Row 1 - End plate in mode 1	209.2	563.4	1263.6	1234.8	640.3
		Row 2 - End plate in mode 2	354.2				640.3
15	W4/24	Row 1 - End plate in mode 1	261.5	636.6	1278.5	1237.0	640.3
		Row 2 - End plate in mode 2	375.1				640.3
16	NON-STANDARD	End plate in mode 1		209.2	637.0	620.3	640.3
17		Row 1 - End plate in mode 1	209.2	481.2	637.0	620.3	435.1
		Row 2 - End plate in mode 2	272.2				435.1
18		Row 1 - End plate in mode 2	350.9	671.7	671.7	625.6	640.3
		Row 2 - Column web in compression	320.8				640.3
		Row 3- Discounted	0				640.3

Table 4 Component forces for moment resistance

Test	Detail	$M_{c,pl,Rd}$	$M_{b,pl,Rd}$	Moment required for full strength appellation	Failure moment	Predicted moment resistance	Strength classification	
		kNm	kNm	kNm	kNm	kNm	Test	Predicted
1	W1/20	272	327	327	158.4	91.2	PS	PS
2	W1/20	326	327	327	125.4	85.2	PS	PS
3	W1/20	326	456	456	187.8	104.6	PS	NP
4	W1/24	326	327	327	231.0	119.7	PS	PS
5	W1/24	326	456	456	275.4	140.4	PS	PS
6	W1/24	326	1060	652	425.4	228.4	PS	PS
7	W2/24	326	456	456	250.2	164.9	PS	PS
8	W3/20	272	327	327	161.4	121.2	PS	PS
9	W3/20	326	456	456	279.0	142.5	PS	PS
10	W3/24	272	327	327	165.6	152.3	PS	PS
11	W4/24	272	456	456	282.0	223.4	PS	PS
12	W4/24	326	456	456	412.8	235.0	PS	PS
13	W4/24	326	1370	652	688.8	462.3	FS	PS
14	W4/24	496	456	456	413.4	240.7	PS	PS
15	W4/24	496	1370	992	664.8	462.3	PS	PS
16	NON-STANDARD	326	456	456	184.8	102.5	PS	NP
17		326	456	456	247.2	208.6	PS	PS
18		326	1060	652	557.4	444.7	PS	PS

FS = Full strength; PS = Partial strength; NP = Nominally pinned

Table 5 Strength classification

Test	Detail	Initial rotational stiffness MNm/rad		Ratio = Test/ Predicted	Stiffness Classification			
					Test		Predicted	
		Test	Predicted		Braced	Unbraced	Braced	Unbraced
1	W1/20	21.3	29.8	0.71	SR	SR	SR	SR
2	W1/20	21.6	42.4	0.51	SR	SR	R	SR
3	W1/20	30.4	46.1	0.66	SR	SR	SR	SR
4	W1/24	37.5	53.9	0.70	R	SR	R	SR
5	W1/24	36.0	55.2	0.65	SR	SR	R	SR
6	W1/24	83.3	177.0	0.47	SR	SR	R	SR
7	W2/24	60.0	116.1	0.52	R	SR	R	SR
8	W3/20	40.0	32.6	1.23	R	SR	SR	SR
9	W3/20	46.7	53.6	0.87	SR	SR	R	SR
10	W3/24	21.3	37.6	0.57	SR	SR	R	SR
11	W4/24	65.0	107.2	0.61	R	SR	R	SR
12	W4/24	100.0	131.1	0.76	R	SR	R	SR
13	W4/24	220.0	355.2	0.62	R	SR	R	SR
14	W4/24	75.0	169.3	0.44	R	SR	R	R
15	W4/24	258.3	489.1	0.53	R	SR	R	R
16	NON STANDARD	35.0	96.1	0.36	SR	SR	R	SR
17		60.0	118.1	0.51	R	SR	R	SR
18		143.8	318.9	0.45	R	SR	R	SR

SR- Semi rigid; R- Rigid

Table 6 Stiffness classification

Beam	Assumed beam length L_b	Flexural rigidity EI_b	Nominally pinned	Rigid	
				Braced	Unbraced
	m	MNm^2	$0.5\ EI_b/L_b$ MNm/rad	$8\ EI_b/L_b$ MNm/rad	$25\ EI_b/L_b$ MNm/rad
406 x 178 UB 60	10	45.2	2.3	36.2	113.0
457 x 191 UB 74	11	70.1	3.2	51.0	159.3
686 x 254 UB 125	17	247.8	7.3	116.6	364.4
762 x 267 UB 147	19	354.9	9.3	149.4	467.0

Table 7 Boundaries for stiffness classification

Test	Detail	Thickness		Components governing moment resistance of joint	Maximum thickness for plastic design	Rotation at failure	Is rotation capacity sufficient for plastic design?	
		End plate mm	Column flange mm		mm	rad	Test	Predicted
12	W4/24	15	17.3	End plate	14.9	0.061	Yes	No
9	W3/20	12	17.3	End plate	13.1	0.053	Yes	Yes
10	W3/24	15	14.2	End plate, column web in compression	14.4	0.051	Yes	No
4	W1/24	15	17.3	End plate	14.9	0.050	Yes	No
8	W3/20	12	14.2	End plate	13.1	0.046	Yes	Yes
5	W1/24	15	17.3	End plate	15.2	0.042	Yes	Yes
14	W4/24	15	25.3	End plate	14.4	0.039	Yes	No
1	W1/20	12	14.2	End plate	13.1	0.038	Yes	Yes
2	W1/20	12	17.3	End plate	10.7	0.036	Yes	No
6	W1/24	15	17.3	End plate	14.9	0.034	Yes	No
16	Note (i)	15	17.3	End plate	14.4	0.034	Yes	No
11	W4/24	15	14.2	End plate, column flange	15.7	0.033	Yes	Yes
7	W2/24	20	17.3	End plate	15.7	0.031	Yes	No
3	W1/20	12	17.3	End plate	13.1	0.025	-	Yes
13	W4/24	15	17.3	End plate	14.4	0.019	No	No
17	Note (ii)	15	17.3	End plate	11.9	0.013	No	No
15	W4/24	15	25.3	End plate	14.4	0.009	No	No
18	Note (iii)	20	17.3	End plate, column web in compression	14.0	0.007	No	No

i) As detail W2/24 except that end plate is 15 (not 20) thick

ii) As detail W4/20 except that end plate is 15 (not 12) thick

iii) As detail W5/24 except that end plate is 20 (not 15) thick

Table 8 Suitability of joints for plastic design

LIST OF FIGURES

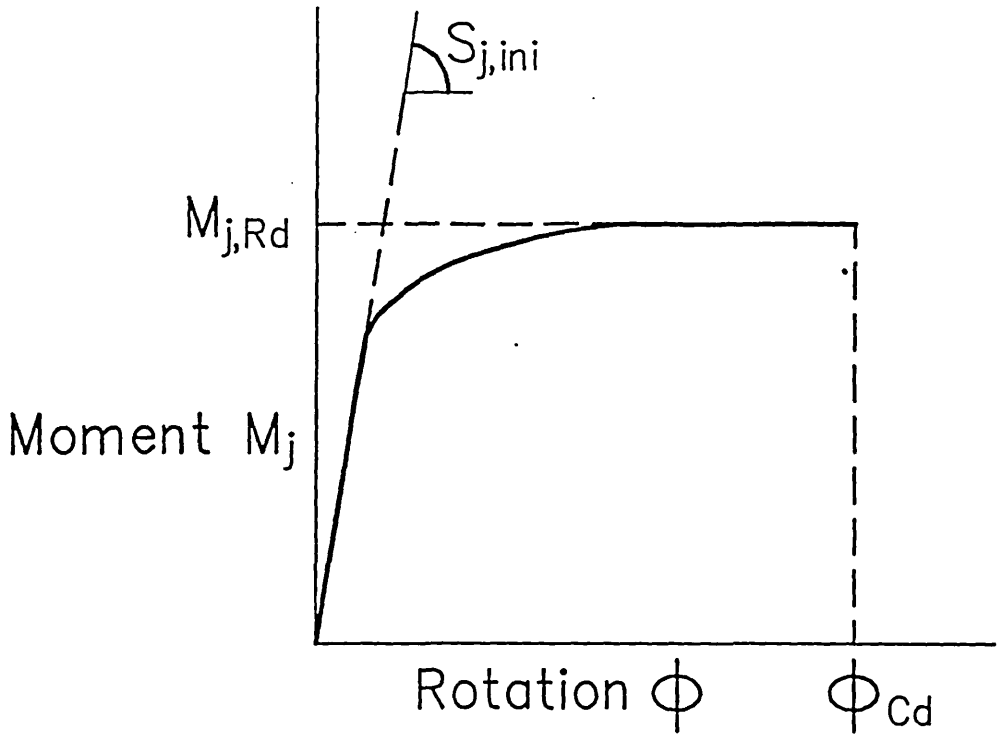

Fig.1

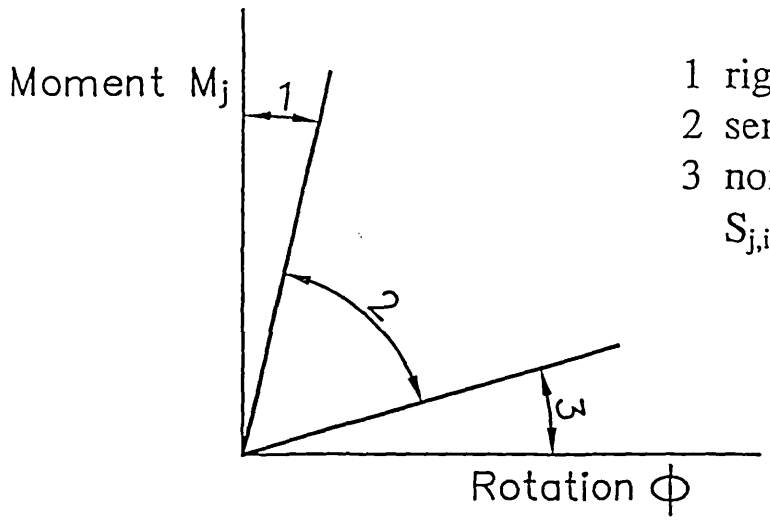

1 rigid, if $S_{j,ini} \geq 8EI_b/L_b$
2 semi-rigid
3 nominally pinned, if $S_{j,ini} \leq 0.5\ EI_b/L_b$

(a) Braced frames

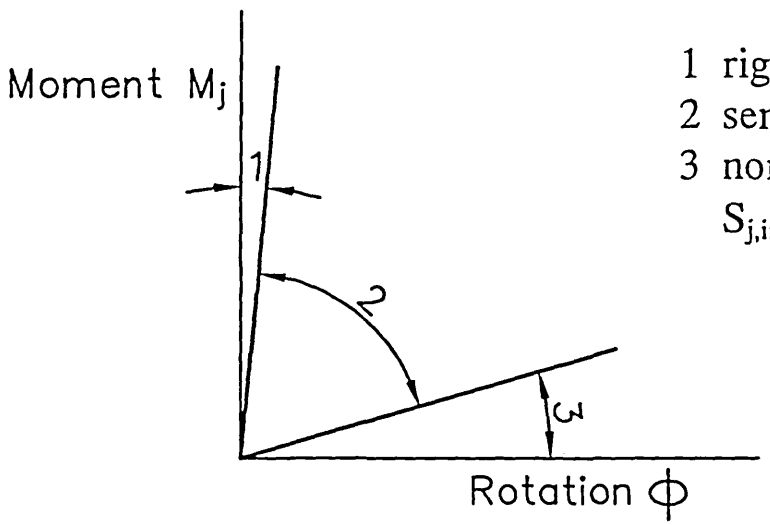

1 rigid, if $S_{j,ini} \geq 25EI_b/L_b$
2 semi-rigid
3 nominally pinned, if $S_{j,ini} \leq 0.5\ EI_b/L_b$

(b) Unbraced frames

Fig.2

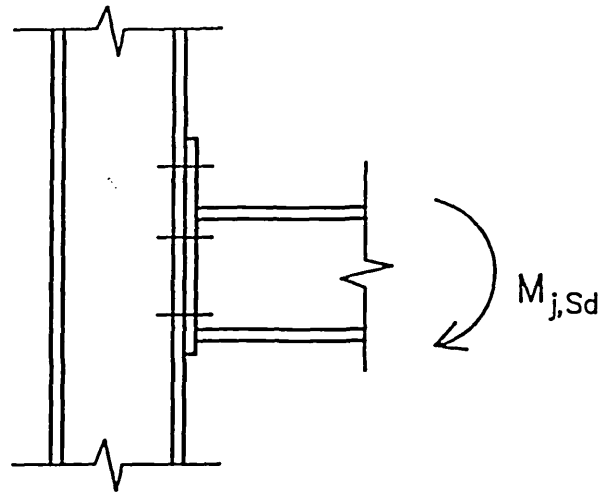

Full strength, if either $M_{j,Rd} \geq M_{b,pl,Rd}$

or $M_{j,Rd} \geq 2M_{c,pl,Rd}$

Nominally pinned, if $M_{j,Rd} < 0.25$ times the moment resistance required for a full strength joint

Fig.3

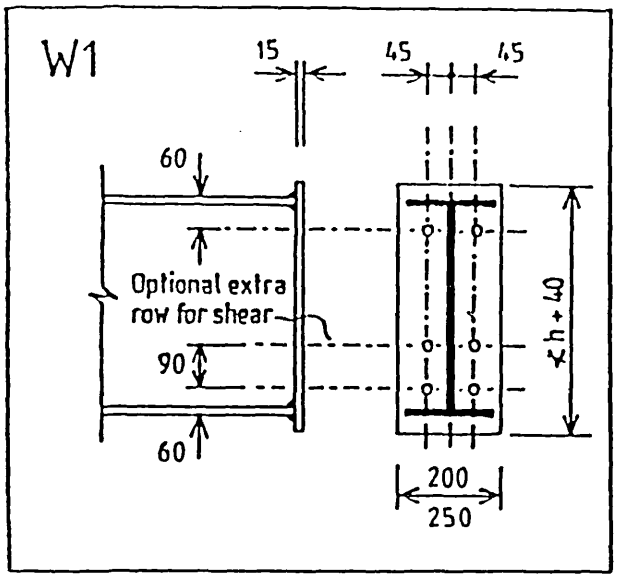

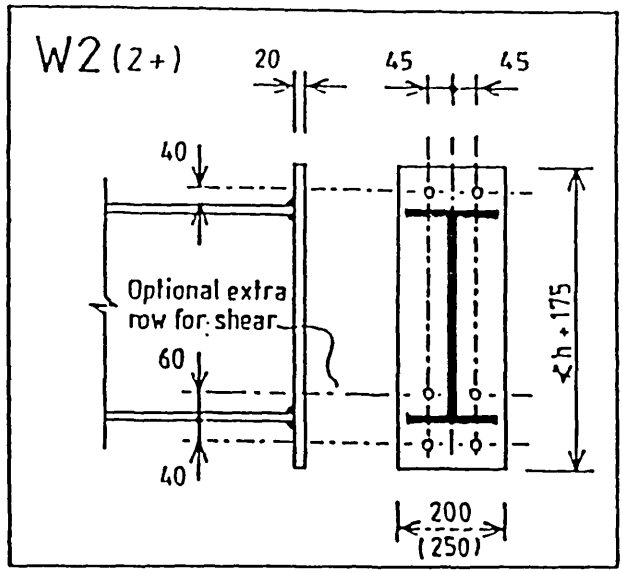

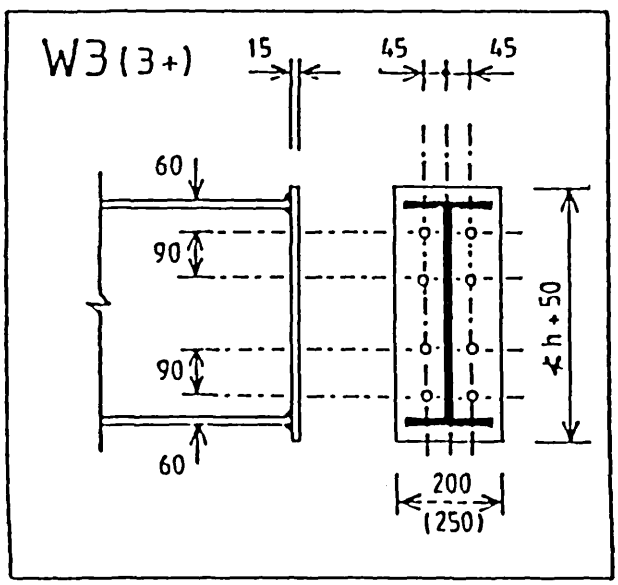

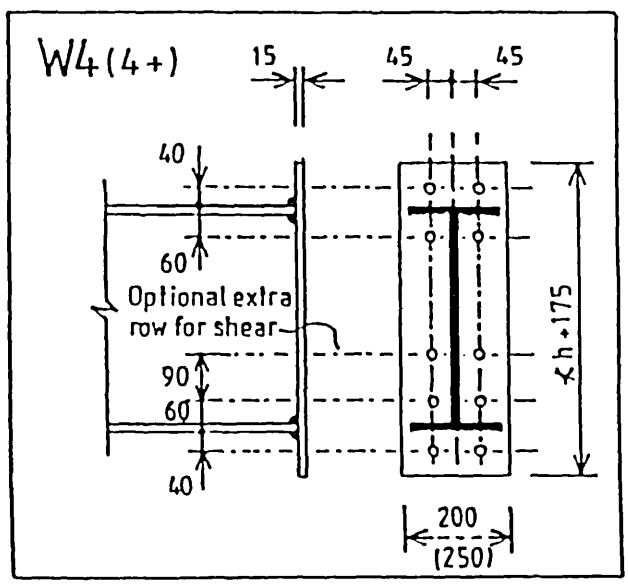

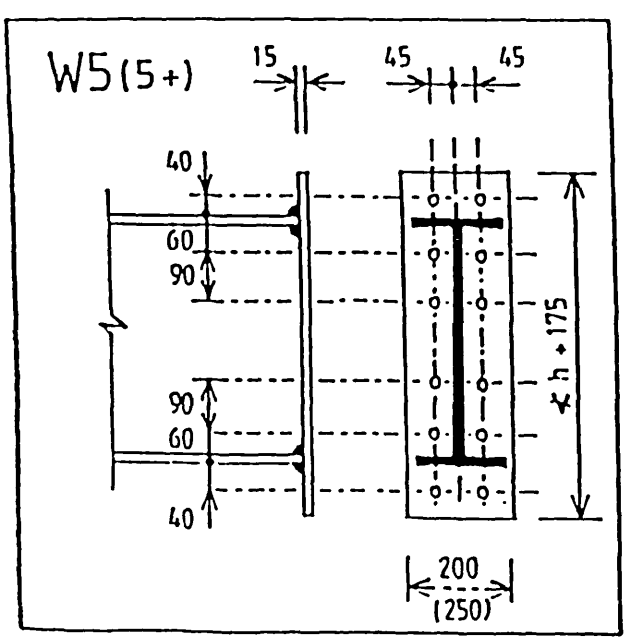

Notes

1. '+' denotes the wider (250) end plate.
2. Optional extra bottom bolt rows for shear are shown on 1, 2 and 4.
3. Flange to end plate weld size to be in the range 10 to 12mm visible fillet.
4. Web to end plate weld 2 X 8 FW as standard.
5. End plates S275.
6. M24 8.8 bolts as standard.
7. Prefix W indicates connections suitable for the wind-moment method, with the bottom half of the detail mirroring the top.

Fig. 4

BOSE/YOUNGSON/WANG

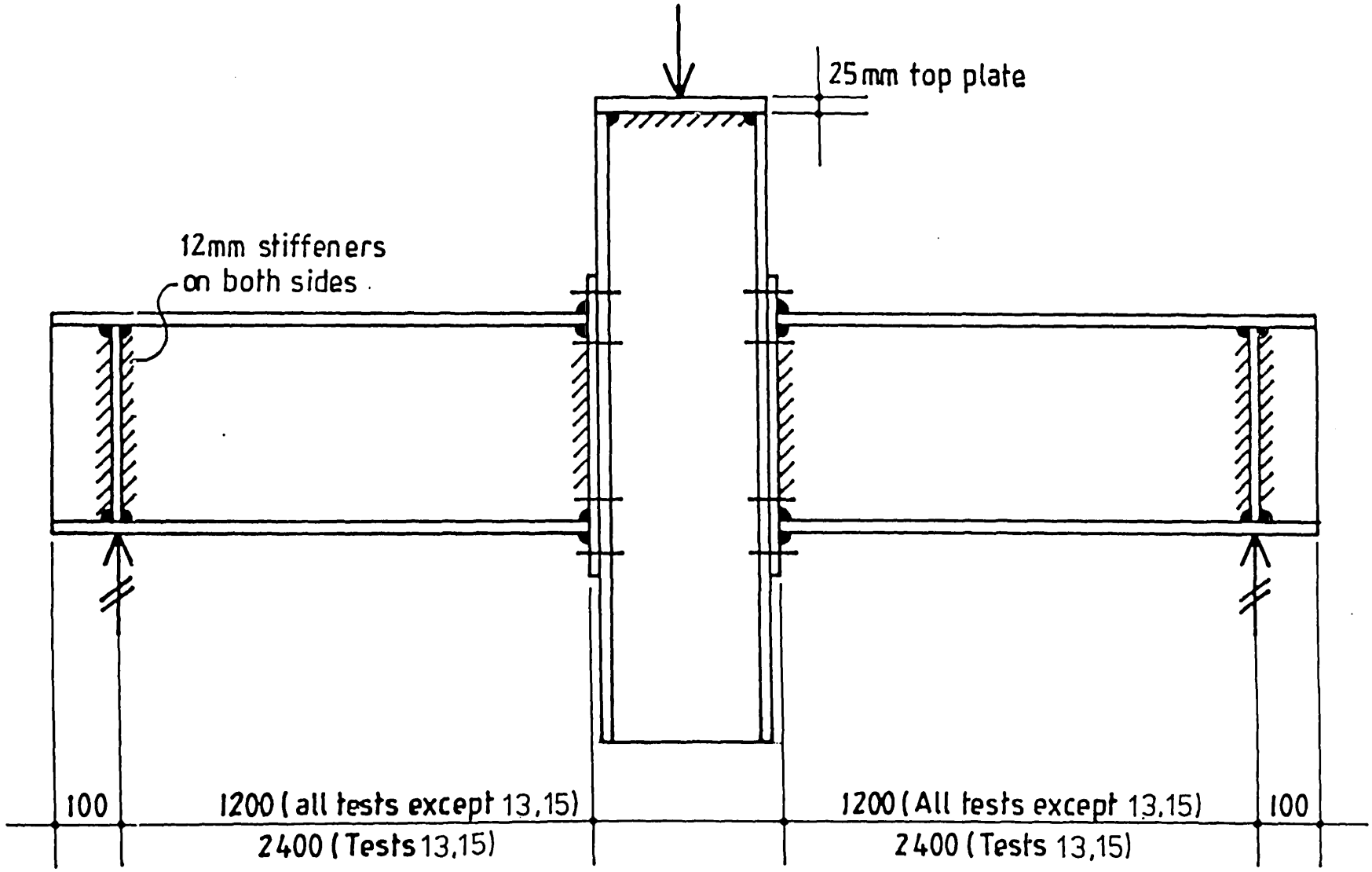

Fig. 5

BOSE/YOUNGSON/WANG

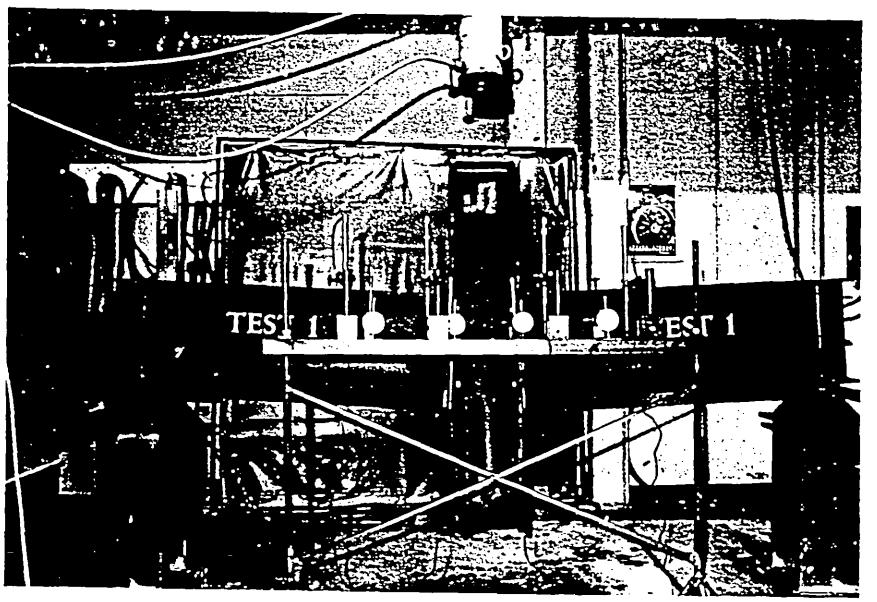

Fig.6

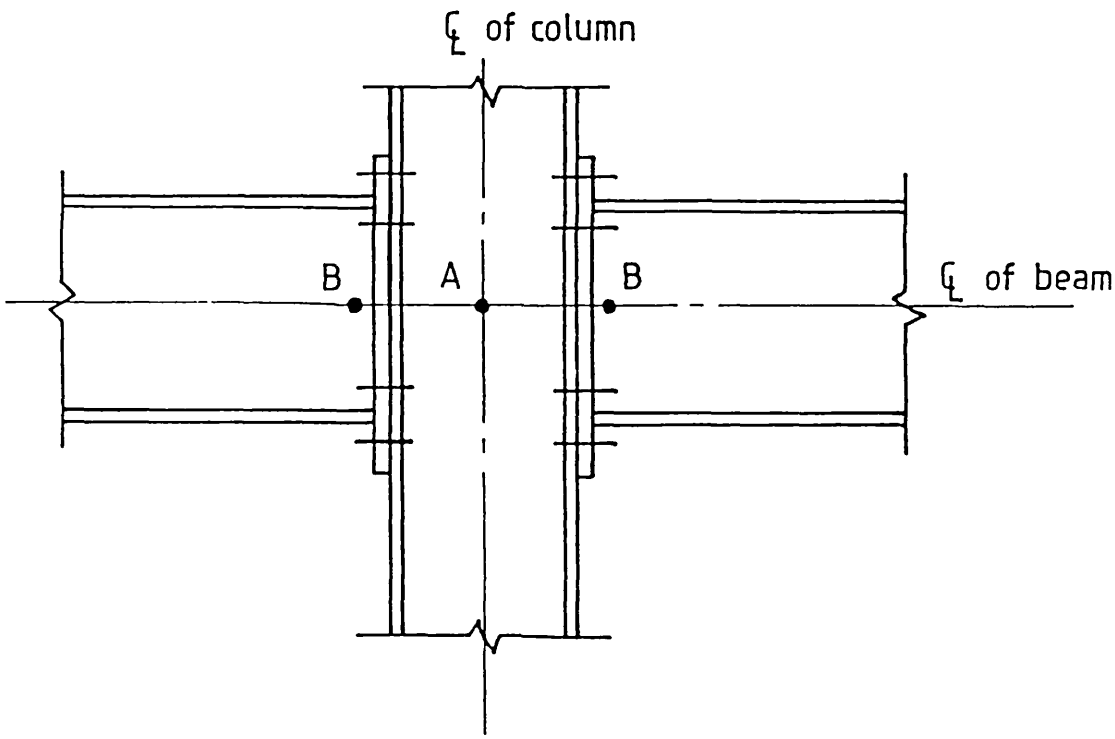

Fig. 7

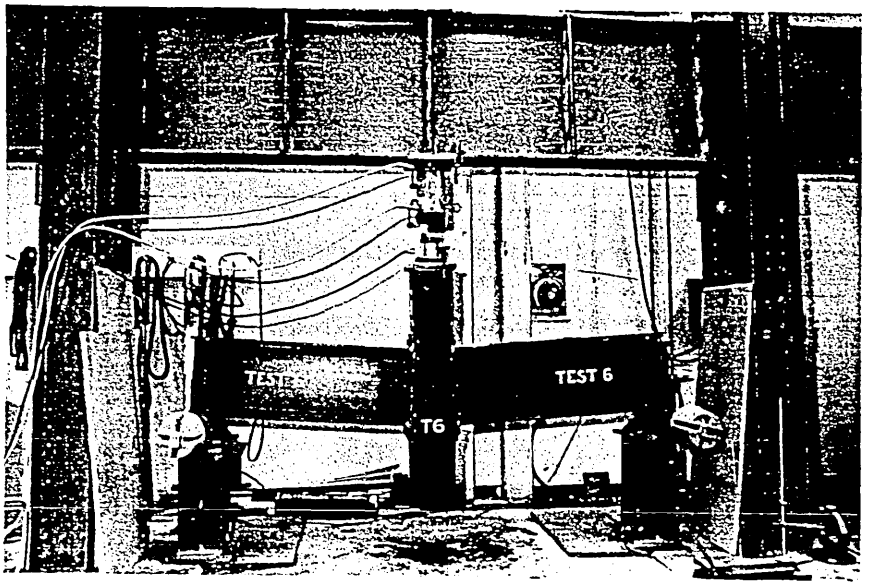

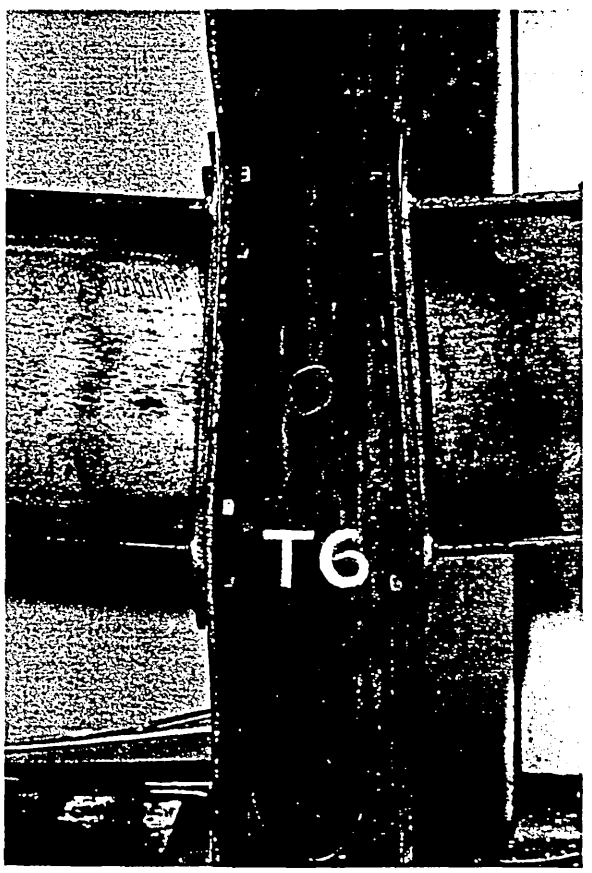

Fig.8

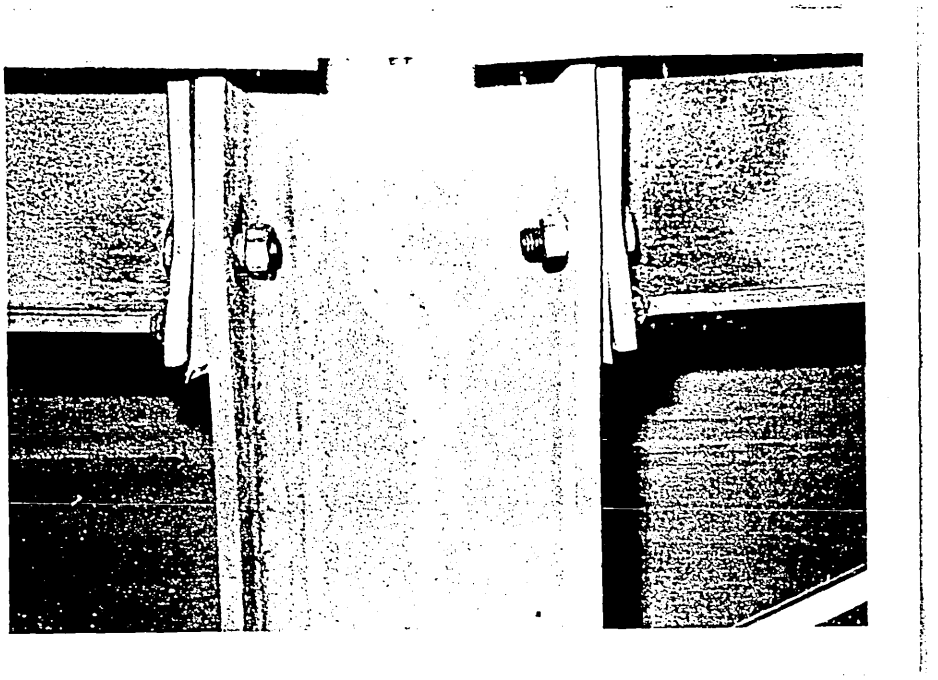

(a)

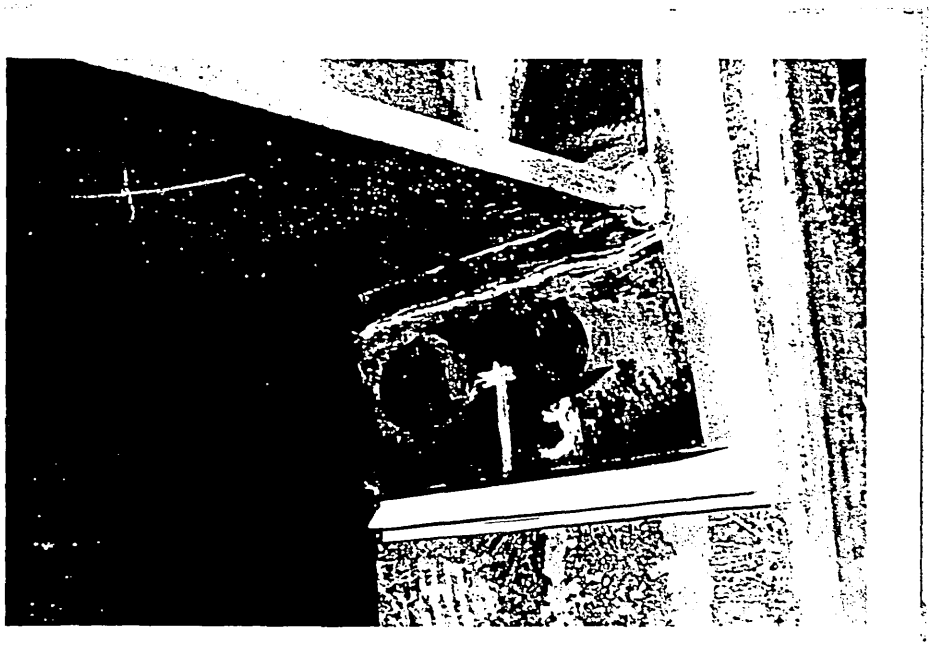

(b)

Fig.9

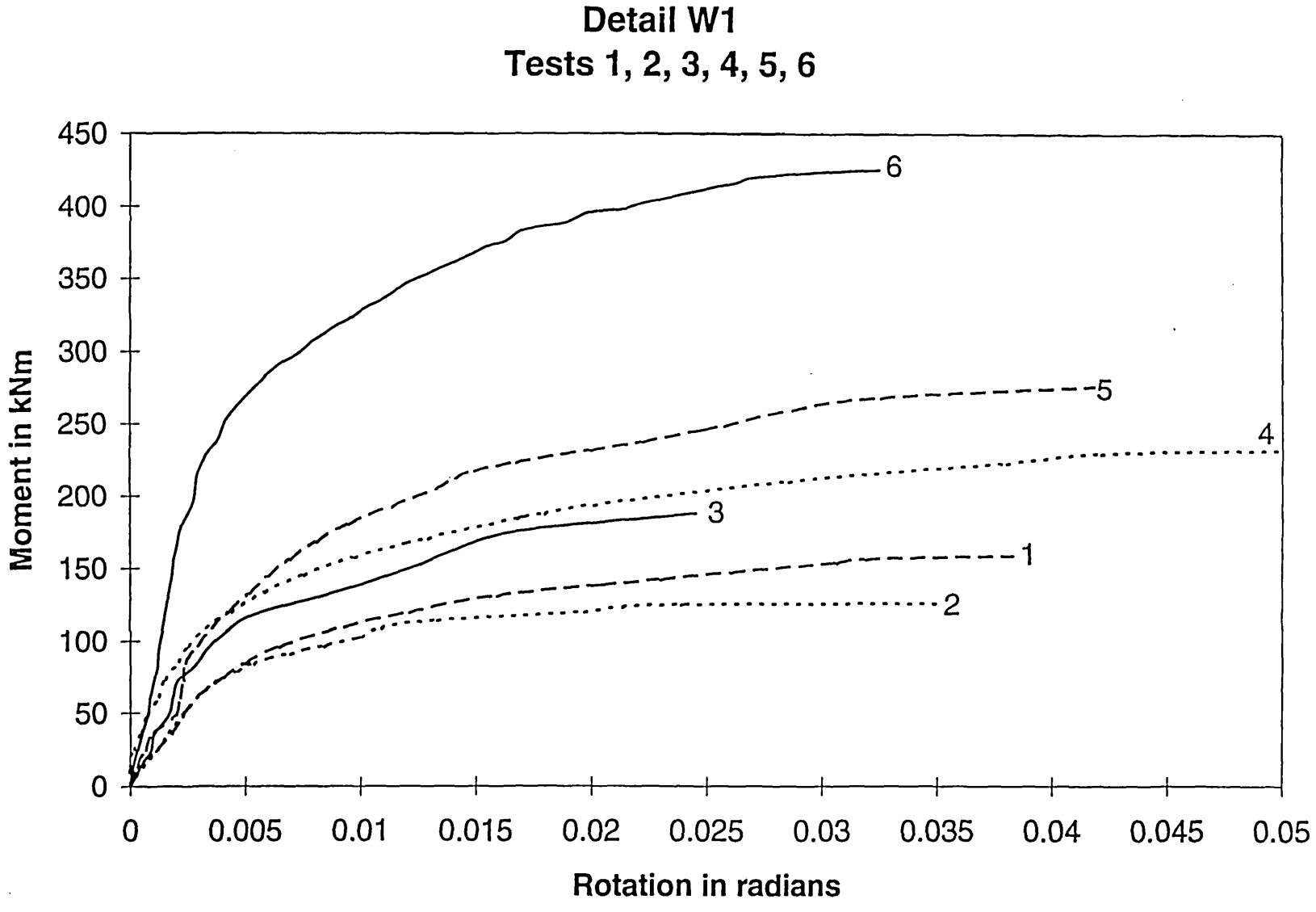

Fig.10

BOSE/YOUNGSON/WANG

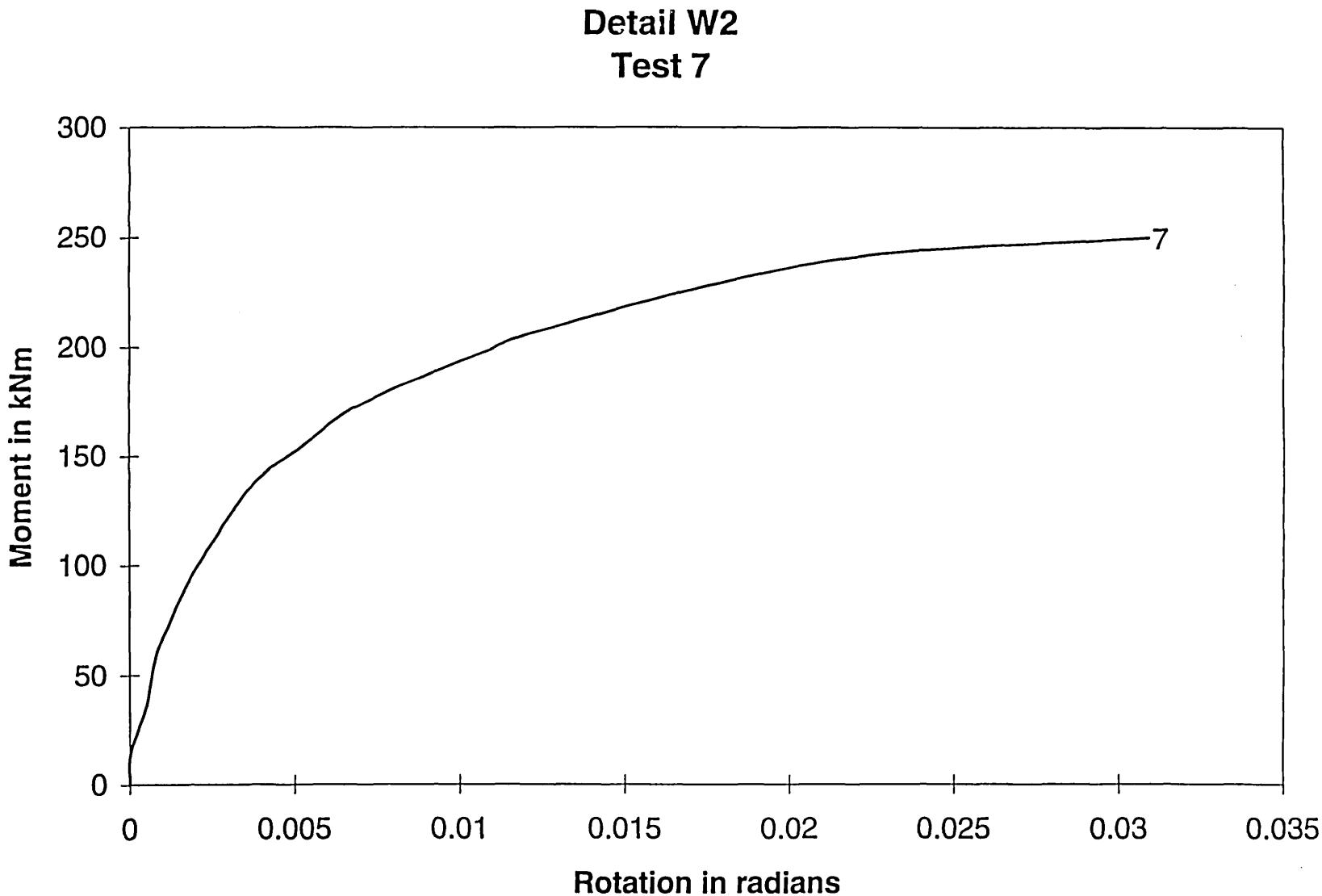
Detail W2
Test 7
300
250
200
150
100
50
0
Moment in kNm
7
0
0.005
0.01
0.015
0.02
0.025
0.03
0.035
Rotation in radians

Fig.11

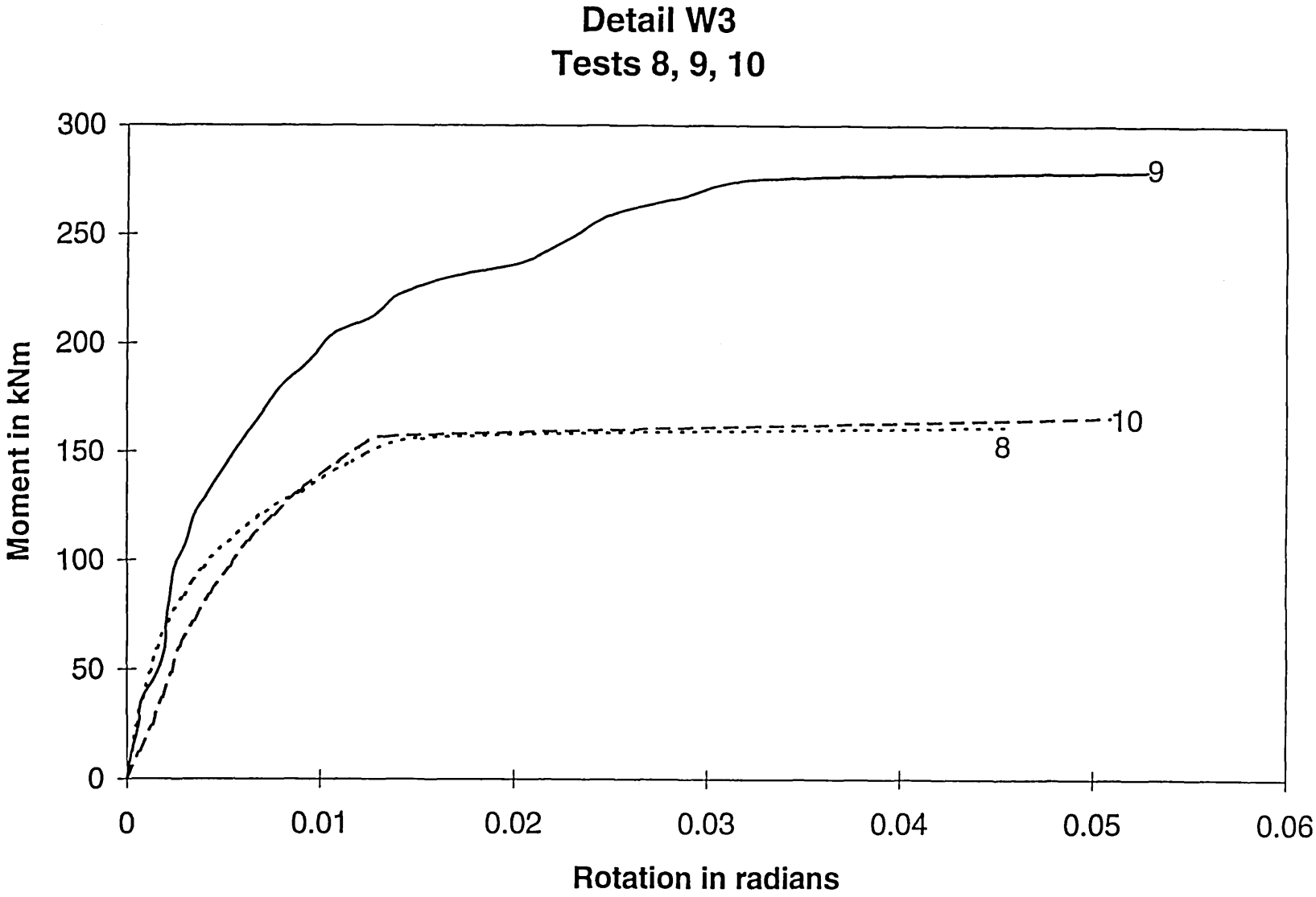
Detail W3
Tests 8, 9, 10
Moment in kNm
300
250
200
150
100
50
0
0
0.01
0.02
0.03
0.04
0.05
0.06
Rotation in radians
9
10
8

Fig.12

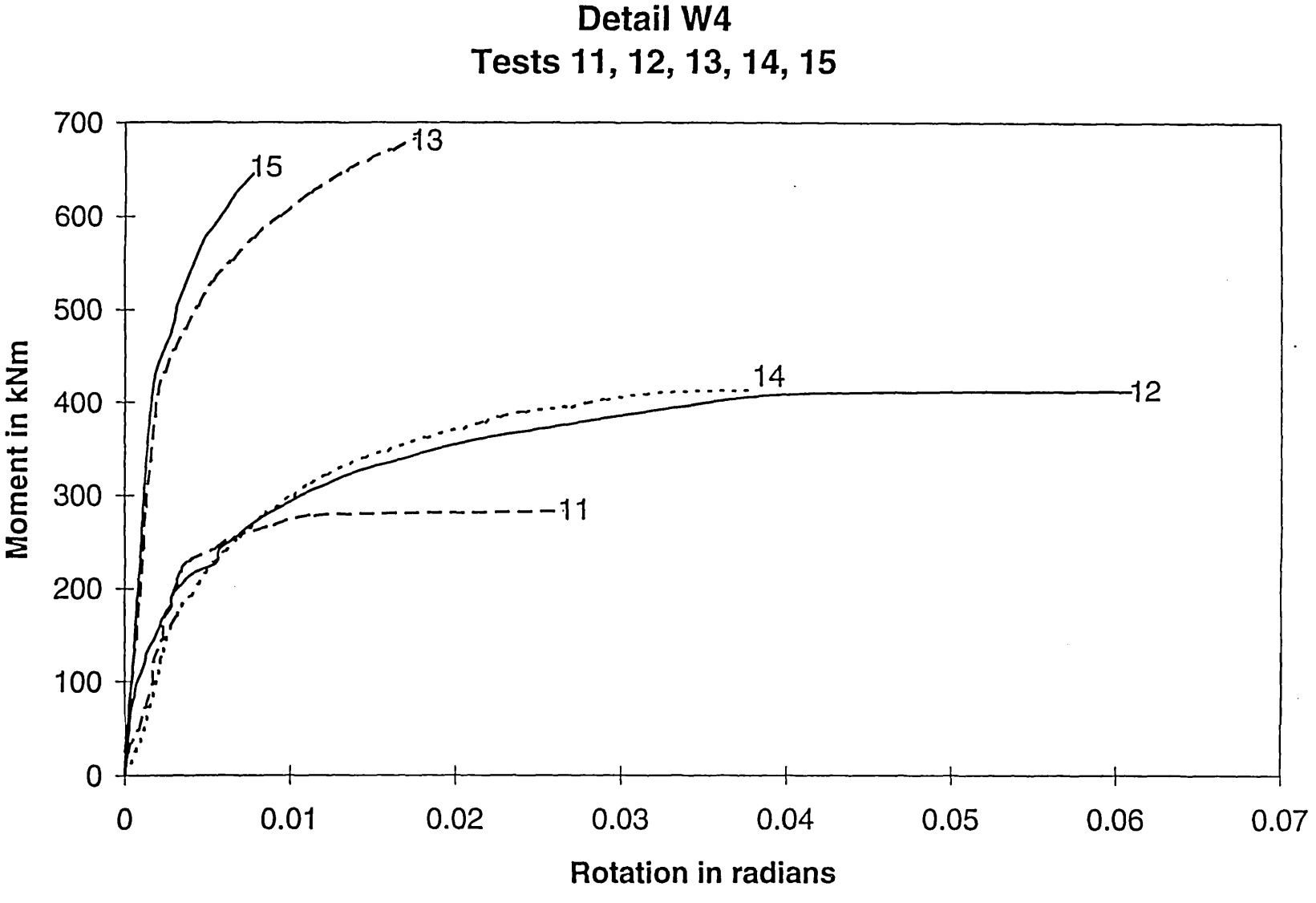

Fig.13

BOSE/YOUNGSON/WANG

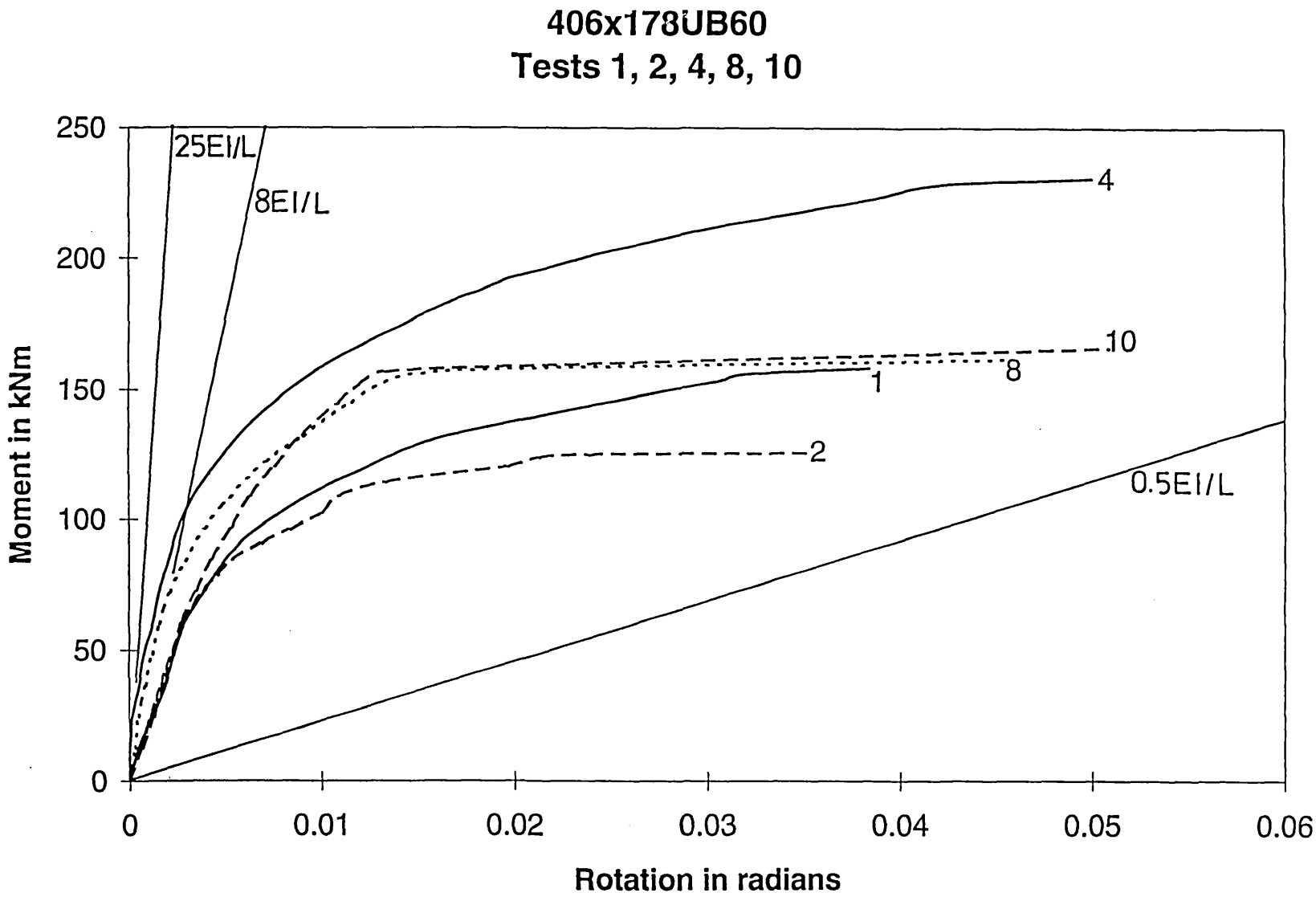

Fig.14

BOSE/YOUNGSON/WANG

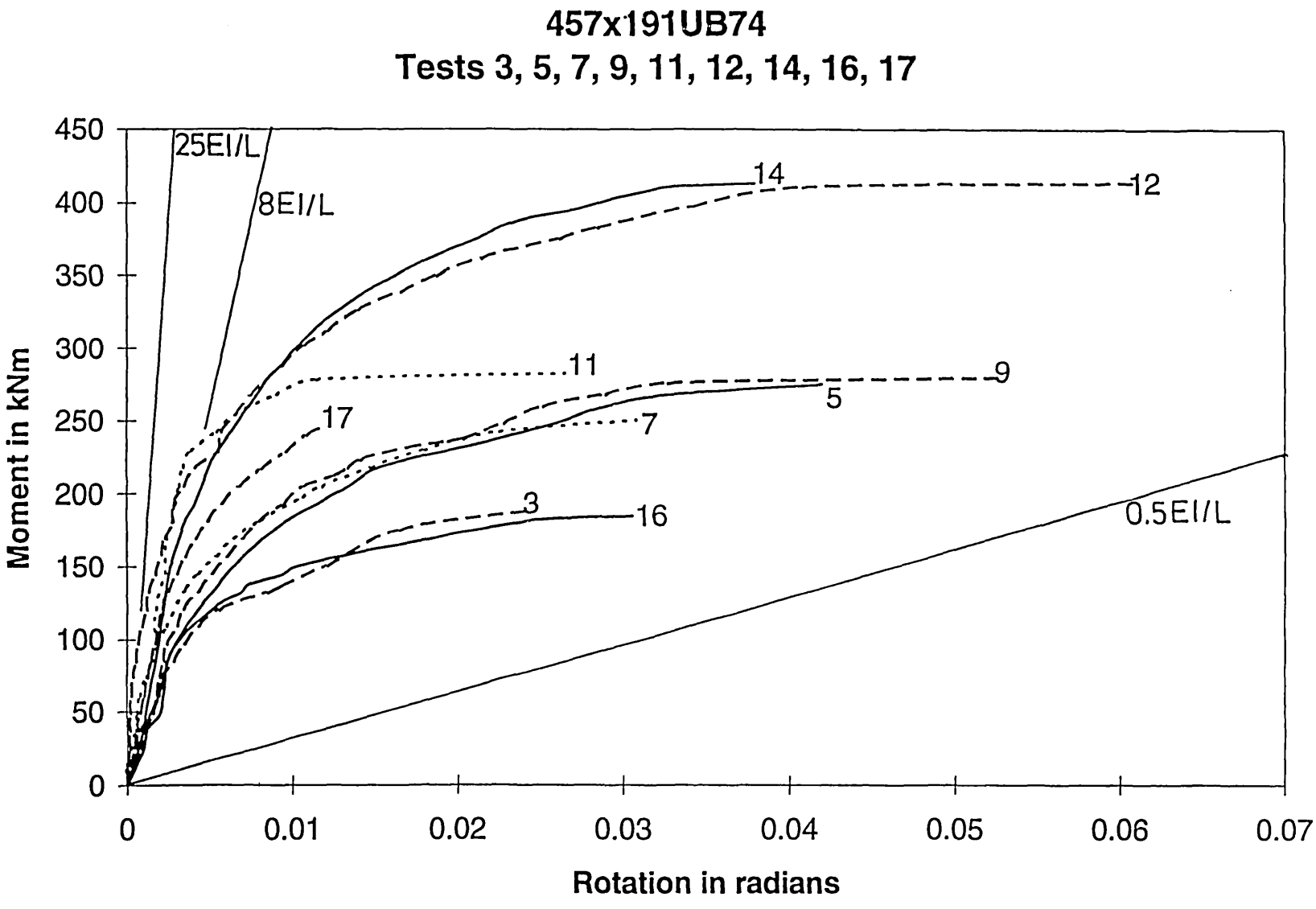

Fig.15

BOSE/YOUNGSON/WANG

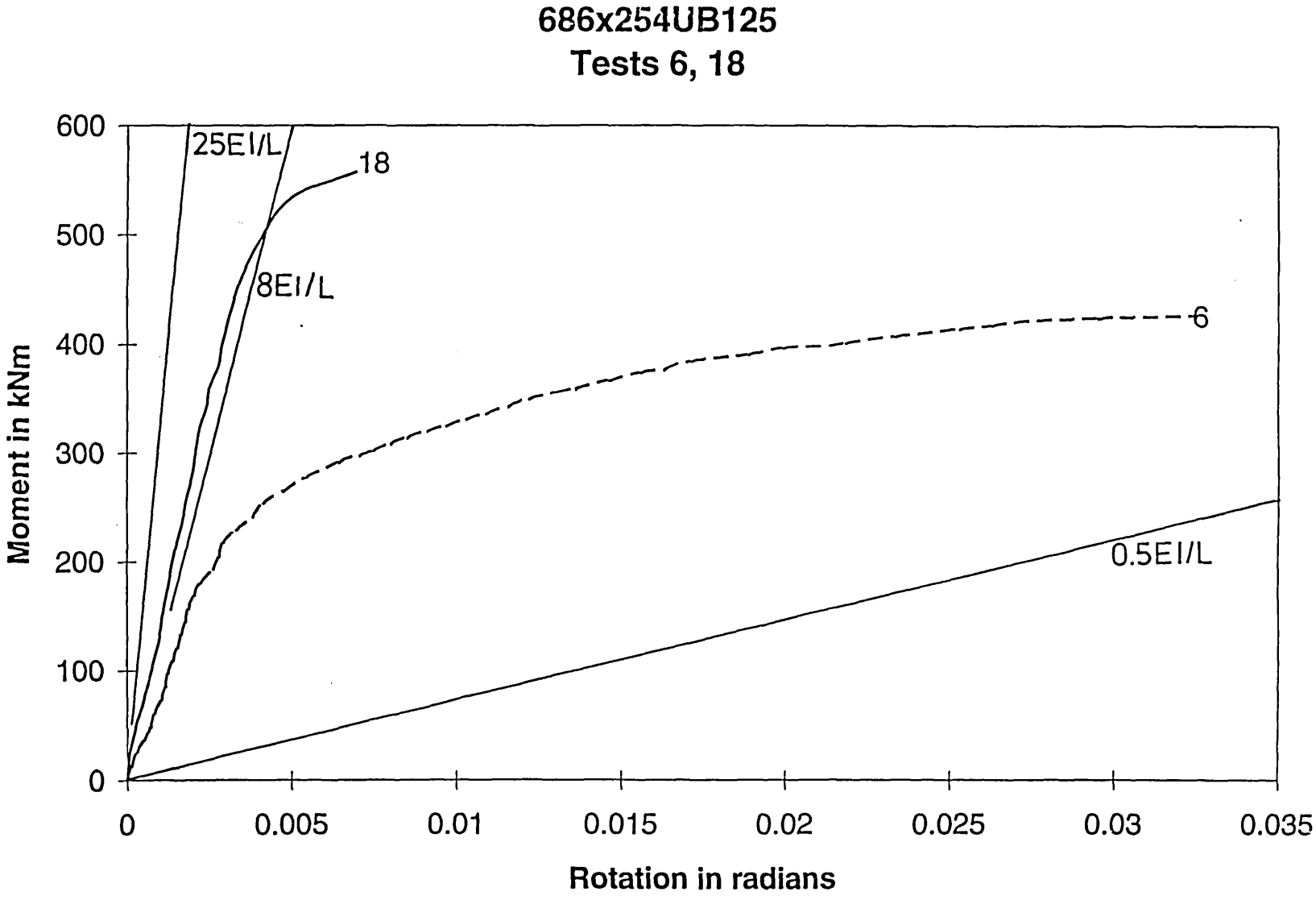

Fig.16

BOSE/YOUNGSON/WANG

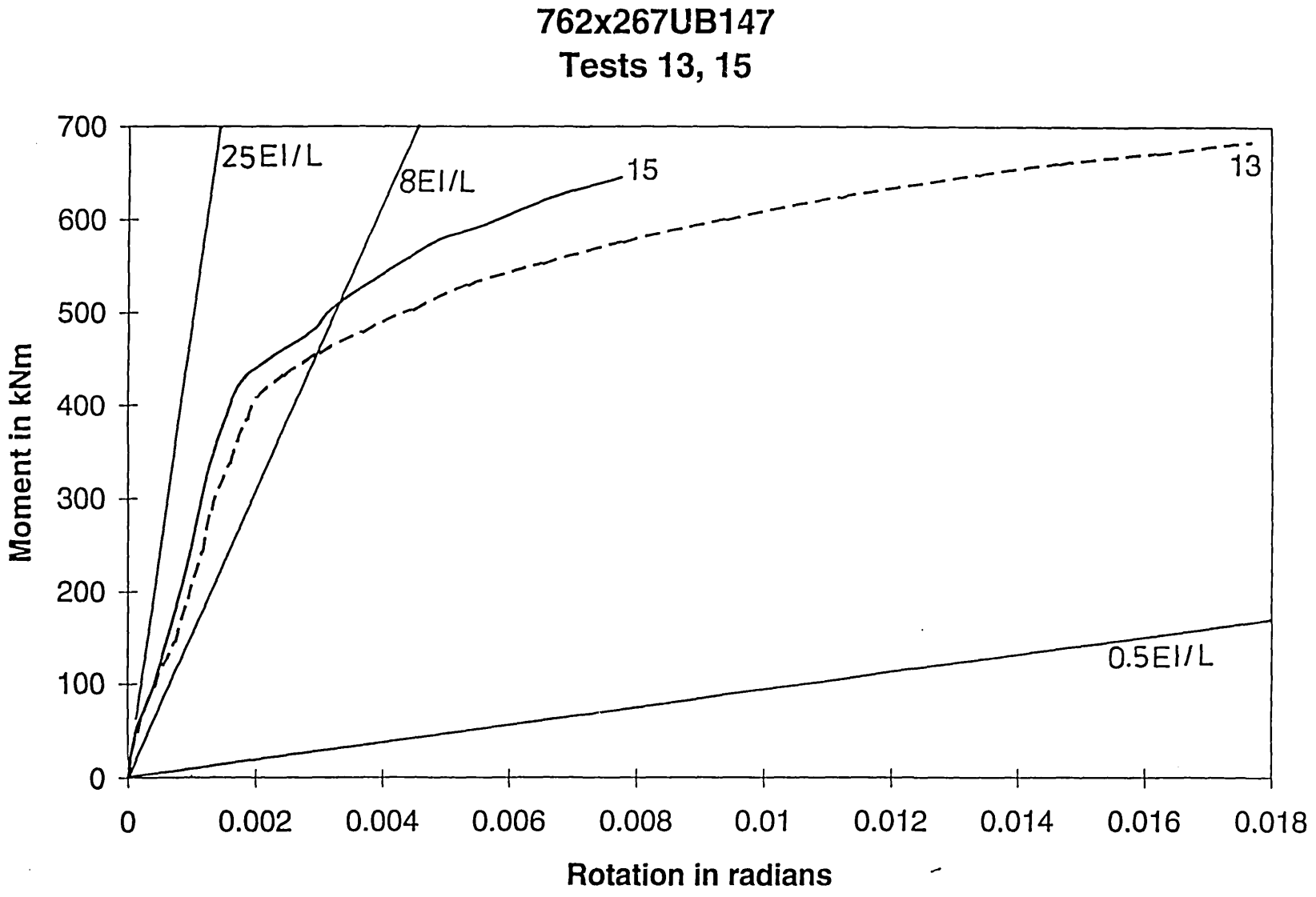

Fig.17

BOSE/YOUNGSON/WANG